Dissertation zur Erlangung des Doktorgrades
der Fakultät für Chemie und Pharmazie
der Ludwig-Maximilians-Universität München

Challenges in Pharmaceutical Quality Control

–

The Use of a Hyphenated HPLC-DAD-HRMS/SPE-NMR System for the Separation, Isolation, Enrichment and Structural Elucidation of Impurities

von
Philipp Martin Schmidt

aus
München, Deutschland

2024

Erklärung

Diese Dissertation wurde im Sinne von § 7 der Promotionsordnung vom 28. November 2011 von Herrn Professor Dr. Konstantin L. Karaghiosoff betreut.

Eidesstattliche Versicherung

Diese Dissertation wurde eigenständig und ohne unerlaubte Hilfe erarbeitet.

München, den 19.12.2024

.....

Philipp Schmidt

Dissertation eingereicht am: 19.12.2024

1. Gutachter: Prof. Dr. Konstantin L. Karaghiosoff

2. Gutachter: Prof. Dr. Thomas M. Klapötke

Mündliche Prüfung am: 14.03.2025

Acknowledgments

There are several people I would like to thank for both the support and the patience they showed me during the research and writing of this thesis. With the structural changes happening at Hexal AG and the Corona pandemic the circumstances were not always easy at times, but they were always willing to answer questions and lend a helping hand, when asked.

First and foremost, I would like to thank my supervisor Prof. Dr. Konstantin L. Karaghiosoff – or Conny – for the opportunity to research and write my PhD thesis in his working group. From my research internship, over my master thesis and now my dissertation, Conny was always supportive and ready to provide his expert insights and aid. His professional, but at the same time light-hearted and kind attitude, made working with him both productive and enjoyable, and I am glad for his support and patience these past years. I would also like to thank him for enabling the opportunity to perform my research at Hexal AG in Holzkirchen, giving me the opportunity to research an interesting topic and at the same time gather experience outside of university.

At this point I would also like to thank Dr. Hans-Christian Müller, who was kind enough to act as my supervisor at Hexal AG. I would like to express my gratitude for his support in organizing the cooperation between Hexal and the LMU, and for enabling me to research a topic that was interesting, insightful and at the same time relevant to my further career path in life. Christian was always supportive and patient, and his insights and experience in regard to the workings of the pharmaceutical industry and pharmaceutical quality control were always much appreciated, especially as I had no prior knowledge in this area before starting my thesis. Even after my time at Hexal, Christian kindly continued to provide his insights, which I would also like to thank him for.

Furthermore, I would like to thank Prof. Dr. Thomas Klapötke for welcoming me in his research group and for taking over the second review of this thesis.

Besides Christian, there are several other people at Hexal AG to whom I would like to express my gratitude. I would like to thank the entire team of the SDC Holzkirchen; Fabian Schmid and Dr. Hannes Dettlaff for making me feel welcome, Markus Philipp for his support, Christine Kolb for showing me the use of many of the analytical instruments and especially Andreas Reiser for his guidance and continued support, even after I had finished working fulltime at Hexal.

I would also like to thank Dr. Markus Godejohann from Bruker for his initial training and further support in the use of the hyphenated system, that produced the bulk of data for this thesis. I would also like to thank him for analyzing the final samples of the Flurbiprofen project with the method I sent him, when I no longer had access to the required analytical equipment, as this added much value to the project.

I would also like to express my gratitude to several of the people at my new workplace, Sykam GmbH. I would like to thank my former colleague Dr. Niko Fischer for introducing me to the company, as the job is a great opportunity and gave me financial stability whilst I finished my thesis. I am also grateful to Dirk and Frank Meier for accepting me into their company. I would also like to thank my colleague Dr. Sarah Linert, not only for proofreading parts of this thesis, but also for being my first point of contact with the working group of Conny, when I did my research internship under her in 2016.

Lastly, I would like to thank my family for their constant support, both financially and morally, as well as their patience, even though they often made sure to remind me how much time had already passed since the start of my PhD.

Table of Content

Abbreviations

AIBN	Azobis(isobutyronitrile)
API	Active Pharmaceutical Ingredient
Arom	Aromatic
au	atomic units
BHT	Dibutylhydroxytoluene
Bu	*n*-Butyl
COSY	Correlation Spectroscopy (NMR)
CV	Column Volume
d	duplet (NMR)
dd	duplet of duplets (NMR)
DAD	Diode-Array Detector
DMF	*N,N*-Dimethylformamide
DMSO	Dimethyl Sulfoxide
ESI	Electrospray Ionization
Et	Ethyl
FDA	Food and Drug Administration
GC	Gas Chromatography
GMP	Good Manufacturing Practice
HFBA	Heptafluorobutyric Acid
HMBC	Heteronuclear Multiple Bond Correlation (NMR)
HPLC	High-Performance Liquid Chromatography
HRMS	High-Resolution Mass Spectrometry
HSQC	Heteronuclear Single Quantum Correlation (NMR)
ICH	International Council for Harmonization
IR	Infrared Spectroscopy
LC	Liquid Chromatography
LCW	Liquid-Core Waveguide (Raman Spectroscopy)
m	multiplet (NMR)
MAT	Medication-Assisted Treatment
MCC	Microcrystalline cellulose
MeOH	Methanol
MS	Mass Spectrometry
m/z	Mass-to-Charge Ratio (MS)
NMR	Nuclear Magnetic Resonance

NOE	Nuclear Overhauser Effect
NSAID	Nonsteroidal Anti-Inflammatory Drug
Oct	*n*-Octyl
ORF	Oral Film
OUD	Opioid Use Disorder
PEG	Polyethylene Glycol
ppm	Parts Per Million (NMR)
PVC	Polyvinyl Chloride
Q	Quadrupole (MS)
q	Radio Frequency Quadrupole (MS), quartet (NMR)
QbD	Quality by Design
qNMR	Quantitative NMR
RRS	Resonance Raman Spectroscopy
s	singlet (NMR)
SPE	Solid-Phase Extraction
t	triplet (NMR)
THF	Tetrahydrofuran
TOF	Time-of-Flight (MS)
UHR	Ultrahigh Resolution
UPLC	Ultraperformance Liquid Chromatography
UV	Ultraviolet
Vis	Visible

1 Introduction

1.1 Problem and Motivation

As in many areas of science, analysis is one of the most important parts of pharmaceutical research. From the discovery and synthesis of new active ingredients, over early product development and clinical trials, to the continuous quality control of products, analysis is indispensable.[1-7]

Drugs are a subject that affects everyone during the course of their life in one way or another, and in some cases, such as Insulin for diabetics and chemotherapy for cancer patients, they are required for survival. As such, continuous and efficient quality assurance is of vital importance, which is why strict regulations and norms have been put in place worldwide in order to ensure that medicine is both safe and reliable.[8-11] To support the implementation and enforcement of these regulations, many organizations have been founded around the globe, such as the american *Food and Drug Administration* (FDA) or the *International Council for Harmonization of Technical Requirements for Pharmaceuticals for Human Use* (ICH), amongst many others.[1-6,12] In order to provide sufficient safety for patients, quality, effectiveness, and compliance to registered specifications of a drug must be guaranteed within its declared expiration date. Additionally, small changes during the shelf life of a medication may not only lead to reduced effectiveness but may even be harmful for the patients consuming them.[1-7,12-18]

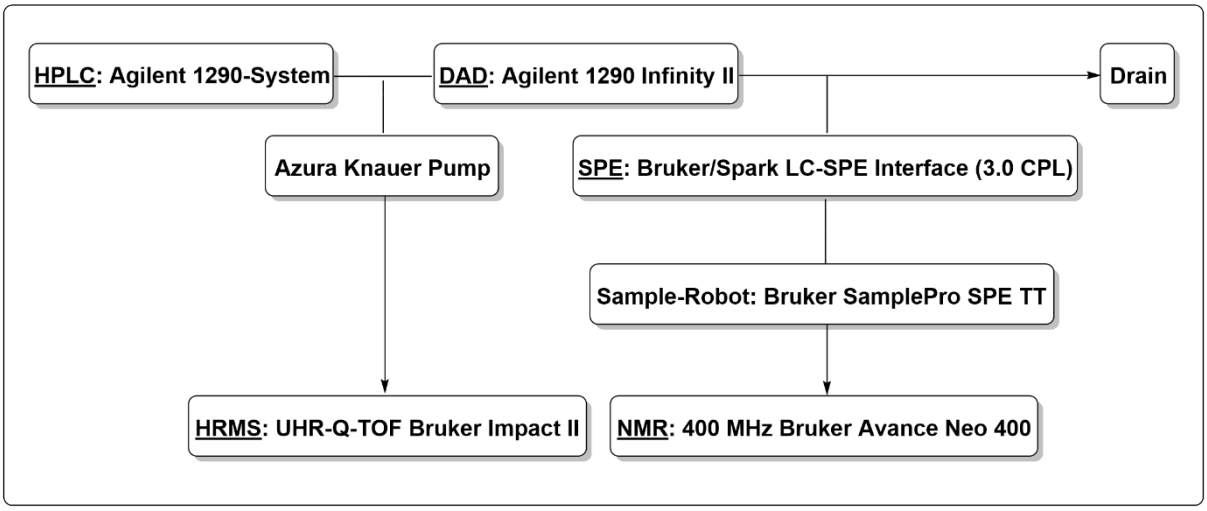

Figure 1: Scheme of the hyphenated HPLC-DAD-HRMS/SPE-NMR system discussed in the dissertation, with individual module names.

Due to their nature as chemical compounds, active ingredients are not inert and may experience changes due to external influences, such as temperature and moisture. Furthermore, the – in some cases very complex – synthesis of an active pharmaceutical ingredient (API) and the production processes of drugs may also lead to unintentional and undesirable side products and impurities.[1-7,12-18] A well-designed synthesis and purification of APIs, as well as continuous and conscious improvements of production processes and storage (Quality by Design – QbD), may decrease the likelihood of the formation of side products and impurities, but unfortunately, their unexpected appearance can never be ruled out entirely.[19-21]

To enable the detection of such impurities, a comprehensive and continuous monitoring by analytical processes is required. While the discovery of a new impurity during product development and stress tests, performed before marketing of the drug, "merely" leads to a delayed launch to market, a discovery during routine quality control of an already marketed product may constitute a real risk to the health and safety of patients.[8-11] Taking the compromised drug may not only be harmful to the affected consumer, but also requires the product to be removed from sale until the safety of the product can once more be guaranteed. The resulting unavailability of the, possibly essential, drug may hereby not only be potentially life threatening to patients but can also cause a loss of revenue for both producers and retailers.[8-11] To once again ensure the safety of the drug, the new impurity must first be identified, quantified, and if necessary subjected to a thorough risk assessment, by performing a toxicological evaluation. Lastly, should this evaluation show that the effectiveness of the drug may no longer be guaranteed, or that the new impurity poses a health risk to patients, actions must be taken to prevent its formation in the future. Only then the improved drug is allowed to once again be sold.[1-7]

As all these processes can be both complex and time consuming, it is of great importance to develop analytical methods that help simplify and thereby expedite them. Additionally, the substances that are to be analyzed are generally only available in small amounts, as they are often trace impurities in a drug. Therefore, methods are required that are capable of effectively and reliably detecting, separating and identifying impurities, even when only small sample amounts are available. In an ideal case, methods are used that combine these three steps in one single process. Such analytical techniques are commonly called "hyphenated methods", and though they have the potential to significantly accelerate analytical processes, their implementation may prove difficult in cases, due to their complexity and the requirements they demand of the personnel operating them.[21-24]

1.2 Objective

One of the most widespread separation and purification techniques, that is both used on a small scale in laboratories as well as on a large scale in routine industrial processes, is chromatography. Especially liquid chromatography, or more specifically high-performance-liquid-chromatography (HPLC), is very popular in the pharmaceutical industry. As most APIs are organic molecules of varying shapes and sizes, so-called "reversed-phase" HPLC is most often applied.[16,23,25-29] Reversed-phase HPLC most commonly utilizes a stationary phase consisting of silica gel, that has been modified with organic side chains, to enable hydrophobic interactions with the organic compounds. The more nonpolar a molecule is, the higher the interaction and the longer the retention time.[25-29]

Due to being one of the most widely used separation techniques, HPLC is well researched and understood, which is a major reason for its application in areas such as product research and development, routine quality control, as well as individual investigations. Most APIs have a defined assay and/or purity method that utilizes HPLC, which can be found in resources such as the *European Pharmacopoeia*. With a base knowledge about HPLC analysis, these methods can be adapted and applied to different materials, products and dosage forms with relative ease. This flexibility enables a broad range of applications for HPLC and is one of the main reasons for its popularity.

Another advantage of HPLC is the ability to couple it to a large number of analytical techniques, in order to combine separation and purification with comprehensive analysis. Amongst these techniques are detection modes such as UV/Vis, IR or Raman spectroscopy, purification methods such as solid-phase extraction (SPE) and methods for structural elucidation like nuclear magnetic resonance (NMR) spectroscopy or mass spectrometry.[7,16,9-11,21,22] Most of these techniques are themselves well established and researched, and while many of them (especially UV/Vis spectroscopy) have been successfully applied in combination with HPLC for a long time, others still present certain challenges when combined with HPLC.[26,28-32] Additionally, the qualifications some of these techniques demand of the personnel operating them, in regard to acquisition and evaluation of data, can be very high in cases. Due to these challenges, the use of complex hyphenated HPLC systems, that are coupled to a variety of analytical and purification techniques, is still limited in regular pharmaceutical quality control.

For these reasons, it was the aim of this dissertation to develop methods for a hyphenated HPLC system, consisting of common purification and analytical techniques, that are quick, effective, and able to perform a complete analysis from identification, over quantification, to structural elucidation using only small amounts of analyte. To this purpose, real case studies, with unknown impurities that occurred in the pharmaceutical industry were chosen. The intention was to show that these hyphenated systems are capable of identifying new, unknown impurities with little personnel and time requirements, while

avoiding the usual time-consuming procedures common in the pharmaceutical industry, such directed stress and enrichment experiments and attempts of synthesizing the impurities before analysis.[21,31,32]

References (Problem and Motivation/Objective)

1. International Conference on Harmonization (ICH) guidelines. Impurities in new Drug Substances Q3A (R2), October 2006.
2. International Conference on Harmonization (ICH) guidelines. Impurities in new Drug Products Q3B (R2), June 2006.
3. International Conference on Harmonization (ICH) Guidance for Industry. Impurities in new Drug Substances Q3A (R2), June 2008.
4. International Conference on Harmonization (ICH) Guidance for Industry. Impurities in new Drug Products Q3B (R2), August 2006.
5. International Conference on Harmonization (ICH) guidelines. Impurities: guideline for residual solvents Q3C (R8), August 2022.
6. International Conference on Harmonization (ICH) guidelines. On elemental impurities Q3D (R2), May 2022.
7. Ahuja SS. Assuring quality of drugs by monitoring impurities. Adv Drug Deliv Rev 2007;59:3-11.
8. Görög S. New safe medicines faster: the role of analytical chemistry. TRAC 2003;22(7+8):407-415.
9. Görög S. The importance and challenges of impurity profiling in modern pharmaceutical analysis. TRAC 2006;25(8):755-757.
10. Singh S, Handa T, Narayanam M, Sahu A, Junwal M, Shah RP. A critical review on the use of modern sophisticated hyphenated tools in the characterization of impurities and degradation products. J Pharm Biomed 2012;69:148-173.
11. International Conference on Harmonization (ICH) specification. Test procedures and acceptance criteria for new drug substances and new drug products: chemical substances – Scientific guideline Q6A, May 2000.
12. FDA Guidance for Industry: ANA's: Impurities in Drug Products; November 2010.
13. Ayre A, Varpe D, Nayak R, Vasa N. Impurity Profiling of Pharmaceuticals. ARPB 2011;1(2):76-90.
14. International Conference on Harmonization (ICH) Guidance for Industry. Impurities: Guidelines for Residual Solvents Q3C (R8), December 2021.
15. Pan C, Liu F, Motto M. Identification of Pharmaceutical Impurities in Formulated Dosage Forms. J Pharm Sci 2011;100(4):1228-1259.

16. Pilaniya K, Chandrawanshi HK, Pilaniya U, Manchandani P, Jain P, Singh N. Recent trends in the impurity profile of pharmaceuticals. J Adv Pharm Tech Res 2010;1(3):302-310.
17. Bari SB, Kadam BR, Jaiswal YS, Shirkhedkar AA. Impurity profile: Significance in Active Pharmaceutical Ingredient. Eurasian J Anal Chem 2007;2:32-53.
18. Ambhore JP, Adhao VS, Cheke RS, Popat RR, Gandhi SJ. Futuristic review on progress in force degradation studies and stability indicating assay method for some antiviral drugs. GSCBPS 2021;16:133-149.
19. Beg S, Hasnain MS, Rahman M, Swain S. Chapter 1 – Introduction to Quality by Design (QbD): Fundamentals, Principles, and Applications. In: Beg S, Hasnain MS, editors. Pharmaceutical Quality by Design. Academic Press; 2019, p. 1-17.
20. Mishra V, Thakur S, Patil A, Shukla A. Quality by design (QbD) approaches in current pharmaceutical set-up. Expert Opin Drug Deliv 2018;15(8):737-758.
21. Jain D, Basniwal PK. Forced degradation and impurity profiling: Recent trends in analytical perspectives. J Pharm Biomed Anal 2013;86:11-35.
22. Kamboj S, Kamboj N, Rawal RK, Thakkar A, Bhardwaj TR. A Compendium of Techniques for the Analysis of Pharmaceutical Impurities. Curr Pharm Anal 2014;10(2):145-160.
23. Landge AK, Deshmukh VK, Chaudhari SR. Impurities in Pharmaceuticals- A Review. Current Pharma Research 2013;4(1):1105-1116.
24. Hirschfeld T. The Hy-phen-ated Methods. Anal Chem 1980;52(2):297A-312A.
25. Colin H, Guiochon G. Introduction to reversed-phase high-performance liquid chromatography. J. Chromatogr. 1977;141:289-312.
26. Gupta MK, Ghuge A, Parab M, AL-Refaei Y, Khandare A, Dand N, Waghmare N. A comprehensive review on High-Performance Liquid Chromatography (HPLC), Ultra Performance Liquid Chromatography (UPLC) & High-Performance Thin Layer Chromatography (HPTLC) with current updates. Curr Issues Pharm Med Sci 2022;35(4):224-228.
27. Patel K, Patel D, Panchal D, Patel K, Upadhyay U. A Review on High Performance liquid Chromatography. IJCRT 2022;10(10):2320-2882.
28. Ali AH. High-Performance Liquid Chromatography (HPLC): A review. Ann Adv Chem 2022;6:10-20.
29. Sudev S, Janardhanan SV. Review on HPLC Method Development Validation and Optimization. Int J Pharm Sci Rev Res 2019;56(2):28-43.
30. Locatelli M, Governatori L, Carlucci G, Genovese S, Mollica A, Epifano F. Recent application of analytical methods to phase I and phase II drugs development: a review. Biomed Chromatogr 2012;26:283-300.

31. Baertschi SW, Alsante KM, Reed RA. Pharmaceutical Stress Testing. 2nd ed. Boca Raton: CRC Press; 2011.
32. Singh S, Bakshi M. Guidance on Conduct of Stress Tests to Determine Inherent Stability of Drugs. Mat Sci 2000;24:1-14.
33. Chew YL, Khor MA, Lim YY. Choices of chromatographic methods as stability indicating assays for pharmaceutical products: A review. Heliyon 2021;7:1-12.
34. Ermer J. The use of hyphenated LC-MS technique for characterization of impurity profiles during drug development. J Pharm Biomed Anal 1998;18:707-714.
35. Dubey S, Pandey RK, Shukla SS. Impurity profiling and drug characterization: backdrop and approach. IAJPS 2018;5(4):2499-2515.
36. Ermer J, Vogel M. Applications of hyphenated LC-MS techniques in pharmaceutical analysis. Biomed Chromatogr 2000;14:373-383.
37. Govaerts C, Adams E, Schepdael AV, Hoogmartens J. Hyphenation of liquid chromatography to ion trap mass spectrometry to identify minor components in polypeptide antibiotics. Anal Bioanal Chem 2003;377:909-921.
38. Magio RM, Calvo NL, Vignaduzzo SE, Kaufman TS. Pharmaceutical impurities and degradation products: Uses and applications of NMR techniques. J Pharm Biomed Anal 2014;101:102-122.
39. Spraul M. Developments in NMR Hyphenation for Pharmaceutical Industry. Modern Magnetic Resonance 2008:1221-1228.
40. Tokunaga T, Akagi K, Okamoto M. Sensitivity enhancement by chromatographic peak concentration with ultra-high performance liquid chromatography-nuclear magnetic resonance spectroscopy for minor impurity analysis. J Chromatogr A 2017;1508:163-168.

1.3 Introductory Review Paper

The following, yet to be published, review is meant to provide a brief overview of common practices and analytical techniques related to HPLC, as they are used in the pharmaceutical industry.

Author contributions:

The author of this dissertation performed the entirety of the literary research and writing of the following Review article "The Use of Hyphenated Liquid Chromatography Systems in Pharmaceutical Analysis".

Dr. Hans-Christian Müller and Professor Konstantin Karaghiosoff had an advisory role in the preparation of the manuscript and aided in proof-reading.

The Use of Hyphenated Liquid Chromatography Systems in Pharmaceutical Analysis

Philipp Schmidt[1], Hans-Christian Müller[2,*], Konstantin Karaghiosoff[1,*]

[†]Department Chemie, Ludwig-Maximilians-Universität München, Butenandtstraße 5-13, Haus D, 81377 Munich, Germany

[‡]Analytical Development, Hexal AG, Industriestraße 25, 83607 Holzkirchen, Germany

***Corresponding Authors:**

*Konstantin Karaghiosoff − Department Chemie, Ludwig-Maximilians-Universität München, 81377 Munich, Germany; orcid.org/0000-0002-8855-730X; Phone: +49 (0)89 2180-77426; Email: klk@cup.uni-muenchen.de

*Hans-Christian Müller − Analytical Development, Hexal AG, 83607 Holzkirchen, Germany; orcid.org/0000-0001-9367-6066; Phone: +49 8024 908 2200; Email: dhcm@gmx.de

Abstract:

In this review we aim to provide an overview of the use of hyphenated liquid chromatography (LC) systems in pharmaceutical analysis, with a focus on the evaluation and identification of impurities. We will first introduce the analytical techniques most commonly used in combination with LC in the pharmaceutical industry, focusing on the advantages they provide and the challenges that may arise by coupling them to LC. We will then present examples of more complex hyphenated LC systems and literature examples of their use in the identification of pharmaceutical impurities. With this review we aim to highlight the great potential of hyphenated LC systems in pharmaceutical analysis, both in routine and specific applications and provide those interested in the topic with an overview and literature sources for further research.

Abbreviations:

API – active pharmaceutical ingredient, COSY – correlation spectroscopy (NMR), DAD – diode-array detector, DMSO – dimethyl sulfoxide, ESI – electrospray ionization, GC – gas chromatography, HMBC – heteronuclear multiple bond correlation (NMR), HPLC – high-performance liquid chromatography, HRMS – high-resolution mass spectrometry, HSQC – heteronuclear single quantum correlation (NMR), ICH – international council for harmonization, IR – infrared spectroscopy, LC – liquid chromatography, LCW – liquid-core waveguide (Raman spectroscopy), MS – mass spectrometry, NMR – nuclear magnetic resonance, NOE – nuclear Overhauser effect, PEG – polyethylene glycol, QbD – quality by design, qNMR – quantitative NMR, RRS – resonance Raman spectroscopy, SPE – solid-phase extraction, UPLC – ultra-performance liquid chromatography, UV – ultraviolet, Vis – visible

Keywords:

LC, UV/Vis, MS, NMR, IR, Raman, 2D-LC, SPE, hyphenation, DAD

I Introduction

According to the ICH guidelines pharmaceutical impurities are defined as “any component of the new drug substance that is not the chemical entity defined as the new drug substance”[1-4] and can generally be classified as organic, inorganic, metal and elemental impurities, as well as residual solvents. These impurities may be formed or introduced into the drug product during substance synthesis, formulation, or storage of the medicinal product.[1-7] As these impurities may lessen the efficacy of the drug or even pose a threat to the health and safety of patients, the identification and quantificational monitoring of impurities is a vital part of regular pharmaceutical quality control during drug development, production and stability testing.[1-14]

If the level of an impurity rises above the defined identification level (for example ICH guidelines) it may lead to the delay of drug development, supply problems or possibly even the withdrawal of a medicinal product already on the market in batches or in its entirety, unless the impurity is identified, specified and if necessary its levels reduced.[1-8] As this can cause risks for the patients who may be dependent on the drug in question as well as financial losses for both the involved pharmaceutical companies and retailers, the swift detection, separation, and identification of these substances is essential.[15-18]

As such, several analytical methods have been, and continue to be developed to improve the efficacy and speed of detection and identification of impurities to increase the pharmaceutical product quality. Amongst these are separation methods, such as gas and liquid chromatography, spectroscopic methods, such as UV, IR, Raman and NMR spectroscopy and spectrometric methods, such as mass spectrometry.[7,12,16-21] Also, in recent years the application of a quality by design (QbD) approach has been encouraged, which aims to prevent the formation of impurities in the first place, by theoretical consideration and determination of possible risk factors during product development.[20,23,24]

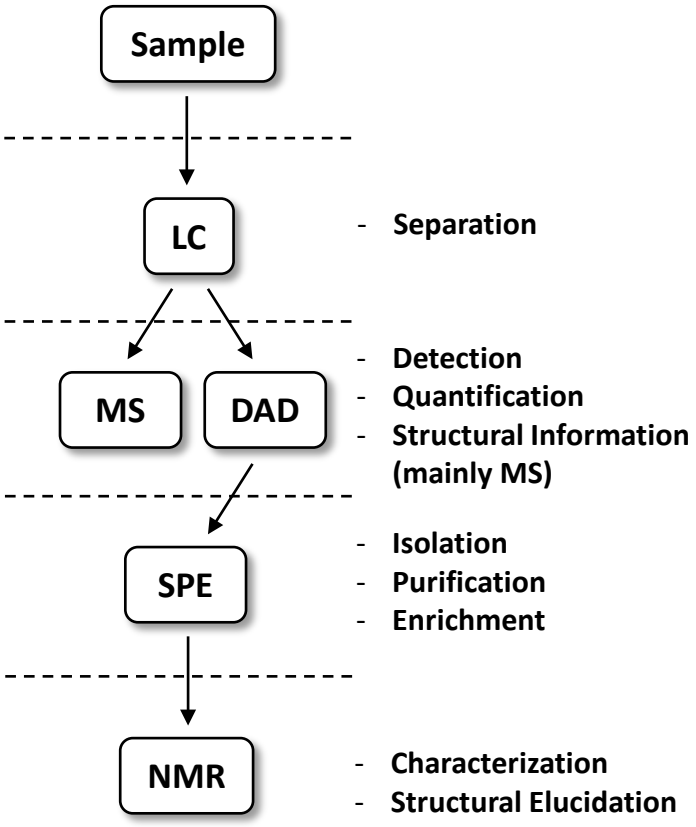

Figure 1. Scheme of a hyphenated liquid chromatography (LC) system containing mass spectrometry (MS), diode-array detection (DAD), solid-phase extraction (SPE) and nuclear magnetic resonance (NMR). The function and type of acquired data is described for each component.

In most cases the identification of an impurity begins by performing degradation experiments. Herein different components of a medicinal product are mixed together under varying conditions (ph-value, temperature, different solvents, moisture etc.) and are stored over a prolonged period of time. Samples are taken from these experiments at regular intervals to determine which conditions and components cause the formation of the new impurity. This provides both information on the nature of the impurity and which conditions should be selected for its artificial synthesis.[20,25,26] Once sufficient amounts of samples have been obtained via degradation experiments or synthesis, these are used for identification of the impurity. This can be achieved by comparing the retention time of the impurity to an analytical standard of the suspected impurity or by using absolute analytical methods, such as MS spectrometry and NMR spectroscopy for complete structural elucidation.[7,12,16-21] Though information obtained during the first detection of an impurity (e.g. retention time corelating to polarity or mass indicating the size and possible origin) may help reduce the number of degradation experiments needed, the process remains overall time consuming.

To increase the efficiency during analysis, hyphenated systems have long since been applied in pharmaceutical product development and quality control.[11,17,21,22,27] Depending on the setup of such systems they may combine everything from separation and detection over isolation and acquisition of

structural data (Fig. 1). By combining all these steps into one, the requirements to both time and sample amount can be significantly reduced, ideally to a point were degradation experiments are no longer required as the amount of impurity obtained from a medicinal sample is sufficient for all steps of analysis. In this review we attempt to highlight the uses and potential of hyphenated systems for the identification of pharmaceutical impurities. Hereby we have limited ourselves to hyphenated systems including LC, as an example of one of the most wide spread separation methods in the pharmaceutical industry.

II Hyphenation

In 1980 Hirschfeld defined hyphenated methods as "the marriage (…) of two separate analytical techniques via appropriate interfaces, usually with the backup of a computer tying everything together."[27] Over time this definition extended to the combination of two or more techniques, usually involving at least one separation technique and a spectroscopic detection method. Also, MS detection, as a spectrometric method has found widespread use.[16-21] Though hyphenated systems may contain any combination of separation, isolation, detection, and analytical methods this review will focus solely on the coupling of liquid chromatographic (LC) methods, as one of the most widespread separation techniques used in the pharmaceutical industry. The main advantages of hyphenated systems are the time that can be saved by directly coupling separation and analysis, without the need for isolation in between. Also, a reduced amount of sample is needed for the characterization of an analyte, as several analytical methods are performed with the same sample.

In the following we first present individual techniques used in hyphenated LC systems, describing their function, advantages, and disadvantages, before addressing more advanced systems, which combine the strengths of the individual analytical methods. In doing so we hope to provide a comprehensive overview of the tools available in pharmaceutical analysis when it comes to hyphenated LC methods.

III LC-Hyphenation

When speaking about LC-hyphenation in general, this review will use the term LC (liquid chromatography) as an umbrella term, which is also meant to include the more advanced HPLC and UPLC techniques.

III.I Liquid Chromatography

In LC analysis samples are dissolved and separated by a chromatographic column. Depending on the column material in combination with eluent properties the varying substances contained within a sample have different degrees of interaction with the solid phase leading to their separation. In most cases this separation is based on the polarity of the individual analytes, however columns based on ion-exchange, size exclusion and chiral chromatography are also available. Aside from the material the column is packed with, factors such as the grain size of said material as well as column length and width may also be adapted in order to improve sample separation and/or the amount of sample that can be analyzed in one run. Broad columns, that allow a higher load, may even be used for preparative HPLC enabling not only the separation but also quantitative isolation of individual analytes.[12,22,28-32]

A further factor strongly influencing the separation is the choice of the solvent system. Most pharmaceutical LC analysis is performed on reversed-phase columns, as most molecules of interest are rather nonpolar, organic compounds.[12,22,28-32] As such, mixtures of either different organic solvents or organic solvents with varying degrees of water are applied. To further influence the separation, factors such as temperature, flow rate and pH-value of the liquid phase may be adjusted by acids, bases, or buffers and coupling reagents may be added to the solvents. In addition, two or more solvent systems can be used in a single analysis. [12,22,28-32] If the composition of the liquid phase is kept constant during an LC-run, the method is called isocratic, whereas a so-called gradient method will change the make-up of the liquid phase over time, by adjusting the relative level of each solvent mixture. A method can also combine both gradient and isocratic run-time sections, allowing the creation of highly specific and complex, time-dependent solvent systems. [28-32]

All these factors make LC a highly versatile separation method that can be easily and effectively adapted for an array of cases and can be used for swift and efficient analysis of a large number of samples with high resolution and excellent recovery. This ease of use and adaptability is the main reason for its popularity in high through-put analytical environments, such as pharmaceutical quality control. [12,22,28-32]

Though highly versatile, there are certain drawbacks to LC. For one, the requirement to dissolve samples excludes insoluble or hard to dissolve samples.[30-32] The types of solvents that can be used in LC analysis is also a limiting factor. Highly viscous solvents such as DMSO or volatile solvents such as

certain ethers cannot be used in LC as they pose the risk of severely changing the pressure within the system altering the conditions of the separation or even leading to a shutdown of the system by exceeding its maximum pressure-limit. In this case, the analyte would be better suited for GC analysis. The evaporation of volatile solvents from solvent mixtures may also alter the polarity of the liquid phase, changing the separation conditions over time, leading to inconsistent results. The cost and environmental impact, potentially caused by use of organic solvents are also factors to be considered. This problem is however reduced for HPLC and UPLC due to less solvent consumption.[29-32] Further limitations may arise from the requirements of the individual detection modes coupled to LC; these will however be addressed in the respective parts of this review.

Despite the adaptability of LC analysis, cases may arise were the peak capacity (column plates), meaning the number of individual compounds that can be properly separated and detected during one, single LC run, may reach its limits.[31,32] This is especially the case when a sample contains a high number of compounds with very similar retention times. In this case, attempts to develop methods capable of separating and individually detecting all desired analytes with classic LC may prove time consuming and the resulting methods may lack in efficiency by, for example, drastically increasing the run and/or column regeneration time. In some cases, several independent methods must be developed for different analytes of interest resulting in both loss of time and material due to several LC methods being required for a single sample.[32-35] To avoid this, the development of two, or higher dimensional LC separation has intensified in the recent decade.

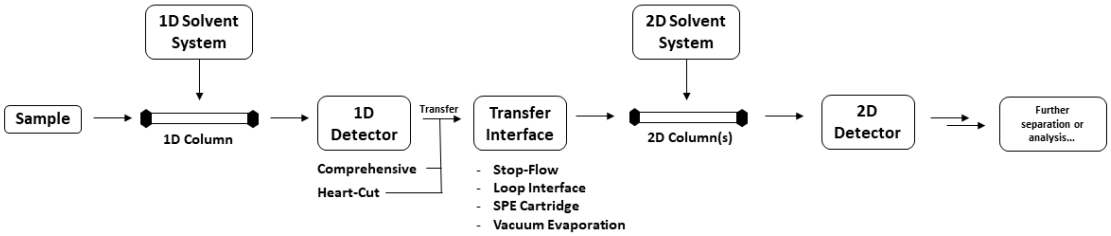

Figure 2. Scheme of a multidimensional LC set-up with different options for sample transfer.

Multidimensional LC separation is itself by definition a hyphenated method and works by combining two or more LC separation mechanisms.[27] As such, two or more columns and liquid phases are linked in series to improve the overall separation of a sample by combining different separation conditions. In general, two modes of operation are applied to multidimensional LC: comprehensive and heart cutting LC (Fig. 2). Comprehensive LC functions by feeding the entire effluent of the first dimension LC into the second dimension LC, whilst heart cutting merely transfers regions or peaks of interest.[33-39]

The main challenges of multidimensional LC lie in the additional efforts necessary for the user, the transfer between the different resolving dimensions and the complexity of the required hardware.

Especially the transfer from one dimension to another requires many considerations that led to the development of several different transfer interfaces.[33-39] One such mode is the application of stop-flow, during which part of the first-dimension separation is performed, feeding the effluent directly into the second system, before it is halted in favor of the second-dimension's completion. Then the first-dimension separation is resumed until the desired amount of effluent has once again been transferred, hereby incrementally feeding the first-dimension effluent into the second-dimension system.[34-35] Drawbacks of this system are a possible decrease in separation quality and increased analytical time. As such, peak broadening may occur in the chromatogram due to the regular halting of the first-dimension flow. Also, as the second-dimension separation must be repeated several times during which the first-dimension separation is delayed the time needed for one complete analytical cycle may increase drastically.[34-35]

A method to prevent this delay is the use of a loop interface, which is usually equipped with two loops. These serve as an intermediate storage for the first-dimension effluent. This allows the second-dimension analysis of the first loop's content, whilst the second is filled and vice versa for the following run. Hereby, both the first- and second-dimension separation can be performed simultaneously to save time. However, the runtime of the second-dimension separation is limited by the time needed to fill the storage loop.[37-39]

A further drawback of both, the stop-flow and loop-interface, is the mixing of solvent systems during the interdimensional transfer, which may cause changes in pressure, polarity, temperature and, worst-case, phase separation or bubble-formation, leading to a decrease in resolution.[34-36,38] A possibility to alleviate the issues arising from incompatible solvents or solvent mixing, is the use of solid phase extraction (SPE) to store samples on solid phase cartridges in-between the first- and second-dimension LC runs. In addition to the possibility of a liquid phase change, this also offers the possibility to switch the conditions to allow varying detection mods.[34,35,37,38] One example would be a switch from a liquid phase, containing a phosphate buffer to a buffer that is more volatile, such as trifluoro acetic acid, in order to enable analysis via methods such as ESI-HRMS.[33,35] This removal of salts may also be achieved by the insertion of a salt removing column in between the first- and second-dimension systems for loop and stop-flow interfaces.[34,35] A final method to remove issues with incompatible solvents is the use of a vacuum evaporation interface that uses heat and reduced pressure to remove solvents. Such a system may be used in cases of solvents that are entirely immiscible or lead to any type of reactions between solvent components and may even be applied in a switch from normal to reversed phase chromatography.[34,35]

If multiple regions in the first-dimension separation are of interest, a further issue arises in multidimensional LC. In this case the second-dimension separation needs to be repeated for each of

these regions, overall increasing the duration of the analysis. For such setups interfaces with parallel columns in the second-dimension have been developed, allowing several fractions to be handled at the same time, even allowing the use of different methods.[34] This application of parallel columns, however, necessitates the use of individual detectors that may cause inconsistent results due to slight differences between them.

Overall multidimensional LC further increases the versatility and efficiency of classic LC, but the complexity of the systems may prove detrimental to its application. Also, all these techniques may come with the drawback, that they potentially modify the analyte, thereby falsifying the results. For example, a large problem with vacuum evaporation is the loss of volatile compounds, whilst stop-flow methods may alter the chromatogram of a sample, as described above. Such considerations need to be taken into account when designing the overall method.

III.II LC-UV and DAD, the Analytical Standard

Whilst LC is one of the most common separation methods in pharmaceutical analysis, the most common detection method it is coupled to is UV/Vis spectroscopy, mostly shortened to UV spectroscopy. The use of this detection mode is so widespread that whenever someone mentions LC analysis without a specified detection mode, the use of UV spectroscopy is usually implied.[29,31,32,40]

UV/Vis spectroscopy uses light in the ultra violet and visible spectrum (160-2000 nm, depending on light source) to irradiate the analytes after separation. When a compound with absorption in this range of the electromagnetic spectrum passes through the detector, the change in intensity of the absorption is depicted in the chromatogram, resulting in individual peaks.[12,21,31,32] Basic UV/Vis detectors only analyze samples with very few selected wavelengths, bearing the risk of failing to detect compounds that absorb at different wavelengths, whereas diode-array detectors (DAD) irradiate the samples with repeated scans of a large range of the UV and visible spectrum, enabling the detection or distinction of more compounds.[7,32,41]

LC-UV spectroscopy is often used in assay and purity analysis to screen for impurities in excipients, APIs and drug formulations that may have formed or contaminated the sample during synthesis, production, or storage. By comparing the retention time and absorbed wavelengths of detected peaks to analytical reference standards, new impurities can hereby be detected. By comparing the integral of any peak to the integral of the corresponding standard with defined concentrations, quantitative statements can be made regarding the amount of analyte in the sample, that corresponds to that peak. Such quantitative information together with additional methods makes LC-UV suitable for long-term degradation and stability studies. If an impurity is known, the retention time, absorption, as well as an

analytical standard can easily and swiftly confirm the compound's identity with reasonable certainty and give information about the impurity's concentration.[19,21,41,42]

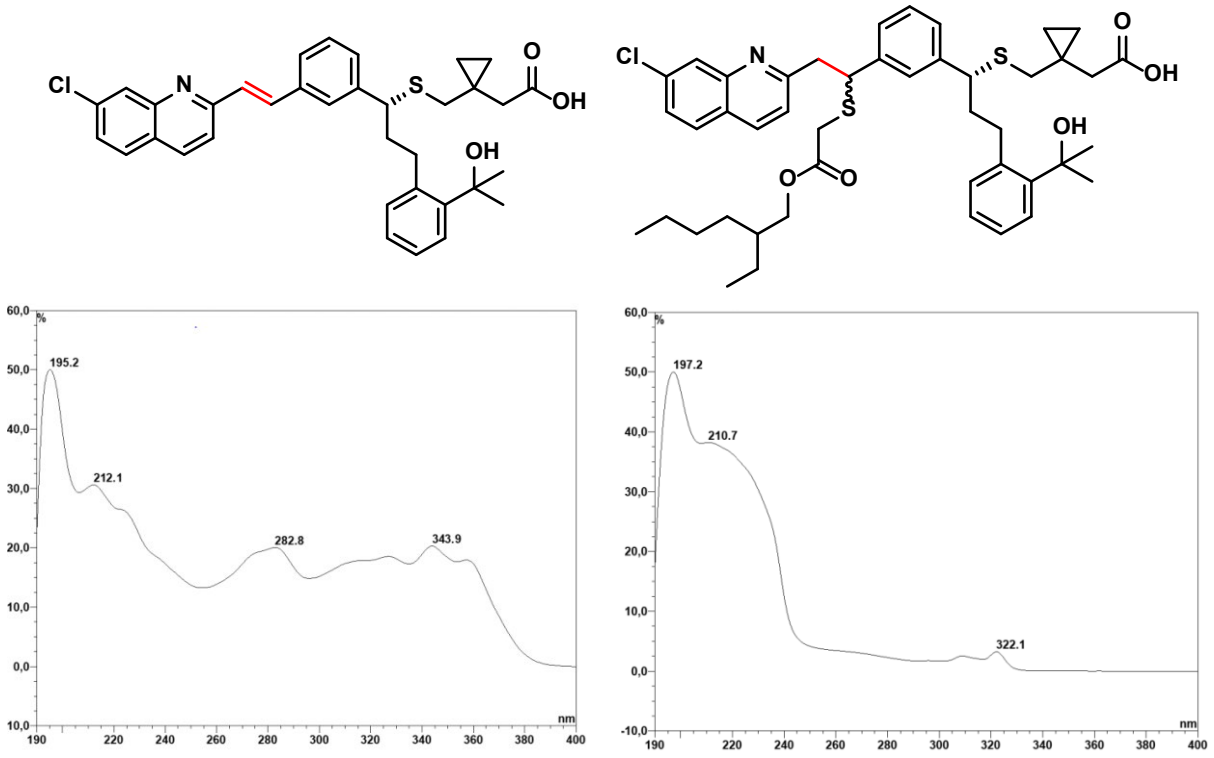

Figure 3. Molecular structure and UV spectrum of asthma medication Montelukast (left) and its degradation product caused by a thiol-ene addition (right). The addition to the double bond (red) decreases the connectivity of the chromophore system, leading to strong changes in the UV spectrum.[45]

If a previously unknown compound is detected, however, UV analysis can only give limited information, as LC-UV analysis provides no information on a compound's identity and absolute concentration, always requiring a reference.[15,19,42] The most structural information UV spectroscopy can provide about a degradation or reaction product of the analyte is whether a change to the chromophore system of a molecule has occurred, by comparing the UV spectrum to that of the analyte.[19] As such, Schmidt *et al.* found that a dimeric degradation product of the API Naloxone (Fig. 7) in an investigational medicinal product showed little to no change to its UV absorption compared to the original API. This led to the conclusion that the aromatic ring of the API had remained unchanged during degradation and that the reaction had occurred at a different location within the molecule. The nearly identical UV spectrum also indicated that the detected impurity was indeed a degradation product of Naloxone and not of an excipient.[43] On the other hand, Görög *et al.* found that different impurities of 3-oxosterioids could be easily distinguished from one another in their UV absorptions due to the π-system's sensitivity to changes (Fig. 4).[44] Schmidt *et al.* also found that a Michael-like, thiol-ene addition of a thioglycolate to the asthma medication Montelukast lead to a strong change in the UV absorption (Fig. 3). The

addition of the thioglycolate led to the removal of the double bond connecting the aromatic systems of the API, thereby severely altering the chromophore system.[45]

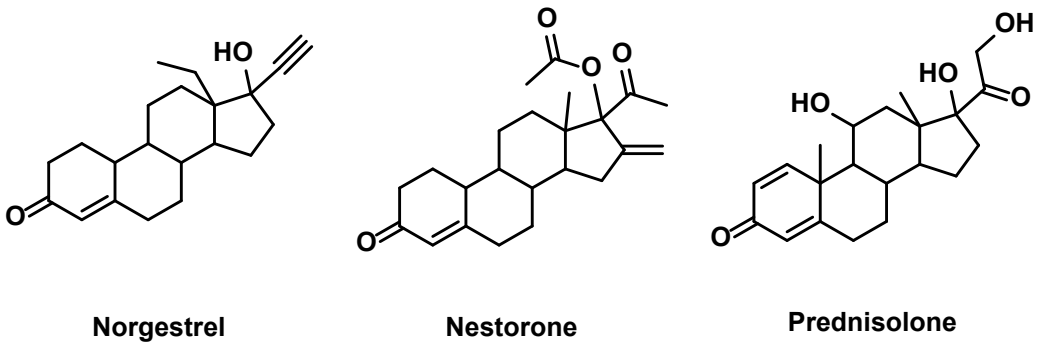

Figure 4. Molecular structures of the 3-oxosterioids Norgestrel, Nestorone and Prednisolone, analyzed by Görög *et al.* Variations to the ring system in impurities formed during synthesis or caused by oxidation lead to detectable variations in the UV spectra.[46]

Aside from gaining little structural information and the need for a reference substance, the prerequisite of needing compounds that absorb well within the UV and visible range is a further limitation of the method. As such, some compounds may only have a low UV sensitivity as pointed out by Pawellek *et al.* for Vigabatrin.[46] This may cause problems for effective impurity profiling and leads to the necessity of implementing alternative detection methods. Also, compounds that are not UV active cannot be analyzed by UV spectroscopy and may, in the worst case, go undetected during analysis. In the case described by Eckers *et al.* the widespread excipient polyethylene glycol (PEG) could not be detected by UV spectroscopy and coeluted with trace impurities contained within a formulation of the APIs Lamivudine and Zidovudine, as proven by mass spectrometry.[47]

There is also a risk of impurities with identical retention times coeluting during UV analysis and therefore going undiscovered. This is especially the case when only one or two UV traces are recorded, instead of using a DAD to measure a broader spectrum, which increases the likelihood, but is no guaranty for detection.[41]

Overall, LC-UV spectroscopy is still one of the most used analytical methods in pharmaceutical quality control due to its ease of use and reliability, but in many cases, especially involving structural questions and unknown compounds it must be supplemented by other detection and analytical methods.

III.III LC-MS

One such method often used in addition or replacement of LC-UV, especially when a new unknown substance is to be identified, is LC-MS.[48-51] LC-MS has become a widespread analytical method with the introduction of atmosphere pressure ionization, that strongly increased the ease of use.[50-52]

Many different types of MS setups exist with varying internal ionization and separation modes. In general, separation of ions according to their mass-to-charge ratio is achieved by using electric or magnetic fields. Ionization modes include hard ionization methods, that often lead to fragmentation of the molecule, and soft ionization methods that reduce or prevent fragmentation.[50,52] Not all types of ionization can be utilized for LC-MS however, with the main limiting factor being the technical requirements for the continuous transition of the material flow from the high-pressure environment of an LC to the vacuum of an MS. In modern, efficient setups this is achieved by ionization taking place at atmospheric pressure, excluding certain ionization methods.[50,52]

The first ionization method suitably fulfilling these requirements was electrospray ionization (ESI), which paved the way for the widespread use of LC-MS and still remains one of the most popular ionization methods for LC-MS.[50-52] Once created, the ions are separated and analyzed by a variety of methods. Many mass spectrometers use more than one separation method (MS/MS) to maximize the separation potential and to compensate for the drawbacks of individual methods.[50-53] More complex tandem mass spectrometers (MS^n) are also used, that combine different separation and fragmentation methods. This allows the combination of soft ionization methods, that provide the mass of the molecule ion, and fragmentation methods that provide ionized molecule fragments.[50,51,53] The table below provides a list of common ionization and separation methods used in LC-MS. It should be noted that only soft ionization methods can be coupled directly to LC and fragmentation methods can only be applied to LC-MS in MS^n systems (Table 1).[49-54]

Table 1. Common ionization methods and mass analyzers used in LC-MS.[49-54]

Ionization Methods			
Atmospheric Pressure Chemical Ionization (APCI)			
Mechanism	**Applications**	**Advantages**	**Limits**
- vaporization of the mobile phase via N_2 stream and heat (100 – 500 °C) - mobile phase vapor is ionized via an electron source - ionized vapor reacts with the sample	- thermally stable molecules - low to medium sized (< 1500 Da) molecules - low to medium polar molecules - volatile molecules (for thermal vaporization)	- efficient, soft ionization - No flow reduction from LC to MS required - few restrictions for solvents and reagents that can be used during LC	- limited use for high polar and ionic samples - unsuitable for large molecules (> 1500 Da)

molecules to create charged sample ions			
Atmospheric Pressure Photo Ionization (APPI)			
Mechanism	**Applications**	**Advantages**	**Limits**
- vaporization of the mobile phase via N_2 stream and heat (100 – 500 °C) - mobile phase vapor or dopant (if solvent cannot be ionized, mostly toluene or acetone) is ionized via a photon source - ionized vapor or dopant reacts with sample molecules to charged sample ions	- thermaly stable molecules - low to medium sized (< 1500 Da) molecules - non-polar to medium polar molecules - volatile molecules (for thermal vaporization)	- efficient, very soft ionization - no flow reduction from LC to MS required - few restrictions for solvents and reagents	- limited use for high polar and ionic samples - unsuitable for large molecules (> 1500 Da)
Electrospray Ionization (ESI)			
Mechanism	**Applications**	**Advantages**	**Limits**
- sample molecules must be previously ionized - samples and mobile phase are nebulized by a charged needle 3 to 5 kV) creating charged droplets - solvent is removed leaving the remaining charged sample	- thermally labile molecules - low to large sized molecules - medium to highly polar molecules - ionic or ionizable molecules (via chemical reactions such as acid or base reactions) - volatile or non-volatile molecules - formation of adduct-ions and ions with multiple charges possible	- very soft ionization - analysis of a wide range of molecule sizes - analysis of thermally labile molecules - analysis of non-volatile molecules, such as ionic samples	- limited use for non-polar molecules - flow reduction necessary - samples must be ionizable in solution - addition of reagents necessary for non-ionic samples - non-volatile reagents may clog the sampling needle over time - ionizable components in the mobile phase and the sample may compete with the ionization of the molecules of interest, lowering sensitivity
Mass Analyzers			
Time-Of-Flight (TOF)			
Mechanism	**Applications**	**Advantages**	**Limits**
- ions are accelerated by an electric field - the accelerated ions pass through a drift	- coupled to pulsed ionization methods or ion traps that can regulate the ion output	- very high mass range (> 100 000 mau) - determination of elemental formular possible	- requires a pulse of ions for analysis - no constant flow of samples possible

tube and strike a detector - the time of flight is used to calculate the ions *m/z* value - ions with lower *m/z* values reach higher velocities - resolution can be improved by a reflectron (electrostatic mirror) that diverts ions into a second drift tube	- molecules with very large sizes - samples containing many analytes	- improved resolution using a reflectron - high sensitivity - simultaneous measurement of a large mass range and a large number of ions	
Sector			
Mechanism	**Applications**	**Advantages**	**Limits**
- a set electric and/or magnetic field is used to divert the ions - according to the degree of the diversion the *m/z* value of the ions is determined - improved resolution by combining a electric and magnetic sector	- used to be the analytical standard and often serves as comparison for other mass analyzers - use has become less common	- high resolution - high sensitivity	- large and expensive - only certain mass ranges are measured at the same time - high vacuum required - difficult to couple with LC
Quadrupole Mass analyzer			
Mechanism	**Applications**	**Advantages**	**Limits**
- consists of four rods that are connected as parallel pairs - a radio frequency electric field is applied to each pair - by variation of the electric fields, only ions of certain *m/z* values can pass through the quadrupole - by variation of the electric field a range of ions can be analyzed - several quadrupoles can be combined (such as a triple quadrupole) to achieve not only	- mass range up to 4 000 mau - very common in LC-MS - triple quadrupole mass analyzers are used to gain a large amount of information for specific analytes of interest	- small and low cost - ease of use - excels at quantification - good selectivity	- limited mass range - lower sensitivity at higher *m/z* values - low resolution

separation but also fragmentation			
Quadrupole Ion Trap			
Mechanism	**Applications**	**Advantages**	**Limits**
- similar to the quadrupole mass analyzer - adds a third-dimension electrical field - the electrical fields change in a set radio frequency, trapping ions within the fields - ions are selectively ejected and analyzed - several variations exist: three-dimensional and linear quadrupole and cylindrical ion traps	- mass range up to 70 000 mau - can be used for fragmentation experiments - can be linked to other mass analyzers that require a pulsed ion source, such as TOF	- small and low cost - ease of automation - higher mass range than the standard quadrupole - drop off in sensitivity for larger ions lower than the standard quadrupole - good selectivity - fragmentation experiments possible	- limited mass range - low resolution (can be improved by applying slower radio-frequency voltage scan rates
Fourier-transform ion-cyclotron resonance (FT-ICR)			
Mechanism	**Applications**	**Advantages**	**Limits**
- ions are forced onto circular paths by a homogenous magnetic field - oscillation takes place with a cyclotron frequency inverse to the *m/z* value of the ion - the ions are excited by an oscillating magnetic frequency, expanding the circular radius - this circular motion is measured resulting in the ions *m/z* value	- samples containing many components - samples with high mass ranges - trace impurity analysis	- extremely high resolution - very high mass range (> 100 000 mau) - determination of elemental formular possible	- very bulky and high maintenance due to superconducting magnet - lower throughput possible
Orbitrap			
Mechanism	**Applications**	**Advantages**	**Limits**
- related to FT-ICR - consist of an outer barrel-like and an inner axial spindle electrode - the electrostatic field created by these	- samples containing many components - trace impurity analysis - mass range up to 6 000 mau	- very high resolution - determination of elemental formular possible - moderate spatial and maintenance cost requirements, as no	- limited mass range - limited ion capacity

electrodes force the ions to orbit and oscillate around the inner spindle - this harmonic oscillation occurs at a frequence proportional to the *m/z* value of the ion	superconducting magnet is required

Either positive or negative detection modes, or both simultaneously, can be selected for a mass spectrometer. These are capable of detecting either cations and anions of analytes, fragments thereof, or adducts consisting of analytes and ions contained within the sample.[50,52,53,55,56] Ions that form adducts may include, sodium cations, that are often present as trace impurities, or ions from reagents used in the LC part of the analysis such as ammonia, carbonate or trifluoro acetate.[48] The pH value of the mobile phase may also influence the ionization by either protonating or deprotonating molecules.[57]

These ions or adducts are detected with high accuracy and resolution, making MS a very sensitive detection mode, capable of analyzing trace impurities that could not be detected by UV analysis. This makes MS an ideal analytical method for sensitive cases, where even trace impurities may be detrimental to patients, such as the analysis of genotoxic or carcinogenic substances, like nitrosamines.[49-51,53,58,59] According to Eckers *et. all*, as mentioned above, LC-MS can also detect certain substances that are not detected by LC-UV due to a lack of a chromophore system, such as the widely used excipient PEG.[47] Furthermore, whilst UV analysis is incapable of detecting coeluting substances with similar UV absorptions (though DAD analysis may circumvent this issue), MS can detect several sample components at the same time. However, as also pointed out by Eckers *et. all*, highly concentrated analytes may lead to overload and overshadow the signals of coeluting substances.[47,50,51,53,58]

In addition to the accurate detection of substances, MS and high-resolution mass spectrometry (HRMS) in particular offers highly accurate information on the mass of detected ions for structural elucidation. HRMS is capable of providing a mass with an accuracy of 1-2 ppm.[50,51,53] In combination with multidimensional MS^n experiments, that provide detailed fragmentation patterns of molecules, this accuracy results in an array of information on the identity and structure of unknown analytes.[50,51,53,55] Using online databases and computational programs MS analysis may even provide molecular structures of analyzed compounds. As such, Neu *et. all*, where capable of identifying impurities in synthetic Thyroxine without the need of prior stress testing (Fig. 5).[60]

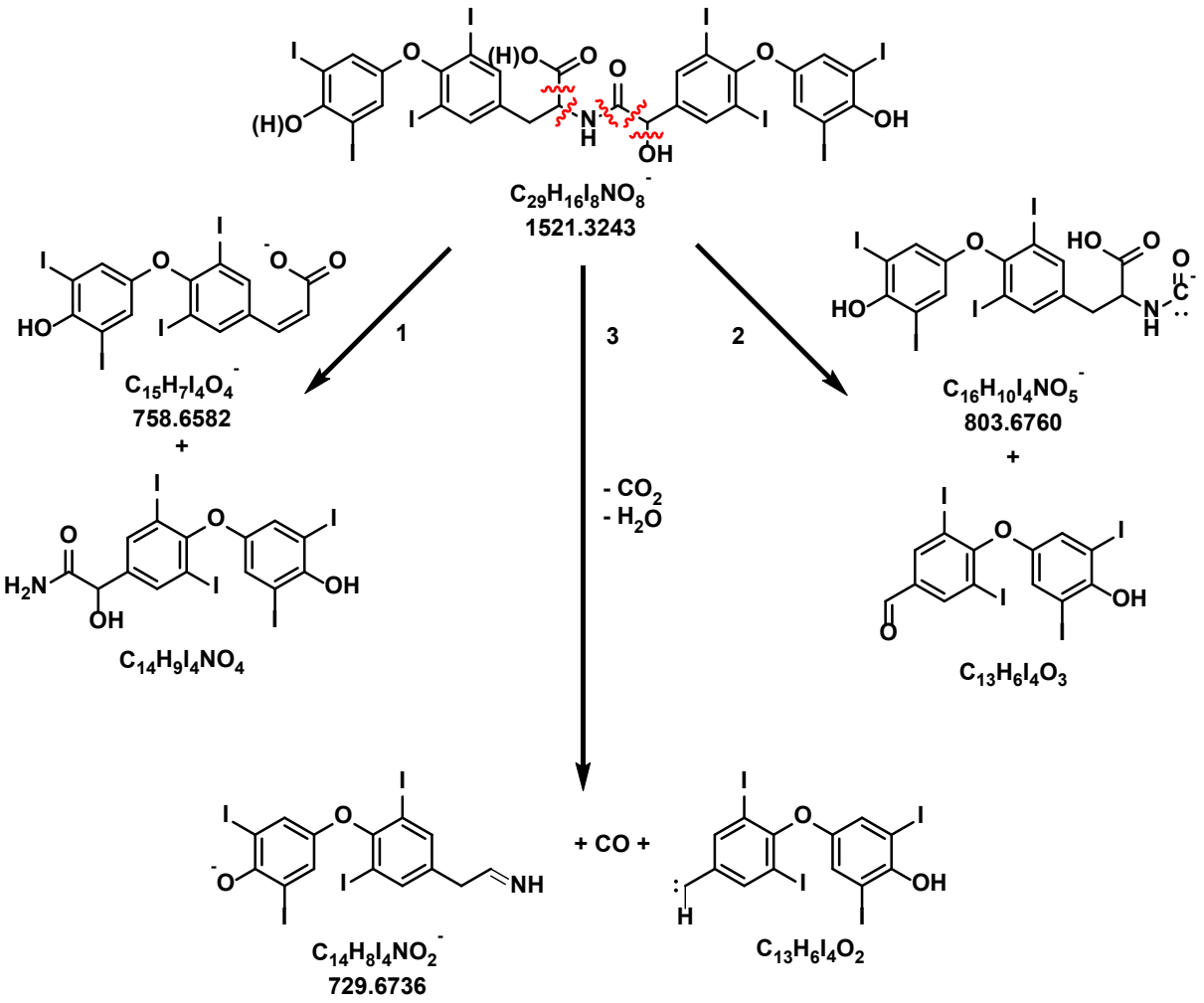

Figure 5. Fragmentation pattern of a dimeric impurity of Thyroxine depicting both the detected anionic fragments with their corresponding *m/z* values, as well as the proposed neutral fragments.[60]

A further method applied in MS analysis to gain information on the structure of an unknown analyte is hydrogen exchange mass spectrometry, using deuterated water or deuterium sulfide. The mass difference between hydrogen and deuterium gives information on the presence of functional groups with exchangeable protons.[52] Other modifications to molecules by reagents or the use of chemical ionization are also possible. These may help circumvent the drawback of MS requiring analytes that can be ionized. None the less, molecules that are not easily modified or ionized cannot be analyzed by LC-MS.[50,61,62]

A further drawback of LC-MS are the reagents that can be used in the LC separation. For mass spectrometry, samples must be transferred into the gas phase for analysis, excluding non-volatile additives such as phosphate, sulfate, borate and citrate buffers, as these are known to clog the ion source over time. Instead, volatile formate, acetate, carbonate, hydroxide and ammonia buffers must be used.[34,48,58,63] In some cases, the none-volatile additives may lead to a better LC separation than the volatile alternatives decreasing the quality of the separation or prolonging the overall method, when

switching to an MS method. Also, as LC-MS analysis is often derived from LC-UV analysis in research and development, this further prolongs the method development or limits the compatibility of methods.[48,57,58,63] Non the less LC-MS is a suitable method for both routine quality control and more specific cases such as structural elucidation of impurities or new drug candidates.

III.IV LC-Infrared and LC-Raman Spectroscopy

In the following section Infrared (IR) and Raman spectroscopy are discussed together, as both fall under the umbrella term of vibrational spectroscopy and rely on very similar technical setups. Both use electromagnetic radiation to excite different vibrational modes of each sample molecule. This leads to the scattering, absorption or wavelength change of the radiated light which can be measured to produce a fingerprint of the analyzed sample. Using this fingerprint, the identity of a sample or functional groups contained in the sample molecules can be determined, allowing both the identification of known and the analysis of unknown compounds. In case of IR spectroscopy light in the range of the near to far infrared spectrum is used, whilst Raman spectroscopy uses monochromatic lasers that usually fall into the range of the visible, near infrared or near ultraviolet light. [64,65,66]

The fast and mostly non-destructive application as well as the ease of use of these methods have made them strong tools in the identification of known substances as well as the characterization of new compounds.[64] Due to the excitation of different vibrational modes, IR and Raman spectroscopy are often used complementary to one another to cover a wider range of samples and increase the amount of information gathered for each compound.[65,66] If a known substance is detected in a sample, its specific IR or Raman fingerprint can be compared to a database of compounds, such as a database of APIs and common pharmaceutical excipients,[67] to determine its identity, or specific functional groups.[66] IR and Raman spectroscopy can also aid in the structural elucidation of unknown compounds by providing information on the functional groups present in a compound. For example, Fukutsu *et al.* used IR spectroscopy to detect certain structural elements within degradation products of the antibiotic Cefpodoxime proxetil, that helped verify structures previously proposed using mass spectrometry and NMR spectroscopy (Fig. 6).[68]

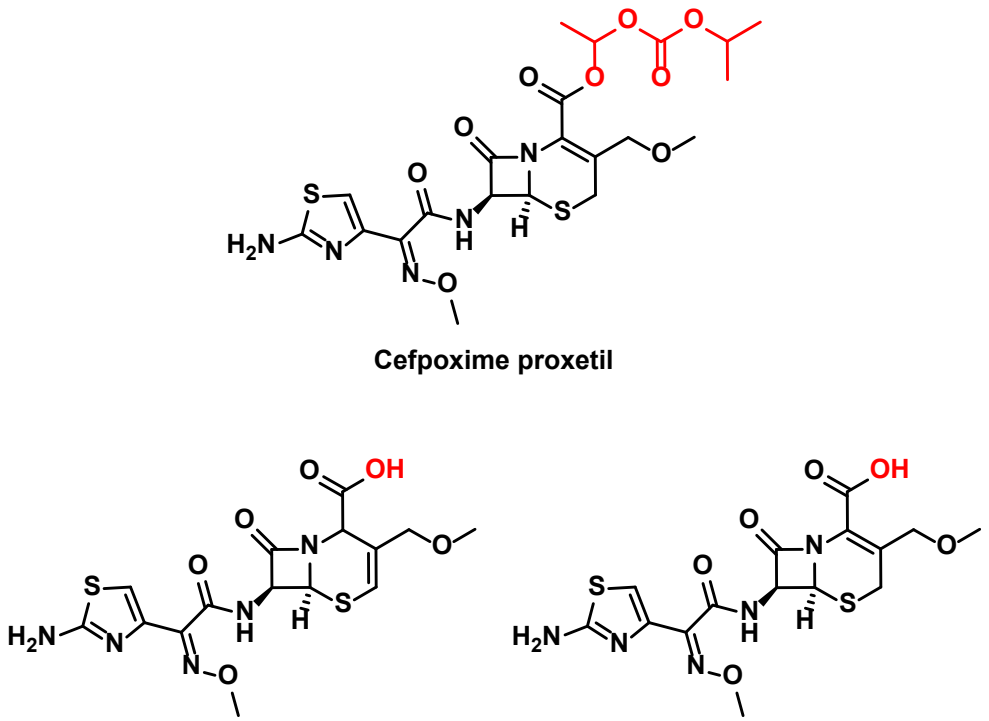

Figure 6. Molecular structures of Cefpoxime proxetil (top) and two of its degradation products (bottom). The replacement of the ester side chain (red) by OH groups leads to the appearance of a strong new signal around 3300 cm^{-1} in the IR spectrum.[68]

The major disadvantages of these two analytical methods, when coupling them with liquid chromatography, lie in their sensitivity. In the case of IR spectroscopy, its high sensitivity leads to issues relating to the mobile phase used during LC. Even more so than for UV spectroscopy, IR spectroscopy interacts with most solvents used during LC analysis, leading to absorption of the IR radiation.[69-71] Water especially leads to interference with the measurements, due to its strong IR absorbance, quickly overshadowing the signals from the analytes.[69,72,73] Due to weak Raman scattering, water causes less issues for Raman spectroscopy. However, the low sensitivity of Raman causes problems for the combination of Raman and LC, as the continuous flow during LC analysis only enables short measurement cycles, insufficient for Raman analysis.[72]

Despite these drawbacks, methods for coupling LC chromatography and vibrational spectroscopy have been developed, both off- and on-line.[70,71] During off-line analysis, the sample is measured after solvent removal. For this purpose, part of the effluent is split to a separate interface, where it is deposited onto a substrate and the solvent is removed, before IR measurement. Though this method eliminates the interference by solvents and, especially for the purpose of Raman measurements, allows extended measurements periods, there are several drawbacks to this approach.[70,71] Compared to an on-line approach, the set-up is more complex, time consuming, and the sample is no longer readily available for follow-up on-line measurements.[71] The time required to deposit sufficient sample amounts onto the substrate also limits the overall LC-method, as samples that elute in quick succession may end up being mixed on the sample holder. Also volatile samples may be lost during the solvent

removal process and uneven deposition of sample on the substrate may lead to complications, when quantitative measurements are desired.[71]

Progress in measurement and computational techniques have led to preferential use of on-line measurement techniques for both Raman and IR spectroscopy. To alleviate the issue of mobile-phase interference with IR spectroscopy, several approaches to subtract background spectra have been developed. In the case of an isocratic LC-method, a background spectrum with the specific solvent composition is measured in advance.[69,70] Gradient methods create a more complex situation. Interactions of individual solvents with one another or with reagents contained in the mobile-phase influence the measured spectra. At each point of the gradient method spectra are obtained, which can differ in signal intensities and individual signals detected. To account for this, gradient methods require several background measurements at different solvent compositions. Using these individual backgrounds, a mathematical matrix can be calculated that is then used as a background for the entire measurement.[69,70]

In the case of LC-Raman, the low sensitivity and resulting measurement time is the major drawback for on-line measurements, however, the possibility to perform measurements in aqueous solutions without interference is an important advantage compared to IR spectroscopy.[72-74] A basic approach to enable LC-Raman measurements is to reduce the volume of the used flow-cell in combination with a lowered LC-flow during the sections of interest. Hereby the sensitivity and measurement time can be increased.[74] This, however, leads to the need of additional considerations for the used LC-method, as the flow rate in particular has to be adjusted for the measurements.[69,71] A different approach to improving the measurement sensitivity is to increase the amount of collected data, by increasing the measurement distance of the Raman laser. This can be achieved by methods such as liquid-core waveguide (LCW), that use special optical capillaries that reflect the laser beam in order to increase the irradiation of the sample.[71-73] Another approach is the use of resonance Raman spectroscopy (RRS) that focuses on the excitation of the analytes Raman signals at specific wavelengths, while avoiding the resonance of the mobile phase. This fine tuning requires prior knowledge of the analyte, complicating the application. Also, any fluorescence by the analyte or impurities in the sample can easily overshadow the Raman signals, requiring suppression of fluorescence, or further fine tuning to avoid it.[71]

Overall, Raman and IR spectroscopy provide data that can be highly specific for structural elucidation and identification, especially by fingerprinting. However, the many considerations needed for the coupling to LC required for method developments and during measurements, as well as the required intensive knowledge of the measurement techniques, significantly reduce the popularity in scientific works.

III.V LC-NMR

The last analytical method covered in this article is NMR spectroscopy. In contrast to the other techniques, NMR spectroscopy is rarely used as a detection method and is mainly applied for identification and structural elucidation.[7,21] NMR spectroscopy uses strong, permanent magnetic fields in conjunction with radiofrequency pulses to excite the nuclei of a sample molecule. The NMR signals obtained are unique for each magnetically active nucleus and its chemical environment. Thus, the combined NMR spectra of a compound are like a fingerprint, allowing the unambiguous identification and structural characterization of the compound.[12,21,79]

Table 2. List of some the most common NMR experiments and the information they provide.[75-79]

NMR Experiment	Obtained Information
1D NMR (decoupled)	Chemical shifts of magnetically active nuclei (e.g. ^{1}H, ^{13}C, ^{15}N, ^{19}F, ^{31}P) without interaction with other magnetically active nuclei, information about the chemical environment of the observed nucleus
1D NMR (coupled)	Chemical shifts and coupling patterns of magnetically active nuclei (e.g. ^{13}C, ^{15}N, ^{19}F, ^{31}P), information about the chemical environment of the observed nucleus
COSY	Homonuclear correlation based on scalar coupling between nuclei (e.g. ^{1}H-^{1}H COSY), several variations thereof used
NOESY	Homonuclear correlation based on through space NOE interactions (e.g. ^{1}H-^{1}H NOESY)
EXSY	Homonuclear correlation based on chemical exchange (e.g. ^{1}H-^{1}H EXSY), information on dynamic phenomena
HSQC	Heteronuclear correlation based on one bond scalar coupling (e.g. ^{1}H-^{13}C, ^{1}H-^{15}N, ^{1}H-^{31}P HSQC)
HMBC	Heteronuclear correlation based on long range coupling over two or more bonds (^{1}H-^{13}C, ^{1}H-^{15}N, ^{1}H-^{31}P HMBC)

Both one- and two-dimensional NMR spectra and combinations thereof are used to identify and characterize chemical compounds.[12,17,21] In some cases, such as large biomolecules like proteins and enzymes, 3D experiments are also utilized.[21] A list of the most commonly used 1D and 2D experiments and the information they provide is listed below in Table 2.[75-79] Using smart combinations of these experiments and the data they provide, information on functional groups, connectivity, conformation, and stereochemistry, as well as the ratio of atoms in a sample molecule can be acquired.[12,17,21,79] Also,

by suppressing the Nuclear Overhauser Effect (NOE) during measurements, the quantification of different compounds in a mixture becomes possible – qNMR spectroscopy.[21,79,80]

The most common and easy to measure nucleus in NMR spectroscopy is the ^{1}H but other magnetically active isotopes such as ^{13}C, ^{15}N, ^{19}F and ^{31}P can also be detected. As many APIs and pharmaceutical excipients contain nuclei of this type, NMR spectroscopy is a useful tool in pharmaceutical analysis.[12,79] Similarly to MS, the quantitative information gained during NMR analysis is absolute. It requires no reference substance when interpreting obtained data for structural elucidation or identification of a sample, compared to methods such as UV analysis.[17,21,79,81] When quantitative analysis is required however, a defined internal standard is required. Overall NMR spectroscopy is a quasi-universal analytical method in pharmaceutical environments that is highly specific, non-destructive in regards to the investigated compounds, and measurements are independent of factors such as molecule size and chemistry.[79]

Despite its analytical strengths, NMR spectroscopy has certain drawbacks that cause unique challenges for pharmaceutical analysis. Compared to methods, such as UV and HRMS analysis, that can detect impurities in the nano and picomolar range respectively, NMR spectroscopy requires comparatively large amounts of sample around the millimolar range. This is especially the case when isotopes with lower abundance are measured or when the recording of 2D spectra is desired. As pharmaceutical analysis often deals with low-quantity impurities, NMR spectroscopy causes many challenges.[11,17,79] Through recent improvements of instrumental equipment, such as stronger magnets and more sensitive probes (e.g. cryoprobes), and measuring techniques, the sensitivity could be reduced to the nanomolar range.[11,17,21,79,82]

Another challenge of NMR spectroscopy may arise from its solvent requirements. As most solvents and reagents used in other pharmaceutical analysis are themselves NMR active, the use of their deuterated variants would be required.[17,79,81] Though there are cases of entire LC runs being performed with deuterated solvents, this method remains expensive when solvents aside of deuterated water are used and is therefore undesirable in routine pharmaceutical analysis.[17,81] Despite several advances in solvent suppression techniques, they are generally not sufficient for LC-NMR coupling when undeuterated solvents are used. However, solvent suppression may be useful in this area by removing the signals of residual solvent peaks, caused by incomplete deuteration of the solvent, or by suppressing water that has entered the solvent via moisture in the air.[17,79,81]

The need for deuterated solvents, together with the high equipment and maintenance costs of NMR instruments, such as the constant need for liquid helium and nitrogen to cool the superconducting magnet, make NMR spectroscopy a very expensive analytical method. A further aspect of NMR spectroscopy that needs to be considered is the personnel requirements. Recording and interpretation

of NMR spectra, especially for complex molecules require trained personnel making the technique less accessible for routine analysis.[15,79]

Despite its high operating cost and limitations, the analytical power of NMR spectroscopy in identifying unknown entities, as in some cases required by international pharmaceutical guidelines (ICH, FDA), has led to increased usage mainly during pharmaceutical product development as well as during routine stability studies. This triggered the development of several hyphenated LC methods, both on- and off-line.[17,21,79]

Some problems of on-line LC-NMR spectroscopy are similar to multidimensional LC and resulted in the development of similar solutions. Alongside sensitivity issues, LC hyphenation also introduces complications relating to measurement time. When measuring samples with a low concentration or when recording more complex 2D measurements or spectra of isotopes with a low natural abundance, the measurement time may increase up to several hours or in extreme cases even days.[7,11,15,79,81]

This sensitivity and time issue is the main reason why NMR spectroscopy is rarely used as a detector, none the less on-flow (or continuous flow) LC-NMR analysis methods exist, that directly couple the LC to the NMR flow probe. However, on-flow LC-NMR analysis requires high sample concentrations in the mmol/mL range, that may be difficult to achieve in purity analysis and even then, the analysis is usually limited to the 1D measurement of abundant isotopes such as ^{1}H and ^{19}F.[17,81-83] Despite its limited application, on-flow LC-NMR spectroscopy has the advantage of continuously recording spectra for all components of a sample, serving as a near-universal detection mode where other methods fail.[79,82]

To increase the time the sample remains in the NMR flow probe a further commonly applied technique is stop-flow LC-NMR spectroscopy. This method halts the LC separation when a peak of interest (usually determined by UV analysis) reaches the NMR flow probe. In theory, this allows unlimited time for the NMR measurement, allowing less sensitive and more time-consuming experiments, including 2D measurements and the analysis of less abundant isotopes.[17,81-83] The halting of the LC separation may, however, lead to certain issues as also mentioned in the multidimensional LC section of this review. For example, the prolonged time that samples remain on the column may cause sensitive compounds to decompose over time, falsifying the results of the analysis. Also, the stopping of the LC-flow, especially in cases where more than one component is to be analyzed by NMR spectroscopy may result in a loss of separation quality. Specifically, the repeated stopping of the flow can result in ghost peaks and peak broadening.[81-83] Finally, a limitation of stop-flow LC-NMR spectroscopy is that the amount of sample available for analysis is limited to the sample concentration present in a single LC run, once again favoring higher concentrations for better results.[17,81,82]

An evolution of stop-flow LC-NMR analysis is the application of loop collection. Instead of stopping the flow for each measurement, this method redirects peaks of interest into individual capillaries for follow-up NMR analysis separate from the LC activities. This eliminates issues regarding separation quality, but limitations such as sample concentration and stability remain.[17,81,83] To avoid decomposition of samples during the storage within the loop, some loop collection models allow the detachment of filled capillaries for storage under cooled conditions, with its own possible issues. This method allows prolonged storage followed by off-line NMR analysis.[17,81,82]

All these on-line LC-NMR methods share a common draw back in regard to the applied solvents and reagents. As samples are obtained directly from the LC-flow, conditions suitable for NMR analysis have to be chosen. Some reagents may cause NMR signals with chemical shifts identical to those of the sample, leading to overlap and a loss of information. Also, these LC-NMR methods require the use of expensive deuterated solvents during the LC separation. Improvements in solvent suppression methods may alleviate this issue, however certain complications can arise, especially in the case of on-flow LC-NMR spectroscopy. Solvent suppression requires the targeting of the chemical shift of the specific solvent's signals. As these are not fixed, but change with the solvent composition, gradient methods require constant adaption. In the case of stop-flow and loop collection, premeasurements can be performed to determine the solvent's chemical shift. Due to the continuous nature of the on-flow LC-NMR analysis such measurements cannot be performed.[17,79,82]

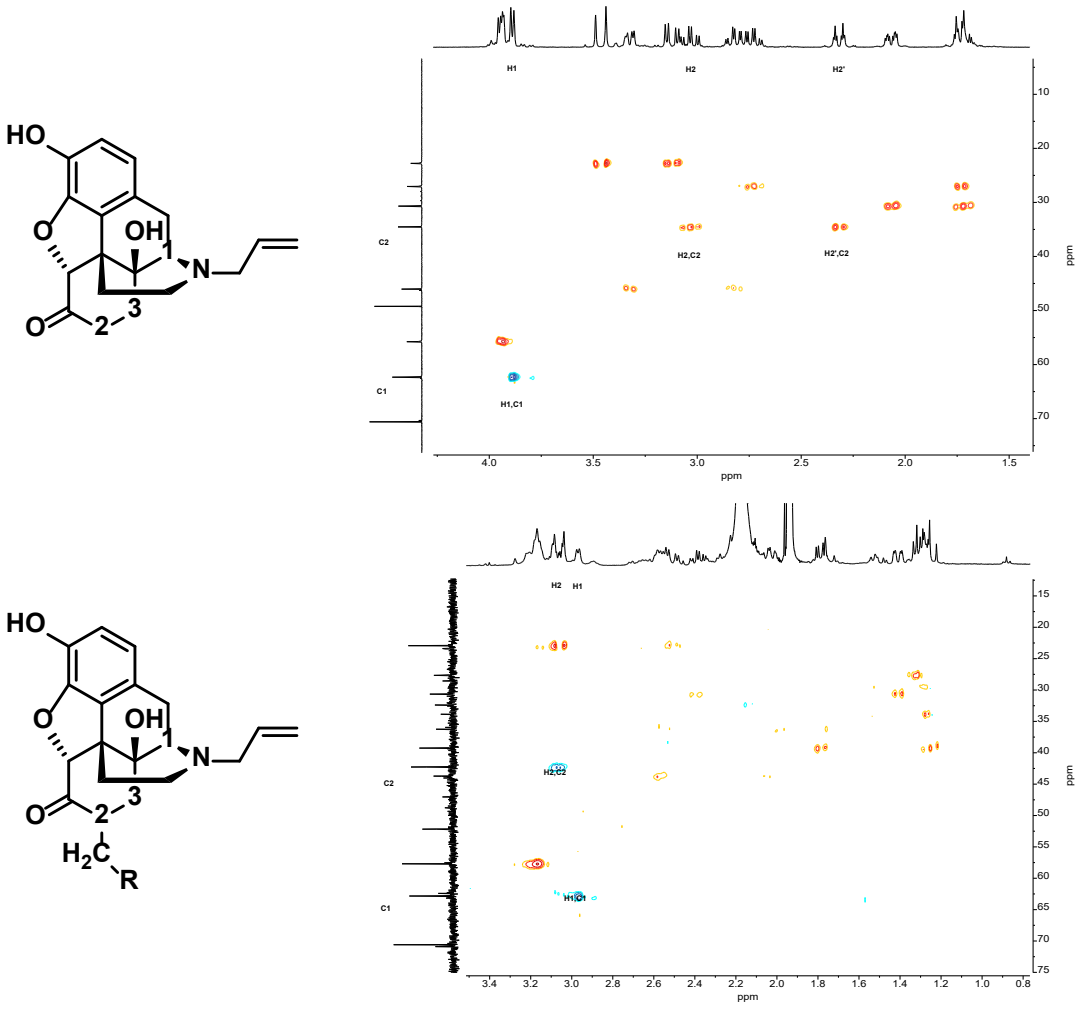

Figure 7. Comparison of a section of the ^{1}H-^{13}C HSQC spectra of Naloxone (above) and a dimeric Naloxone impurity (below), with R representing a second Naloxone unit. ^{1}H-^{13}C HSQC spectra depict the correlation between carbon atoms and their attached protons, with the phase for CH_2 groups depicted in orange and for CH and CH_3 groups depicted in blue. Compared to the spectrum of the API, an additional CH group to the signal originating of the carbon marked as **1** can be observed in the aliphatic region with the signal of the CH_2 group originating from **2** disappearing. Hereby the location of the bridging methylene group could be confirmed at position **2** as its signal had changed from a CH_2 to a CH group.[43]

Classically, the way to avoid issues relating to solvents after LC separation is the use of preparative LC, however this still has the disadvantage of the isolated samples containing non-volatile reagents used in the LC mobile phase. Also, samples have to be stable during the removal of solvents.[79] A hyphenated method to avoid these drawbacks is the use of solid-phase extraction (SPE). During SPE, components of interest are trapped on cartridges. This process can be performed for several components within one run and may be repeated for several consecutive runs.[17,79,82,83] Hereby components of interest can be enriched on individual SPE cartridges, enabling the collection of larger amounts of analyte even with samples of low concentration.[17,79,82] Samples trapped this way can also be washed and dried, removing both reagents and solvents from the LC mobile phase. The enriched and purified sample is then eluted into NMR capillaries using strong eluting, deuterated solvents, such as methanol or acetonitrile.[17,79]

As a sample of interest can be stored on several cartridges and then pooled together in the NMR tube, pure samples of high concentration can be obtained, with the only limiting factors being sample stability, instrument availability and the run time of the LC method.[17,79,82]

Using SPE Schmidt *et al.* isolated sufficient amounts of analyte for complete NMR characterization from a sample solution containing a dimeric impurity of the opioid antagonist Naloxone. Previous HRMS experiments had suggested a dimeric structure with a methylene bridge connecting the two Naloxone units. Using 2D experiments the structure was confirmed and the position of the methylene bridge was determined (Fig. 7 and 8).[43]

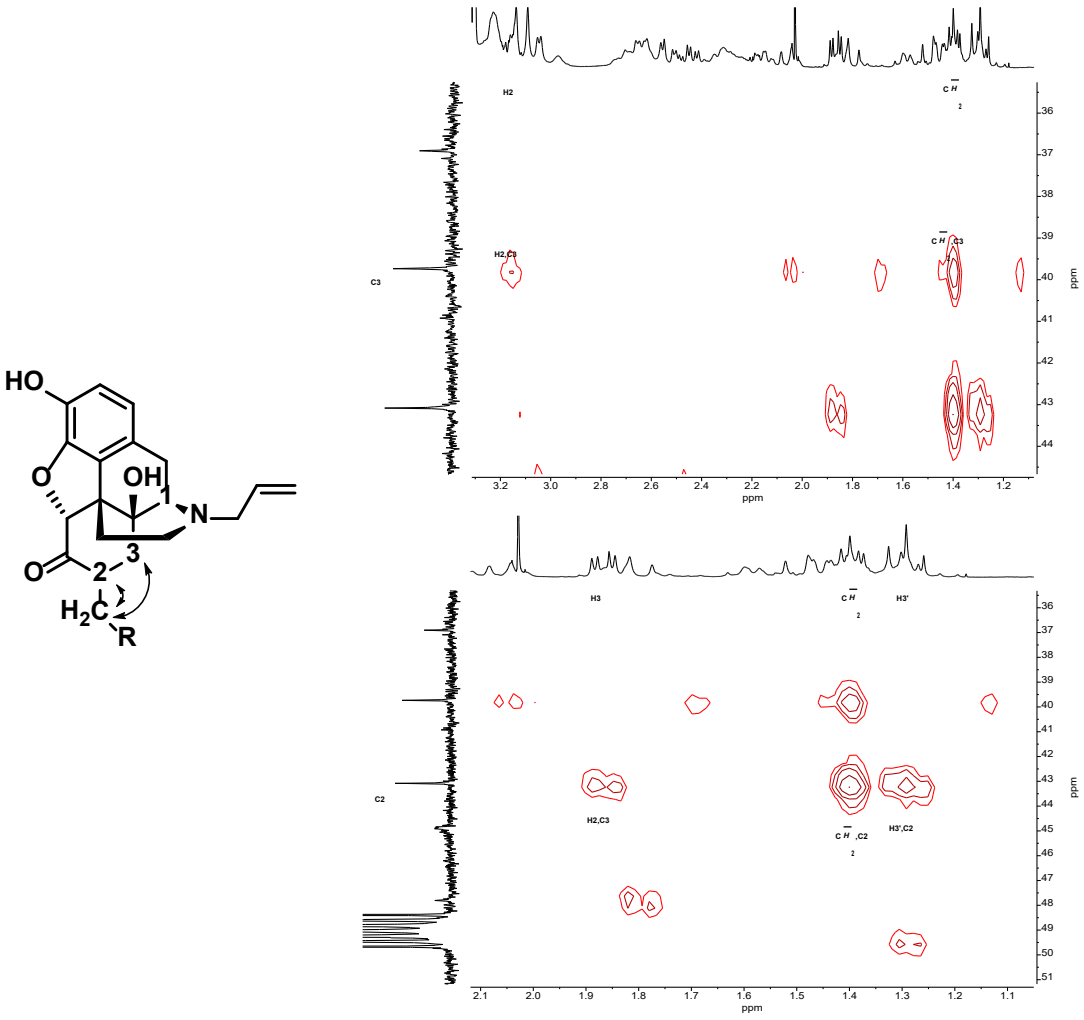

Figure 8. Sections of the ^{1}H-^{13}C HMBC of a dimeric Naloxone impurity showing the correlations between the carbons marked as **2** and **3** with the protons of the bridging methylene group used amongst other signals to confirm the location of the methylene bridge by Schmidt *et al.*[43]

III.VI Complex LC-Hyphenated Systems

In the following chapter, examples are provided of the previously mentioned analysis methods used in conjunction in more complex hyphenated LC system setups. Hereby we intend to highlight the advantages these systems provide by combining the different strong points of each method, thereby compensating for weaknesses. However, we also demonstrate the challenges that arise by these combinations, e.g. caused by the need to create one single method that is compatible with all analytical techniques.

The use of such systems, which combine several analytical modes, provides many advantages. For one, the combination of different detection modes ensures a more comprehensive analysis of a sample, reducing the risk of sample components going undetected. Additionally, the combination of different analytical modes provides a wider range of data that expedites and makes the identification and/or structural elucidation of a sample compound easier and more conclusive. By combining these methods into a hyphenated system, detection and data acquisition is streamlined, saving both time and material, as all necessary information can be obtained from one single sample. This makes the use of multicomponent hyphenated systems especially interesting in areas, where comprehensive data must be acquired from little sample in as short a time as possible, such as impurity analysis.[84] The reduced material requirements may even enable the identification of impurities solely from samples of the medicinal product batch in question. This eliminates the need for extensive and time-consuming stress tests in order to acquire the amount of sample, that would be necessary when each analytical step is performed by itself.[84]

Though examples in literature exist, the complete structural elucidation of an unknown impurity from a medicinal product by itself is still rather uncommon.[85,86] However, two areas of pharmaceutical analysis where complex hyphenated systems are commonly used are the identification of potential drug candidates in plant extracts and in metabolomics.[87-96] As this review focuses on pharmaceutical analysis in product development, routine and stability testing, the following paragraphs will mainly present examples from this area

In multicomponent hyphenated systems, UV/Vis or DAD are usually used mainly for detection purposes. As LC-UV is one of the most widespread analytical methods in routine pharmaceutical quality control, LC-UV methods often serve as the basis for further method development, when adapting to the expanded hyphenated system, that additionally use modes such as MS or NMR.[29,31,32,40] The wide range of applicability, ease of use and high sensitivity, resulting in low sample consumption during method development, make LC-UV ideal for adapting the method for compatibility with other analytical modes and to improve qualities such as separation or LC run time. As mentioned above in the LC-UV section, first bits of information can be acquired about a sample in some cases, like the origin

of the impurity, by comparing the obtained DAD spectra to those of known components of the analyzed medicinal product, such as the API or excipients.[19] In the formerly mentioned example by Schmidt *et al.* a thiol-ene addition to the double bond of the asthma medication Montelukast (Fig. 3) lead to a strong change in UV absorption in the area around 240 to 380 nm by severing the conjugation between Montelukast's two phenyl rings.[45] Also, Pan *et al.* found a red shift in the degradation product of the Parkinson's medication TCH346 caused by an expansion of the conjugated system by replacing a methylene bridged amino group by an aldehyde group (Fig. 9).[97] Though these observations give indications for a change in the chromophore system and may provide clues where and how a molecule was modified, further analytical methods have to be applied, as UV data alone is insufficient for structural elucidation.

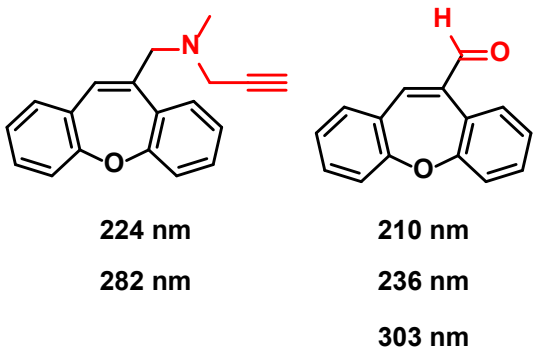

Figure 9. Comparison of the major UV absorption bands of TCH346 (left) and the impurity (right) analyzed by Pan *et. al.*[97]

Whilst LC-UV serves mainly as detection method,[29,31,32,40] LC-MS provides more extensive data for identification or characterization of samples. In some cases, this acquired data is already sufficient to identify impurities.[60] One such case is the degradation product of the pain killer Flurbiprofen and the excipient PEG which form an array of mono and diesters with varying size due to the different chain lengths of PEG (Fig. 10).[84] In this case MS data is sufficient to infer the structure of the impurity, as an esterification reaction between PEG and Flurbiprofen, with unambiguous products can be assumed.[84] LC-MS also serves as an additional detection method to cover substances that cannot be detected by LC-UV as they are not UV active.[49-51] Such substances may include small molecules like certain nitrosamines or as mentioned above, excipients like PEG that do not contain chromophore systems.[47] Like LC-UV, LC-MS requires only small amounts of substance, enabling detection and identification of trace amounts of sample, without the need for enrichment.[19,21,49-51] This makes these two methods in combination extremely effective and time efficient, as there is no need for extensive degradation experiments for identification. Due to this, LC-UV and LC-MS are the most widespread used LC analytical methods used in pharmaceutical analysis.[29,31,32,50-52]

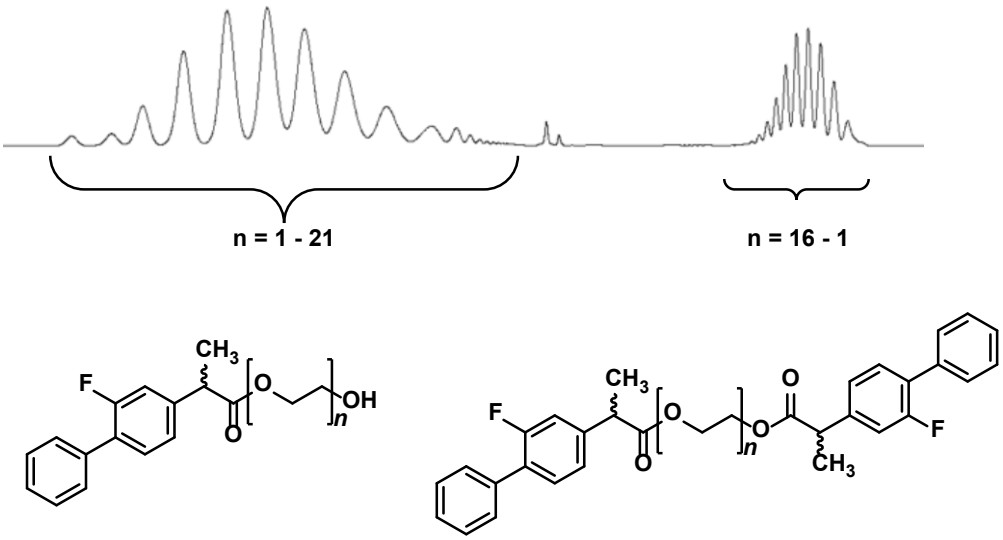

Figure 10. UV chromatogram of two Flurbiprofen-PEG mono- (left) and diester (right) impurities with varying chain lengths. The numbers beneath the chromatogram depict which chain lengths were detected during HRMS analysis.[84]

Of course, despite the advantages of the combination of LC-UV and LC-MS certain drawbacks exist. Adaption to LC-MS methods requires certain considerations.[48,57,58] As substances must be present in cationic or ionic state for detection via LC-MS, agents such as acids or bases are usually added to the mobile phases to ionize substances.[48,58,63] Depending on the required pH value this may lead to the exclusion of certain columns that may be sensitive to acid, limiting the options during method development and in some cases necessitating the change of the column when adapting to the combined LC-UV-MS method. The change of the pH value may also lead to a change of retention time and possibly even switching the order of elution of substances. Also, substances that cannot be ionized cannot be detected by LC-MS. In the former mentioned case of Pan *et. al.* both these observations were made.[97] As different pH values were applied in the LC method in order to ionize the unknown impurity, the retention time of the impurity remained nearly consistent at 11 min, whilst the API's retention time shifted between 5 and 13 min. The unknown impurity could however not be ionized and remained undetectable in LC-MS both in acidic and basic conditions.[97] Lastly, there are cases where even the most extensive MS data, including molecule size, fragmentation patterns, chemical formula, and knowledge of the impurity source may not suffice for structural elucidation. This is especially the case when several constitutional isomers exist. For the case of the thiol-ene reaction of Montelukast, an addition to either end of the double bond is possible and though the consideration of transitional states in the reaction may give indications to the final product, an unambiguous identification was only possible *via* 1D and 2D NMR experiments (Fig. 11).[45]

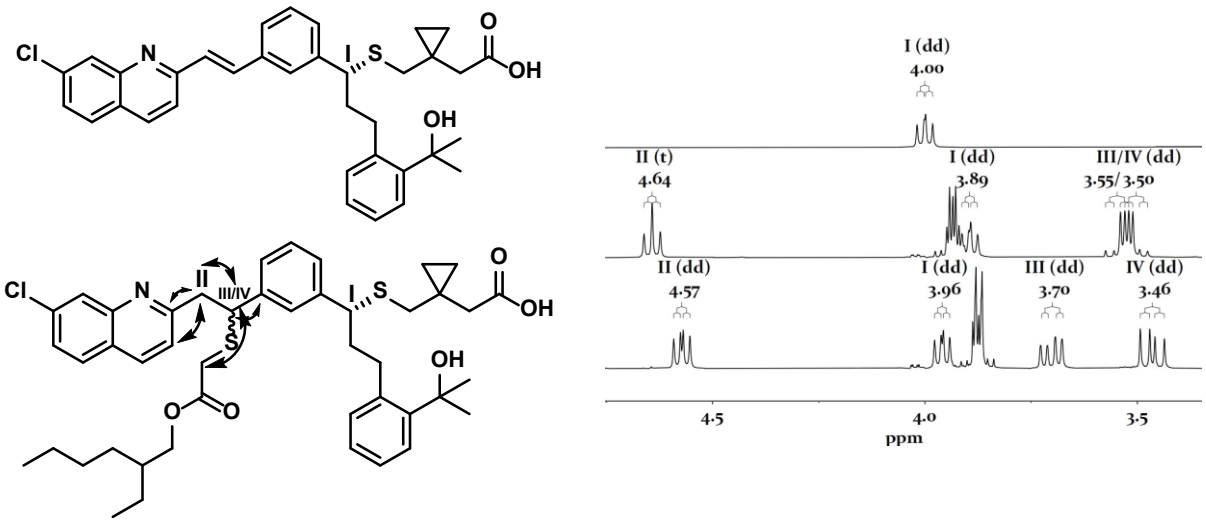

Figure 11. Chemical structures of the asthma medication Montelukast (top-left) and an impurity formed by addition of a thioglycolate (bottom-left). The arrows (bottom-left) depict which correlations between carbons and protons were observed in the ^{1}H-^{13}C HMBC NMR spectra. The right depicts a section of the aliphatic region of the ^{1}H NMR spectra of Montelukast (top-right) and the two stereo isomers of the impurity (middle- and bottom-right) as well of the spin systems of the protons. The protons (II, III and IV) introduced by the thiol-ene addition to the double bond of Montelukast can be clearly observed in the impurities.[45]

Methods such as NMR spectroscopy provide additional information on constitution and connectivity that cannot be obtained via LC-MS. Where applicable, NMR spectroscopy provides the most extensive information on a sample molecule and, if the adequate experiments are chosen leads to the unambiguous identification of an analyte. In the case of Kesting *et al.* HRMS and NMR data were used in conjunction to identify three adulterants in preparations of Chinese herbal medication.[98] Here HRMS data served to obtain a molecular formular that could be compared with literature to identify possible API candidates. In a following step SPE was used to collect the compounds of interest and confirm their identity by NMR analysis. For the structural elucidation ^{1}H NMR data were collected for all three compounds and additional 2D experiments were performed for the third adulterant that had the highest concentration.[98] Similarly, Murakami *et al.* identified three degradation products of the pain killer Loxoprofen in adhesive tapes by MS and NMR analysis (Fig. 12).[99] Here MS data, including fragmentation experiments and H/D exchange experiments served to provide information on molecular formulas, functional groups and chemical behavior. In addition, a cell for pressurized liquid extraction was coupled to an SPE unit to isolate the impurities of interest which were then identified by ^{1}H NMR analysis via a loop collection LC-NMR device.[99]

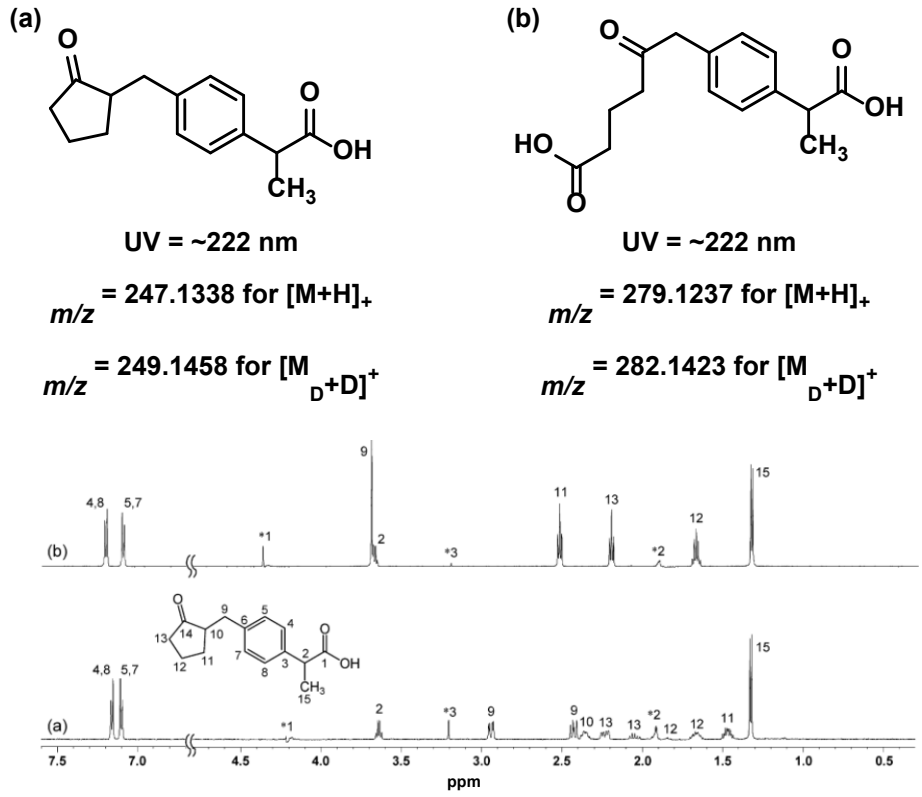

Figure 12. Selected UV, HRMS, H/D exchange HRMS and ^{1}H NMR data of Loxoprofen (a) and one of three of its impurities (b) described by Murakami *et al*.[99]

In both these cases SPE was used for isolation of compounds prior to NMR analysis.[98,99] Due to the ability to enrich compounds of interest on SPE cartridges and purify them in a follow-up step, SPE is one of the most useful tools for LC-NMR analysis. Also, as the mobile phase of the LC separation is removed on the SPE cartridge, the amount of deuterated solvent required in this procedure is reduced, as there is no need to run the LC method using deuterated solvents allowing an easier combination with other analytical methods such as LV-UV and MS.[17,53,79,82] However, SPE requires certain considerations. In particular, it is necessary to optimize the conditions for the trapping on the cartridges. This can be achieved by choosing cartridge types that optimally retain the peak of interest and by adjusting the quantity and composition of the make-up flow, e.g. the eluent that is added when trapping a substance of interest on the SPE cartridge. In both above-mentioned cases, pre-tests were performed to improve the SPE retention.[97,98] In some cases, these tests may prove trivial, whilst in others they may become more complex. In the case of Schmidt et al. the isolation of three methylene bridged dimers of the opioid antagonist Naloxone (Fig. 7) onto SPE cartridges required several adjustments for optimization.[43] The use of different types of cartridges with varying polarity or ion exchange properties proved insufficient for the isolation. The retention was finally optimized by addition of a basic buffer to the make-up flow which served to convert the impurities to their neutral state, thereby decreasing polarity and improving retention on a nonpolar cartridge.[43] Though the combination of UV, MS and NMR analysis provides data for the unambiguous identification of

impurities, the high amounts of substance required for NMR analysis still proves challenging when analyzing a sample directly obtained from a medical product. As shown by the above examples, even when successfully isolated from a medical product, LC-SPE-NMR analysis often only provides sample amounts sufficient for ^{1}H NMR data.[43,97,98] However, in the case of Schmidt et al. it was shown that isolation and complete structural elucidation including 2D NMR spectra can be performed directly from medical products containing as little as 0.016 % impurity.[84] In this article, eighteen different samples of the above mentioned Flurbiprofen-PEG mono- and diesters (Fig. 10) were isolated and identified from extracts of Flurbiprofen Lozenges. Using an HPLC-DAD-HRMS/SPE-NMR system data for the unambiguous structural elucidation of the individual esters, including COSY, HSQC and in many cases also HMBC data could be obtained.[84]

In most cases, the methods mentioned up to this point are sufficient for complete structural elucidation, however, the use of vibrational spectroscopy can provide additional information that may prove helpful in the identification process and further strengthen conclusions drawn from data. In the case of Storalzyk et al. a degradation product of the breast cancer medication Exemestane was identified by MS and NMR analysis in stressed samples of the API.[55] In this case, IR spectroscopy was used additionally, providing data that further supported the proposed structure. Specifically, the presence of a hydroxyl group, that had replaced a keto group during degradation could be confirmed by IR spectroscopy.[55] It should be noted that this example serves to highlight the use of addition IR analysis but does not constitute a case of a complex LC-IR hyphenated system.

IV Conclusion

Overall, LC hyphenated systems are widely used in many areas of the pharmaceutical industry from the discovery and characterization of new drug candidates over product development to routine screenings and quality control. Especially “simple” hyphenated systems such as LC-UV or LC-MS have continuously grown in popularity in all these areas since their conception due to their high sensitivity and ease of use. Methods such as LC-IR and LC-RS on the other hand remain less popular due to their limitations and the knowledge required for the measurements and data interpretation. Similarly, LC-NMR is not as widespread in many areas of pharmaceutical analysis, despite the breadth of data it provides. Here the relatively large amounts of sample in the millimolar range required, as well as the necessity for deuterated solvents are the limiting factors. However, the introduction of solid-phase extraction has vastly improved the popularity and applicability of LC-NMR analysis as it eliminates or reduces most of these issues.

Whilst the use of more complex hyphenated LC systems that go beyond simple LC-UV-MS systems such as LC-UV-MS/SPE-NMR are growing in popularity in areas such as the analysis of plant extracts or metabolomics, they are still rather uncommon in impurity analysis and quality control. Here LC-UV and LC-MS are still the most widespread analytical methods, with NMR analysis mainly performed on samples acquired from artificially synthesized impurities after extensive degradation experiments. A few recent examples however have shown that measuring techniques have progressed enough to enable LC-NMR analysis directly from medicinal samples. This would enable the use of hyphenated LC systems that combine effective detection modes such as UV and IR spectroscopy with powerful analytical methods such as MS spectrometry and NMR spectroscopy in quality control. This would save both time and money and help ensure the availability and safety of medication.

Conflict of Interest

The authors declare that there is no conflict of interest.

Declaration of Interest

None.

Author Agreement

The manuscript was written through contributions of all authors. All authors have given approval to the final version of the manuscript.

References

1. International Conference on Harmonization (ICH) guidelines. Impurities in new Drug Substances Q3A (R2), October 2006.
2. International Conference on Harmonization (ICH) guidelines. Impurities in new Drug Products Q3B (R2), June 2006.
3. International Conference on Harmonization (ICH) Guidance for Industry. Impurities in new Drug Substances Q3A (R2), June 2008.
4. International Conference on Harmonization (ICH) Guidance for Industry. Impurities in new Drug Products Q3B (R2), August 2006.

5. International Conference on Harmonization (ICH) guidelines. Impurities: guideline for residual solvents Q3C (R8), August 2022.
6. International Conference on Harmonization (ICH) guidelines. On elemental impurities Q3D (R2), May 2022.
7. Ahuja SS. Assuring quality of drugs by monitoring impurities. Adv Drug Deliv Rev 2007;59:3–11.
8. Ayre A, Varpe D, Nayak R, Vasa N. Impurity Profiling of Pharmaceuticals. ARPB 2011;1(2):76–90.
9. International Conference on Harmonization (ICH) Guidance for Industry. Impurities: Guidelines for Residual Solvents Q3C (R8), December 2021.
10. FDA Guidance for Industry: ANA's: Impurities in Drug Products; November 2010.
11. Pan C, Liu F, Motto M. Identification of Pharmaceutical Impurities in Formulated Dosage Forms. J Pharm Sci 2011;100(4):1228–1259.
12. Pilaniya K, Chandrawanshi HK, Pilaniya U, Manchandani P, Jain P, Singh N. Recent trends in the impurity profile of pharmaceuticals. J Adv Pharm Tech Res 2010;1(3):302–310.
13. Bari SB, Kadam BR, Jaiswal YS, Shirkhedkar AA. Impurity profile: Significance in Active Pharmaceutical Ingredient. Eurasian J Anal Chem 2007;2:32–53.
14. Ambhore JP, Adhao VS, Cheke RS, Popat RR, Gandhi SJ. Futuristic review on progress in force degradation studies and stability indicating assay method for some antiviral drugs. GSCBPS 2021;16:133–149.
15. Görög S. New safe medicines faster: the role of analytical chemistry. TRAC 2003;22(7+8):407–415.
16. Görög S. The importance and challenges of impurity profiling in modern pharmaceutical analysis. TRAC 2006;25(8):755–757.
17. Singh S, Handa T, Narayanam M, Sahu A, Junwal M, Shah RP. A critical review on the use of modern sophisticated hyphenated tools in the characterization of impurities and degradation products. J Pharm Biomed 2012;69:148–173.
18. International Conference on Harmonization (ICH) specification. Test procedures and acceptance criteria for new drug substances and new drug products: chemical substances – Scientific guideline Q6A, May 2000
19. Görög S, Babják M, Balogh G, Brlik J, Csehi A, Dravecz F, Gazdag M, Horváth P, Laukó A, Varga K. Drug impurity profiling strategies. Talanta 1997;44:1517–1526.
20. Jain D, Basniwal PK. Forced degradation and impurity profiling: Recent trends in analytical perspectives. J Pharm Biomed Anal 2013;86:11–35.

21. Kamboj S, Kamboj N, Rawal RK, Thakkar A, Bhardwaj TR. A Compendium of Techniques for the Analysis of Pharmaceutical Impurities. Curr Pharm Anal 2014;10(2):145–160.
22. Landge AK, Deshmukh VK, Chaudhari SR. Impurities in Pharmaceuticals- A Review. Current Pharma Research 2013;4(1):1105–1116.
23. Beg S, Hasnain MS, Rahman M, Swain S. Chapter 1 – Introduction to Quality by Design (QbD): Fundamentals, Principles, and Applications. In: Beg S, Hasnain MS, editors. Pharmaceutical Quality by Design. Academic Press; 2019, p. 1–17.
24. Mishra V, Thakur S, Patil A, Shukla A. Quality by design (QbD) approaches in current pharmaceutical set-up. Expert Opin Drug Deliv 2018;15(8):737–758.
25. Baertschi SW, Alsante KM, Reed RA. Pharmaceutical Stress Testing. 2nd ed. Boca Raton: CRC Press; 2011.
26. Singh S, Bakshi M. Guidance on Conduct of Stress Tests to Determine Inherent Stability of Drugs. Mat Sci 2000;24:1–14.
27. Hirschfeld T. The Hy-phen-ated Methods. Anal Chem 1980;52(2):297A–312A.
28. Colin H, Guiochon G. Introduction to reversed-phase high-performance liquid chromatography. J. Chromatogr. 1977;141:289–312.
29. Gupta MK, Ghuge A, Parab M, AL-Refaei Y, Khandare A, Dand N, Waghmare N. A comprehensive review on High-Performance Liquid Chromatography (HPLC), Ultra Performance Liquid Chromatography (UPLC) & High-Performance Thin Layer Chromatography (HPTLC) with current updates. Curr Issues Pharm Med Sci 2022;35(4):224–228.
30. Patel K, Patel D, Panchal D, Patel K, Upadhyay U. A Review on High Performance liquid Chromatography. IJCRT 2022;10(10):2320–2882.
31. Ali AH. High-Performance Liquid Chromatography (HPLC): A review. Ann Adv Chem 2022;6:10–20
32. Sudev S, Janardhanan SV. Review on HPLC Method Development Validation and Optimization. Int J Pharm Sci Rev Res 2019;56(2):28–43.
33. Zhang K, Li Y, Tsang M, Chetwyn NP. Analysis of pharmaceutical impurities using multi-heartcutting 2D LC coupled with UV-charged aerosol MS detection. J Sep Sci 2013;36:2986–2992.
34. Francois I, Sandra K, Sandra P. Comprehensive liquid chromatography: Fundamental aspects and practical considerations–A review. Anal Chim Acta 2009;641:14–31.
35. Pirok BWJ, Stoll DR, Schoenmakers PJ. Recent Developments in Two-Dimensional Liquid Chromatography: Fundamental Improvements for Practical Applicationa. Anal Chem 2019;91:240–263.

36. Stoll DR, Carr PW. Two-Dimensional Liquid Chromatography: A State of the Art Tutorial. Anal Chem 2017;89:19–31.
37. Marlot L, Faure K. Preparative two dimensional separation involving liquid-liquid chromatography. J Chrom A 2017;1494:1–17.
38. Yang P, Pursch M. Recent Advances in Two-dimensional Liquid Chromatography. Chromatography Today 2018:24–29.
39. Pirok BWJ, Gargano AFG, Schoenmakers PJ. Optimizing separations in online comprehensive two-dimensional liquid chromatography. J Sep Sci 2018;41:68–98.
40. Locatelli M, Governatori L, Carlucci G, Genovese S, Mollica A, Epifano F. Recent application of analytical methods to phase I and phase II drugs development: a review. Biomed Chromatogr 2012;26:283–300.
41. Chew YL, Khor MA, Lim YY. Choices of chromatographic methods as stability indicating assays for pharmaceutical products: A review. Heliyon 2021;7:1–12.
42. Qui F, Norwood DL. Identification of Pharmaceutical Impurities. J Liq Chromatogr Relat Technol 2007;30:877–935.
43. Schmidt P, Kolb C, Reiser A, Philipp M, Müller HC, Karaghiosoff K. Isolation, Identification and Structural Verification of a Methylene-Bridged Naloxon “Dimer” Formed by Formaldehyde. J Pharm Sci 2021;11(6):1682–1689.
44. Görög S, Babják M, Balogh G, Brlik J, Csehi A, Dravecz F, Gazdag M, Horváth P, Laukó A, Varga K. Estimation of impurity profiles of drugs and related materials. Part 19: Theme with variation. Identification of impurities in 3-oxosteroids. J Pharm Biomed Anal 1998;18:511–525.
45. Schmidt P, Kolb C, Reiser A, Philipp M, Godejohann M, Helmboldt H, Müller HC, Karaghiosoff K. Formation of a Thiol-Ene Addition Product of Asthma Medication Montelukast Caused by a Widespread Tin-Based Thermal Stabilizer. Chem Res Toxicol 2020;33:2963–2971.
46. Pawellek R, Holzgrabe U. Influence of the mobile phase composition on hyphenated ultraviolet and charged aerosol detection for the impurity profiling of vigabatrin. J Pharm Biomed 2021;201:1–8.
47. Eckers C, Laures AMF, Giles K, Major H, Pringle S. Evaluating the utility of ion mobility separation in combination with high-pressure liquid chromatography/ mass spectrometry to facilitate detection of trace impurities in formulated drug products. Rapid Commun Mass Spectrom 2007;21:1255–1263.
48. Ermer J. The use of hyphenated LC-MS technique for characterization of impurity profiles during drug development. J Pharm Biomed Anal 1998;18:707–714.

49. Dubey S, Pandey RK, Shukla SS. Impurity profiling and drug characterization: backdrop and approach. IAJPS 2018;5(4):2499–2515.
50. Ermer J, Vogel M. Applications of hyphenated LC-MS techniques in pharmaceutical analysis. Biomed Chromatogr 2000;14:373–383.
51. Govaerts C, Adams E, Schepdael AV, Hoogmartens J. Hyphenation of liquid chromatography to ion trap mass spectrometry to identify minor components in polypeptide antibiotics. Anal Bioanal Chem 2003;377:909–921.
52. Glish GL, Vachet RW. The basics of mass spectrometry in the twenty-first century. Nat Rev 2003;2:140–150.
53. Gillespie TA, Winger BE. Mass spectrometry for small molecule pharmaceutical product development: a review. Mass Spectrom Rev 2011;30:479–490.
54. Hart-Smith G, Blanksby SJ, Mass Spectrometry in Polymer Chemistry. 1st ed. Weinheim:Wiley; 2012.
55. Stolarczyk EU, Rosa A, Kubiszewski M, Zagrodzka J, Cybulski M, Kaczmarek L. Use of hyphenated LC-MS/MS technique and NMR/IR spectroscopy for the identification of exemestane stress degradation products during the drug development. Eur J Pharm Sci 2017;109:389–401.
56. Testen A, Plevnik M, Stefane B, Cigic IK. Identification of new process-related impurity in the key intermediate in the synthesis of TCV-116. Acta Pharm. 2019;69:63–74.
57. Studzinska S, Nuckowski L, Kilanowska A. Ultra-High-Performance Reverse-Phase Liquid Chromatography Hyphenated with ESI-Q-TOF-MS for the Analyses of Unmodified and Antisense Oligonucleotides. Chromatographia 2020;83:349–360.
58. Ermer J, Kibat PG. A quality concept for impurities during drug development – use of the hyphenated LC-MS technique. PSTT 1998;1(2):76–82.
59. Pucciarini L, Gilardoni E, Ianni F, D'Amato A, Marrone V, Fumagalli L, Regazzoni L, Aldini G, Carini M, Sardella R. Development and validation of a HPLC method for the direct separation of carnosine enantiomers and analogues in dietary supplements. J Chromatogr B 2019;1126–1127:1–7.
60. Neu V, Bielow C, Gostomski I, Wintringer R, Braun R, Reinert K, Schneider P, Hermann S, Huber CG. Rapid and Comprehensive Impurity Profiling of Synthetic Thyroxine by Ultrahigh-Performance Liquid Chromatography–High-Resolution Mass Spectrometry. Anal Chem 2013;85:3309–3317.
61. Vyas VK, Ghate M, Ukawala RD. Recent Advances in Characterization of Impurities – Use of Hyphenated LC-MS Technique. Curr Pharm Anal 2010;6(4):299–306.

62. Wijk AMV, Niederländer HAG, Siebum AHG, Vervaart MAT, Jong GJD. A new derivatization reagent for LC-MS/MS screening of potential genotoxic alkylation compounds. J Pharm Biomed Anal 2013;74:133–140.
63. Debremaeker D, Visky D, Chepkwony HK, Schepdael AV, Roets E, Hoogmartens J. Analysis of unknown compounds in azithromycin bulk samples with liquid chromatography coupled to ion trap mass spectrometry. Rapid Commun Mass Spectrom 2003;17:342–350.
64. Mendez ASL, Garcia CV, da Silva FEB, Paula FR. Identification and Quantification Methodologies for Active Substances in Natural Products: The Hole of Chromatographic and Spectroscopic Techniques. Churr Chromatogr 2015;2(1):2–19.
65. Pilaniya K, Chandrawanshi HK, Pilaniya U, Manchandani P, Jain P, Singh N. Recent trends in the impurity profile of pharmaceuticals. J Adv Pharm Tech Res 2010;1(3):302–310.
66. Krysa M, Szymanska-Chargot M, Zdunek A. FT-IR and FT-Raman fingerprints of flavonoids – A review. Food Chem 2022;393:1–9.
67. De Veij M, Vandenabeele P, De Beer T, Remon JP, Moens L. Reference database of Raman spectra of pharmaceutical excipients. J Raman Spectrosc 2009;40:297–307.
68. Fukutsu N, Kawasaki T, Saito K, Nakazawa H. Application of high-performance liquid chromatography hyphenated techniques for identification of degradation products of cefpodoxime proxetil. J Chromatogr A 2006;1129:153–159.
69. Boelens HFM, Dijkstra RJ, Eilers PHC, Fitzpatrick F, Westerhuis JA. New background correction method for liquid chromatography with diode array detection, infrared spectroscopy detection and Raman spectroscopy detection. J Chromatogr A 2004;1057:21–30.
70. Kuligowski J, Quntás G, Garrigues S, Lendl B, de la Guardia M. Recent advances in on-line liquid chromatography – infrared spectrometry (LC-IR). TRAC 2010;28(6):544–552.
71. Dijkstra RJ, Ariese F, Gooijer C, Brinkman UAT. Raman spectroscopy as a detection method for liquid-separation techniques. TRAC 2005;24(4):304–323.
72. Dijkstra RJ, Slooten CJ, Stortelder A, Buijs JB, Ariese F, Brinkman UAT, Gooijer C. Liquid-core waveguide technology for coupling column liquid chromatography and Raman spectroscopy. J Chromatogr A 2001;918:25–36.
73. Dijkstra RJ, Bader AN, Hoornweg GP, Brinkman UAT, Gooijer C. On-Line Coupling of Column Liquid Chromatography and Raman Spectroscopy Using a Liquid Core Waveguide. Anal Chem 1999;71:4575–4579.
74. Lo YH, Hiramatsu H. Online Liquid Chromatography-Raman Spectroscopy Using the Vertical Flow Method. Anal Chem 2020;92:14601–14607.
75. Webb GA. Modern Magnetic Resonance. Heidelber: Springer; 2007.
76. Keeler J. Understanding NMR Spectroscopy. New York: Wiley; 2013

77. Heise H, Matthews S. Modern NMR Methoddology. Heidelberg: Springer; 2013.
78. Jacobsen NE, NMR Spectroscopy Explained: Simplidied Theory, Applications and Examples for Organic Chemistry and Structural Biology. New York: Wiley; 2007.
79. Magio RM, Calvo NL, Vignaduzzo SE, Kaufman TS. Pharmaceutical impurities and degradation products: Uses and applications of NMR techniques. J Pharm Biomed Anal 2014;101:102–122.
80. Singh S, Roy R. The application of absolute quantitative ^{1}H NMR spectroscopy in drug discovery and development. Expert Opin Drug Discov 2016;11(7),695–706.
81. Peng SX. Hyphenated HPLC-NMR and its applications in drug discovery. Biomed Chromatogr 2000;14:430–441.
82. Spraul M. Developments in NMR Hyphenation for Pharmaceutical Industry. Modern Magnetic Resonance 2008:1221–1228.
83. Tokunaga T, Akagi K, Okamoto M. Sensitivity enhancement by chromatographic peak concentration with ultra-high performance liquid chromatography-nuclear magnetic resonance spectroscopy for minor impurity analysis. J Chromatogr A 2017;1508:163–168.
84. Schmidt P, Kolb C, Godejohann M, Reiser A, Philipp M, Müller HC, Karaghiosoff K. Separation and identification of a complex flurbiprofen-polyethylene glycol mono- and diester mixture via a hyphenated HPLC-DAD-HRMS/SPE-NMR system. J Pharm Biomed Anal 2023;222:1–12.
85. Corcoran O, Spraul M. LC-NMR-MS in drug discovery. Drug discov today 2003;8(14)624–631.
86. Garcia-Manteiga JM, Mari S, Godejohann M, Spraul M, Napoli C, Cenci S, Musco G, Sitia R, Metabolomics of B to cell differentiation, J Proteome Res 2011;10:4165–4176.
87. Godejohann M, Tseng LH, Braumann U, Fuchser J, Spraul M. Characterization of paracetamol metabolite using on-line LC-SPE-NMR-MS and cryogenic NMR probe. J Chromatogr A. 2004;1058:191–196.
88. Nicholls AW, Wilson ID, Godejohann M, Nicholson JK, Shockcor JP. Identification of phenacetin metabolites in human urine after administration of phenacetin-C2H3: measurement of futile metabolic deacetylation via HPLC/MS-SPE-NMR and HPLC-ToF MS. Xenobiotica 2006;46(7):615–629.
89. Tang H, Xiao C, Wang Y. Important roles of hyphenated HPLC-DAD-MS-SPE-NMR technique in metabonomics. Magn Reason Chem 2009;47:157–162.
90. Fu J, Wang YN, Ma SG, Li L, Wang XJ, Li Y, Liu YB, Qu J, Yu SS. Xanthanoltrimer A-C: three xanthanolide sesquiterpene trimers from fruit of Xanthium italicum Moretti isolated by HPLC-MS-SPE-NMR. Org Chem Front 2021;8:1288–1293.
91. Gummadi S, Siyyadri DS. Nuclear magnetic resonance and hyphenations – a review. IJPSR 2020;11(12):5932–5950.

92. Iqbal K, Iqbal J, Staerk D, Kongstad KT. Characterization of antileishmanial compounds from lawsonia intermis L. leaves using semi-high resolution antileishmanial profiling combined with HPLC-HRMS-SPE-NMR. Front Pharmacol 2017;8(337):1–7.
93. Johansen KT, Ebild, Christensen SB, Godejohann M, Jaroszewski JW. Alkaloid analysis by high-performance liquid chromatography-solid phase extraction-nuclear magnetic resonance: new strategies going beyond the standard. J Chromatogr A 2012;1270:171–177.
94. Johansen KT, Wubshet SG, Nyber NT. HPLC NMR revisited: using time-slice high-performance liquid chromatography-solid phase extraction-nuclear magnetic resonance with database-assisted dereplication. Anal Chem 2013;85:3183–3189.
95. Liu F, Wang YN, Li Y, Ma SG, Qu J, Liu YB, Niu CS, Tang ZH, Li YH, Li L, Yu SS. Triterpenoids from the twigs and leaves of Rhododendron latoucheae by HPLC-MS-SPE NMR. Tetrahedron. 2019;75:296–307.
96. Seger C, Godejohann M, Tseng LH, Spraul M, Girtler A, Sturm S, Stuppner H. LC-DAD-MS/SPE NMR Hyphenation. A tool for the analysis of pharmaceutically used plant extracts: identification of isobaric iridoid glycoside regioisomers from harpagophytum procumbens. Anal Chem 2005;77:878–885.
97. Pan C, Liu F, Ji Q, Wang W, Drinkwater D, Vivilecchia R. The use of LC/MS, GC/MS and LC/NMR hyphenated techniques to identify a drug degradation product in pharmaceutical development. J Pharm Biomed 2006;40:581–590.
98. Kesting JR, Huang JQ, Sorensen D. Identification of adulterants in a Chinese herbal medicine by LC-HRMS and LC-MS-SPE/NMR and comparative in vivo study with standards in a hyphenated rat model. J Pharm Biomed 2010;51:705–711.
99. Murakami T, Kawasaki T, Takemura A, Fukutsu N, Kishi N, Kusu F. Identification of degradation products in loxoprofen sodium adhesive tapes by liquid chromatography-mess spectrometry and dynamic pressurized liquid extraction-solid-phase extraction coupled to liquid chromatography-nuclear magnetic resonance spectroscopy. J Chromatogr A 2008;1208:164–174.

1.4 Concept

Alongside HPLC as one of the most popular separation techniques, the following, widely used and effective purification and analytical techniques were selected for this work:

As the most common detection method that is coupled to HPLC, as well as the tool that is most often used for the initial detection of an impurity during routine quality control, UV/Vis-Spectroscopy was selected in the form of diode-array detection (DAD). DAD enables the simultaneous recording of a broad area of the UV and visible spectrum, increasing the probability of detecting substances, that would otherwise go undetected when recording only one or two wavelengths. UV/Vis-spectroscopy was hereby mainly applied as a method for detection, but in some cases information on the structure of the analyte was deduced from the recorded spectra nonetheless.[1-3]

The second most common analytical technique, that is coupled to HPLC, is mass spectrometry, which was implemented into the system as high-resolution mass spectrometry (HRMS). Aside from functioning as a detector, which is complementary to DAD, HRMS also provides important information on the structure of an analyte, which in some cases may be enough to fully identify an impurity.[4-7]

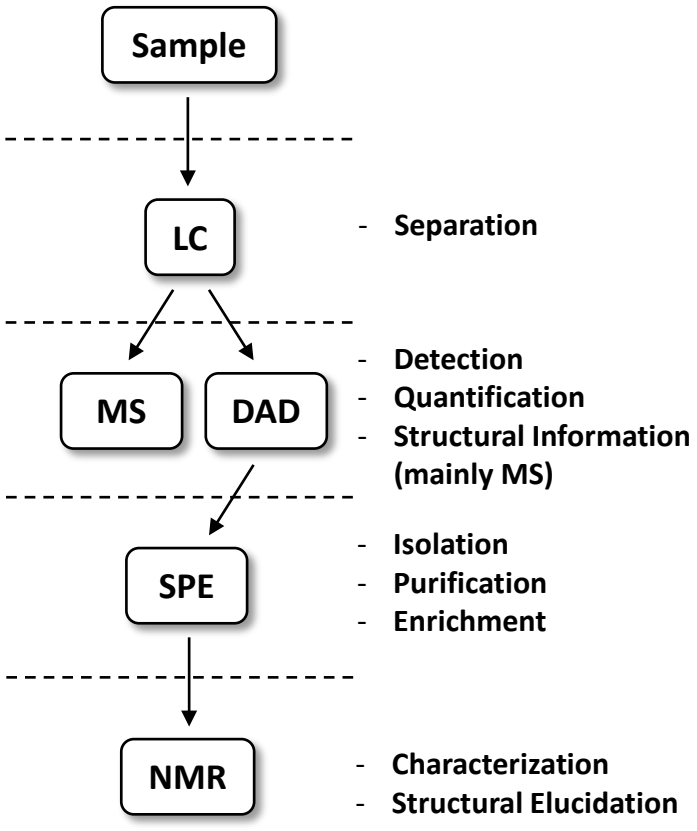

Figure 1. Flowchart of the hyphenated System used in this dissertation. The different analytical methods are depicted alongside their function and the data they provide.

The final analytical technique selected for the system, was nuclear magnetic resonance (NMR) spectroscopy, which was not utilized for detection, but was implemented exclusively as a tool for structural elucidation. Though NMR spectroscopy is one of the most powerful analytical methods available in chemistry and pharmacy, its coupling to HPLC is the most challenging out of all the selected techniques. Chief among these challenges are the large amounts of substance needed, the long measurement times, and the solvent requirements.[1-8,11]

Finally, to balance out the disadvantages of NMR spectroscopy, the last component selected for the hyphenated system was solid-phase extraction (SPE).

SPE is capable of simultaneously isolating, purifying, and concentrating a sample, thereby enabling NMR measurements, independent of the time and chromatographic restraints of HPLC separation. By performing several, consecutive HPLC runs, sufficient analyte amounts can be gathered on SPE cartridges to perform NMR measurements despite the generally low concentrations of impurities within a pharmaceutical sample.[11-14]

The aim of this work was to gage the efficiency of this HPLC-DAD-HRMS/SPE-NMR system by using real case studies found in the pharmaceutical industry. At first synthetic samples were used to:

- gage the system's capabilities in regard to quantification and elucidation of formation mechanisms of impurities.
- evaluate the capabilities and limitations of the system when separating, purifying, and concentrating a sample.
- perform complete structural elucidations of several real pharmaceutical impurities.

Lastly, as proof-of-concept, the entire quantification, isolation, and structural elucidation was performed on an actual medical product. For this purpose, real drug samples from a long-term stability test were used, without subjecting them to any further procedures to enrich the impurity in question. In doing so, it was shown that by using this hyphenated system, the complete analysis of an impurity can be performed with real samples and available quantities, as they occur in everyday quality control, without the need for additional experiments to enrich or synthesize the impurity.

The following chapters present three case studies of varying APIs, dosage forms and their impurities. After a brief introduction, original research papers containing the results of the studies are presented, followed by a summary of their contents and comments meant to embed the research in the overall thesis.

References (Concept)

1. Ahuja SS. Assuring quality of drugs by monitoring impurities. Adv Drug Deliv Rev 2007;59:3-11.
2. Sudev S, Janardhanan SV. Review on HPLC Method Development Validation and Optimization. Int J Pharm Sci Rev Res 2019;56(2):28-43.
3. Chew YL, Khor MA, Lim YY. Choices of chromatographic methods as stability indicating assays for pharmaceutical products: A review. Heliyon 2021;7:1-12.
4. Ermer J. The use of hyphenated LC-MS technique for characterization of impurity profiles during drug development. J Pharm Biomed Anal 1998;18:707-714.
5. Dubey S, Pandey RK, Shukla SS. Impurity profiling and drug characterization: backdrop and approach. IAJPS 2018;5(4):2499-2515.
6. Ermer J, Vogel M. Applications of hyphenated LC-MS techniques in pharmaceutical analysis. Biomed Chromatogr 2000;14:373-383.
7. Govaerts C, Adams E, Schepdael AV, Hoogmartens J. Hyphenation of liquid chromatography to ion trap mass spectrometry to identify minor components in polypeptide antibiotics. Anal Bioanal Chem 2003;377:909-921.
8. Pan C, Liu F, Motto M. Identification of Pharmaceutical Impurities in Formulated Dosage Forms. J Pharm Sci 2011;100(4):1228-1259.
9. Singh S, Handa T, Narayanam M, Sahu A, Junwal M, Shah RP. A critical review on the use of modern sophisticated hyphenated tools in the characterization of impurities and degradation products. J Pharm Biomed 2012;69:148-173.
10. Kamboj S, Kamboj N, Rawal RK, Thakkar A, Bhardwaj TR. A Compendium of Techniques for the Analysis of Pharmaceutical Impurities. Curr Pharm Anal 2014;10(2):145-160.
11. Singh S, Handa T, Narayanam M, Sahu A, Junwal M, Shah RP. A critical review on the use of modern sophisticated hyphenated tools in the characterization of impurities and degradation products. J Pharm Biomed 2012;69:148-173.
12. Magio RM, Calvo NL, Vignaduzzo SE, Kaufman TS. Pharmaceutical impurities and degradation products: Uses and applications of NMR techniques. J Pharm Biomed Anal 2014;101:102-122.
13. Spraul M. Developments in NMR Hyphenation for Pharmaceutical Industry. Modern Magnetic Resonance 2008:1221-1228.
14. Tokunaga T, Akagi K, Okamoto M. Sensitivity enhancement by chromatographic peak concentration with ultra-high performance liquid chromatography-nuclear magnetic resonance spectroscopy for minor impurity analysis. J Chromatogr A 2017;1508:163-168.

2 Montelukast: System Functionality and Elucidation of Formation Mechanisms

As a first example to demonstrate the functionality of the HPLC-DAD-HRMS/SPE-NMR system, a previously elucidated impurity was chosen. This impurity was a degradation product of the asthma medication Montelukast, which forms via the reaction of a component of the thermal stabilizer used in the primary packaging material of the Montelukast chewable tablets. Although the impurity had already been quantified and identified, the goal of the project was to transfer the analytical method to the hyphenated system, to ascertain, whether the thus obtained data is of sufficient quality and quantity for a complete quantification and identification of the impurity.

2.2 Montelukast Research Article

Author contributions:

Philipp Schmidt:

- *Design and performance of experiments to clarify the formation mechanism of the Montelukast impurity*
- *HPLC analysis and evaluation of these experiments*
- *Artificial synthesis of the impurity samples for analysis using the HPLC-DAD-HRMS/SPE-NMR system*
- *Method transfer to the HPLC-DAD-HRMS/SPE-NMR system*
- *Separation, enrichment, isolation and data acquisition using the HPLC-DAD-HRMS/SPE-NMR system*
- *Evaluation of the data, followed by the complete structural elucidation of the two diastereomers of the Montelukast impurity, including the assignment of all ^{1}H and ^{13}C NMR signals*
- *Synthesis, analysis and structural elucidation of the two diastereomers of the Montelukast-Thiophenol addition product using the HPLC-DAD-HRMS/SPE-NMR system*
- *Writing of the Research Article*

Christine Kolb and Andreas Reiser:

- *Performed the initial investigations regarding the identity and formation of the Montelukast impurity, when it was first discovered, including degradation and enrichment experiments*

Markus Philipp:

- *Performed a role as supervisor of the project*

Markus Godejohann:

- *Aided in the initial NMR analysis and elucidation of the Montelukast impurity, when it was first discovered*

Hannes Helmboldt:

- *Isolation of the sodium salts of the Montelukast impurity by flash chromatography*

Hans-Christian Müller and Konstantin Karaghiosoff:

- *Performed an advisory role in the preparation of the manuscript and aided in proof-reading*

Chemical Research in Toxicology

pubs.acs.org/crt

Article

Formation of a Thiol−Ene Addition Product of Asthma Medication Montelukast Caused by a Widespread Tin-Based Thermal Stabilizer

Philipp Schmidt, Christine Kolb, Andreas Reiser, Markus Philipp, Markus Godejohann, Hannes Helmboldt, Hans-Christian Müller,* and Konstantin Karaghiosoff*

Cite This: *Chem. Res. Toxicol.* 2020, 33, 2963−2971

Read Online

ACCESS | Metrics & More | Article Recommendations | Supporting Information

ABSTRACT: We report the formation and characterization of two diastereomeric thiol−ene addition products of the asthma medication Montelukast within chewing tablets. Widespread tin-based thermal stabilizers dioctyltin bis(2-ethylhexyl thioglycolate) and monooctyltin tris(2-ethylhexyl thioglycolate), used in the manufacturing process of the medication's forming foil, were identified as the source of the thiol reactant, showing that these stabilizers may play a part in the degradation of Montelukast and APIs with functionalities similar to those of Montelukast, which should be considered during development of medication. The isolation and analysis of these impurities was performed by HPLC and UV−vis spectroscopy. HRMS and NMR data were collected to characterize and determine the structures of these compounds.

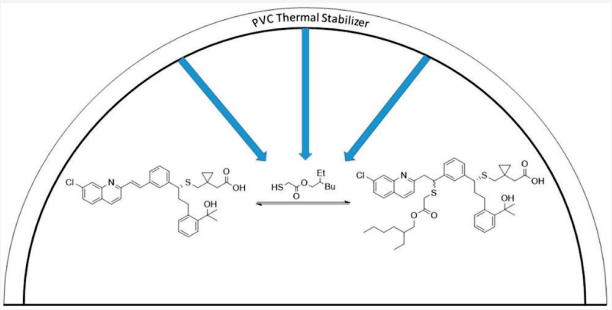

INTRODUCTION

Montelukast (**1**) (Figure 1) is a leukotriene receptor antagonist used in the treatment of asthma and allergic

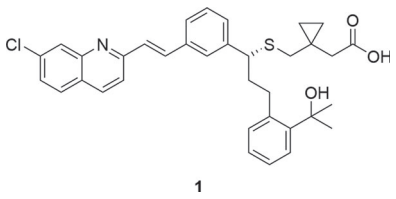

1

Figure 1. Chemical structure of asthma medication Montelukast (**1**).

rhinitis. It is commonly given in addition to inhaled corticosteroids, should the treatment with an inhaler be insufficient. By blocking the $CysLT_1$ receptors in the lungs, Montelukast helps decrease inflammation and bronchoconstriction in asthma patients.[1−3]

Unlike most asthma medications, the sodium salt of Montelukast can be taken orally in forms such as granulates, film, and chewing tablets.[3] The foil commonly used as packaging for such tablets consists partially of PVC, which contains the thermal stabilizers dioctyltin bis(2-ethylhexyl thioglycolate) and monooctyltin tris(2-ethylhexyl thioglycolate).[4,5] These organotin compounds are introduced to prevent the thermal or light induced degradation of the PVC foil, during which polyenes are formed, and hydrochloric acid is released.[4,5] These stabilizers also play a role as traps for the released HCl, a process during which the tin compounds are chlorinated and 2-ethylhexyl thioglycolate is released (Figure 2).[5,6]

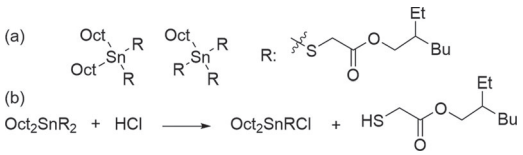

Figure 2. (a) Chemical structures of thermal stabilizers dioctyltin bis(2-ethylhexyl thioglycolate) and monooctyltin tris(2-ethylhexyl thioglycolate) and (b) representative reaction of dioctyltin bis(2-ethylhexyl thioglycolate) with HCl and the subsequent release of 2-ethylhexyl thioglycolate.[6]

During HPLC analysis of Montelukast chewing tablets, the presence of two formerly unknown impurities was detected. After isolation and NMR studies, these impurities were determined to be two stereoisomers formed by a Michael-like, thiol−ene addition of 2-ethylhexyl thioglycolate to the double bond present in Montelukast. Here, we describe in detail the identification, isolation, formation, and synthesis, as

Received: June 30, 2020
Published: November 11, 2020

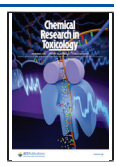

https://dx.doi.org/10.1021/acs.chemrestox.0c00261
Chem. Res. Toxicol. 2020, 33, 2963−2971

well as the properties, of these two impurities. These do not include biological properties.

Disclamer. The details outlined in this article only constitute a small part of a large-scale investigation following a recorded quality event during routine follow-up stability testing of a product batch. The whole process initiated thereafter was governed by a fully compliant and repeatedly authority inspected pharmaceutical quality system, which is in full accordance with all relevant national and international pharmaceutical and medicine laws and guidelines. The full investigation involved all relevant technical and scientific functions from different managerial levels as well as all relevant authorities. No risk for the consumers of the marketed product was evident at any point in time. This event was completely unexpected and never seen before at any storage or stress conditions.

It is the intention of the authors to keep the focus of this article on the scientific chemical and analytical aspects of this investigation; therefore, the large amount of procedural and regulatory information required to understand the complete process and all its risk mitigating aspects is not included and the focus of this work is kept on the identification and structural elucidation of the compounds in question.

RESULTS AND DISCUSSION

Identification. During LC−UV purity analysis of bulk Montelukast chewing tablets that had been stored for 12 months at 25 °C and a relative humidity of 60%, two previously unknown impurities were detected at levels of 0.26 and 0.28 area-% relative to the Montelukast content in the tablets (Figure S1 of the Supporting Information). This prompted further investigations into the origin and structure of these unknown substances. At first, LC−MS analysis was applied to identify the mass of the two impurities (Figures S4 and S10). In both cases, an m/z value of 790 for $[M + H]^+$ was observed, as opposed to the value of 586 for the original active pharmaceutical ingredient (API). The difference in the m/z value of 204 fits to the mass of 2-ethylhexyl thioglycolate, giving the first indications for the formation of the two diastereomers of the thiol−ene addition product **2** (Figure 3).

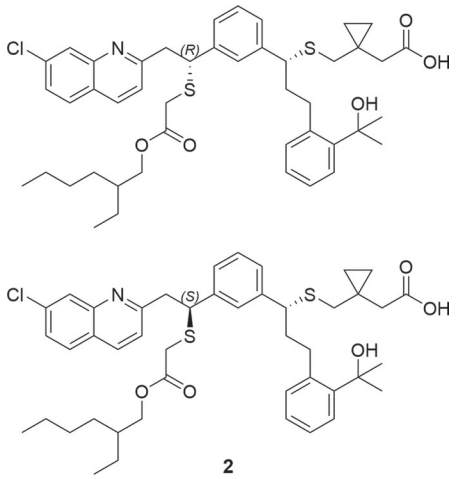

2

Figure 3. Proposed structures of the (*R*)- and (*S*)-diastereomers resulting from the thiol−ene addition of 2-ethylhexyl thioglycolate to Montelukast.

Further conducted UV−vis spectroscopy resulted in near identical spectra for both impurities and showed two maxima in areas of 192 to 196 and 209 to 213 nm, whereas any signals beyond around 230 nm, which are significant in the case of Montelukast, were no longer detectable (Figures S6 and S7). This suggests a drastic change of the chromophore system within the molecule, as would be the case for the loss of the double bond connecting the aromatic systems of the quinoline and phenyl rings within the API.

The final structural elucidation was performed after enrichment and LC−NMR analysis, identifying the two impurities as the proposed (*R*)- and (*S*)-diastereomers of the thiol−ene addition of 2-ethylhexyl thioglycolate to Montelukast (**2**, Figure 3). To obtain NMR samples of higher quality and concentration, **2** was later directly synthesized and isolated using a hyphenated HPLC−DAD−HRMS/SPE−NMR (high performance liquid chromatography−diode array detector−high resolution mass spectrometry/solid phase extraction−nuclear magnetic resonance) system that used UV information to selectively trap each of the two diastereomers onto separate solid phase cartridges during several consecutive HPLC runs (Figure S2).

After we used this method, the two expected diastereomers of **2** could be isolated. However, the NMR techniques applied, though showing differences between the two substances, were not sufficient to identify which of the isolated fractions was the (*R*)- and (*S*)-diastereomer.

For Montelukast (**1**), two doublets are visible in the ^{1}H NMR spectrum at around 7.78 and 7.44 ppm, originating from the olefinic protons of its double bond. In comparison, these signals have disappeared from the aromatic region of both diastereomers of **2**, and an overall high field shift of many aromatic signals can be observed, likely caused by the interruption of the electron delocalization previously created by the double bond (Figure 4).

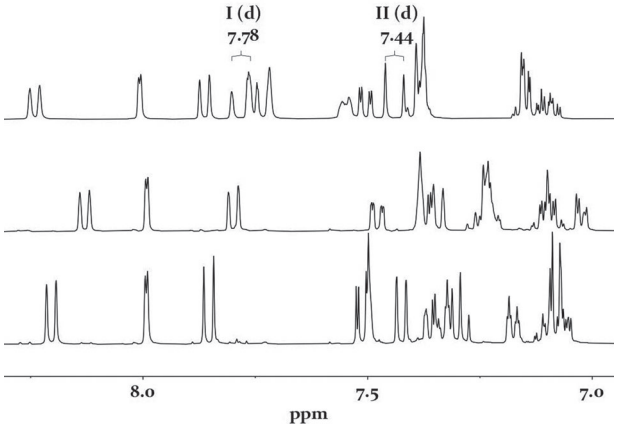

Figure 4. NMR spectra of the aromatic regions of Montelukast (top) and the two diastereomers of the thiol−ene addition product (middle and bottom). The signals arising from Montelukast's double bond are marked (I/II) and given in ppm.

Also, the ^{1}H NMR spectrum of Montelukast shows one single doublet of doublets at around 4.00 ppm, caused by the proton of the stereocenter adjacent to the sulfur atom. The NMR spectra of the diastereomers of **2**, aside from having overall more signals in the aliphatic region due to the glycolate side chain, additionally show new signals in this region around

https://dx.doi.org/10.1021/acs.chemrestox.0c00261
Chem. Res. Toxicol. 2020, 33, 2963−2971

4.00 ppm (Figure 5). These are caused by the new protons introduced to the location of the former double bond during

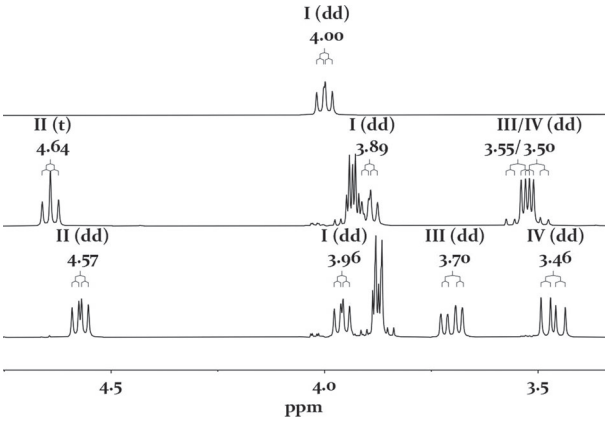

Figure 5. NMR spectra of the aliphatic regions of Montelukast (top) and the two diastereomers of the thiol−ene addition product (middle and bottom). The signals arising from the original stereocenter present in Montelukast (I), as well as the newly formed CH- and CH_2-groups (II and III/IV) in the diastereomers of impurity **2**, are marked and given in ppm.

the thiol−ene addition, creating an ABX spin system. For the first isomer, this is visible as a triplet at 4.64 ppm, caused by the coupling of the proton of the CH-group at the stereo center (X-part) with the neighboring diastereotopic protons of the CH_2-group (AB-part), which in turn produces a set of doublets of doublets at 3.55 and 3.50 ppm. While the signal of the X-part produces a triplet due to near identical coupling with the adjacent diastereotopic protons, the X-part of the second isomer shows a doublet of doublets at 4.57 ppm. Also, the signals of the AB-part, which almost merge into one another for the first isomer, are split much further apart for the second. As such, they are visible as individual doublets of doublets at 3.70 and 3.46 ppm, respectively. To further confirm the addition pattern of the thiol−ene reaction, additional ^{13}C and 2D spectra (COSY, HSQC, HMBC) were recorded (Figures S12−S21). For both diastereomers, a coupling of the CH_2-group into the quinoline ring and the CH-group into the phenyl ring can be observed in the HMBC spectra, confirming the postulated structure of **2**. The HMBC spectrum of the first diastereomer also shows the coupling between the newly formed stereo center with the first ethylene group of the thioglycolate side chain.

Formation and Synthesis. Alongside the structural elucidation, research into the formation of **2** was conducted. For this purpose, different degradation experiments of Montelukast were performed under varying conditions. These were then followed by HPLC analysis to determine whether **2** could be detected.

First, photostress experiments were performed by exposing the powdered chewing tablets to laboratory light at room temperature and to a solar simulator at 30 °C for 4 h each. Also, powder of the pure API was exposed to a solar simulator at 30 °C for 1−4 days and to X-rays at room temperature for 15 min (Table S1). Next, the powdered chewing tablets were exposed to thermic and hydrolytic stress by adding ultrapure water and storing the samples at 50 and 70 °C for 6 days (Table S2). **2** could not be detected in either photo, thermic, or hydrolytic stress of the powdered chewing tablets or the pure API.

Only a thermic stress trial of the tablets, wrapped in the packaging material, at 50 and 70 °C for 8 days showed the formation of the two diastereomers of impurity **2**, leading to the conclusion that the wrapping material was involved in their formation (Table S3). Following these results, stress experiments with samples of varying compositions were performed at 50 °C for up to 8 days (Tables S4−S6). It was found that the PVC part of the packaging foil was essential in the formation of **2** but that **2** could not be detected in mixtures consisting solely of the API and the PVC foil. Formation of **2** was only observed in the presence of croscarmellose sodium (internally cross-linked sodium carboxymethyl cellulose) or microcrystalline cellulose (MCC), both part of the chewing tablets formulation.

Because these two substances may contain reactive impurities, such as formaldehyde, formic acid, and peroxides,[7,8] further stress experiments were performed with these components (Table S7). It was found that formic acid and formaldehyde, as precursor to formic acid,[7] both led to the formation of **2**, while hydrogen peroxide led to no changes. Owing to these findings, the enrichment of **2** for analytical purposes was performed by adding formic acid to the API and pieces of forming foil in DMF, at 50 °C for 20 h (Table S9).

Drawing from the conclusions of the structural elucidation and the stress experiments, a synthesis for **2** was devised. Instead of degrading the tin stabilizers, 2-ethylhexyl thioglycolate was directly reacted with Montelukast. In order to clarify whether acid is needed solely to release the thioglycolate from the forming foil, or whether it also plays a part in the reaction mechanism, two parallel experiments were conducted, one with and one without formic acid.

For this purpose, two samples of the Montelukast sodium salt were dissolved in DMF and heated to 50 °C, under exclusion of light. Formic acid was given to the first sample, before an excess of 2-ethylhexyl thioglycolate was added to both reactions. After 2 h, a sample of each reaction was taken and analyzed by HPLC. The approximate yield was then determined by comparing the area percentages of the combined yield of the two diastereomers of **2** to that of Montelukast.

Formation of **2** was observed for both reactions, with approximately 97% of Montelukast having reacted to **2**, in the case of the acidic sample, and 24% for the acid free sample. These results show that the thiol−ene reaction occurs regardless of the presence of acid, though the acid clearly increases the yield. As such, the formic acid appears to play two roles in the formation of **2**: first by degrading the tin stabilizers, releasing 2-ethylhexyl thioglycolate as reactant, and second by acting as a catalyst (Scheme 1).

In order to further clarify the reaction mechanism, other experiments were conducted, and the approximate yields were once again determined by comparing area percentages of **2** and Montelukast during HPLC analysis. As most thiol−ene reactions occur via either a radical or Michael-like mechanism, similar conditions were explored.[9−16]

First, a radical pathway was investigated. Most radical thiol−ene reactions use a radical starter such as AIBN for initiation, so the question arose how this initiation may occur for Montelukast.[9,11,12] A known reaction of Montelukast is a reversible, light induced, internal isomerization, during which the double bond rotates from its initial *trans*-conformation to a *cis*-conformation (Scheme 2).[1,2]

https://dx.doi.org/10.1021/acs.chemrestox.0c00261
Chem. Res. Toxicol. 2020, 33, 2963−2971

Scheme 1. Acid Catalyzed Formation of the Diastereomers of Impurity 2[a]

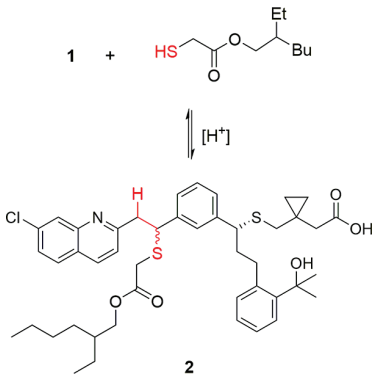

[a]This formation is completed by addition of 2-ethylhexyl thioglycolate to the double bond of Montelukast (**1**) or Montelukast sodium.

Scheme 2. Proposed Mechanism of the Light Induced Transition of *trans*-Montelukast to *cis*-Montelukast[a]

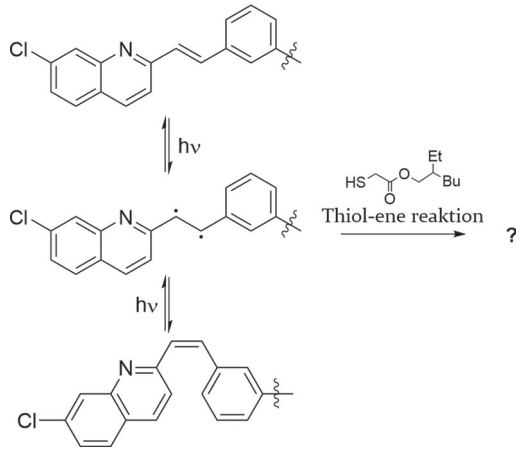

[a]Proposed mechanism is via a biradical transition state.

As one possible mechanism for such a photoisomerization occurs via a biradical transition state (Scheme 2),[17−19] the question of whether Montelukast may serve as its own radical starter arose. To clarify whether this self-catalysis truly takes place, an attempt was made to suppress the reaction using the radical catcher BHT (2,6-Di-*tert*-butyl-4-methylphenol). A reaction under identical conditions as those of previous experiments was performed with the addition of an excess of BHT. HPLC analysis showed that the reaction occurs despite the presence of BHT. With 76% the yield was slightly lower than that in previous experiments, but seeing as BHT was detected as unchanged and there were no further side products that would suggest the suppression of a radical mechanism by a radical catcher, a radical mechanism seems unlikely.

These and further results indicate that the thiol−ene addition occurs via an ionic, Michael-like mechanism, initiated by the nucleophilic attack of sulfur. Such a mechanism usually occurs in the presence of a base or nucleophile as initiator or catalyst,[10−15] though additive free reactions are known.[9,15,16] Also, a thiol-Michael addition would provide a possible explanation for the specific addition pattern of the reaction. Due to the electron pulling nature of the quinoline ring's nitrogen atom, an attack of the thiol group at the carbon adjacent to the benzene ring leads to the delocalization of the negative charge over the entire quinoline ring, thereby stabilizing the transition state.

These results coincide with similar known synthesis byproducts of Montelukast. These are formed during the introduction of the 2-(1-(mercaptomethyl)cyclopropyl) acetic acid side chain during the synthesis of Montelukast and result from the addition of a further unit of 2-(1-(mercaptomethyl)-cyclopropyl) acetic acid to the double bond (Figure 6).[20,21]

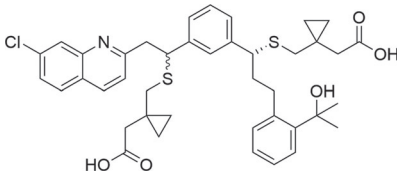

Figure 6. Addition product of 2-(1-(mercaptomethyl)cyclopropyl) acetic acid to Montelukast formed as byproduct of the synthesis of the API.[20,21]

This reaction also follows a Michael-like mechanism and, as in the case of 2-ethylhexyl thioglycolate, leads to the formation of two new stereoisomers with an identical addition pattern to those of **2**.[21]

Lastly, the effect of the acid on the reaction was explored, to see whether its catalytic role lies solely in protonating the Montelukast sodium salt or whether further effects are in play. As such, only an equimolar amount of formic acid was added to the reaction. This resulted in a yield of 69%, lower than that of the reaction with an excess of acid, indicating that the acid does not accelerate the reaction solely by protonating the sodium salt of Montelukast but plays a further catalytic role. As such, the protonation of quinolin's nitrogen atom may increase the electron withdrawing effect, further activating the carbon adjacent to the benzene ring by increasing its electrophilicity. This would constitute an unusual case of an acid catalyzed thiol-Michael addition.

Parallel to investigation of the mechanism and conditions of the formation of **2**, attempts to isolate the individual stereoisomers were performed. In a first step, flash chromatography and subsequent preparative HPLC were applied, to afford the two diastereomers of compound **2** as colorless oils in 98.7 and 98.1% isomer purity, respectively. Both stereoisomers were then treated with sodium hydroxide, before final purification by flash chromatography, affording the sodium salts of the two diastereomers of **2** as very hygroscopic, white powders.

A major reason for the conversion of the diastereomers to their sodium salts was the observation that the thiol−ene addition products, especially the free acids, were unstable. As such, the observation was made that samples, analyzed by NMR spectroscopy in deuterated acetonitrile or methanol, showed signals of Montelukast reemerging in the spectrum within a span of 24 h, proving the thiol−ene addition to be reversible.

The conditions of this reversible reaction were further explored in stability tests. Samples of the crude reaction solution, i.e., Montelukast with an excess of the 2-ethylhexyl thioglycolate and formic acid in DMF, as well as a mixture of the sodium salts of the two diastereomers of **2**, dissolved once

https://dx.doi.org/10.1021/acs.chemrestox.0c00261
Chem. Res. Toxicol. 2020, 33, 2963−2971

in benzene and once in THF, were prepared. These three samples were each analyzed every 24 h by HPLC over the course of 4 days to observe the change in Montelukast and **2** levels.

In the case of the sodium salts of **2**, dissolved in benzene and THF, an equilibrium between Montelukast and the thiol−ene addition product formed within 3 days. With 90 area-%, the amount of **2** remaining in benzene was significantly higher than that in THF; yet, interestingly, only 3 area-% of Montelukast was detected in THF. Instead, two unknown peaks were observed in the UV detector which could be identified as the sulfoxides of Montelukast and the diastereomers of **2** via LC−MS measurements.

HPLC analysis of the reaction solution showed no significant changes, with the equilibrium remaining in favor of **2**. This is likely caused by an excess of 2-ethylhexyl thioglycolate present in the solution that drives the equilibrium onto the side of the two diastereomeric products.

A further reaction with equimolar amounts of Montelukast and 2-ethylhexyl thioglycolate and an excess of formic acid was performed to observe the equilibrium without an excess of reactants. This reaction resulted in a level of 48 area-% of the thiol−ene addition product, which increased over the course of 4 days until an equilibrium was reached at 89 area-%. These values are similar to those of the equilibrium reached in the benzene solution of **2**, indicating that the thiol−ene addition product is favored over Montelukast, despite the disruption of the delocalized π-system during the formation of **2**.

Further Experiments with Thiophenol. In addition to experiments with 2-ethylhexyl thioglycolate, Montelukast was treated with thiophenol to see whether the API is also capable of reacting with other thiols. Under identical conditions to those of 2-ethylhexyl thioglycolate, thiophenol was allowed to react with Montelukast in the presence of an excess of formic acid. Two new compounds were observed during HPLC analysis. Their combined yield of approximately 96% was determined by comparison to the area percentage of Montelukast (Figure S2). LC−MS analysis (Figures S6 and S11) showed the expected m/z value of 696 for $[M + H]^+$, and once again, a change in the chromophore system was observed in the UV−vis spectra, showing maxima at 196.1 and around 250.0 nm (Figure S8).

Samples of **3** for NMR studies were once more collected by using a hyphenated HPLC−DAD−HRMS/SPE−NMR system (Figures S22−S31). As in the case of **2**, the individual NMR spectra measured for the two isomers could not be linked to the individual (*R*)- and (*S*)-diastereomers.

Similar to impurity **2**, the disappearance of the double bond signals in the aromatic region was once more observed for **3**. A high field shift along with new signals from the additional phenyl ring were also visible. As observed before, for **2**, the first diastereomer isolated during LC−SPE separation had a less distinct ABX spin system at the site of the thiol−ene addition than that of the second. In fact, no ABX system could be observed at all for the first isolated isomer of **4**, as the signal of the CH-group at 4.99 ppm was not the only signal to produce a triplet; however, the signal of the CH_2-group at 3.59 ppm was visible as a doublet. The second isomer however showed a triplet at 4.93 ppm for the X-part and two separate doublets of doublets at 3.68 and 3.57 ppm for the AB-part. The coupling of the CH_2−group with carbon atoms of the quinoline ring, visible in the HMBC spectra, once more confirmed the pattern of the thiol−ene addition (Figure 7).

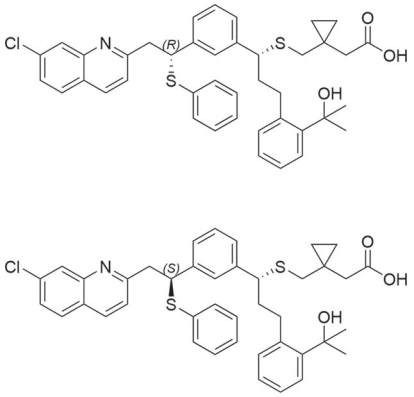

3

Figure 7. (*R*)- and (*S*)-diastereomers of the thiol−ene addition of thiophenol to Montelukast.

Additionally, an attempt to isolate a sample, previously collected by solid phase extraction, was made by slowly evaporating the solvent under a nitrogen flow. However, NMR and HPLC analysis showed that this procedure led to the complete decomposition of **3**, reforming Montelukast. Analysis of the reaction solution of **3** after 4 weeks also showed a significant decrease of the diastereomeric products down to 42 area-%, proving the thiol−ene addition products of thiophenol and Montelukast to be even more unstable than those of 2-ethylhexyl thioglycolate.

CONCLUSION

Our studies led to the conclusion that the thermal stabilizers dioctyltin bis(2-ethylhexyl thioglycolate) and monooctyltin tris(2-ethylhexyl thioglycolate), widely used in PVC foil, were responsible for releasing 2-ethylhexyl thioglycolate, which migrated into the medication and reacted with Montelukast. Other APIs with similar functionalities to those of Montelukast may potentially be affected by this discovery, requiring a proper risk assessment during product development in case PVC foil is considered as primary packaging material for these medications.

It should once more be emphasized that the impurities described in this paper posed no risk to patients consuming the commercially available products. The discovery of impurities within medication during long-term stability tests is a not an uncommon occurrence, which is addressed in all pharmaceutical quality systems according to international laws and guidelines. Even the detection of a toxic substance does not automatically pose a health risk, as other factors such as the detected levels, resorption behavior, and its own stability also play a large role. The biological properties of the two diastereomers of **2** are yet to be explored in detail, but the low levels detected (0.26/0.28 area-%) suggest that patient safety is not compromised. Also, many experiments described in this work involve the deliberate manipulation of the formulation to provoke the formation of **2** and do not imply high levels of impurities in products available for patients.

EXPERIMENTAL SECTION

Materials. All chemicals and solvents were used as purchased without further purification. Montelukast chewing tablets (4 mg strength), packaging materials, and PVC foil were commercially available samples. Concentrated hydrochloric acid, formaldehyde, and

https://dx.doi.org/10.1021/acs.chemrestox.0c00261
Chem. Res. Toxicol. 2020, 33, 2963−2971

solvents for synthesis, liquid chromatography, and mass spectrometry, in their respective qualities, were purchased from Merck. The Montelukast sodium salt was provided by Teva Pharmaceutical Industries. BHT was purchased from Cayman Chemical Company, and formulation substances MCC and Crosscarmellose sodium were acquired from FMC BioPolymer. Formic acid and deuterated acetonitrile were purchased from Sigma-Aldrich. Lastly, 2-ethylhexyl thioglycolate and thiophenol were acquired from TCI and Merck, respectively. Ultrapure water was produced by an in-house Merck Millipore Milli-Q system.

General Procedures. Equipment used during degradation experiments included an Ametek Atlas Suntester XLS+, PANalytical X'Pert Pro X-ray source and a reQutec Weiss WKL64 climate chamber.

All ^{1}H and ^{13}C NMR spectra were recorded in deuterated acetonitrile at 297 K and were referenced to residual solvent signals using literature values (1.94 ppm for ^{1}H spectra and 118.26 ppm for ^{13}C spectra).[22] The spectra were acquired using a 400 MHz Bruker Avance Neo 400 (400.15 MHz for ^{1}H and 100.63 MHz for ^{13}C).

High resolution mass spectrometry was performed on a UHR-Qq-TOF Bruker impact II and a spherical high capacity ion trap Bruker HCT ultra in positive ESI mode.

HPLC analysis for LC−UV and LC−MS (HCT ultra) measurements were performed using Agilent 1100 and a Dionex UltiMate 3000 systems, respectively, with column ovens set to 30 °C and detection set to 225 and 324 nm. The hyphenated HPLC−DAD−MS/SPE−NMR system consisted of an Agilent 1290 Infinity II system, a Bruker impact II mass spectrometer, and a Bruker/Spark LC−SPE Interface (3.0 CPL). After separation via HPLC, 5% of the effluent was split to the mass spectrometer, and the remaining sample was channeled through the DAD unit. Once a preset UV intensity was reached within a certain time, the sample was diluted with water (1 mL/min), using an Azura Knauer pump, and redirected to the LC−SPE interface in order to trap each peak on Spark SPE cartridges (10 × 2 mm^2, Hysphere-Resin GP, 10−12 μm pore size). This trapping was performed for 12 HPLC runs with each cartridge being used for 6 trapping cycles (12 trappings of each peak on two separate cartridges). Finally, the loaded cartridges were dried for 30 min under a nitrogen flow, before each of the 12 combined samples were eluted into 2.5 mm NMR tubes by 140 μL of deuterated acetonitrile, using an automated Bruker SamplePro SPE TT system.

The HPLC parameters, solvents, and columns used are listed below alongside the respective experiment. All analytical data of compounds **2** and **3** and their isomers are listed at the end of the Experimental Section. All experiments were performed under exclusion of light by wrapping reaction vessels in aluminum foil, in order to prevent the photoisomerization of Montelukast.

Purity Analysis. Montelukast chewing tablets were ground, and powder, equivalent to 10 mg of Montelukast sodium, was dissolved in 10 mL of acetonitrile/water (3:2), to produce an API solution with an approximately 0.5 mg/mL concentration. A 0.5 mg/mL solution of pure API in acetonitrile water (3:2) was prepared, and the two samples were analyzed via HPLC. The individual diastereomers of impurity **2** were detected at retention times of 36.29 and 37.17 min.

The column used for LC−UV analysis was a Thermo Hypersil BDS C18 with 3.0 μm particle size (125 × 4.0 mm), with a solvent system consisting of a 0.025 M NaH_2PO_4 buffer (pH 3.7) in a 4:1 water/acetonitrile mixture (A) and a 0.025 M NaH_2PO_4 buffer (pH 3.7) in a 4:1 acetonitrile/water mixture (B). Sample solution (20 μL) was injected, and the separation was performed at a flow rate of 1.0 mL/min and a gradient of 47% B, held for 35 min, before switching to 95% B, held for 27 min, and finally returning to 47% B for 10 min.

For LC−MS analysis, a Thermo Hypersil Gold C18 column with 1.9 μm particle size (50 × 3.0 mm) was used, with a solvent system consisting of a 0.010 M ammonium formate buffer (pH 3.7, A) and acetonitrile (B). Sample solution (6 μL) was injected, and the separation was performed at a flow rate of 0.9 mL/min and a gradient of 48.2% B, held for 8.9 min, before switching to 77% B, held for 6.8 min, and finally returning to 48.2% B for 2.5 min.

Degradation and Enrichment Experiments. Both whole and powdered Montelukast chewing tablets, as well as pure API (Montelukast sodium), were used during these experiments. The conditions, time, and additives during degradation and enrichment experiments are listed in the Supporting Information.

For analysis, via HPLC, 0.5 mg/mL solutions of each sample were prepared, as described above, in the purity analysis section. The methods used for LC−MS and LC−UV analyses are also identical.

For LC−NMR analysis, a 20 min isocratic method was applied using an XBridge C8 column with 3.5 μm particle size (250 × 4.6 mm) and a solvent system of 18 and 0.1% formic acid (A) and 82% acetonitrile (B). Sample solution (100 μL) with a concentration of approximately 2.5 mg/mL was injected and separated at a flow of 1.0 mL/min.

The sample for NMR analysis was prepared by dissolving Montelukast (1 equiv, 252.67 mg, 0.42 mmol) in 4.5 mL of DMF and adding 5 g of shredded PVC foil. The mixture was then heated for 14 h at 50 °C and was then twice extracted with 10 and 5 mL of chloroform and filtered by a 1 μm glass fiber filter. The solvent was then removed by rotary evaporation, diluted with a 1:4 water/acetonitrile solution, and once again filtrated.

Synthesis and Mechanism Experiments: General Procedures. Both the synthesis and experiments for the clarification of the mechanism were performed under identical conditions. Analysis and determination of reaction yields were done by application of a short 6 min isocratic LC−UV method using a Thermo Hypersil Gold C18 column with 1.9 μm particle size (50 × 3.0 mm). Sample solution (0.1 μL) was injected, and the analysis was performed at a flow rate of 0.8 mL/min and a solvent system of 20 and 0.1% formic acid (A) and 80% acetonitrile (B).

The general procedure for these experiments consisted of dissolving Montelukast sodium in DMF and heating it to 50 °C. Then, 2-ethylhexyl thioglycolate and the respective additives were added, and the solution was stirred at 50 °C for 2 h. Finally, a sample of 100 μL was diluted with 400 μL of an acetonitrile/water (3:2) solution and analyzed by LC−UV.

Synthesis of 2-(1-((((1*R*)-1-(3-((1*R*/*S*)-2-(7-Chloroquinolin-2-yl)-1-((2-((2-ethylhexyl)oxy)-2-oxoethyl)thio)-ethyl)phenyl)-3-(2-(2-hydroxypropan-2-yl)phenyl)-propyl)thio)methyl)-cyclopropyl)acetic Acid (2), Using Formic Acid. The synthesis was performed via the general procedure. Montelukast sodium (1 equiv, 518.73 mg, 0.85 mmol) was dissolved in DMF (10 mL), and formic acid (200 μL) and 2-ethylhexyl thioglycolate (2.8 equiv, 500 μL, 2.38 mmol) were added. Yield = 97%. Yield after 4 days = 96%.

Synthesis of 2, without Formic Acid. The synthesis was performed via the general procedure. Montelukast sodium (1 equiv, 518.46 mg, 0.85 mmol) was dissolved in DMF (10 mL), and 2-ethylhexyl thioglycolate (2.8 equiv, 500 μL, 2.38 mmol) was added. Yield = 24%. Yield after 4 days = 23%.

Synthesis of 2, with BHT. The synthesis was performed via the general procedure. Montelukast sodium (1 equiv, 608.04 mg, 1.00 mmol) was dissolved in DMF (25 mL), and formic acid (200 μL), 2-ethylhexyl thioglycolate (2.8 equiv, 500 μL, 2.38 mmol), and BHT (2.5 equiv, 549.31 mg, 2.50 mmol) were added. Yield = 76%.

Synthesis of 2, with Equimolar Amounts of Formic Acid. The synthesis was performed via the general procedure. Montelukast sodium (1 equiv, 608.94 mg, 1.00 mmol) was dissolved in DMF (25 mL), and formic acid (1 equiv, 37.73 μL, 1.00 mmol) and 2-ethylhexyl thioglycolate (2.8 equiv, 500 μL, 2.38 mmol) were added. Yield = 69%.

Synthesis of 2, with Equimolar Amounts of 2-Ethylhexyl Thioglycolate. The synthesis was performed via the general procedure. Montelukast sodium (1 equiv, 608.73 mg, 1.00 mmol) was dissolved in DMF (25 mL), and formic acid (200 μL) and 2-ethylhexyl thioglycolate (1 equiv, 210.21 μL, 1.00 mmol) were added. Yield = 51%. Yield after 4 days = 89%.

Synthesis and Isolation of the Sodium Salts of 2. Montelukast sodium (1 equiv, 20.0 g, 32.90 mmol) was dissolved in acetonitrile (300 mL) and water (150 mL), and 2-ethylhexyl thioglycolate (2.9 equiv, 20 mL, 95.00 mmol) was added at room

https://dx.doi.org/10.1021/acs.chemrestox.0c00261
Chem. Res. Toxicol. 2020, 33, 2963−2971

temperature. The solution was stirred for 3 days before the solvent was removed *in vacuo*. The resulting yellow oil was dissolved in an acetonitrile/water mixture (2:3, 150 mL) and was purified by reversed-phase flash chromatography, using a Biotage Isolera LS system with a 100 g YMC ODS AQ C18 column with 20 μm particle size. The solvent system consisted of 0.1% acetic acid (A) and 0.1% acetic acid in acetonitrile (B). Per run, 70 mL of the sample was injected, and purification was performed at a flow of 200 mL/min and a gradient that increased from 75 to 100% within 5.5 column volumes (CV) and remained at 100% until 9 CV were reached. The detection mode was set to 210 and 280 nm. After flash chromatography, an aliquot of the resulting colorless oil was separated into the two isomers by preparative HPLC using a Knauer Azura system and a Phenomenex Gemini NX C18 column with 5 μm particle size (30 × 250 mm). A 12 min isocratic method was applied with a solvent system of 18 and 0.1% acetic acid (A) and 82 and 0.1% acetic acid in acetonitrile (B). The sample (50 mg/mL, 2 mL) was injected per run, and the isolation was performed at a flow rate of 80 mL/min. This isolation was performed twice for isomer **2**. After separation, the two isomers were converted into their sodium salts by addition of a 1 M sodium hydroxide solution, until a pH value of 10 was reached. The two fractions were immediately treated by reversed-phase flash chromatography once more, using the previous conditions; however, replacing the solvent system with water (A) and methanol (B). The resulting fractions were lyophilized to obtain the sodium salts of **2** as white hygroscopic powder. Isomer 1 = 890.00 mg (1.10 mmol). Isomer 2 = 475.00 mg (0.58 mmol). Combined yield = 5%.

Analysis and Separation of the Diastereomers of 2 via a Hyphenated HPLC−DAD−MS/SPE−NMR System. The synthesis was performed via the general procedure. Montelukast sodium (1 equiv, 1012.47 mg, 1.66 mmol) was dissolved in DMF (10 mL), and formic acid (400 μL) and 2-ethylhexyl thioglycolate (2.9 equiv, 1 mL, 4.76 mmol) were added.

Analysis and separation were performed by application of a 30 min isocratic method using a ProntoSIL EuroBOND C18 column with 5.0 μm particle size (125 × 4.0 mm). Undiluted sample solution (5 μL) was injected, and the analysis was performed with a flow rate of 0.7 mL/min and a solvent system of 20 and 0.1% formic acid (A) and 80 and 0.1% formic acid in acetonitrile (B). Trapping onto the SPE cartridges was performed during a 14−20 min time period at an intensity of 180 mAU in the 324 nm detection range. Peak 1 was trapped in a time period of approximately 15.36−16.44 min, and peak 2 was trapped in a time period between 16.74 and 18.05 min.

Synthesis of 2-(1-((((*R*)-1-(3-((*R/S*)-2-(7-Chloroquinolin-2-yl)-1-(phenylthio)ethyl)phenyl)-3-(2-(2-hydroxypropan-2-yl)-phenyl)propyl)thio)methyl)cyclopropyl)acetic Acid (3). Analysis and determination of reaction yields were done by application of a 15 min isocratic LC−UV method using a Thermo Hypersil Gold C18 column with 1.9 μm particle size (50 × 3.0 mm). Sample solution (0.1 μL) was injected, and the analysis was performed at a flow rate of 0.8 mL/min and a solvent system of 20 and 0.1% formic acid (A) and 80% acetonitrile (B).

Montelukast sodium (1 equiv, 2.00 g, 3.29 mmol) was dissolved in DMF (25 mL) and heated to 50 °C. Then, formic acid (800 μL) and thiophenol (2 equiv, 800 μL, 7.84 mmol) were added, and the reaction was stirred at 50 °C for 2 h. Finally, a sample of 100 μL was diluted with 400 μL of a 3:2 acetonitrile/water solution and analyzed by LC−UV. Yield = 96%. Yield after 4 weeks = 42%.

Analysis and Separation of the Two Diastereomers of 3 via a Hyphenated HPLC−DAD−MS/SPE−NMR System. The synthesis was performed, as described above. Montelukast sodium (1 equiv, 2000.36 mg, 3.29 mmol) was dissolved in DMF (25 mL), and formic acid (800 μL) and thiophenol (2.5 equiv, 840 μL, 8.23 mmol) were added.

Analysis and separation were performed by application of a 22 min isocratic method using a ProntoSIL EuroBOND C18 column with 5.0 μm particle size (125 × 4.0 mm). Undiluted sample solution (5 μL) was injected, and the analysis was performed at a flow rate of 0.7 mL/min and a solvent system of 30 and 0.1% formic acid (A) and 70 and 0.1% formic acid in acetonitrile (B). Trapping onto the SPE cartridges was performed during a 15−18 min period of time at an intensity of 1050 mAU in the 324 nm detection range. Peak 1 was trapped in a time period of approximately 16.05−16.66 min, and peak 2 was trapped in a time period between 16.78 and 17.39 min.

Analytical Data of 2. The data for the diastereomers of compound **2** were collected during the different experiments described above (Figure 8). Isomers 1 and 2 do not refer to the individual (*R*)- and (*S*)-diastereomers, respectively, but describe the order in which the samples were detected and collected during HPLC analysis and isolation. NMR, UV−vis, and MS data were collected for the free acids of **2**, whereas the melting point was measured for the isolated sodium salts.

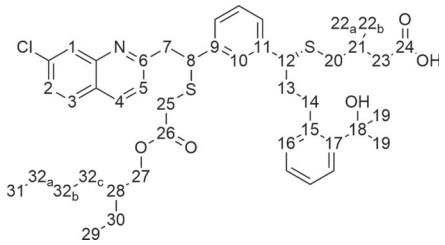

Figure 8. Numbering scheme for the assignment of ^{1}H and ^{13}C NMR signals of **2**.

Isomer 1. ^{1}H NMR (400.15 MHz, CD_3CN): δ 8.13 (d, ^{3}J(H4,H5) = 8.4 Hz, 1H, H4), 7.99 (d, ^{4}J(H1,H2) = 2.1 Hz, 1H, H1), 7.80 (d, ^{3}J(H2,H3) = 8.8 Hz, 1H, H3), 7.48 (dd, ^{3}J(H2,H3) = 8.7, ^{4}J(H1,H2) = 2.1 Hz, 1H, H2), 7.38 (s, 1H, H10), 7.39−7.36 (m, 1H, H_{arom}), 7.34 (d, ^{3}J(H4,H5) = 8.4 Hz, 1H, H5), 7.29−7.20 (m, 3H, H_{arom}), 7.17−7.05 (m, 2H, H_{arom}), 7.02 (dd, J = 6.8, 2.4 Hz, 1H, H16), 4.64 (t, ^{3}J(H7/7′,H8) = 7.6 Hz, 1H, H8), 3.97−3.90 (m, 2H, H27), 3.89 (dd, J = 8.4, 6.3 Hz, 1H, H12), 3.55 (dd, ^{2}J(H7,H7′) = 13.8, ^{3}J(H7,H8) = 7.7 Hz, 1H, H7), 3.50 (dd, ^{2}J(H7,H7′) = 13.9, ^{3}J(H7′,H8) = 7.5 Hz, 1H, H7′), 3.10 (d, ^{2}J(H25,H25′) = 15.0 Hz, 1H, H25), 3.02−2.92 (m, 1H, H14), 2.95 (d, ^{2}J(H25,H25′) = 15.3 Hz, 1H, H25′), 2.65 (ddd, J = 13.1, 11.4, 5.2 Hz, 1H, H14′), 2.41 (d, ^{2}J(H20,H20′) = 13.4 Hz, 1H, H20), 2.35 (d, ^{2}J(H23,H23′) = 16.2 Hz, 1H, H23), 2.34 (d, ^{2}J(H20,H20′) = 13.2 Hz, 1H, H20′), 2.27 (d, ^{2}J(H23,H23′) = 16.2 Hz, 1H, H23′), 2.15−1.95 (m, 2H, H13), 1.54−1.41 (m, 1H, H28), 1.46 (s, 6H, H19), 1.34−1.16 (m, 8H, H30 and $H32_{a-c}$), 0.88−0.77 (m, 6H, H29 and H31), 0.46−0.36 (m, 2H, $H22_a$ or $H22_b$), 0.38−0.25 ppm (m, 2H, $H22_a$ or $H22_b$). ^{13}C NMR (100.63 MHz, CD_3CN): δ 173.8 (C24), 171.2 (C26), 161.7 (C6), 148.6 (C_{arom}), 147.1 (C17), 144.2 (C11), 142.0 (C9), 141.1 (C15), 137.5 (C4), 135.9 (C_{arom}), 132.3 (C16), 130.4 (C3), 129.6 (C_{arom}), 129.1 (C10), 128.1 (C_{arom}), 127.8 (C_{arom}), 127.7 (C_{arom}), 127.4 (C_{arom}), 126.4 (C_{arom}), 123.6 (C5), 73.5 (C18), 68.0 (C27), 50.6 (C12), 50.3 (C8), 45.2 (C7), 40.5 (C13), 40.3 (C23), 39.6 (C28), 39.2 (C20), 33.5 (C25), 33.1 (C14), 32.1 (C19), 31.0 (C32), 29.5 (C32), 24.4 (C30), 23.6 (C32), 17.5 (C21), 14.3 (C31), 13.0 (C22), 12.6 (C22), 11.3 ppm (C29). HRMS (ESI): m/z calculated for $C_{45}H_{56}ClNO_5S_2$ + H^+ [M + H^+] = 790.3361, found = 790.3368. Melting point: 94.7 °C.

Isomer 2. ^{1}H NMR (400.15 MHz, CD_3CN): δ 8.20 (d, ^{3}J(H4,H5) = 8.4 Hz, 1H, H4), 7.99 (d, ^{4}J(H1,H2) = 2.1 Hz, 1H, H1), 7.85 (d, ^{3}J(H2,H3) = 8.8 Hz, 1H, H3), 7.51 (dd, ^{3}J(H2,H3) = 8.8, ^{4}J(H1,H2) = 2.1 Hz, 1H, H2), 7.49 (s, 1H, H10), 7.42 (d, ^{3}J(H4,H5) = 8.4 Hz, 1H, H5), 7.38−7.27 (m, 3H, H_{arom}), 7.21−7.16 (m, 1H, H_{arom}), 7.14−7.04 (m, 3H, H_{arom}), 4.57 (dd, ^{3}J(H7′,H8) = 9.0, ^{3}J(H7,H8) = 6.3 Hz, 1H, H8), 3.96 (dd, J = 8.3, 6.0 Hz, 1H, H12), 3.91−3.84 (m, 2H, H27), 3.70 (dd, ^{2}J(H7,H7′) = 13.7, ^{3}J(H7,H8) = 6.3 Hz, 1H, H7), 3.46 (dd, ^{2}J(H7,H7′) = 13.8, ^{3}J(H7′,H8) = 9.0 Hz, 1H, H7′), 3.03 (d, ^{2}J(H25,H25′) = 14.9 Hz, 1H, H25), 3.03−2.91 (m, 1H, H14), 2.91 (d, ^{2}J(H25,H25′) = 15.1 Hz, 1H, H25′), 2.73 (d, ^{2}J(H23,H23′) = 16.2 Hz, 1H, H23), 2.78−2.66 (m, 1H, H14′), 2.44 (d, ^{2}J(H20,H20′) = 12.4 Hz, 1H, H20), 2.18 (d, ^{2}J(H20,H20′) = 12.4 Hz, 1H, H20′), 2.08 (d, ^{2}J(H23,H23′) = 16.7 Hz, 1H, H23′), 2.18−1.97 (m, 2H, H13), 1.49−1.39 (m, 1H, H28), 1.45 (s, 6H, H19),

https://dx.doi.org/10.1021/acs.chemrestox.0c00261
Chem. Res. Toxicol. 2020, 33, 2963−2971

1.28−1.10 (m, 8H, H30 and H32$_{a-c}$), 0.86−0.78 (m, 3H, H31), 0.76 (td, ^3J(H29,H30) = 7.5, ^4J(H28,H30) = 3.4 Hz, 3H, H29), 0.51−0.38 (m, 2H, H22$_a$ or H22$_b$), 0.40−0.27 ppm (m, 2H, H22$_a$ or H22$_b$). ^{13}C NMR (100.63 MHz, CD_3CN): δ 174.1 (C24), 171.2 (C26), 161.9 (C6), 148.4 (C$_{arom}$), 147.1 (C17), 143.8 (C11), 142.7 (C9), 141.1 (C15), 137.9 (C4), 136.1 (C$_{arom}$), 132.4 (C16), 130.6 (C3), 129.6 (C$_{arom}$), 128.9 (C$_{arom}$), 128.7 (C$_{arom}$),128.0 (C$_{arom}$), 127.6 (C$_{arom}$), 127.3 (C$_{arom}$), 127.0 (C$_{arom}$), 126.5 (C$_{arom}$), 126.4 (C$_{arom}$), 126.4 (C$_{arom}$), 124.2 (C5), 73.5 (C18), 67.9 (C27), 51.0 (C8), 50.6 (C12), 44.9 (C7), 41.2 (C13), 40.0 (C23), 39.5 (C28), 39.3 (C20), 33.4 (C25), 33.0 (C14), 32.1 (C19), 30.9 (C32), 29.5 (C32), 24.3 (C30), 24.0 (C32), 17.0 (C21), 14.3 (C31), 12.9 (C22), 12.7 (C22), 11.2 ppm (C29). HRMS (ESI): m/z calculated for $C_{45}H_{56}ClNO_5S_2$ + H^+ [M + H^+] = 790.3361, found = 790.3363. Melting point: 59.4 °C.

Analytical Data of 3. The data for the diastereomers of compound **3** were collected during the different experiments described above (Figure 9). Isomers 1 and 2 do not refer to the individual (*R*)- and (*S*)-diastereomers, respectively, but describe the order in which the samples were detected and collected during HPLC analysis and isolation.

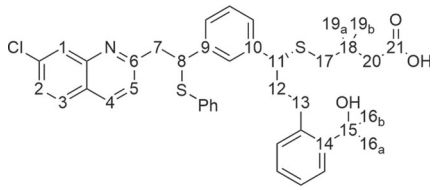

Figure 9. Numbering scheme for the assignment of ^{1}H and ^{13}C NMR signals of **3**.

Isomer I. ^{1}H NMR (400.15 MHz, CD_3CN): δ 8.10 (d, ^3J(H4,H5) = 8.5 Hz, 1H, H4), 7.99 (d, ^4J(H1,H2) = 2.1 Hz, 1H, H1), 7.78 (d, ^3J(H2,H3) = 8.8 Hz, 1H, H3), 7.47 (dd, ^3J(H2,H3) = 8.7, ^4J(H1,H2) = 2.1 Hz, 1H, H2), 7.41−7.28 (m, 5H, H$_{arom}$), 7.22−7.05 (m, 8H, H$_{arom}$), 6.99−6.93 (m, 1H, H$_{arom}$), 4.98 (t, ^3J(H7,H8) = 7.7 Hz, 1H, H8), 3.83 (dd, J = 8.3, 6.4 Hz, 1H, H11), 3.58 (d, ^3J(H7,H8) = 7.7 Hz, 1H, H7), 2.94 (ddd, J = 13.2, 11.5, 4.9 Hz, 1H, H13), 2.54 (ddd, J = 13.0, 11.4, 5.1 Hz, 1H, H13′), 2.40−2.22 (m, 4H, H17 and H20), 2.06−1.86 (m, 2H, H12), 1.48 (s, 3H, H16$_a$ or H16$_b$), 1.47 (s, 3H, H16$_a$ or H16$_b$), 0.47−0.36 (m, 2H, H19$_a$ or H19$_b$), 0.33−0.21 ppm (m, 2H, 192$_a$ or H19$_b$). ^{13}C NMR (100.63 MHz, CD_3CN): δ 174.0 (C21), 161.7 (C6), 149.0 (C$_{arom}$), 147.0 (C14), 144.1 (C10), 142.2 (C9), 141.0 (C$_{arom}$), 137.3 (C4), 135.8 (C$_{arom}$), 132.6 (C$_{arom}$), 132.3 (C$_{arom}$), 130.4 (C3), 129.7 (C$_{arom}$), 129.2 (C$_{arom}$), 128.7 (C$_{arom}$), 127.3 (C$_{arom}$), 128.0 (C$_{arom}$), 127.8 (C$_{arom}$), 127.8 (C$_{arom}$), 127.8 (C$_{arom}$), 127.4 (C$_{arom}$) 126.4 (C$_{arom}$), 126.4 (C$_{arom}$), 126.3 (C$_{arom}$), 126.3 (C$_{arom}$), 123.6 (C$_{arom}$), 127.6 (C$_{arom}$), 127.6 (C$_{arom}$), 73.5 (C15), 53.2 (C8), 50.5 (C11), 45.5 (C7), 40.5 (C12), 40.2 (C17 or C20), 39.2 (C17 or C20), 33.0 (C13), 32.1 (C16), 17.5 (C18), 14.3 (C31), 12.9 (C19), 12.5 ppm (C19). HRMS (ESI): m/z calculated for $C_{41}H_{42}ClNO_3S_2$ + H^+ [M + H^+] = 696.2367, found = 696.2370.

Isomer II. ^{1}H NMR (400.15 MHz, CD_3CN): δ 8.15 (d, ^3J(H4,H5) = 8.4 Hz, 1H, H4), 7.98 (d, ^4J(H1,H2) = 2.1 Hz, 1H, H1), 7.81 (d, ^3J(H2,H3) = 8.8 Hz, 1H, H3), 7.49 (dd, ^3J(H2,H3) = 8.7, ^4J(H1,H2) = 2.1 Hz, 1H, H2), 7.40 (d, ^3J(H4,H5) = 8.4 Hz, 1H, H5), 7.40−7.37 (m, 2H, H$_{arom}$), 7.29−7.04 (m, 10H, H$_{arom}$), 6.99 (dd, J = 7.2, 2.0 Hz, 1H, H$_{arom}$), 4.93 (t, ^3J(H7/7′,H8) = 7.6 Hz, 1H, H8), 3.87 (dd, J = 8.1, 6.4 Hz, 1H, H11), 3.68 (dd, ^2J(H7,H7′) = 13.9, ^3J(H7,H8) = 7.4 Hz, 1H, H7), 3.57 (dd, ^2J(H7,H7′) = 13.9, ^3J(H7′,H8) = 7.5 Hz, 1H, H7′), 2.92 (ddd, J = 13.1, 11.6, 5.0 Hz, 1H, H13), 2.55 (d, ^2J(H20,H20′) = 16.4 Hz, 1H, H20), 2.65− (m, 1H, H13′), 2.35 (d, ^2J(H17,H17′) = 12.8 Hz, 1H, H17), 2.21 (d, ^2J(H17,H17′) = 12.8 Hz, 1H, H17′), 2.18 (d, ^2J(H20,H20′) = 16.2 Hz, 1H, H20′), 2.06−1.86 (m, 2H, H12), 1.48 (s, 3H, H16$_a$ or H16$_b$), 1.47 (s, 3H, H16$_a$ or H16$_b$), 0.50−0.39 (m, 2H, H19$_a$ or H19$_b$), 0.35−0.24 ppm (m, 2H, H19$_a$ or H19$_b$). ^{13}C NMR (100.63 MHz, CD_3CN): δ 174.0 (C21), 161.8 (C6), 148.5 (C$_{arom}$), 147.1 (C14), 143.9 (C10), 142.9 (C9), 141.1 (C$_{arom}$), 137.6 (C4), 137.5 (C$_{arom}$), 135.9 (C$_{arom}$), 135.5 (C$_{arom}$), 132.7 (C$_{arom}$), 132.4 (C$_{arom}$), 130.5 (C3), 130.1 (C$_{arom}$), 129.7 (C$_{arom}$), 129.3 (C$_{arom}$), 128.5 (C$_{arom}$), 127.2 (C$_{arom}$), 128.0 (C$_{arom}$), 127.9 (C$_{arom}$), 127.6 (C$_{arom}$), 127.5 (C$_{arom}$), 127.1 (C$_{arom}$) 126.4 (C$_{arom}$), 126.4 (C$_{arom}$), 126.4 (C$_{arom}$), 124.0 (C5), 73.6 (C15), 53.8 (C8), 50.5 (C11), 45.4 (C7), 40.9 (C12), 40.0 (C20), 39.2 (C17), 32.9 (C13), 32.1 (C16$_a$ and C16$_b$), 17.2 (C18), 12.8 ppm (C19$_a$ and C19$_b$). HRMS (ESI): m/z calculated for $C_{41}H_{42}ClNO_3S_2$ + H^+ [M + H^+] = 696.2367, found = 696.2372.

■ ASSOCIATED CONTENT

Supporting Information

The Supporting Information is available free of charge at https://pubs.acs.org/doi/10.1021/acs.chemrestox.0c00261.

Additional figures and spectra, experimental procedures for degradation tests, and NMR spectra (PDF)

■ AUTHOR INFORMATION

Corresponding Authors

Konstantin Karaghiosoff − *Department Chemie, Ludwig-Maximillians-Universität München, 81377 Munich, Germany*; orcid.org/0000-0002-8855-730X; Phone: +49 (0)89 2180-77426; Email: Konstantin.Karaghiosoff@cup.uni-muenchen.de; Fax: +49 (0)89 2180-77398

Hans-Christian Müller − *Analytical Development, Hexal AG, 83607 Holzkirchen, Germany*; Phone: +49 8024 908 2200; Email: dhcm@gmx.de

Authors

Philipp Schmidt − *Department Chemie, Ludwig-Maximillians-Universität München, 81377 Munich, Germany*; orcid.org/0000-0001-9401-0434

Christine Kolb − *Analytical Development, Hexal AG, 83607 Holzkirchen, Germany*

Andreas Reiser − *Analytical Development, Hexal AG, 83607 Holzkirchen, Germany*

Markus Philipp − *Analytical Development, Hexal AG, 83607 Holzkirchen, Germany*

Markus Godejohann − *Bruker BioSpin GmbH, 76287 Rheinstetten, Germany*

Hannes Helmboldt − *LGC GmbH, D-14943 Luckenwalde, Germany*

Complete contact information is available at: https://pubs.acs.org/10.1021/acs.chemrestox.0c00261

Author Contributions

The manuscript was written through contributions of all authors. All authors have given approval to the final version of the manuscript.

Notes

The authors declare no competing financial interest.

■ ACKNOWLEDGMENTS

We thank the Hexal AG (Industriestraße 25, 83607 Holzkirchen, Germany) for providing funds and materials, as well as the facilities, equipment, and analytical machines, necessary for the research of this paper. We also gratefully acknowledge Bruker BioSpin GmbH for their support and expertise in the measurements and evaluation of NMR data. We would also like to thank the staff of LGC for the isolation of the two stereoisomers.

■ ABBREVIATIONS

AIBN, azobis(isobutyronitrile); API, active pharmaceutical ingredient; arom, aromatic; BHT, dibutylhydroxytoluene; Bu, *n*-butyl; COSY, correlation spectroscopy (NMR); CV, column volume; DAD, diode array detector; DMF, *N,N*-dimethylformamide; ESI, electrospray ionization; Et, ethyl; HMBC, heteronuclear multiple bond correlation (NMR); HPLC, high performance liquid chromatography; HRMS, high resolution mass spectrometry; HSQC, heteronuclear single quantum correlation (NMR); LC, liquid chromatography; MCC, microcrystalline cellulose; MS, mass spectrometry; NMR, nuclear magnetic resonance; Oct, *n*-octyl; PVC, polyvinyl chloride; Q, quadrupole (MS); q, radio frequency quadrupole (MS); SPE, solid phase extraction; THF, tetrahydrofuran; TOF, time-of-flight (MS); UHR, ultrahigh rsolution; UV−vis, ultraviolet−visible

■ REFERENCES

(1) Maafi, M., and Maafi, W. (2014) Montelukast photodegradation: Elucidation of Φ-order kinetics, determination of quantum yields and application to actinometry. *Int. J. Pharm. 471*, 544−552.

(2) Roman, J., Breier, A. R., and Steppe, M. (2011) Stability Indicating LC Method to Determination of Sodium Montelukast in Pharmaceutical Dosage Form and its Photodegradation Kinetics. *J. Chromatogr. Sci. 49*, 540−546.

(3) Scott, J. P., and Peters-Golden, M. (2013) Antileukotriene Agents for the Treatment of Lung Disease. *Am. J. Respir. Crit. Care Med. 188*, 538−544.

(4) Fisch, M. H., Bacaloglu, R., Biesiada, K., and Brecker, L. R. (1999) Mechanism of Organotin Stabilization of Poly(Vinyl Chloride). 2: Significance for PVC Stabilization of Structure and Equilibria of Alkyltin ThiogIycolates/Chlorides. *J. Vinyl Addit. Technol. 5*, 45−51.

(5) Seidler, H., Woggon, H., Härtig, M., and Uhde, W.-J. (1969) Beitrag zur Prüfung von Bedarfsgegenständen aus Plasten. Untersuchungen über die Auswanderung von Di-n-octyl-(l-^{14}C)-zinndithioglykolsäure-2-äthylhexylester aus Hart-PVC in Speiseöl. *Nahrung 3*, 257−264.

(6) Costlow, R. D., Nasshan, H., and Frenkel, P. (2017) Simulated gastric hydrolysis and developmental toxicity of dioctyltin bis(2-Ethylhexylthioglycolate) [DOTE] in rabbits and mice. *Regul. Toxicol. Pharmacol. 87*, 23−29.

(7) del Barrio, M.-A., Hu, J., Zhou, P., and Cauchon, N. (2006) Simultaneous determination of formic acid and formaldehyde in pharmaceutical excipients using headspace GC/MS. *J. Pharm. Biomed. Anal. 41*, 738−743.

(8) Wasylaschuk, W. R., Harmon, P. A., Wagner, G., Harman, A. B., Templeton, A. C., Xu, H., and Reed, R. A. (2007) Evaluation of Hydroperoxides in Common Pharmaceutical Excipients. *J. Pharm. Sci. 96*, 106−116.

(9) Sinha, A. K., and Equbal, D. T. (2019) Thiol-Ene Reaction: Synthetic Aspects and Mechanistic Studies of an Anti-Markovnikov-Selective Hydrothiolation of Olefins. *Asian J. Org. Chem. 8*, 32−47.

(10) Harvison, M. A., and Lowe, A. B. (2011) Combining RAFT Radical Polymerization and Click/Highly Efficient Coupling Chemistries: A Powerful Strategy for the Preparation of Novel Materials. *Macromol. Rapid Commun. 32*, 779−800.

(11) Hoyle, C. E., Lowe, A. B., and Bowman, C. N. (2010) Thiol-click chemistry: a multifaceted toolbox for small molecule and polymer synthesis. *Chem. Soc. Rev. 39*, 1355−1387.

(12) Lowe, A. B. (2010) Thiol-ene 'click' reactions and recent applications in polymer and materials synthesis. *Polym. Chem. 1*, 17−36.

(13) Nair, D. P., Podgórski, M., Chatani, S., Gong, T., Xi, W., Fenoli, C. R., and Bowman, C. N. (2014) The Thiol-Michael Addition Click Reaction: A Powerful and Widely Used Tool in Materials Chemistry. *Chem. Mater. 26*, 724−744.

(14) Wang, T., Hu, B., Huang, J., Li, Q.-F., and Wang, Z. (2019) Luminescent mesoporous hybrid materials grafted with lanthanide complexes synthesized by Michael-like addition reaction. *J. Porous Mater. 26*, 567−574.

(15) Frayne, S. T. (2018) Ph.D. Thesis, *Thiol-Michael Reaction: From First Principles to Applications in Macromolecular Synthesis*, Wesleyan University, Middletown, CT.

(16) Movassagh, B., and Shaygan, P. (2006) Michael addition of thiols to α,β-unsaturated carbonyl compounds under solvent-free conditions. *ARKIVOC 7*, 130−137.

(17) Budyka, M. F. (2012) Diarylethene photoisomerization and photocyclization mechanisms. *Russ. Chem. Rev. 81*, 477−493.

(18) Görner, H., Fojtik, A., Wróblewski, J., and Currell, L. J. (1985) Singlet Mechanism of Trans -> Cis Photoisomerization of Quaternary Salts of 4- Substituted 4'-Azastilbenes (R = CN, H, CH_3, and OCH_3) and theri Quinolinium Analogues. *Z. Naturforsch., A: Phys. Sci. 40a*, 525−537.

(19) Oshkin, I. V., and Budyka, M. F. (2010) Quantum-Chemical Study of the Photoisomerization and Photocyclization Reactions of Styrylquinolines: Potential Energy Surfaces. *High Energy Chem. 44*, 506−515.

(20) Halama, A., Jirman, J., Bouškova, O., Gibala, P., and Jarrah, K. (2010) Improved Process for the Preparation of Montelukast: Development of an Efficient Synthesis, Identification of Critical Impurities and Degradants. *Org. Process Res. Dev. 14*, 425−431.

(21) Kumar, S., Anjaneyulu, G. S. R., and Bindu, V. H. (2011) Identification, Synthesis and Characterization of Impurities of Montelukast Sodium. *Asian J. Cjem. 23*, 4536−4546.

(22) Babij, N. R., McCusker, E. O., Whiteker, G. T., Canturk, B., Choy, N., Creemer, L. C., De Amicis, C. V., Hewlett, N. M., Johnson, P. L., Knobelsdorf, J. A., Li, F., Lorsbach, B. A., Nugent, B. M., Ryan, S. J., Smith, M. R., and Yang, Q. (2016) NMR Chemical Shifts of Trace Impurities: Industrially Preferred Solvents Used in Process and Green Chemistry. *Org. Process Res. Dev. 20*, 661−667.

https://dx.doi.org/10.1021/acs.chemrestox.0c00261
Chem. Res. Toxicol. 2020, 33, 2963−2971

2.3 Supporting Information

Formation of a Thiol-Ene Addition Product of Asthma Medication Montelukast Caused by a Widespread Tin-Based Thermal Stabilizer

Philipp Schmidt[†], Christine Kolb[‡], Andreas Reiser[‡], Markus Philipp[‡], Markus Godejohann[§], Hannes Helmboldt[ǁ], Hans-Christian Müller[‡*], Konstantin Karaghiosoff[†*]

[†]Department Chemie, Ludwig-Maximillians-Universität München, Butenandtstraße 5-13, Haus D, 81377 Munich, Germany, [‡]Analytical Development, Hexal AG, Industriestraße 25, 83607 Holzkirchen, Germany, [§]Bruker BioSpin GmbH, 76287 Rheinstetten, Germany, [ǁ]LGC GmbH, Louis-Pasteur-Str. 30, D-14943 Luckenwalde, Germany

Table of Contents

The programs used to produce the images in these supporting informations were *Compass Hystar* from Bruker, *Chromeleon* from Thermo Scientific as well as *MestreNova* from Mestrelab Research.

I Degradation Experiments

Degradation experiments were performed with pure API (Montelukast-Na), whole and ground bulk Montelukast chewing tablets. Experiments with the API used 1 g of Montelukast-Na powder and ground tablets used 1 g of powdered tablets taken from a total of ten powdered bulk tablets. Aside from photo stress experiments this powder was weighed in amber glass phials and stored for the listed time and temperature along with the mentioned additive.

Table S1: List of performed photo stress experiments.

Material	Additives	Stress Conditions	Temperature	Time	Detection of 2
Ground Montelukast chewing tablets	-	Laboratory light	rt	4 h	No
Ground Montelukast chewing tablets	-	Solar simulator (E = 250 W/m^2)	30 °C	4 h	No
Montelukast-Na powder	-	Solar simulator (E = 250 W/m^2)	30 °C	22 – 104 h	No
Montelukast-Na powder	-	X-Ray radiation Cu Kα: λ = 1.546 Å	rt	15 min	No
Montelukast-Na powder	Mannitol	Laboratory light	rt	4 h	No
Montelukast-Na powder	Mannitol	Solar simulator (E = 250 W/m^2)	30 °C	4 h	No
No detection of **2** during photo stress					

Table S2: Performed thermal and hydrolytic stress experiment.

Material	Additives	Stress Conditions	Temperature	Time	Detection of 2
Ground Montelukast chewing tablets	Ultra-pure water	Stored in amber vial	50 and 70 °C	140 h	No
No detection of **2** during combined thermal and hydrolytic stress of powdered Montelukast chewing tablets					

Table S3: Performed thermal stress tests with Montelukast chewing tablets and added packaging foil.

Material	Stress Conditions	Temperature	Time	Detection of 2
Whole Montelukast chewing tablet	Tablet wrapped in blister material	50 and 70 °C	183 h	Yes
Ground Montelukast chewing tablets	Pieces of lidding foil (not printed) added to powder	50 °C	44 h – 7 d	No
Ground Montelukast chewing tablets	Pieces of printed lidding foil added to powder	50 °C	44 h – 7 d	No
Ground Montelukast chewing tablets	Pieces of forming foil added to powder	50 °C	44 h – 7 d	Yes
Ground Montelukast chewing tablets	Powder wrapped in forming foil (PVC side in contact with mixture)	50 °C	2 d	Yes
Detection of **2** during thermal stress of powdered tablets in combination with forming foil (PVC side in contact with powder)				

Table S4: Performed thermal stress experiments of API and placebo mixtures (25/75 %) with added packaging foil.

Material	Stress Conditions	Temperature	Time	Detection of 2
Montelukast-Na/Placebo Mixture	Mixture wrapped in forming foil (PVC side in contact with mixture)	50 °C	5/8 d	Yes
Montelukast-Na/Placebo Mixture	Mixture wrapped in forming foil (PA side in contact with mixture)	50 °C	5/8 d	No
Montelukast-Na/Placebo Mixture	Pieces of forming foil added to mixture	50 °C	5/8 d	No
Detection of **2** during thermal stress of Montelukast-Na/placebo mixture (25/75 %) in combination with forming foil (PVC side in contact with mixture)				

Table S5: Thermal stress tests of API and selected excipient mixtures with added forming foil.

Material	Additives	Stress Conditions	Temperature	Time	Detection of 2
Montelukast-Na powder	Crosscarmellose-Na	Mixture wrapped in forming foil (PA side in contact with mixture)	50 °C	7 d	Yes
Montelukast-Na powder	Ferric oxide (red)		50 °C	7 d	No
Montelukast-Na powder	MCC		50 °C	7 d	Yes
Montelukast-Na powder	Hydroxypropyl Cellulose		50 °C	7 d	No
Montelukast-Na powder	Aroma		50 °C	7 d	No
Montelukast-Na powder	Mannitol		50 °C	7 d	No
Montelukast-Na powder	Magnesium Stearate		50 °C	7 d	No
Montelukast-Na powder	MCC, Crosscarmellose-Na		50 °C	6 d	Yes
Detection of **2** during thermal stress of Montelukast-Na mixed with Crosscarmellose-Na and/or MCC in combination with formin foil (PVC side in contact with mixture)					

Table S6: Thermal stress tests of API powder and added packaging foil.

Material	Stress Conditions	Temperature	Time	Detection of 2
Montelukast-Na powder	Wrapped in forming foil (dull PA side in contact with powder)	50 °C	8 d	No
Montelukast-Na powder	Wrapped in forming foil (PVC side in contact with powder)	50 °C	8 d	No
Montelukast-Na powder	Pieces of lidding foil (not printed) added to powder	50 °C	8 d	No
Montelukast-Na powder	Pieces of forming foil added to powder	50 °C	44 h – 7 d	No
Montelukast-Na powder	Pieces of printed lidding foil added to powder	50 °C	44 h – 7 d	No
Montelukast-Na powder	Pieces of forming foil added to powder	50 °C	44 h – 7 d	No
No detection of **2** during thermal stress of Montelukast-Na in combination with packaging material alone				

Table S7: Stress tests of API/ground chewing tablets with selected reagents and pieces of forming foil added.

Material	Additives	Stress Conditions	Temperature	Time	Detection of 2
Ground Montelukast chewing tablets	Water	Pieces of forming foil added to mixture	50 °C	15 h	No
Ground Montelukast chewing tablets	Formic acid		50 °C	15 h	Yes
Montelukast-Na powder	0.3 % Hydrogen peroxide		50 °C	15 h	No
Montelukast-Na powder	Water and DMF		50 °C	15 h	Yes
Montelukast-Na powder	Formic acid and DMF	Pieces of forming foil added to mixture	50 °C	15 h	Yes
Montelukast-Na powder	37 % hydrochloric acid and DMF		50 °C	15 h	Yes
Montelukast-Na powder	30 % Hydrogen peroxide and DMF		50 °C	15 h	No
Montelukast-Na powder	Formic acid and MeOH		50 °C	15 h	Yes
Montelukast-Na powder	30 % Hydrogen peroxide and MeOH	Pieces of forming foil added to mixture	50 °C	15 h	No
Montelukast-Na powder	Formaldehyde and water		50 °C	15 h	Yes
Montelukast-Na powder	Formaldehyde and MeOH		50 °C	15 h	Yes
Montelukast-Na powder	Formaldehyde and DMF		50 °C	15 h	Yes
Detection of **2** during thermic stress of Montelukast-Na in combination with forming foil and in the presence of acid (hydrochloric and formic acid) or precursors to acid (formaldehyde)					

Table S8: Stress tests with blanc values of API powder in combination with selected additives and no packaging foil added.

Material	Additives	Temperature	Time	Detection of 2
Montelukast-Na powder	MeOH and pieces of forming foil	50 °C	15 h	No
Montelukast-Na powder	DMF and pieces of forming foil	50 °C	15 h	No
Montelukast-Na powder	Formic acid and DMF	50 °C	15 h	No
Montelukast-Na powder	DMF	50 °C	15 h	No
Montelukast-Na powder	Formic acid	50 °C	15 h	No
Montelukast-Na powder	Aluminum foil, formic acid and DMF	50 °C	20 h	No
No detection of **2** the blanc values				

Table S9: Thermal stress of API powder with PVC foil, formic acid and DMF for enrichment of 2.

Material	Additives	Temperature	Time	Detection of 2
Montelukast-Na powder	PVC foil, formic acid and DMF	50 °C	20 h	Yes
Detection of **2** during the enrichment experiment leading to the conclusion, that the reactant causing the formation of **2** is present in the forming foil				

II UV and MS Chromatograms

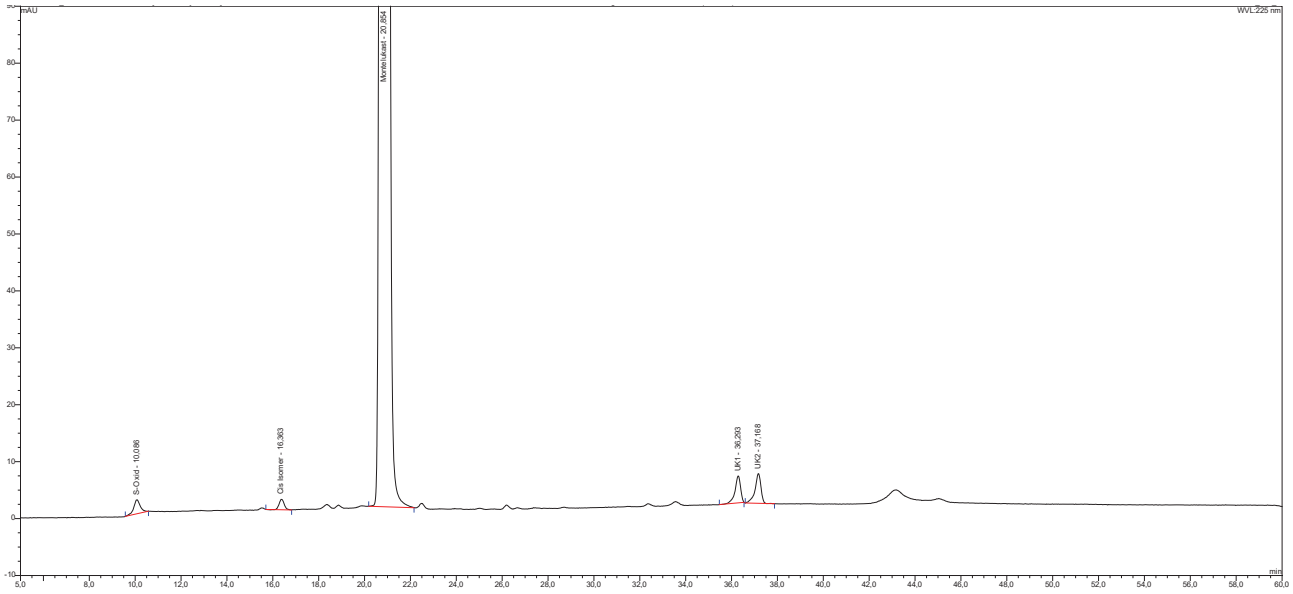

Figure S1: UV chromatogram from stability tests of Montelukast 4 mg chewing tablets stored for 12 months at 25 °C at a relative humidity of 60% in packaging blisters (zoom 5 – 60 min). Montelukast (**1**) is visible at 20.9 min and the new diastereomers of unknown compound (**2**) are visible at 36.3 and 37.2 min.

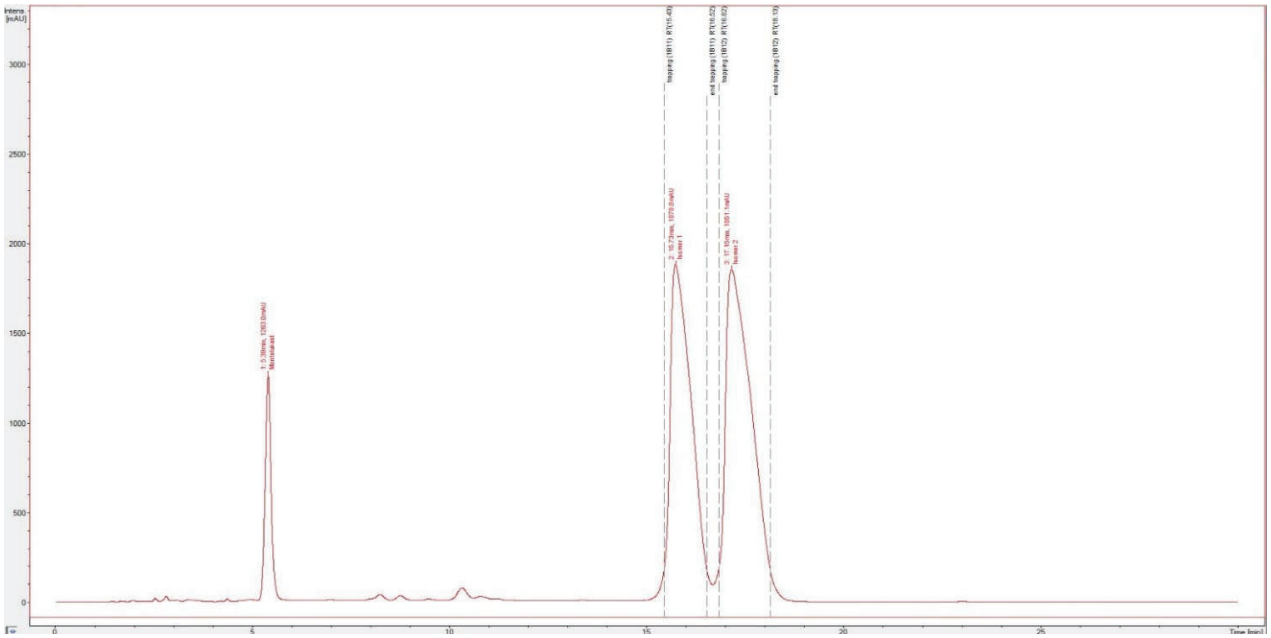

Figure S2: UV chromatogram of the isolation of the diastereomers of compound **2** from the reaction solution, using a hyphenated HPLC-DAD-HRMS/SPE system. Montelukast is visible at 5.4 min and both isomers of the Montelukast-thioglycolate addition product are visible at 15.7 and 17.2 min. The time during which the compounds were trapped on SPE cartridges is marked by dashed lines.

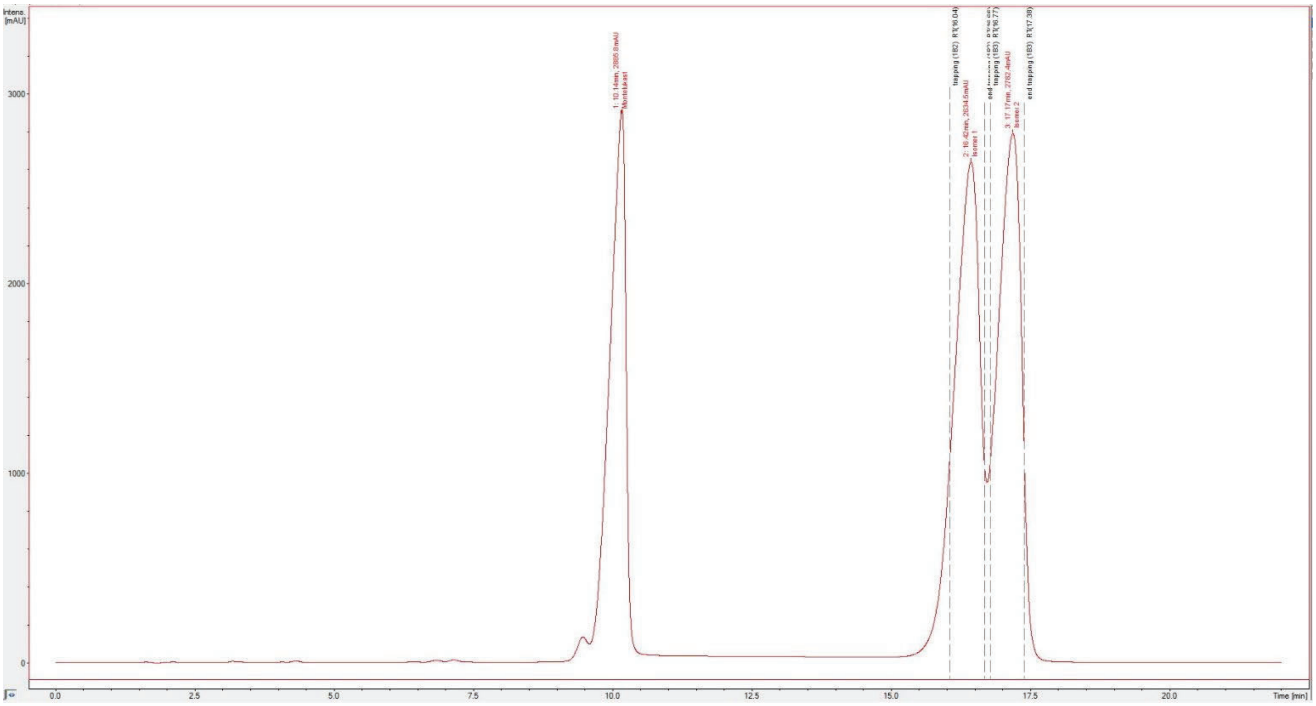

Figure S3: UV chromatogram of the isolation of the diastereomers of compound **3** from the reaction solution, using a hyphenated HPLC-DAD-HRMS/SPE system. Montelukast is visible at 10.1 min and the two isomers of the Montelukast-thiophenol addition product are visible at 16.4 and 17.2 min. The time during which the compounds were trapped on SPE cartridges is marked by dashed lines.

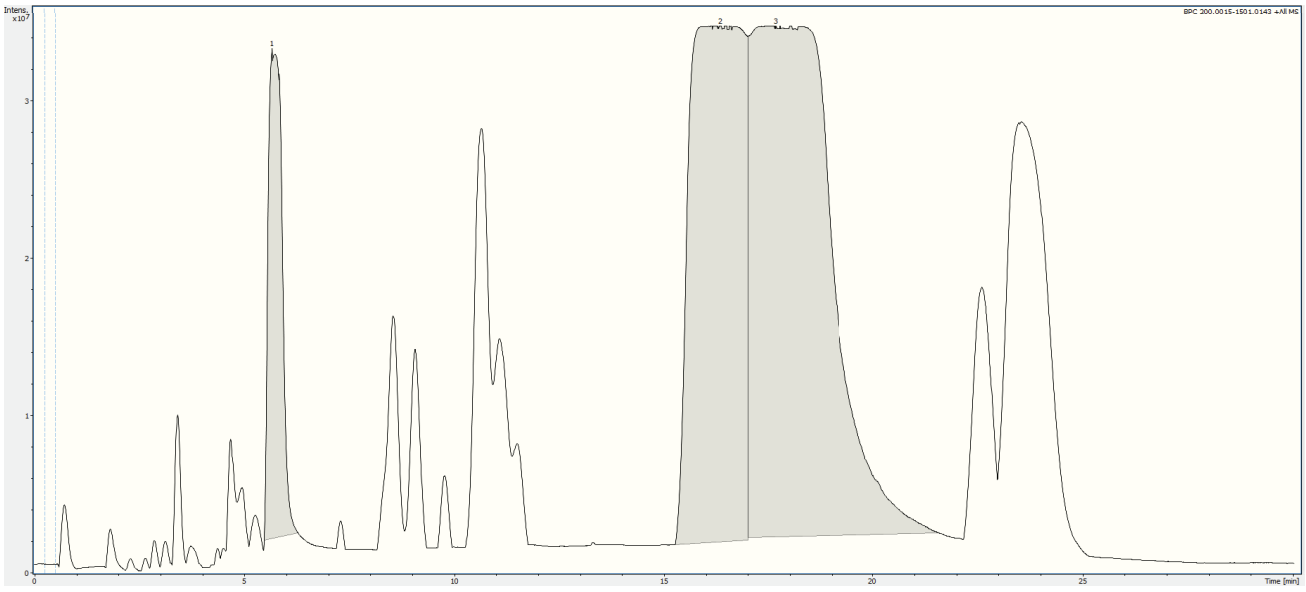

Figure S4: MS chromatogram of the reaction solution of Montelukast and 2-ethylhexyl thioglycolate under acidic conditions. Montelukast is visible at 5.7 min and both isomers of the Montelukast-thioglycolate addition product are visible at 16.4 and 17.7 min.

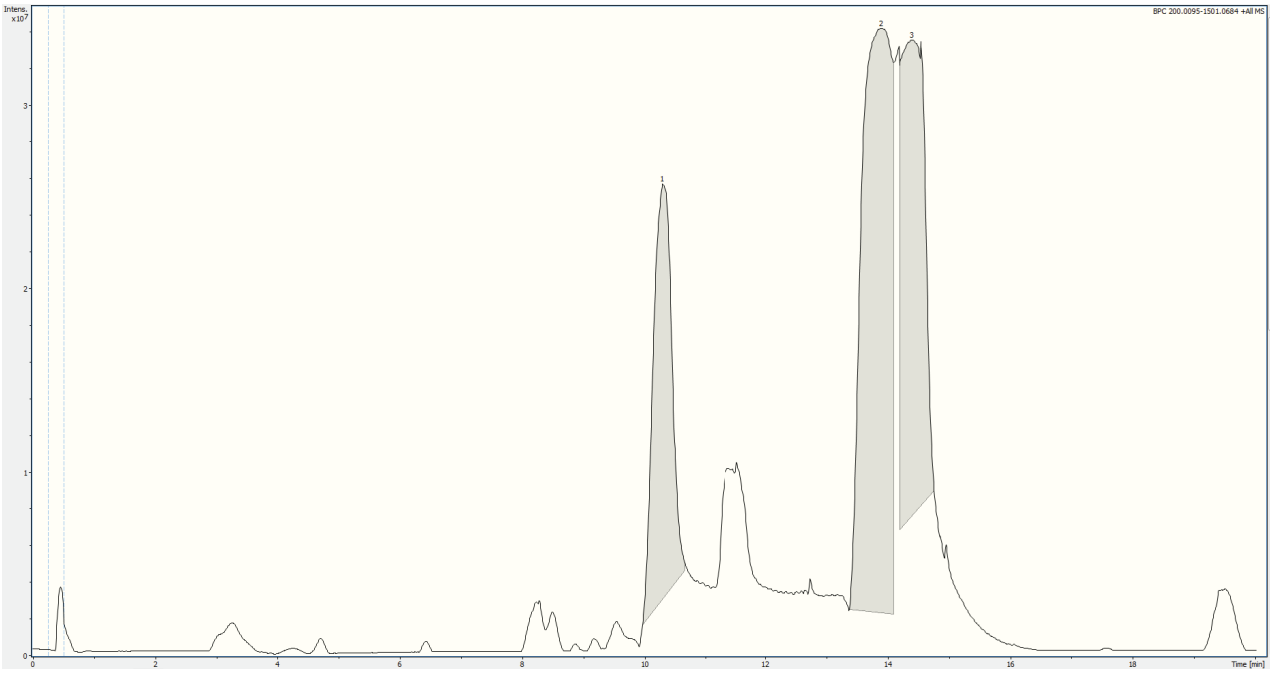

Figure S5: MS chromatogram of the reaction solution of Montelukast and thiophenol under acidic conditions. Montelukast is visible at 10.3 min and both isomers of the Montelukast-thioglycolate addition product are visible at 13.9 and 14.4 min.

III UV-Vis and MS Spectra

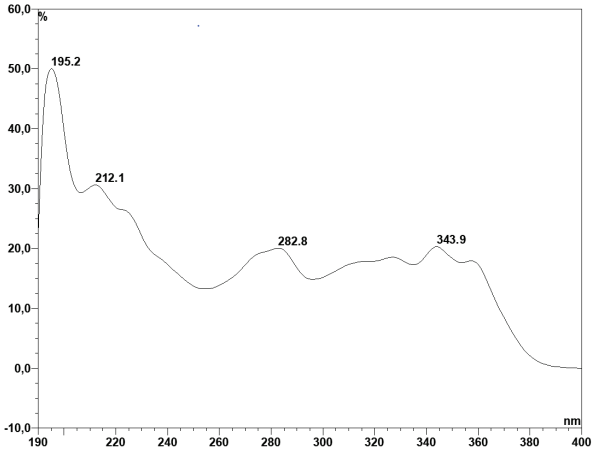

Figure S6: UV-vis spectrum of Montelukast (**1**) recorded by LC-UV spectroscopy.

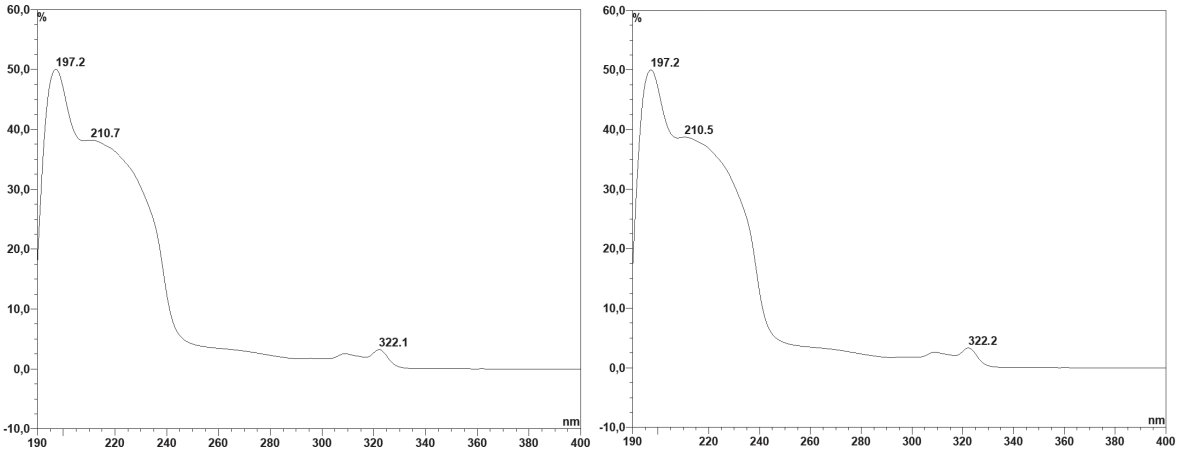

Figure S7: UV-vis spectra of the diastereomers of the Montelukast-thioglycolate addition product (**2**), isomer **1** (left) and **2** (right) recorded by LC-UV spectroscopy.

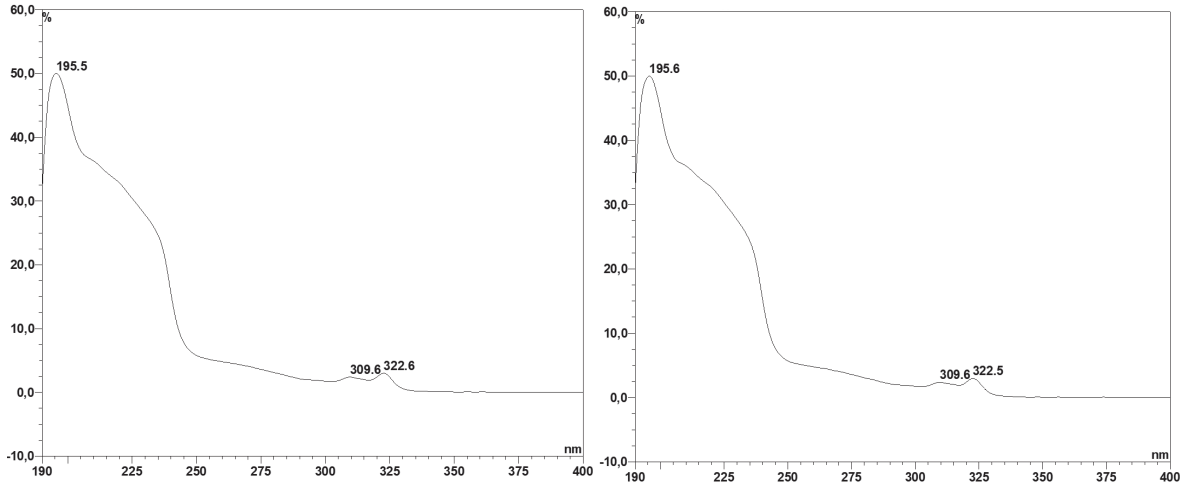

Figure S8: UV-vis spectrum of the diastereomers of the Montelukast-thiophenol addition product (**3**), isomer **1** (left) and **2** (right) recorded by LC-UV spectroscopy.

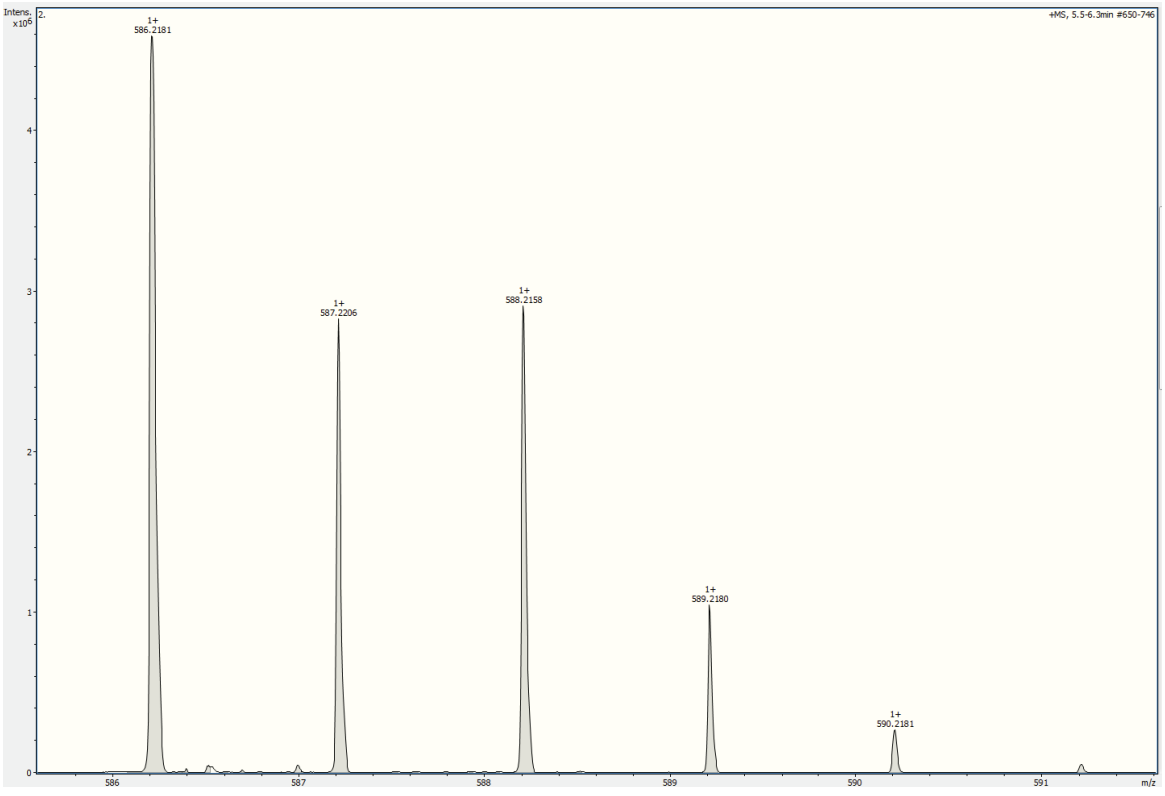

Figure S9: HRMS Data of Montelukast (**1**) recorded by LC-MS spectroscopy.

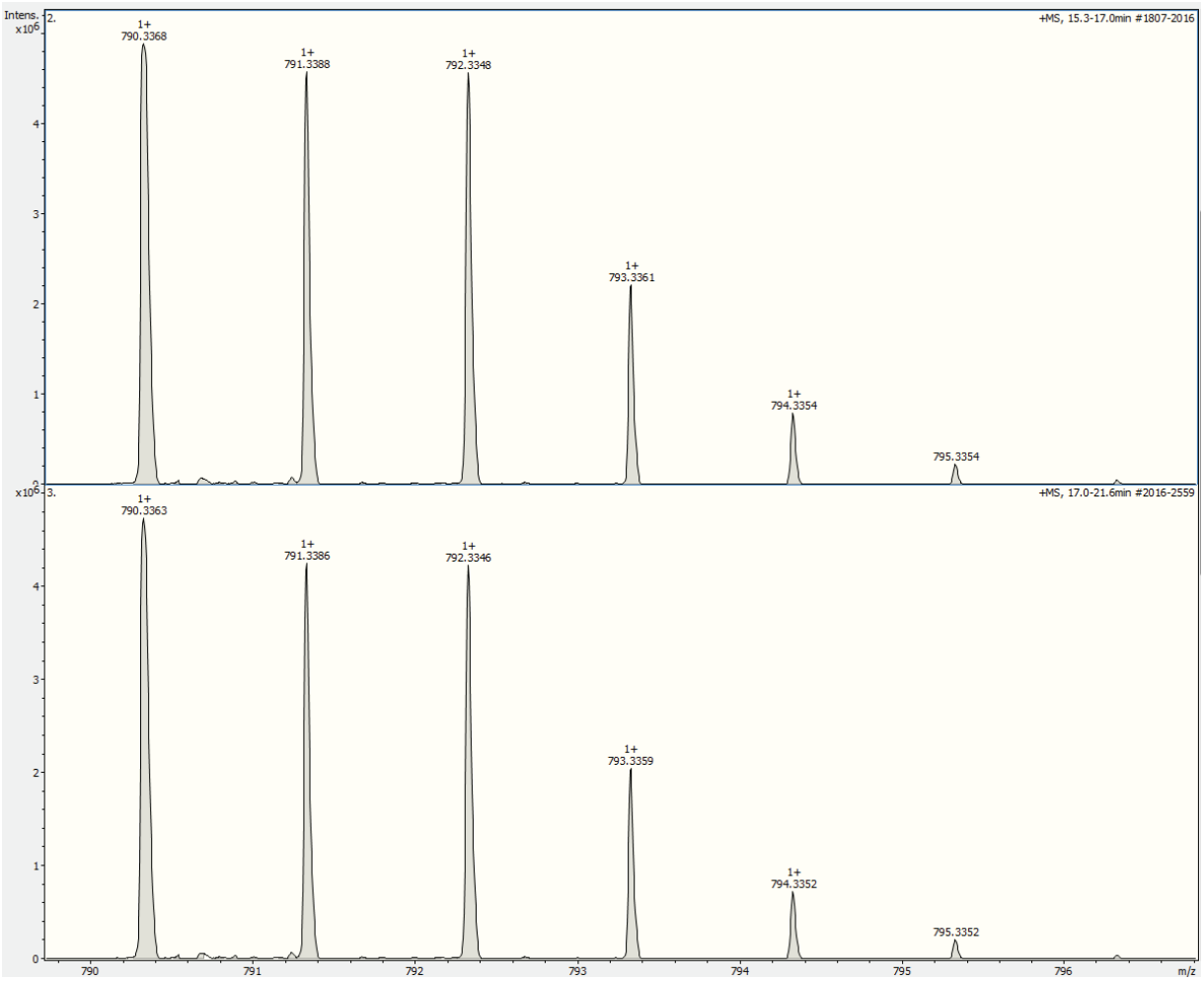

Figure S10: HRMS Data of the diastereomers of the Montelukast-thioglycolate addition product (**2**), isomer **1** (left) and **2** (right) recorded by LC-MS spectroscopy.

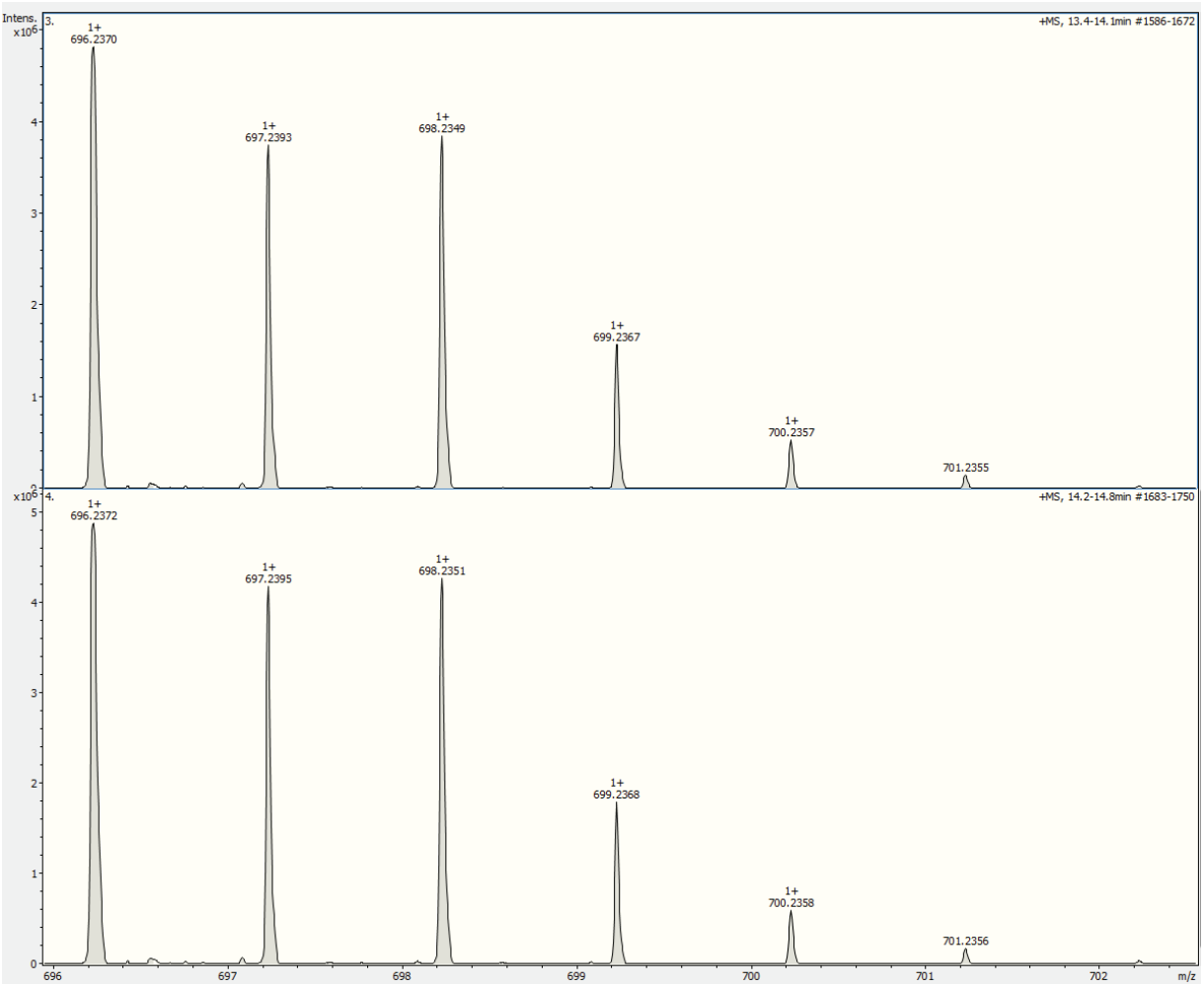

Figure S11: HRMS Data of the diastereomers of the Montelukast-thiophenol addition product (**3**), isomer **1** (left) and **2** (right) recorded by LC-MS spectroscopy.

IV NMR-Spectra

IV.I NMR Spectra of Isomer 1 of the Montelukast-Thioglycolate Addition Product

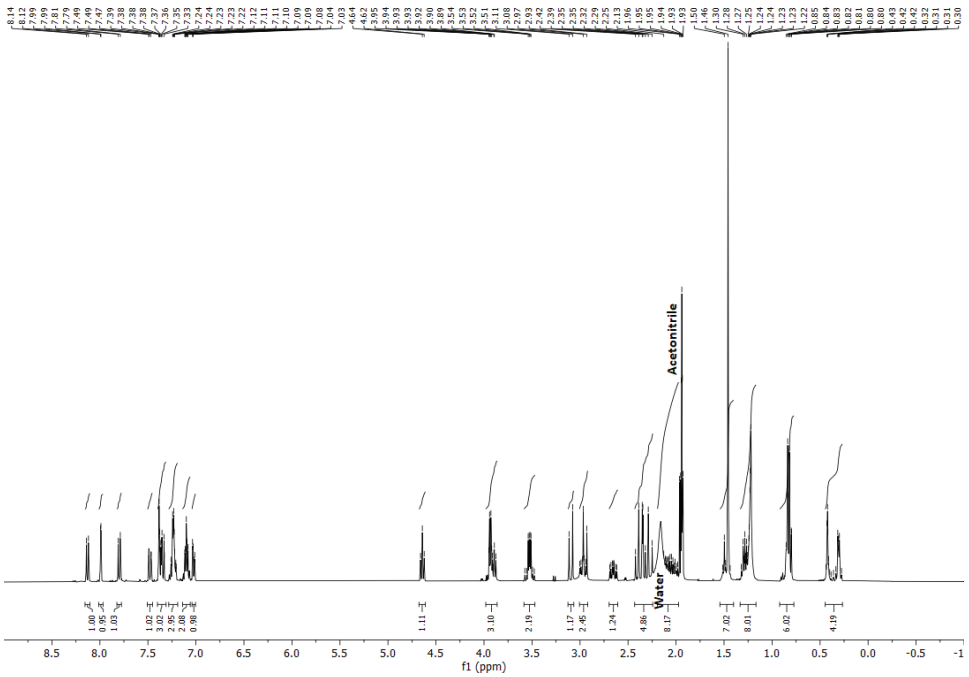

Figure S12: ^{1}H NMR spectrum of **2** (Isomer 1).

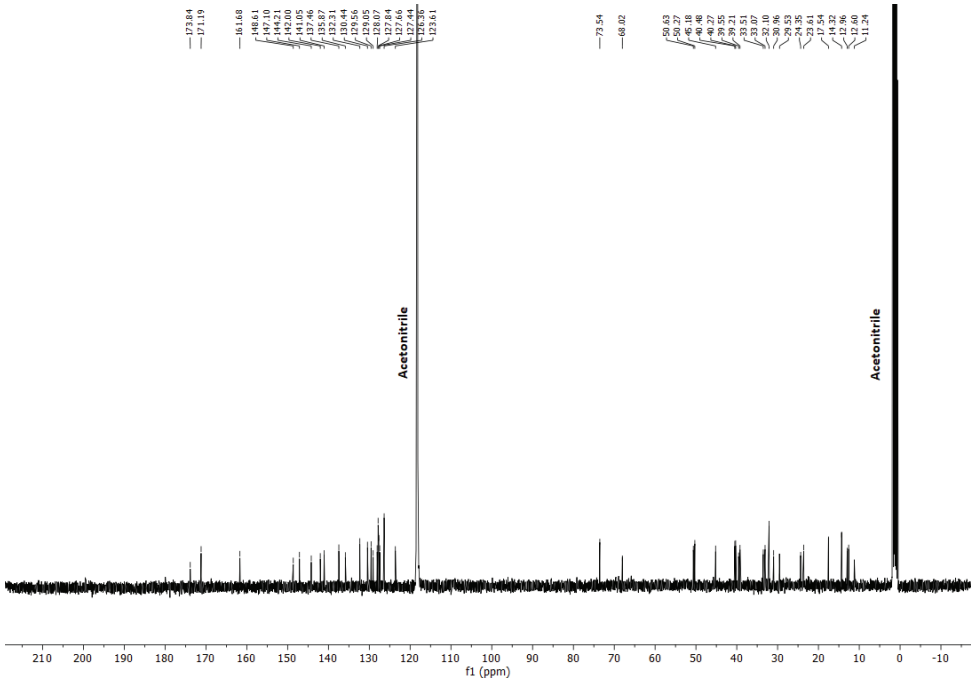

Figure S13: ^{13}C NMR spectrum of **2** (Isomer 1).

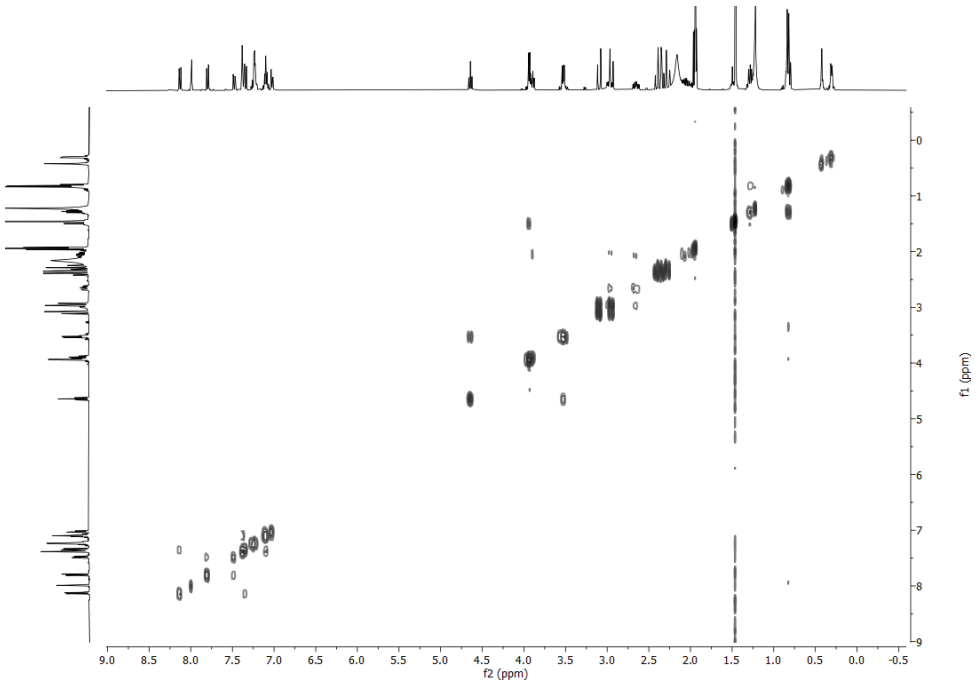

Figure S14: ^{1}H-^{1}H COSY NMR spectrum of **2** (Isomer 1).

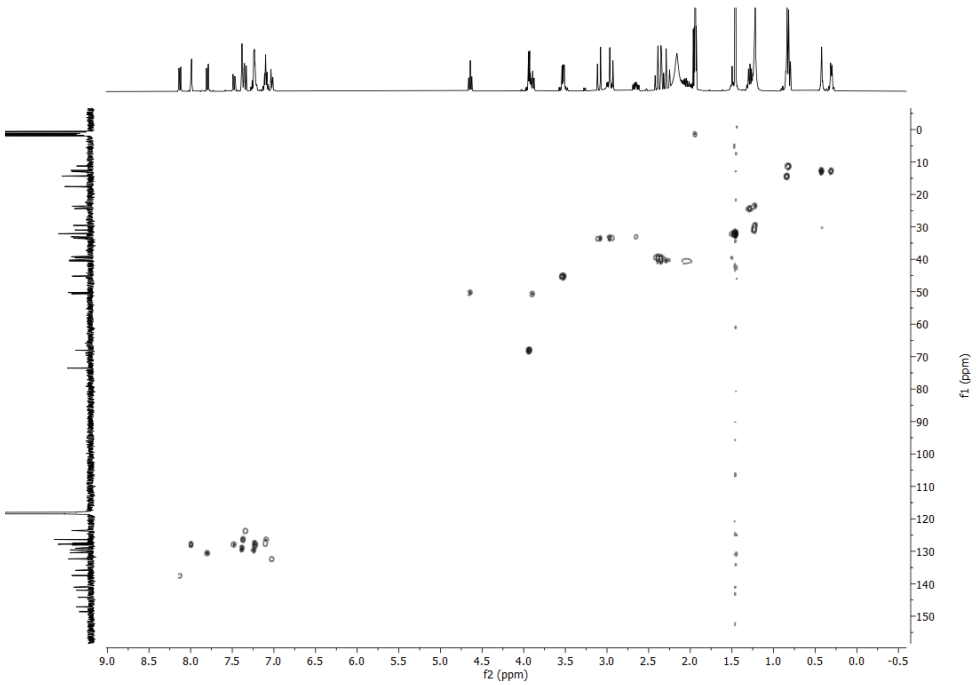

Figure S15: ^{1}H-^{13}C HSQC NMR spectrum of **2** (Isomer 1).

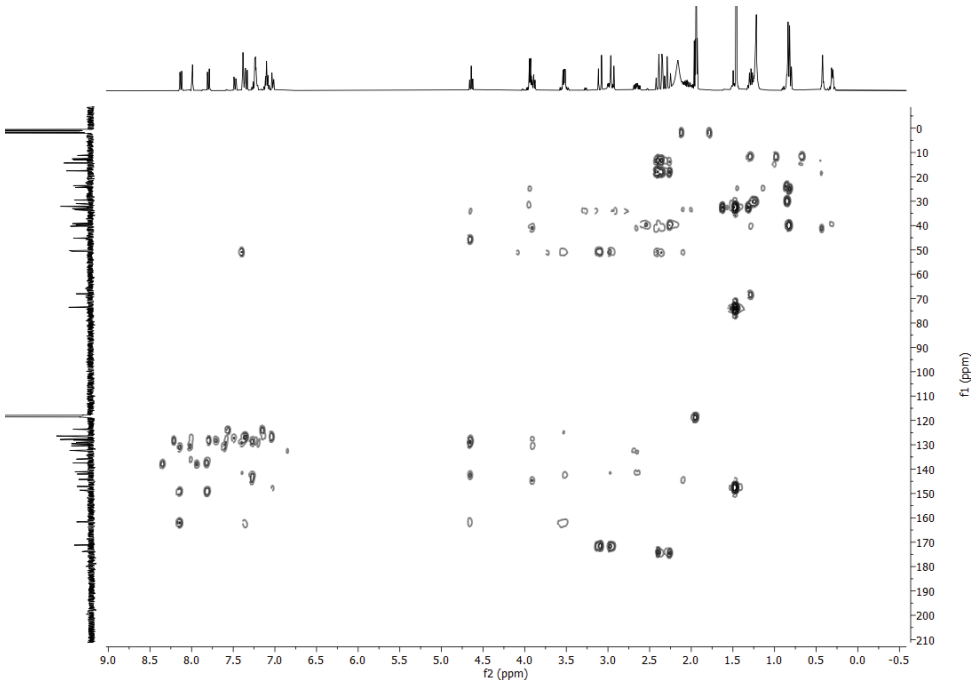

Figure S16: ^{1}H-^{13}C HMBC NMR spectrum of **2** (Isomer 1).

IV.II NMR Spectra of Isomer 2 of the Montelukast-Thioglycolate Addition Product

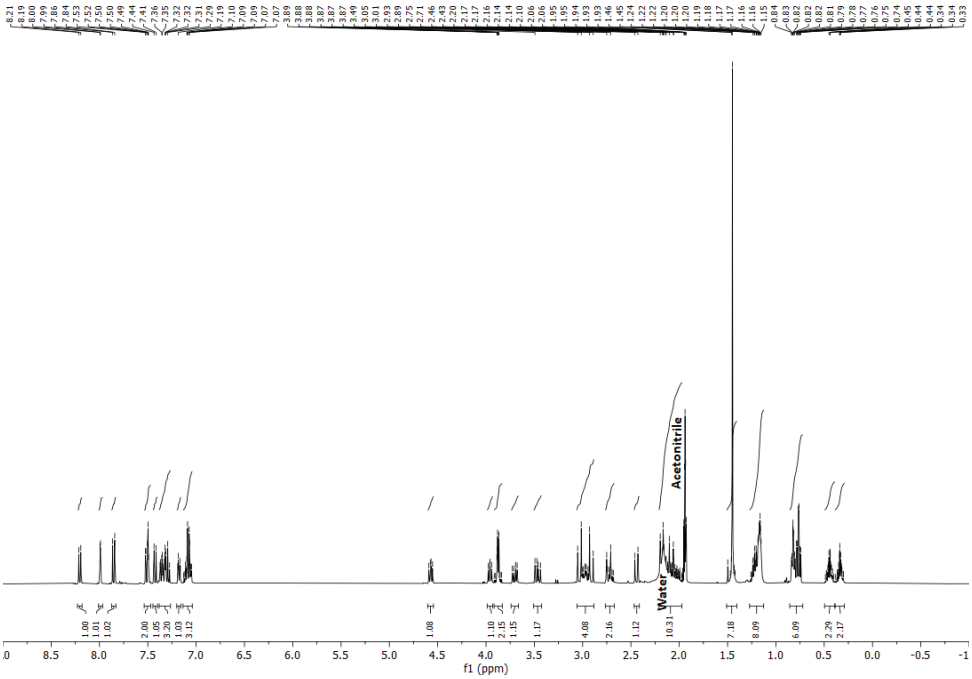

Figure S17: ^{1}H NMR spectrum of **2** (Isomer 2).

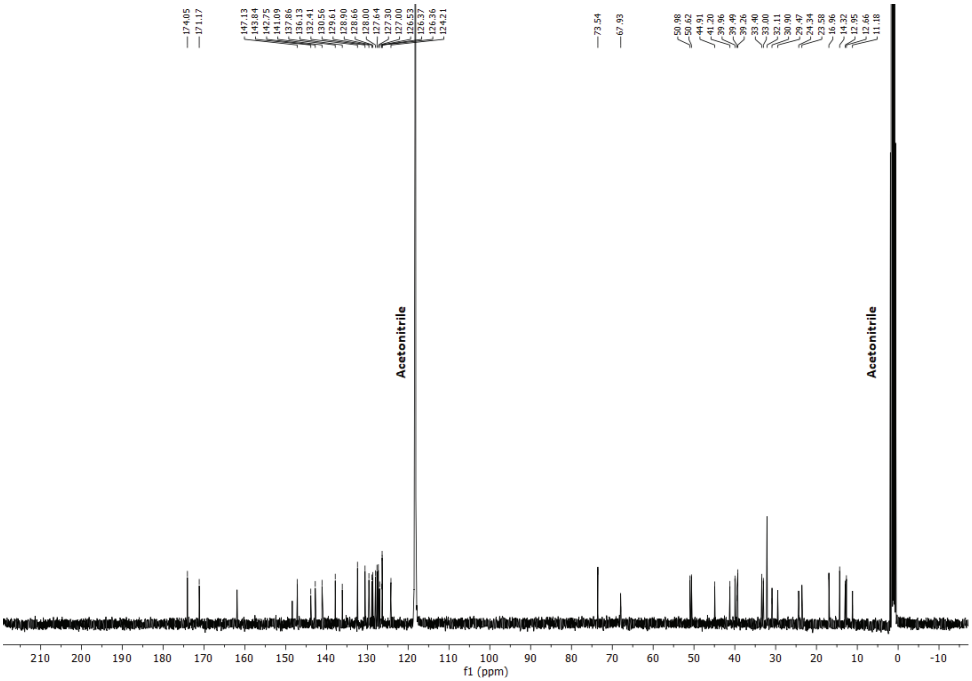

Figure S18: ^{13}C NMR spectrum of **2** (Isomer 2).

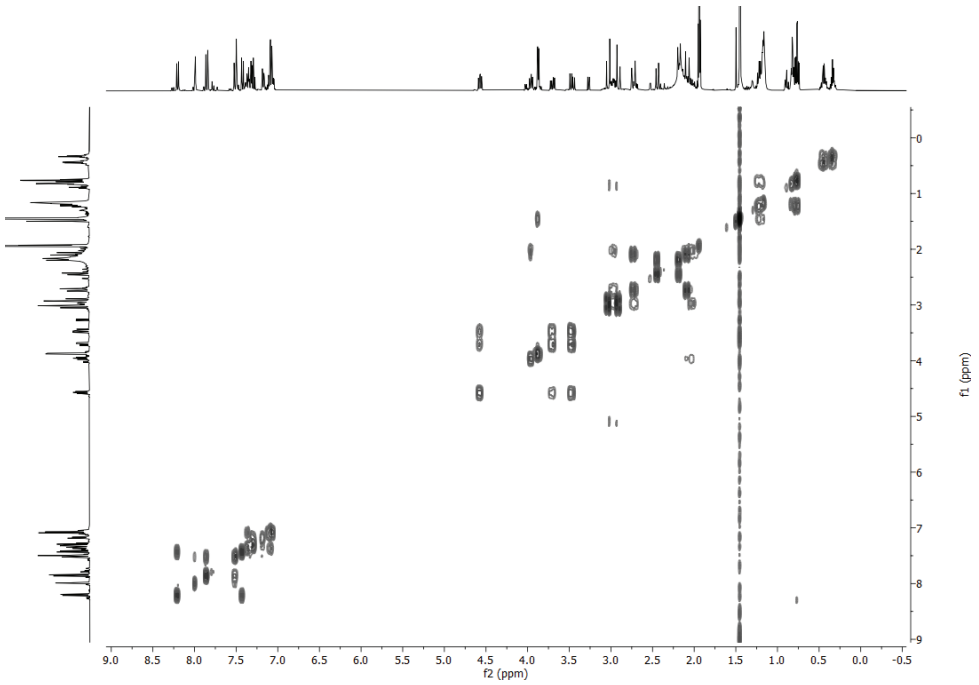

Figure S19: ^{1}H-^{1}H COSY NMR spectrum of **2** (Isomer 2).

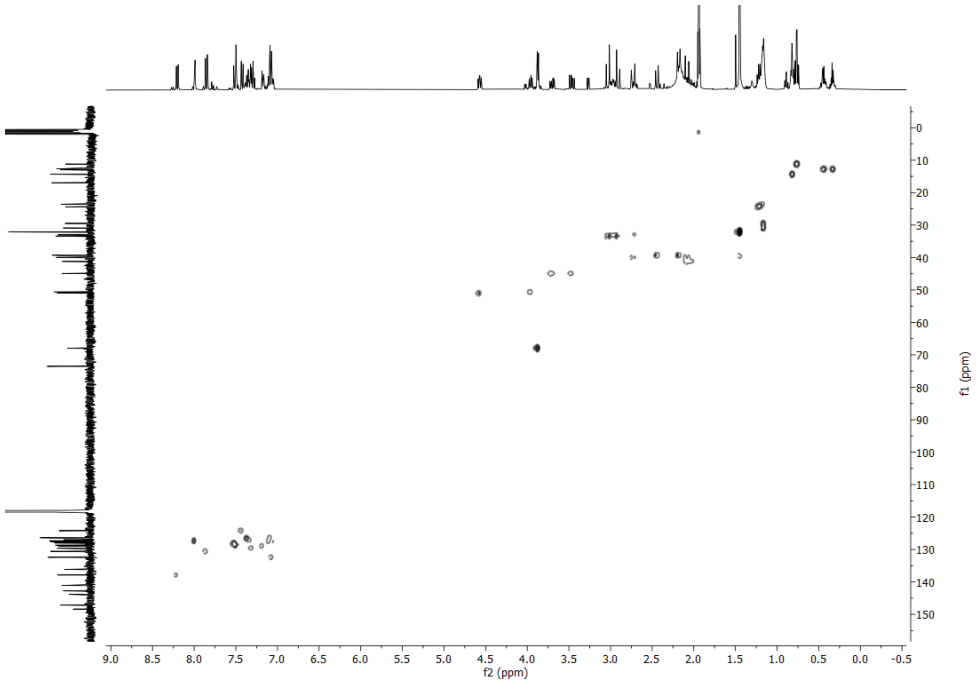

Figure S20: ^{1}H-^{13}C HSQC NMR spectrum of **2** (Isomer 2).

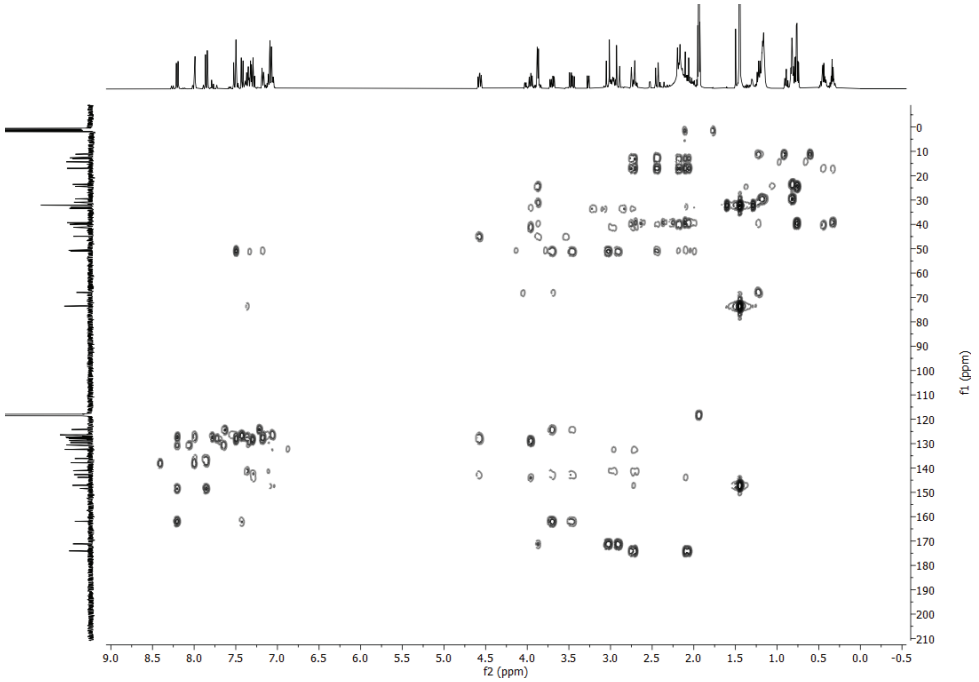

Figure S21: ^{1}H-^{13}C HMBC NMR spectrum of **2** (Isomer 2).

IV.III NMR Spectra of Isomer 1 of the Montelukast-Thiophenol Addition Product

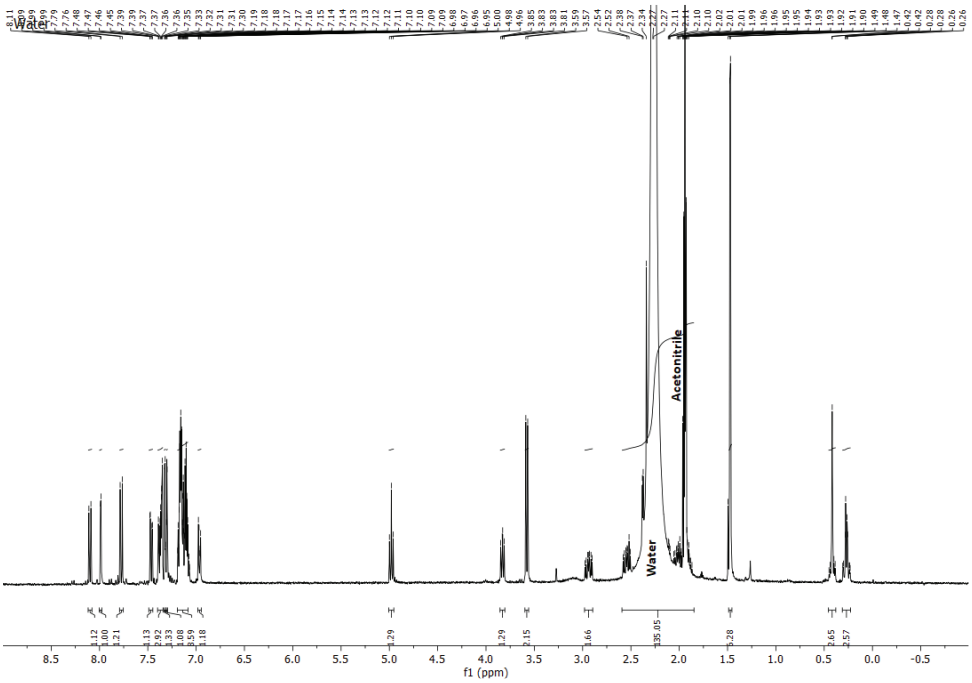

Figure S22: ^{1}H NMR spectrum of **3** (Isomer 1).

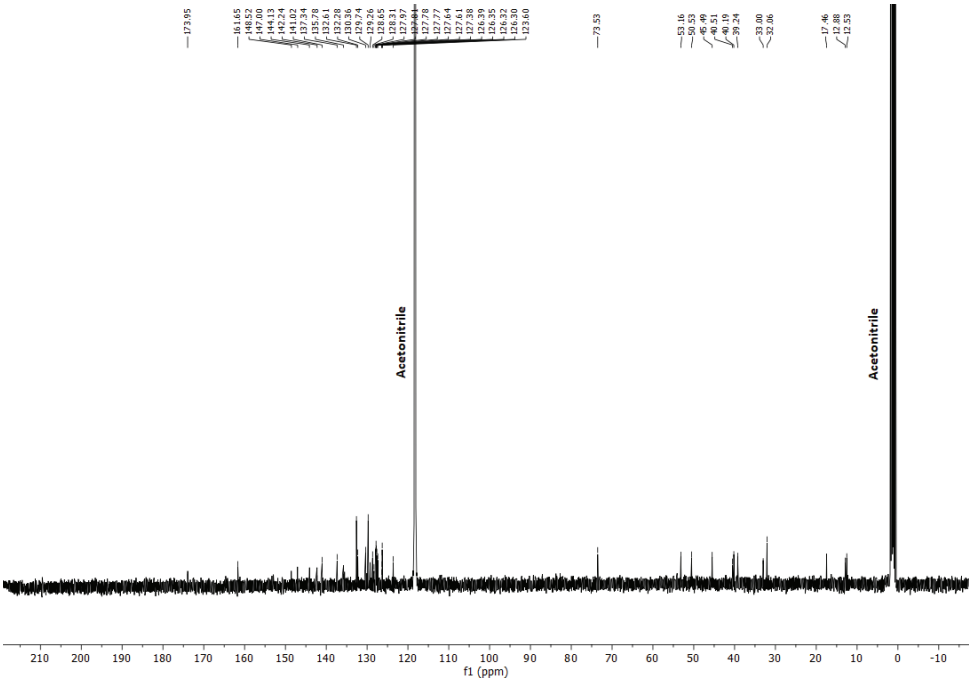

Figure S23: ^{13}C NMR spectrum of **3** (Isomer 1).

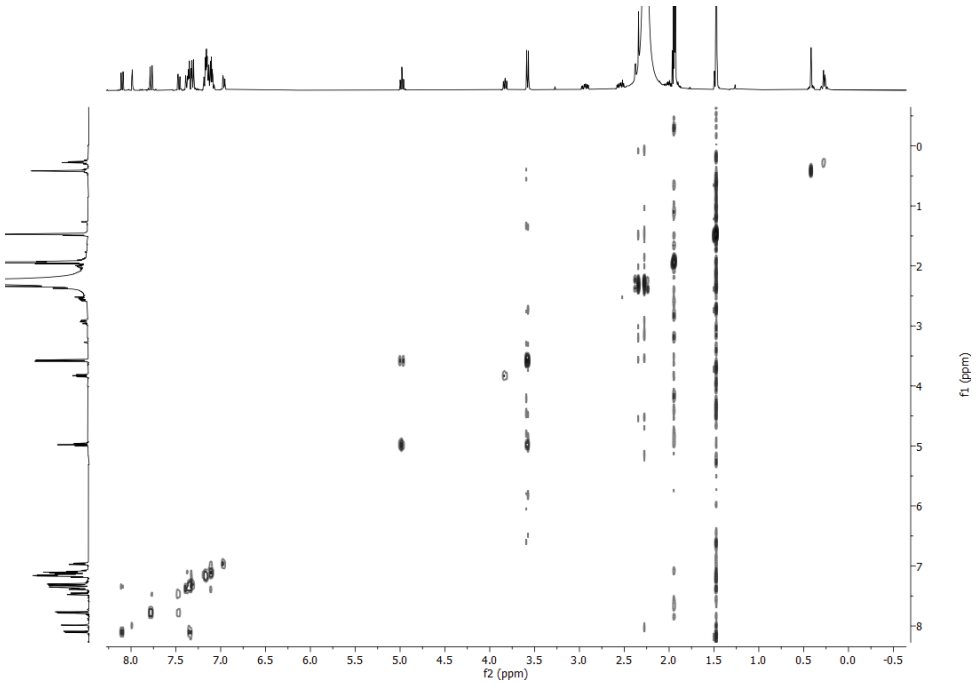

Figure S24: ^{1}H-^{1}H COSY NMR spectrum of **3** (Isomer 1).

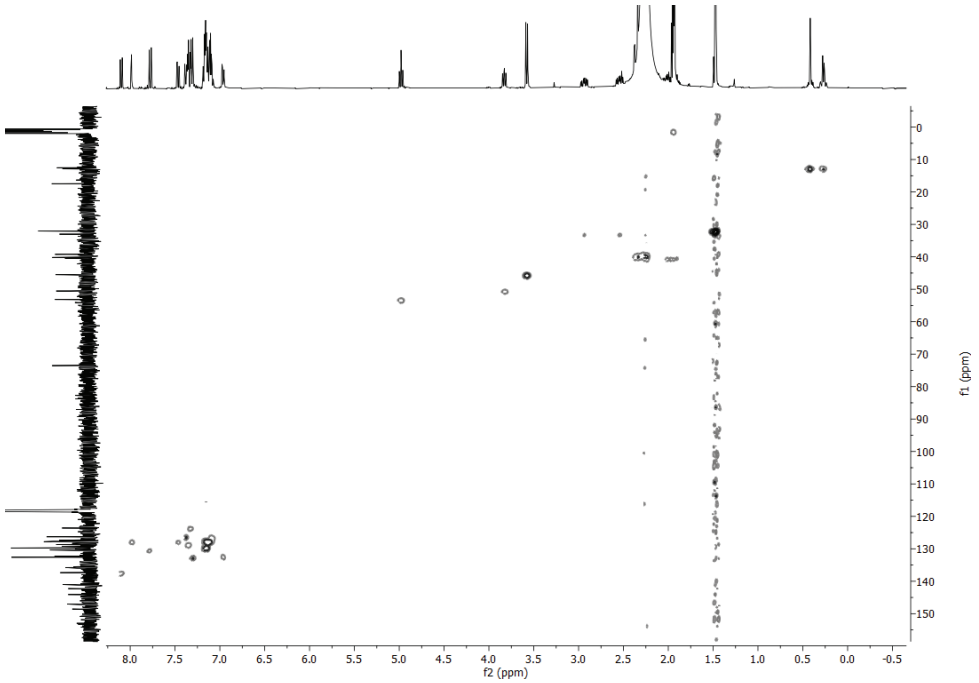

Figure S25: ^{1}H-^{13}C HSQC NMR spectrum of **3** (Isomer 1).

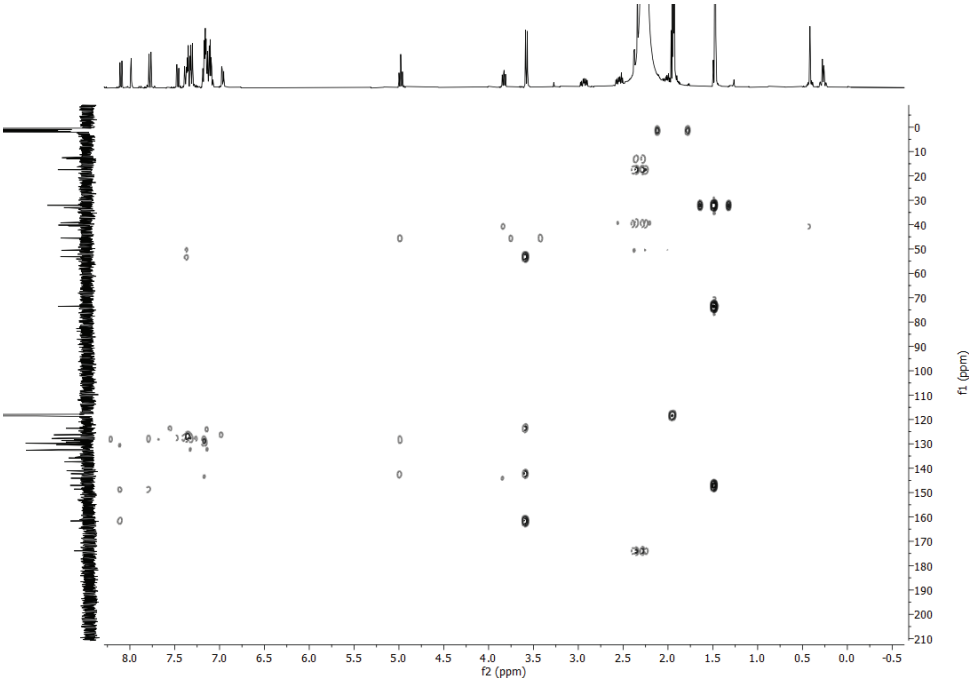

Figure S26: ^{1}H-^{13}C HMBC NMR spectrum of **3** (Isomer 1).

IV.IV NMR Spectra of Isomer 2 of the Montelukast-Thiophenol Addition Product

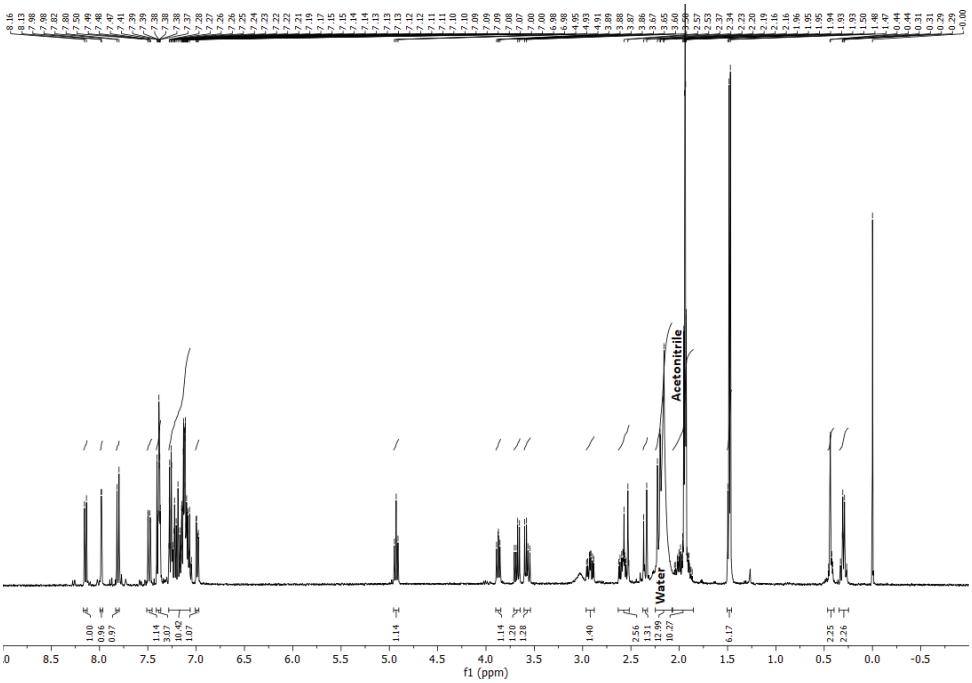

Figure S27: ^{1}H NMR spectrum of **3** (Isomer 2).

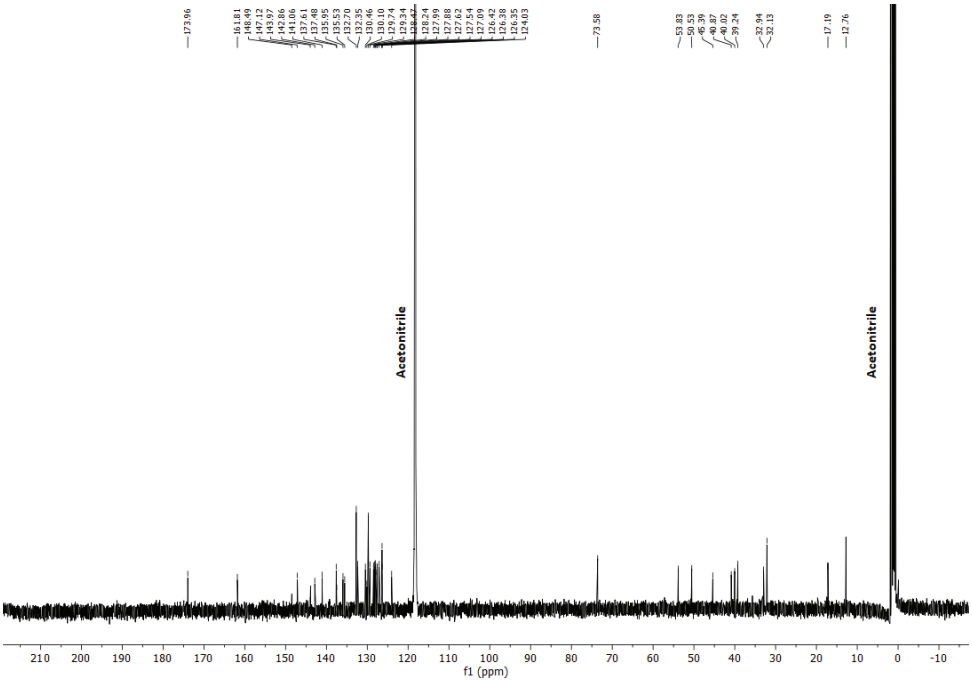

Figure S28: ^{13}C NMR spectrum of **3** (Isomer 2).

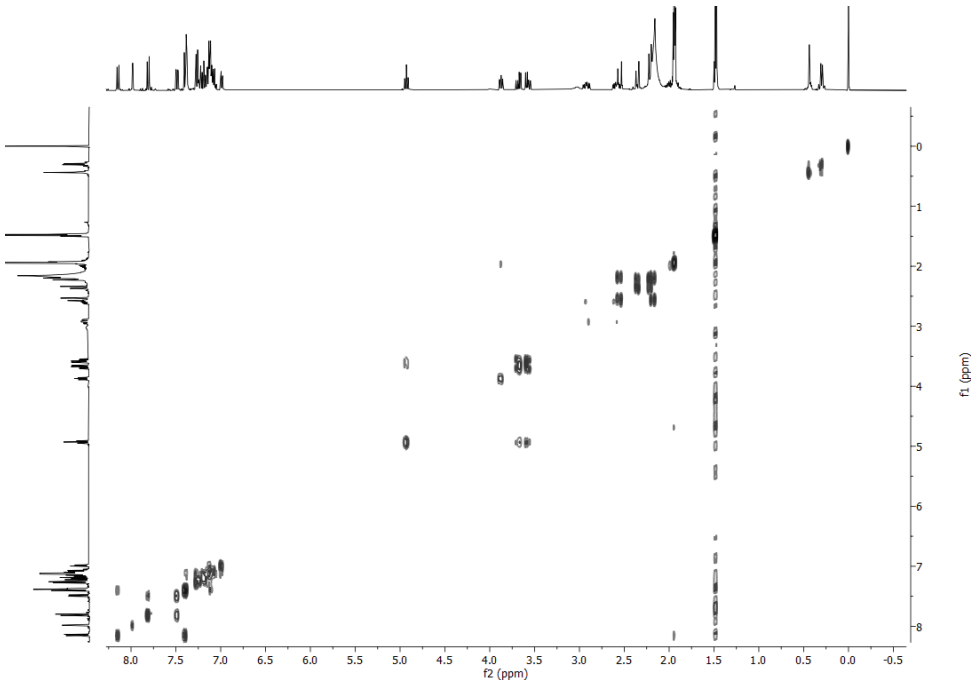

Figure S29: ^{1}H-^{1}H COSY NMR spectrum of **3** (Isomer 2).

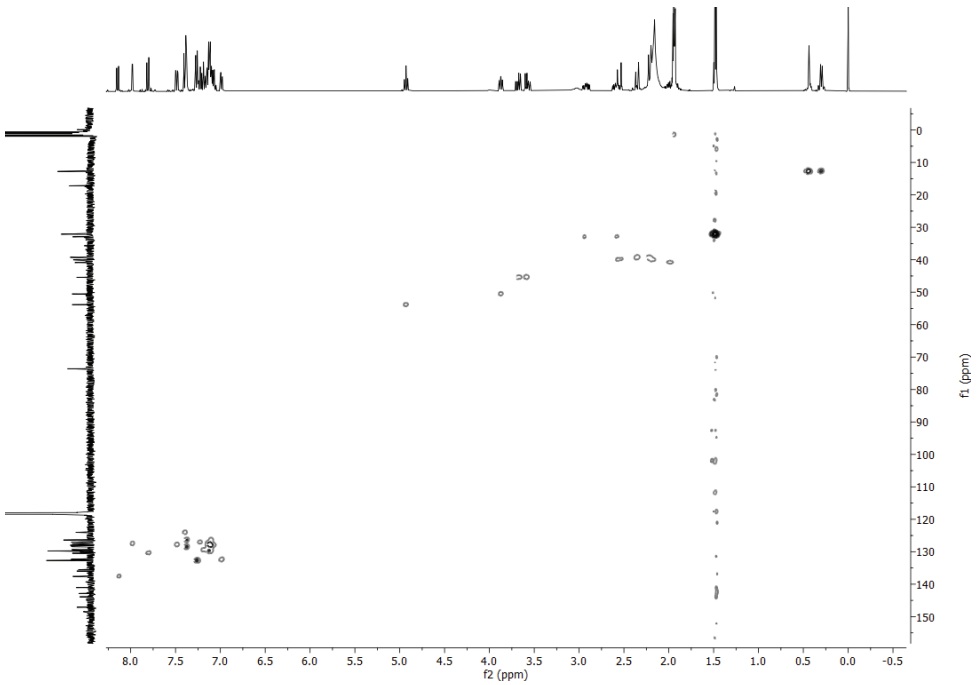

Figure S30: ^{1}H-^{13}C HSQC NMR spectrum of **3** (Isomer 2).

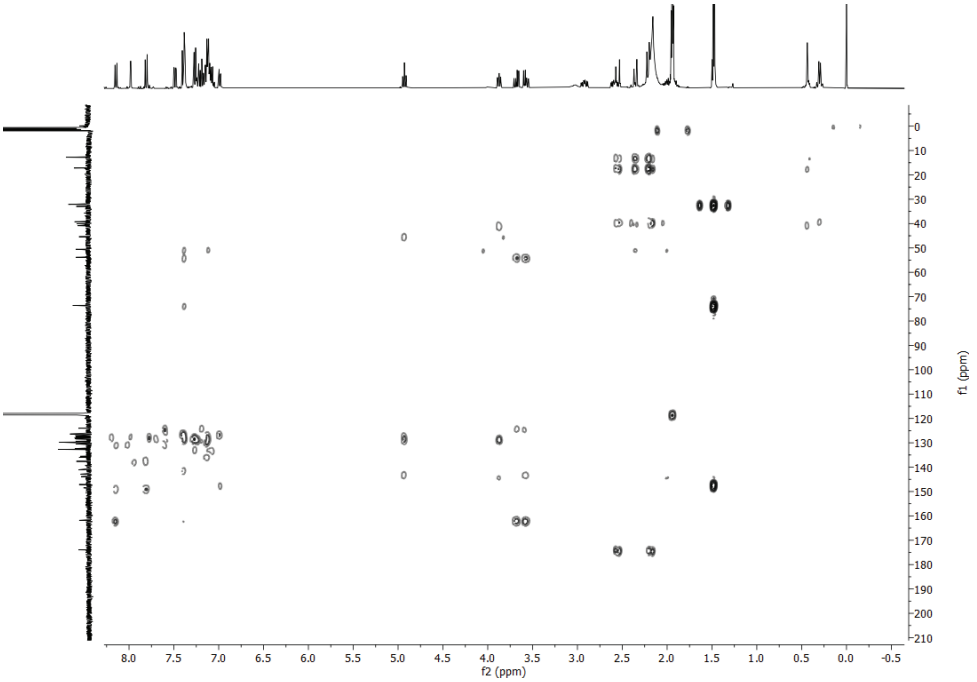

Figure S31: ^{1}H-^{13}C HMBC NMR spectrum of **3** (Isomer 2).

2.4 Discussion

Based on the structure of the impurity and the degradation experiments performed on its first discovery, a synthesis was devised to obtain it artificially. Following the synthesis, the method transfer of the standard analytical method for Montelukast to the hyphenated system was attempted. This transfer was successfully achieved in less than a day. The synthesis solution was analyzed without further work-up, and sufficient UV/Vis, HRMS and NMR Data for complete structural elucidation could be obtained using only the hyphenated system.

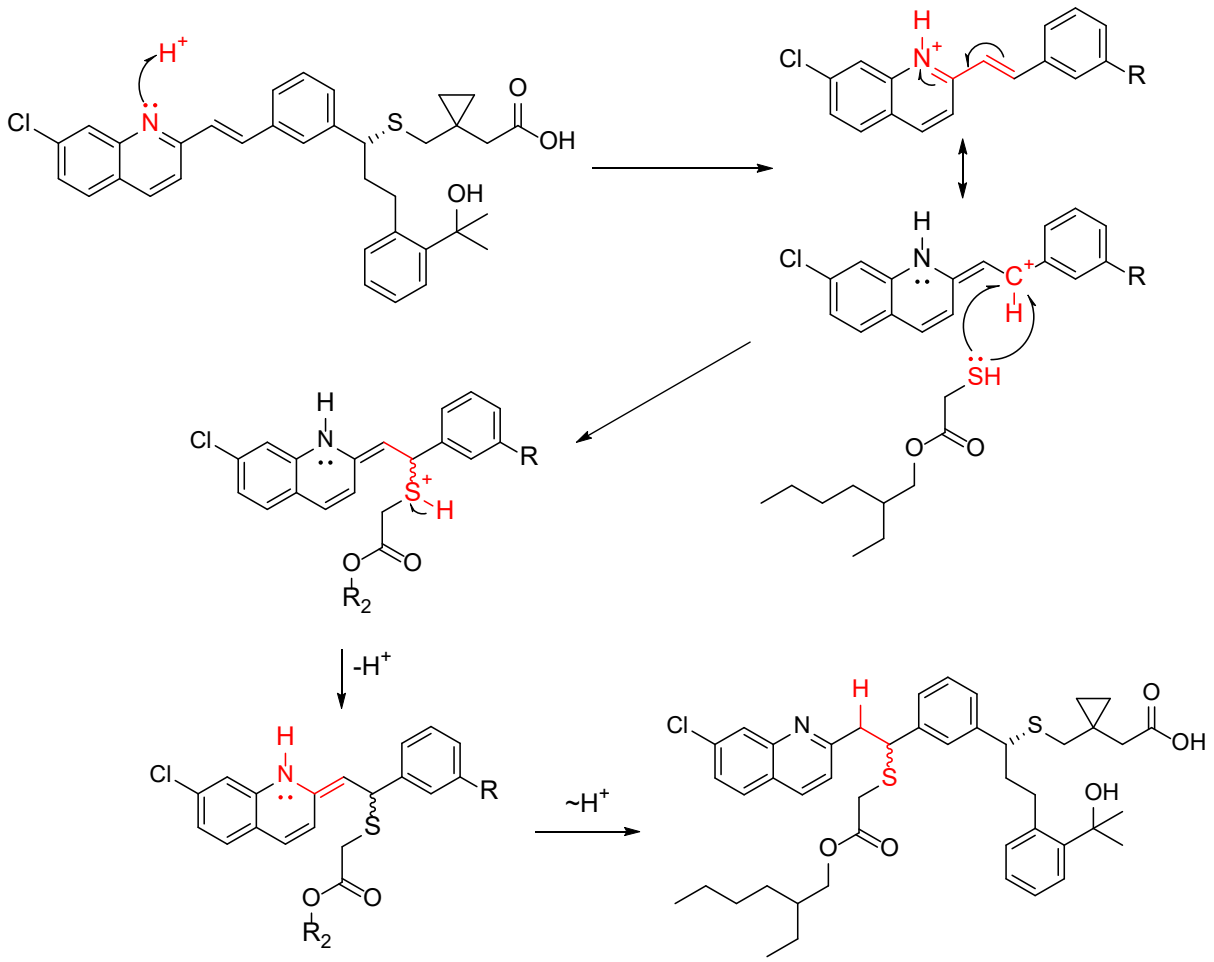

Figure 1. Proposed reaction mechanism of the acid catalyzed thiol-ene addition of 2-ethylhexyl thioglycolate to Montelukast.

Based on the obtained structure, the reaction mechanism that led to the formation of the impurity was investigated. This is an important step to understand the circumstances and conditions that promote the formation of an impurity and to determine appropriate measures to prevent this formation from occurring in the future. Usually, the formation mechanism is determined during degradation tests. However, as these are unspecific and are performed following trial-and-error methods, this process can be time consuming and may not necessarily result in clear results regarding the reaction mechanism. Using a known molecular structure on the other hand, allows scientists to draw conclusions on the reaction mechanism more easily and efficiently.

In this case, the previously performed degradation experiments had shown, that the reaction is expedited by the presence of acid. By comparing the molecular structure of the API to the impurity it could be determined that a thiol-ene addition had taken place, which mostly occur via a radical mechanism or a Michael reaction. Based on this knowledge, a number of experiments were devised to clarify the reaction mechanism. These experiments led to the conclusion that no radical mechanism was involved, but that the reaction had occurred via an atypical acid catalyzed Michael-like reaction.

Overall, these experiments showed that the transfer of standard analytical methods to the hyphenated system can be performed quickly and with relative ease, yielding data of sufficient quantity and quality for a complete structural elucidation. Hereby, the potential to perform a comprehensive identification of an impurity, within a short amount of time and with little substance was demonstrated. Lastly, the thus obtained knowledge was successfully used to identify the formation mechanism of the impurity, which in a real case can be used to adapt the synthesis, formulation, packaging, or storage of a drug in a targeted fashion to prevent conditions that favor the reaction mechanism.

3 Naloxone: Elucidation of Complex Structures

As previously mentioned, one of the major advantages of the used hyphenated system is the ability to perform complete isolation and identification of a new impurity, solely with the data it produces, without the need to perform additional, time-consuming, degradation experiments. To underline this advantage, experiments were performed to investigate whether the thus obtained data was also sufficient for the complete structural elucidation of complex molecules. For these experiments, an impurity was selected that forms by the reaction of two units of the opioid antagonist Naloxone with one unit of formaldehyde. The formaldehyde was present in the drug in amounts harmless to consumers, but high enough to cause the formation of the detected impurity.

3.1 Naloxone Research Article

Author contributions:

Philipp Schmidt:

- *Optimization of the artificial synthesis of the Naloxone impurity, accompanied by studies into the formation mechanism*
- *Artificial synthesis of the Naloxone impurity samples for analysis using the HPLC-DAD-HRMS/SPE-NMR system*
- *Method transfer to the HPLC-DAD-HRMS/SPE-NMR system*
- *Separation, enrichment, isolation and data acquisition using the HPLC-DAD-HRMS/SPE-NMR system*
- *Evaluation of the data, followed by the complete structural elucidation of the four stereoisomers of the Naloxone impurity, including the assignment of all ^{1}H and ^{13}C NMR signals*
- *Writing of the Research Article*

Christine Kolb and Andreas Reiser:

- *Performed the initial investigations regarding the identity and formation of the Naloxone impurity, when it was first discovered, including degradation and enrichment experiments*

Markus Philipp:

- *Performed a role as supervisor of the project*

Hans-Christian Müller and Konstantin Karaghiosoff:

- *Performed an advisory role in the preparation of the manuscript and aided in proof-reading*

Journal of Pharmaceutical Sciences 000 (2021) 1–8

Contents lists available at ScienceDirect

Journal of Pharmaceutical Sciences

journal homepage: www.jpharmsci.org

Pharmaceutics, Drug Delivery and Pharmaceutical Technology

Isolation, Identification and Structural Verification of a Methylene-Bridged Naloxone "Dimer" Formed by Formaldehyde

Philipp Schmidt[a], Christine Kolb[b], Andreas Reiser[b], Markus Philipp[b], Hans-Christian Müller[b,*], Konstantin Karaghiosoff[a,**]

[a] Department Chemie, Ludwig-Maximilians-Universität München, Butenandtstraße 5-13, Haus D, 81377 Munich, Germany
[b] Analytical Development, Hexal AG, Industriestraße 25, 83607 Holzkirchen, Germany

ARTICLE INFO

Article history:
Received 22 July 2021
Revised 17 November 2021
Accepted 17 November 2021
Available online xxx

Keywords:
Naloxone
NMR
Solid-phase extraction (SPE)
HPLC-SPE-NMR
HPLC-HRMS
Hyphenation
Impurity
Aldol condensation
Michael reaction

ABSTRACT

We report the isolation and characterization of a methylene bridged "dimer" of the opioid antagonist Naloxone, previously detected in experimental Buprenorphine-Naloxone oral films. This compound was found to form via an aldol addition followed by a condensation reaction under acidic conditions between two units of Naloxone and one unit of formaldehyde. HPLC-UV-HRMS analysis revealed the formation of three individual stereoisomers during this reaction, which were separately isolated using solid-phase extraction. These isomers were shown to freely react into one another in solvent, forming an equilibrium. The structure of the unknown compound was determined via HRMS spectrometry and 1D and 2D NMR spectroscopy.

Abbreviations

API	active pharmaceutical ingredient
au	atomic units
COZY	correlation spectroscopy (NMR)
DAD	diode array detector
ESI	electrospray ionization
HFBA	heptafluorobutyric acid
HMBC	heteronuclear multiple bond correlation (NMR)
GMP	good manufacturing practice
HPLC	high performance liquid chromatography
HRMS	high resolution mass spectrometry
HSQC	heteronuclear single quantum correlation (NMR)
LC	liquid chromatography
MAT	medication-assisted treatment
MCC	microcrystalline cellulose
MS	mass spectrometry
NMR	nuclear magnetic resonance
NSAID	nonsteroidal anti-inflammatory drug
ORF	oral film
OUD	opioid use disorder
PEG	polyethylene glycol
Q	quadrupole (MS)
q	radio frequency quadrupole (MS)
SPE	solid phase extraction
TOF	time-of-flight (MS)
UHR	ultra-high resolution
UV-Vis	ultraviolet-visible

Introduction

Increasing opioid dependency and the deaths caused by resulting overdose are an ever-growing public health hazard, worldwide.[1] Over 40,000 people died alone in the USA due to opioid abuse in 2017 and the numbers are continuously rising.[2] Opioids effect the central nervous system and overdose can quickly lead to respiratory depression, heart failure and stroke.[3]

* Corresponding author at: Analytical Development, Hexal AG, 83607 Holzkirchen, Germany.
** Corresponding author at: Department Chemie, Ludwig-Maximilians-Universität München, 81377 Munich, Germany.
E-mail addresses: dhcm@gmx.de (H.-C. Müller), klk@cup.uni-muenchen.de (K. Karaghiosoff).

https://doi.org/10.1016/j.xphs.2021.11.014
0022-3549/

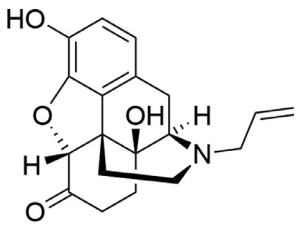

1

Fig. 1. Chemical structure of the opioid antagonist Naloxone (**1**).

Several approaches to the treatment of opioid use disorder (OUD) have been made, but due to the social and medical complexities of OUD no, one ideal method has yet been developed.[4] A long used substance in medication-assisted treatment (MAT) is Methadone.[4] As opioid agonist Methadone causes similar effects to other opioids, and is used in controlled doses to suppress the OUD patient's withdrawal symptoms.[4,5] This similarity to other opioids however, also poses a risk to the use of Methadone in MAT, as inappropriate periods of treatment or abuse may lead to relapse or death by overdose.[6]

Another approach in MAT is the use of Buprenorphine, a partial agonist to the μ-opioid receptor.[4,7-9] With its strong affinity to the μ-receptor, small doses lead to the normal opioid effects which are prolonged instead of intensified by increased dose.[8] Buprenorphine, like Methadone, carries the risk of abuse and overdose, which is why it is often combined with a treatment by Naloxone.[10-12]

Naloxone (Fig. 1) is an effective opioid antagonist and is commonly used to reverse the symptoms of opioid overdose.[3,4,9,13] Used by itself in the treatment of OUD it poses the threat of eliciting withdrawal symptoms,[4,14] but in combinatory treatment with other medication it can help stem the negative effects of these substances.[9,15] In form of take-home emergency kits it may also be administered in acute cases of opioid overdose to reverse the resulting respiratory depression.[4,16] These kits are available for intramuscular administration, but easier to handle intranasal kits have also been developed.[4]

During the development of a (not yet submitted for approval) Buprenorphine-Naloxone and a Naloxone oral film (ORF), HPLC analysis showed the presence of an unknown impurity resulting from the degradation of the active pharmaceutical ingredient (API). Experiments indicated the involvement of formaldehyde in the formation of this impurity. Formaldehyde is a common impurity in several widespread pharmaceutical excipients, such as croscarmellose sodium (internally crosslinked sodium carboxymethyl cellulose), microcrystalline cellulose (MCC), polyethylene glycol (PEG) and hydroxypropyl methylcellulose.[17-23]

Research showed that three stereo isomers of the found impurity exist. Here we describe the synthesis, isolation, identification and formation, as well as the properties of these compounds.

Materials and Methods

Chemicals and Reagents

All chemicals and solvents were used as purchased without further purification. Formic acid (98%) was purchased from Flucka. The reagents ammonium hydrogen carbonate, ammonia solution, heptafluorobutyric acid (HFBA), formaldehyde (37% in water, stabilized by 10% methanol) and sodium hydroxide were purchased from Merck. The solvents acetonitrile, THF and methanol for liquid chromatography and mass spectrometry, in their respective qualities, were purchased from Merck. Deuterated acetonitrile, water and Methanol were acquired from Sigma-Aldrich. Naloxone was acquired from Cilag AG. Ultra-pure water was produced by an in-house Merck Millipore Milli-Q system. All chemicals used in this study, as well as chemicals used in the formulation of the investigational ORFs were of GMP grade.

NMR Spectroscopy

All ^{1}H and ^{13}C NMR spectra were recorded in deuterated acetonitrile, methanol and water at 298 K and were referenced to residual solvent signals using literature values (1.94 ppm for ^{1}H spectra and 118.26 ppm for ^{13}C spectra for acetonitrile, 3.31 ppm for ^{1}H spectra and 49.03 ppm for ^{13}C spectra for methanol and 4.79 ppm for ^{1}H spectra for water).[24] The spectra were acquired using a 400 MHz Bruker Avance Neo 400 (400.15 MHz for ^{1}H, 100.63 MHz for ^{13}C and 376.46 MHz for ^{19}F) and a 400 MHz Bruker AV400TR (400.13 MHz for ^{1}H, 100.62 MHz for ^{13}C and 376.44 MHz for ^{19}F).

HPLC-DAD System

HPLC-UV analysis was performed using an Agilent 1100 system.

Hyphenated HPLC-DAD-HRMS/SPE System

The system consisted of an Agilent 1290 Infinity II system, a Bruker/Spark LC-SPE Interface (3.0 CPL), an UHR-Q-TOF Bruker impact II in ESI positive mode and an Azura Knauer pump. Spark SPE cartridges (10 × 2 mm, Hysphere-Resin GP, 10–12 μm pore size, polyvinyl benzene) were used for collection of the samples. Elution into 2.5 mm Bruker NMR capillaries was performed by a Bruker SamplePro SPE TT system.

Synthesis of the Three Stereoisomers of the Methylene-Bridged Naloxone Dimer (2)

Naloxone hydrochloride dihydrate (1 equiv, 622.76 mg, 1.56 mmol) was dissolved in 10 mL of a 0.4 mol/L sodium hydroxide solution and formaldehyde (excess, 2.18 mmol, 60 μL) was added. The solution was heated to 55 °C and was stirred for 3 h under reflux, before 1 mL concentrated acetic acid was added.

LC-UV-Analysis for Reaction and Post-separation Control

The analysis was performed using a XBridge^{TM} BEH C18 Column with 2.5 μm particle size and dimensions of 100 × 3.0 mm, using a 29 min HPLC method at a temperature of 40 °C. The solvent system consisted of 0.1% HFBA in water (mobile phase A) and acetonitrile (mobile phase B). The UV detector was set to 230 nm with a DAD range from 190 to 450 nm. The injection volume was 20 μL and the flow rate was set to 0.85 mL/min. For the first 2 min the solvent composition was set to 8% B, before it was increased to 14.8% B within 7 min. The composition was further increased to 30.8% B over the course of 11 min and then to 46% B within 1 min. This level was held for 2 min, after which B was returned to 8% within 1 min and held at this level for the remaining 5 min.

Separation and Isolation via a Hyphenated HPLC-DAD-MS/SPE-NMR System

Samples were taken from the synthesis solution without further work-up or dilution. The separation was performed using a Symmetry Shield^{TM} RP_{18} Column with 3.5 μm particle size and dimensions of 100 × 4.6 mm, using a 67 min HPLC method at a temperature of 40 °C. The solvent system consisted of 0.1% HFBA in water (mobile phase A) and acetonitrile (mobile phase B). The injection volume was 10 μL and the flow rate was set to an initial value of 1.7 mL/min. For the first 2 min the solvent composition was set to 8% B, before it was increased to 15% B and the flow rate was reduced to 0.85 mL/min

within 7 min. These values were held for 12 min, before the solvent composition was changed to 20% B over the course of 15 min. After 14 min, the value of B was increased to 30.8% and the flow rate was increased back to 1.7 mL/min. Within 2 min the value of B was further increased to 46% and held at this level for 2 min, before it was returned to 8% within 1 min. This level was held for the remaining 5 min of the HPLC method.

After separation via HPLC, 5% of the eluting solution was split off, diluted by acetonitrile, and analyzed by HRMS in ESI positive mode. At the beginning of every sample injection the HRMS was calibrated using a 0.1% trifluoroacetic acid solution. The remaining solution was directed through a UV detector with a DAD range of 190 – 640 nm that recorded a separate chromatogram at 230 nm. This UV data was combined with input time ranges to determine slices of the chromatogram for isolation. Whenever the recorded UV intensity exceeded an input value within the determined time ranges, the eluting solution was diverted, and the fraction was trapped on an SPE cartridge. A separate cartridge was used for each of the three peaks of interest and each set of cartridges was reused for up to six consecutive runs, before a new set was used.

A threshold of 150 mAU was applied for all three peaks of interest, with the time frame of collection set to 28.0 – 29.1 for the first, 30.3 – 32.8 for the second and 41.0- 43.1 min for the third peak respectively. The time range in which each individual fraction was collected, as well as the number of fractions collected is listed below with the analytical data. In order to ensure the retention of the fractions on the SPE cartridges an additional make-up flow consisting of a 0.1 mol/L ammonium bicarbonate that had been adjusted to a pH value of 8.4 using an ammonia solution, was mixed to the eluting solution before the trapping process. This pH value was chosen due to the pK_s value of Naloxone's amino group,[25] in order to form neutrally charged molecules that would be better retained on the polyvinyl benzene cartridges. This make-up flow was set to 0.01 mL/min for most of the HPLC run, and was increased to 2.5 mL/min during 26 – 48 min.

After the isolation was complete, the loaded cartridges were then dried for 30 min under nitrogen flow and eluted using 70 μL deuterated acetonitrile per cartridge, pooling all collected samples of the three peaks of interest into 5.0 mm NMR capillaries for samples measured in deuterated acetonitrile and into HPLC vials for samples measured in deuterated methanol. The deuterated methanol samples were then dried under nitrogen flow and were transferred into 2.5 mm NMR tubes using 140 μL deuterated methanol.

Analytical Data of 2

NMR and HRMS data, as well as the time frames of collection during HPLC-SPE separation for the three stereo isomers of **2** are listed below. It should be mentioned, that though the isomers of **2** could be separated via HPLC, the isolated isomers were capable of reacting into one another, swiftly forming an equilibrium in solution. As such, HRMS data is given for the individual isomers in order of elution, whereas the NMR data is given as a mixture of the three.

NMR Samples were measured in both deuterated methanol and acetonitrile for a wider range of data. However, only the NMR data of the sample measured in deuterated methanol is listed below, as the sample in deuterated acetonitrile had too many residual solvent signals overlapping with the signals of the compound in the ^{1}H NMR spectra. The spectra recorded in deuterated acetonitrile are however, depicted in the supplementary information. As the two Naloxone units within one molecule could not be differentiated from one another, the molecules are treated as symmetric, with one signal arising from each mirrored set of nuclei (Fig. 2). These mirrored sets may each show up to three signals as all three stereoisomers are contained within the measured sample. In cases where these individual signals

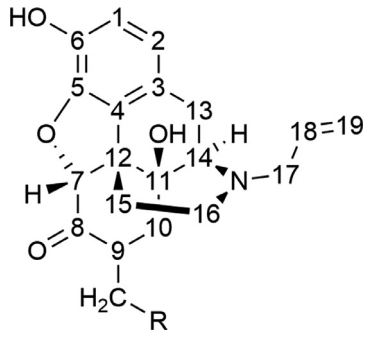

Fig. 2. Numbering scheme for the assignment of ^{1}H and ^{13}C NMR signals of **2**. With R representing a second Naloxone unit with an identical numbering scheme to the first.

were not visible, the region of the chemical shifts is given. Should the signal of an individual isomer be visible in one of these regions, it is listed separately. However, no integral is given in these cases, as they are already included in the listed region. The signals in both the proton and carbon spectra are never assigned to a specific stereoisomer. The combined yield of the three isomers was calculated by approximation, using the UV chromatogram and does not represent the isolated yield.

^{1}H NMR (400.15 MHz, CD_3OD): δ = 6.65, 6.62, 6.61 (d, ^3J(H1, H2) = 8.2, 8.2, 8.1 Hz, 2H, H1), 6.56, 6.56, 6.55 (d, ^3J(H1,H2) = 8.1, 8.1, 8.1 Hz, 2H, H2), 5.97 – 5.76 (m, 2H, H18), 5.38 – 5.12 (m, 4H, H19), 4.75, 4.71, 4.65 (s, 2H, H7), 3.28 – 2.92 (m, 10H, H9, H13, H14, H17), 3.11 (d, ^2J(H13,H13') = 18.4 Hz, H13), 2.77 – 2.00 (m, 8H, H9, H13', H15, H16'), 2.64 (dd, ^2J(H16,H16') = 12.6, ^3J(H15, H16) = 5.4 Hz, H16), 2.53 (dd, ^2J(H14,H14') = 18.8, ^3J(H13',H5) = 5.5 Hz, H13'), 2.45 (td, $^{2,3}J$(H15,H15' and H16') = 12.8, ^3J(H15,H16) = 5.3 Hz, H15), 2.15 (td, $^{2,3}J$(H16',H15 and H16) = 12.8, ^3J(H15',H16') = 3.1 Hz, H16'), 1.87 (dd, ^2J(H10,H10') = 13.3, ^3J(H9,H10) = 4.4 Hz, 2H, H10), 1.65 – 1.17 (m, 6H, H10', H15', CH_2), 1.45 (dd, ^2J(H10,H10') = 13.3, ^3J(H9,H10) = 4.4 Hz, H10), 1.29 ppm (t, $^{2,3}J$(H10',H9 and H10) = 13.3 Hz, H10'). ^{13}C NMR (100.63 MHz, CD_3OD): δ = 212.7, 212.5 (C8), 146.3, 145.0, 144.8 (C5), 140.9, 140.9, 139.7 (C6), 136.5, 136.4, 136.4 (C17), 130.4 (C4), 125.1, 125.1 (C3), 120.8, 119.8 (C2), 119.1, 119.0, 119.0 (C1), 118.6, 118.4 (C19), 93.3, 92.2, 89. 4 (C7), 72.1, 72.0, 71.6 (C11), 64.0, 63.5, 63.0 (C14), 58.6, 58.3 (C17), 52.8 (C12), 45.0 – 44.8 (C16), 43.1 (C9), 39.7 (C10), 31.2 (C15), 34.4, 29.3, 28.3 (CH_2), 24.0, 23.6, 23.6 ppm (C13). HRMS (ESI): *m/z* calculated for $C_{39}H_{42}N_2O_8 + H^+$ [M + H^+] = 667.3014, found = 667.3023 (Isomer I), 667.3020 (Isomer II) and 667.3023 (Isomer III). Isolation time frame: 30.30 – 31.36 min (Isomer I), 32.31 – 34.79 min (Isomer II) and 42.64 – 44.74 min (Isomer III). Combined yield: 0.56 mmol, 72%.

Results and Discussion

Analysis

The impurity was first discovered during LC-UV analysis as part of regular stability and purity testing of an investigational medicinal product. The substance in question showed near identical UV –Vis responses to the API Naloxone, with a maximum present at around 205 nm and a smaller response at 282 nm. This gave the first indication that the impurity originated from degradation of the API and not an excipient. The unchanged responses indicated that no change to the chromophore system had occurred, suggesting that the aromatic system had not changed compared to Naloxone, and that the reaction had taken place in a different region of the molecule.

Further information on the nature of the impurity was acquired during HPLC—HRMS analysis. ESI analysis in positive mode detected a single charged ion with an *m/z* value of 667 for [$M + H$]$^+$ and a

double charged ion with an *m/z* value of 334 for $[M + 2H]^{2+}$, suggesting a molecule with an *m/z* value of approximately 666, compared to 327 for Naloxone. The increase of molecular weight and the presence of a double charged ion indicate that two Naloxone units are involved in the formation of this impurity. 2,2′-BisNaloxone is a known dimeric structure of Naloxone, linked via the aromatic ring. With an *m/z* value 652 however,[26,27] this leaves a difference of 14 atomic units (au) compared to the detected impurity.

This *m/z* value of 14 coincides with the weight of a CH_2 group indicating the involvement of an additional methylene unit in the formation of the impurity in question. Several literature sources report on formaldehyde forming a methylene bridge linking two units of APIs such as hydrochlorothiazide or Melatonin.[22,28-30] As such, formaldehyde was considered as a possible source of the additional methylene group and was therefore implemented in degradation experiments.

Synthesis

Before the synthesis, experiments regarding the formation of the impurity were performed. As formaldehyde had been identified as likely cause of the reaction, experiments were conducted using formaldehyde. First acidic and neutral conditions were explored using formic acid. Though the impurity in question was detected during HPLC-UV/HRMS analysis for acidic conditions, the amounts were insufficient for a potential synthetic route. No traces of the impurity were found under neutral conditions. As such base conditions were explored using sodium hydroxide, resulting in higher yields, prompting the application of a synthesis under basic conditions.

One equivalent of Naloxone hydrochloride was allowed to react with approximately half an equivalent of formaldehyde in a solution of sodium hydroxide in methanol. The solution was heated to 55 °C for 3 h. Reactions were performed in concentrations of 0.2 and 0.4 mol/L sodium hydroxide, with the later resulting in higher yields. After 3 h the reaction solution was neutralized using acetic acid and analyzed as is.

Identification

During LC—HRMS analysis of synthesized samples, two additional peaks in the chromatogram were detected that also had an *m/z* value of 666. This observation indicated that the impurity in question possesses three stereoisomers and therefore contains at least two stereo centers. Also the observation was made, that three, new compounds with an *m/z* value of 1006 for $[M + H]^+$, 503 for $[M + 2H]^{2+}$ and 336 for $[M + 3H]^{3+}$ had formed in small amounts. These values could indicate the presence of additional compounds containing three Naloxone units linked by two methylene bridges. Increased amounts of formaldehyde may favor the formation of these compounds, but no investigations of such kind were made as part of this work.

In combination with the information gained during HPLC-DAD-HRMS, NMR data enabled the final structural elucidation. In order to acquire pure samples in sufficient amounts for NMR analysis, a hyphenated HPLC-DAD-HRMS/SPE-NMR system was applied, that uses time correlated UV data to selectively trap compounds of interest on solid phase cartridges during several consecutive HPLC runs. NMR analysis was first performed for the second of the three peaks of interest, as this was the signal with the largest area in the UV chromatogram.

Assessment of the data led to the conclusion that the impurity in question was a methylene bridged product (**2**) of two units of Naloxone, likely formed in an aldol condensation followed by a Michael addition (Fig. 3).

For better comparability, a series of 1D (^1H, ^{13}C) and 2D (COZY, HSQC, HMBC) spectra of Naloxone hydrochloride were recorded. Due to solubility reasons, the spectra of the API were measured in

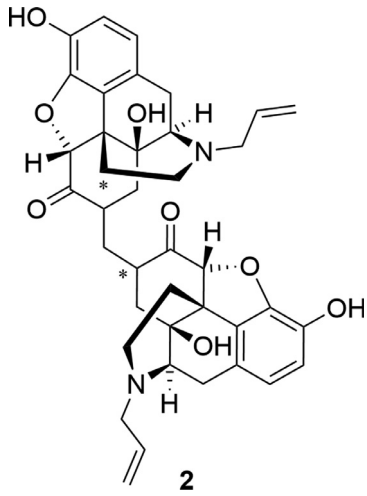

Fig. 3. Structure of the methylene bridged Naloxone impurity (**2**). The steric centers created during formation are marked by stars.

deuterated water, whereas **2** was measured in deuterated methanol (Fig. 4) as well as deuterated acetonitrile, leading to differences in chemical shifts. Using the knowledge gained from the analysis of the API, the signals arising from the aromatic protons, the vinyl group, as well as the proton attached to the furan ring and the cyclohexanone ring could be identified serving as basis for the further analysis of **2** *via* 2D NMR spectroscopy (COZY, HSQC, HMBC).

Using the aforementioned groups, especially the single proton attached to the carbon atom (**I**) connecting the cyclohexanone and the furan ring, the shifts, and in many cases coupling patterns, of the remaining protons were identified via the 2D spectra. For better visualization, a simplified version of the cyclohexanone and the furan ring of **2** is depicted in Fig. 5 with a numbering scheme for the relevant groups.

As the mass difference of 14 au detected during HRMS analysis indicated the presence of a newly formed methylene group with two Naloxone units, the question of the location of this CH_2 group arose. Observation of the phases of the cross peaks in the HSQC spectra of **2** revealed the presence of one additional signal, representing a CH group, at approximately 3.17 ppm compared to the original API. Due to strong overlap of signals in the ^1H NMR spectra, this new CH group's coupling pattern could not be identified, but using the information obtained from all 2D spectra its location within **2** was determined. Starting from the distinct singlet arising from the single proton attached to **I** and the ^{13}C signal of the adjacent keto group (**II**) the location of this new CH group was identified as position **III**.

The chemical shift of the carbon of **III** was found to be 43.1 (in methanol) and 42.3 ppm (in acetonitrile). By observing the cross peaks involving the carbon atoms **I, II** and **III** within the HSQC and HMBC spectra the ^{13}C signals of the newly introduced methylene group (**V**) were located at 27.7 and 28.3 ppm in deuterated acetonitrile and methanol respectively. More cross peaks between protons and carbon atoms in these areas were also observed in the HSQC spectra, however no clear cross peaks could be observed in the HMBC spectra. These signals likely arise from the additional isomers of **2** previously suggested by HRMS analysis. The signals in the HMBC spectra are best visible for the primarily formed stereoisomer, as this is the compound with the most substance, whereas the secondary formed stereoisomers make up less substance, lowering the quality of the HMBC spectra.

This observation was also made for several other protons and carbon atoms in the NMR spectra, where up to three, well resolved signals could be observed. However, due to signal overlap the coupling patterns could not always be determined in the ^1H NMR spectra. In

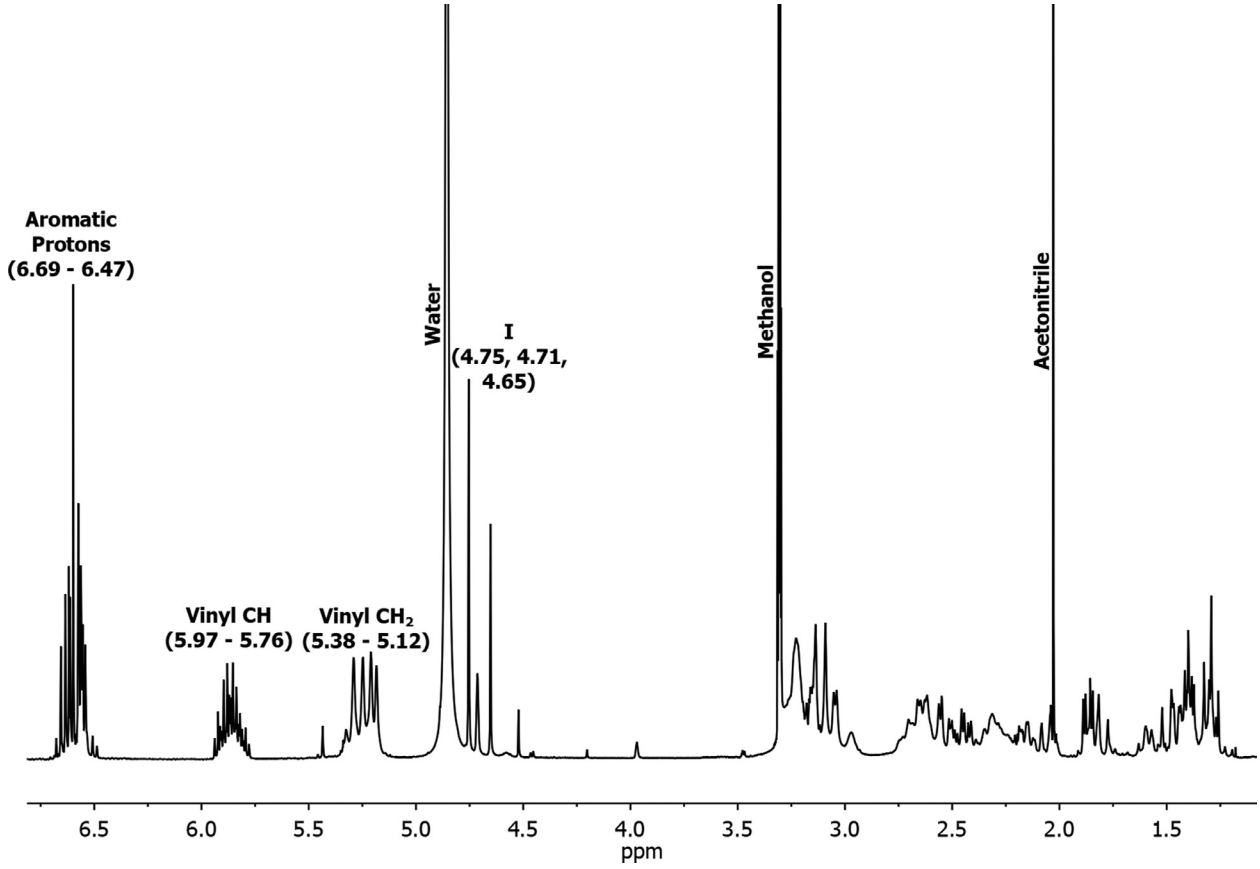

Fig. 4. ^{1}H—NMR spectrum of **2**, recorded in deuterated methanol.

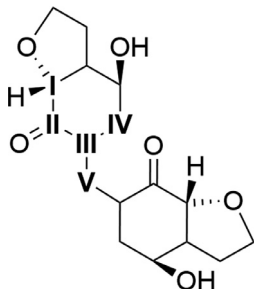

Fig. 5. Simplified depiction of the cyclohexanone and furan ring of **2**, with a numbering scheme for easier assignment of NMR signals.

the case of the protons attached to **I** and the aromatic protons, clear assignments for three sets of ^{1}H and ^{13}C signals could be made. As such, the aromatic protons showed two times three sets of doublets (Fig. 6) and the proton attached to **I** was visible as three individual singlets (Fig. 7).

As previously mentioned, NMR spectra were measured for the isolated fraction of the second relevant of three peaks observed in the UV chromatogram and therefore only one of the three stereoisomers should have been observed. The presence of three different sets of signals in the NMR spectra indicates that isomerization took place, forming an equilibrium between the three possible isomers. To confirm this assumption, all three isolated fractions were once more analyzed by UV chromatography directly after isolation. In all cases the observation was made that the three stereoisomers had reformed in the same ratio observed in the original sample.

As there are two new additional stereo centers present in **2** compared to Naloxone, four sets of stereoisomers can be proposed; (*R*,*R*), (*S*,*S*), (*R*,*S*) and (*S*,*R*). 3D models of the molecules showed that the (*R*,*S*) and (*S*,*R*) isomers are interchangeable by rotation of the molecule, leaving three distinct stereoisomers as is supported by the experimental data. A possible explanation for the change of conformation in the stereocenters is a keto-enol tautomerization taking place between the keto groups and the newly formed stereocenters in the individual Naloxone units. During this intramolecular proton transfer a change between *R* and *S* conformation may occur.

Formation

As formaldehyde was identified as likely cause of the formation of **2**, investigations into possible sources were conducted. Examination of the ORF's formulation revealed PEG and hydroxypropyl methylcellulose as potential sources (Substances used in the formulation are listed in the Supplementary Information). Even in GMP grade, both these excipients are literature known to contain varying amounts of formaldehyde and formic acid due to synthetic routes and degradation, such as oxidation.[17-21,31] Since the initial aldol-like reaction is known to proceed under both base and acidic catalysis, as supported by the previously mentioned experiments, the formic acid formed via excipient degradation and citric acid in the formulation might serve as initiator for the formation of **2** within the ORFs.

Base catalysis is likely to initiate the reaction *via* deprotonation of Naloxone at the methylene group neighboring the keto group, forming an enolate intermediate, whereas acid catalysis activates formaldehyde by protonation of the oxygen atom. In the base catalyzed case, aldol condensation likely leads to intermediate **3** (Fig. 8), which then reacts with a second unit of Naloxone in a Michael addition reaction to form **2**. The acidic reaction likely proceeds via an aldol addition to form compound **4**, followed by a condensation reaction to

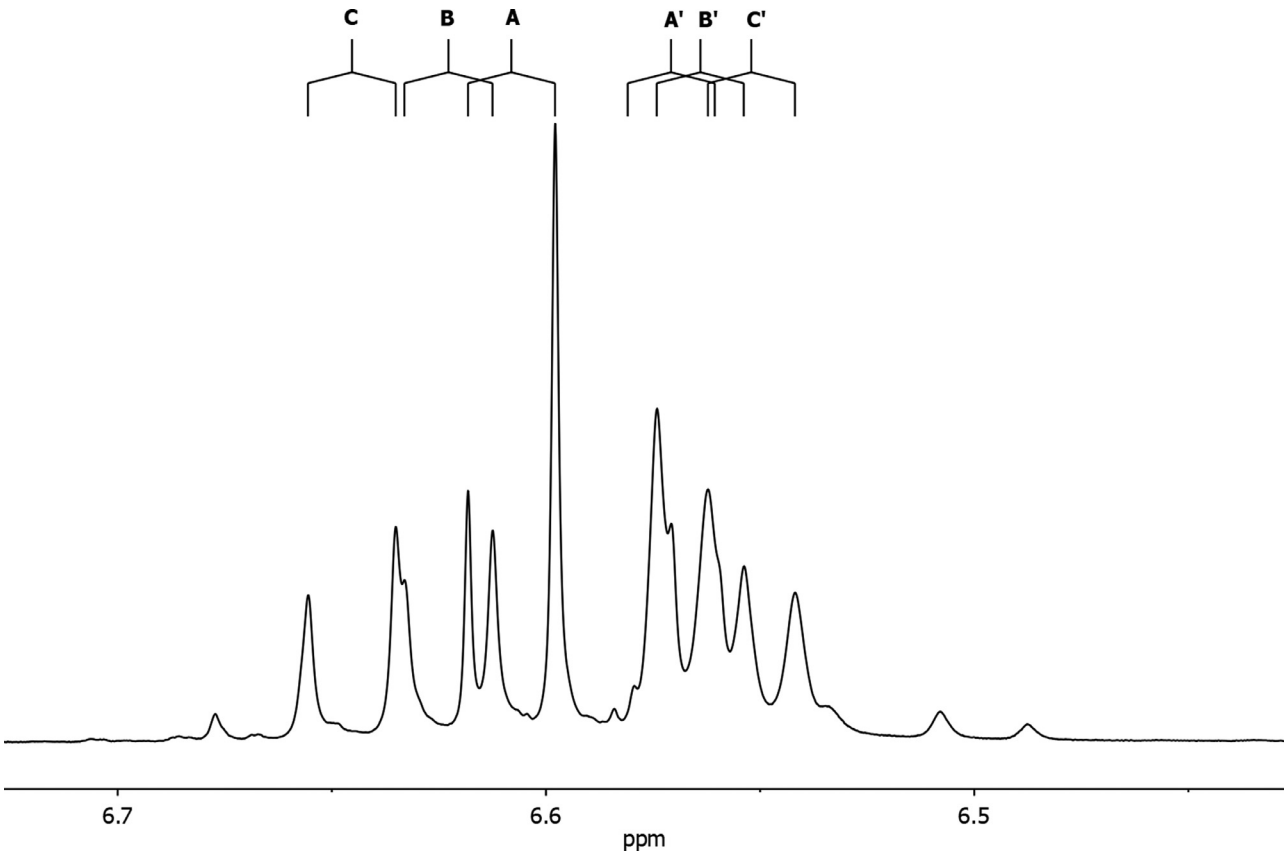

Fig. 6. ^{1}H NMR spectrum of the signals arising from the aromatic protons of **2**, recorded in deuterated methanol.

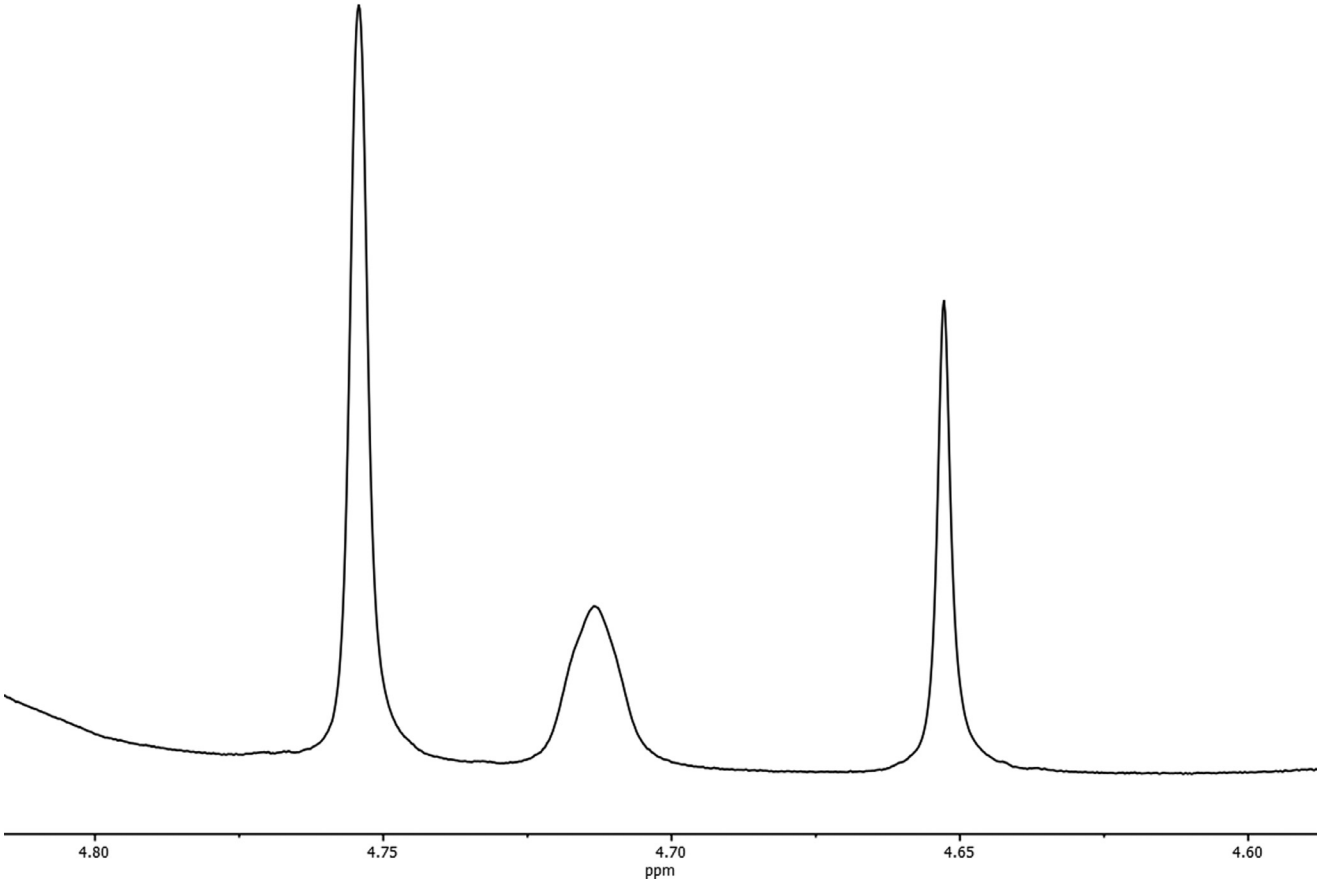

Fig. 7. ^{1}H NMR spectrum of the signals arising from the protons attached to I for the individual stereoisomers of **2**, recorded in deuterated methanol.

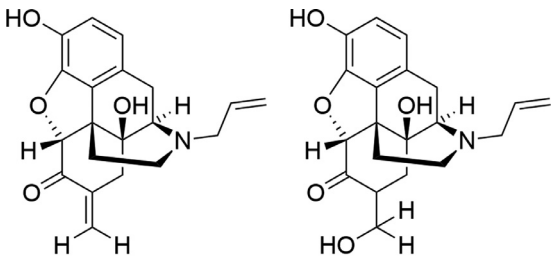

Fig. 8. Proposed intermediate compounds of the reaction of Naloxone with formaldehyde under basic (**3**) and acidic (**4**) conditions.

form **2**. Similar reactions are known for cyclohexanone derivatives and aldehydes (The proposed mechanisms are depicted in the Supplementary Information).[32,33]

Conclusion

In our research we identified three stereoisomers of a previously unknown degradation product of the opioid antagonist Naloxone, discovered in experimental Buprenorphine-Naloxone ORFs. This new compound was shown to form via an aldol condensation followed by a Michael addition, involving two units of Naloxone and one unit of formaldehyde.

Using a hyphenated HPLC-DAD-HRMS/SPE-NMR system, attempts were made to isolate the individual stereoisomers. However, isolation could not be achieved due to rapid racemization, supposedly via keto-enol tautomerization. Nevertheless, using HRMS and NMR analysis the constitution of the new compound was determined.

As formaldehyde is a common trace impurity in several widely applied pharmaceutical excipients,[17-21,31] the possibility of similar reactions in other APIs containing comparable functional groups as Naloxone should be noted. These findings should be considered when putting together a drugs formulation to prevent the formation of unwanted degradation products.

Author Agreement

The manuscript was written through contributions of all authors. All authors have given approval to the final version of the manuscript.

Statement on Funding

Hexal AG, Industriestraße 25, 83607 Holzkirchen, Germany.

Statement on Research Data

Research data used in the preparation of the manuscript is available, and can be requested from the corresponding authors.

Declaration of Competing Interests

The authors declare that they have no known competing financial interests or personal relationships that could have appeared to influence the work reported in this paper.

Acknowledgements

We thank the Hexal AG for providing funds, materials as well as the facilities, equipment and analytical machines necessary for the research of this paper.

Supplementary Materials

Supplementary material associated with this article can be found in the online version at doi:10.1016/j.xphs.2021.11.014.

References

1. World Health Organization. *Guidelines For the Psychosocially Assisted Pharmacological Treatment of Opioid Dependence*. Geneva: World Health Organization; 2009.
2. Scholl L, Seth P, Kariisa M, Wilson N, Baldwin G. Drug and opioid-involved overdose deaths – United States, 2013-2017. *MMWR*. 2019;67:1419–1427.
3. Landers A. Nonprescription availability of the opioid antagonist naloxone. *Am. J. Health-Syst. Pharm*. 2018;75(14):1069–1072.
4. Bell J, Strang J. Medication treatment of opioid use disorder. *Biol. Psychiatry*. 2020;87:82–88.
5. Davis AM, Inturrisi CE. Methadone blocks morphine tolerance and *N*-methyl-$_D$-aspartate-induced hyperalgesia. *JPET*. 1999;289(2):1048–1053.
6. Mattick RP, Kimber J, Breen C, Davoli M, Been R. Buprenorphine maintenance versus placebo or methadone maintenance for opioid dependence. *CDSR*. 2003;2 (CD002207):1–31.
7. Elarabi HF, Hasan N, Marsden J. Therapeutic drug monitoring in buprenorphine/naloxone treatment for opioid use disorder: clinical feasibility and optimizing assay precision. *Pharmacopsychiatry*. 2020;53:115–121.
8. Walsh SL, Eissenberg T. The clinical pharmacology of buprenorphine: extrapolating from the laboratory to the clinic. *Drug Alcohol Depend*. 2003;70:13–27.
9. Orman JS, Keating GM. Buprenorphine/Naloxone: a review of its use in the treatment of opioid dependence. *Drugs*. 2009;69(5):577–607.
10. Mendelson J, Jones RT. Clinical and pharmacological evaluation of buprenorphine and naloxone combinations: why the 4:1 ratio for treatment? *Drug Alcohol Depend*. 2003;70:29–37.
11. Stoller KB, Bigelow GE, Walsh SL, Strain EC. Effects of buprenorphine/naloxone in opioid-dependent humans. *Psychopharmacology (Berl.)*. 2001;154:230–242.
12. Raisch DW, Fye CL, Boardman KD, Sather MR. Opioid dependence treatment, including buprenorphine/naloxone. *Ann Pharmacother*. 2002;36:312–321.
13. Pergolizzi JV, LeQuang JA, Taylor R, Raffa RB. The place of community rescue naloxone in a public health crisis of opioid overdose. *Pharmacol. Pharm*. 2019;10:61–81.
14. Wermeling DP. Review of naloxone safety for opioid overdose: practical considerations for new technology and expanded public access. *Ther Adv Drug Saf*. 2015;6:20–31.
15. Fudala PJ, Bridge TP, Herbert S. Office-based treatment of opiate addiction with a sublingual-tablet formulation of buprenorphine and naloxone. *N Engl J Med*. 2003;349(10):949–958.
16. Kim HK, Connors NJ, Mazer-Amirshahi ME. The role of take-home naloxone in the epidemic of opioid overdose involving illicitly manufactured fentanyl and its analogs. *Expert Opin. Drug Saf*. 2019;18:465–475.
17. Qiu F, Norwood DL. Identification of Pharmaceutical Impurities. *J. Liq. Chrom. Relat. Tech*. 2007;30:877–935.
18. Del Dario M–A, Hu J, Zhou P, Cauchon N. Simultaneous determination of formic acid and formaldehyde in pharmaceutical excipients using headspace GC/MS. *J. Pharm. Biomed. Anal*. 2006;41:738–743.
19. Bergh M, Magnusson K, Nilsson JGN, Karlberg AT. Formation of formaldehyde and peroxides by air oxidation of high polyoxyethylene surfactants. *Contact Derm*. 1998;39:14–20.
20. Bindra DS, Williams TD, Stella VJ. Degradation of O^6-benzylguanine in aqueous polyethhylene glycol 400 (PEG 400) solutions: concerns with formaldehyde in PEG 400. *Pharm. Res*. 1994;11:1060–1064.
21. Fujita M, Ueda T, Handa T. Generation of Formaldehyde by pharmaceutical excipients and its absorption by meglumine. *Chem. Pharm. Bull*. 2009;57:1096–1099.
22. Nassar MN, Nesarikar VN, Lozano R. Influence of formaldehyde impurity in polysorbate 80 and PEG-300 on stability of parenteral formulation of BMS-204352: identification and control of degradation product. *Pharm. Dev. Technol*. 2004; 9:189–195.
23. Qin X-Z, Ip DP, Chang KH-C, Dradransky PM, Brooks MA, Sakuma T. Pharmaceutical application of LC-MS. 1 – Characterization of a famotidine degradates in a package screening study by LC-APCI MS. *J. Pharm. Biomed. Anal*. 1994;12:221–233.
24. Babij NR, McCusker EO, Whiteker GT. NMR chemical shifts of trace impurities: industrially preferred solvents used in process and green chemistry. *Org. Process Res. Dev*. 2016;20:661–667.
25. Llinàs P;, Glen RC, Goodman JM. Solubility challenge: can you predict solubilities of 32 molecules using a database of 100 reliable measurements? *J. Chem. Inf. Moedl*. 2008;48(7):1289–1303.
26. Rafelsberger B. *Stabilization of Naloxonhydrochlorid*. 1998. WO 98/35679, August 20.
27. Hansen P, Hofmann H, Schumann C. Stabilisiertes Kombinationsarzneimittel enthaltend Naloxone und ein Opiatanalgetikum. *EP 0 913 152 A1*. 1999. Mai 6.
28. Franolic JD, Lehr GJ, Barry TL, Petzinger G. Isolation of a 2:1 hydrochlorothiazide-formaldehyde adduct impurity in hydrochlorothiazide drug substance by preparative chromatography and characterization by electrospray ionization LC-MS. *J. Pharm. Biomed. Anal*. 2001;26:651–663.
29. Laforce R., Rigozzi M., Mossi W., Guainazzi P., Calderari G., Aspects of melatonin manufacturing and requirements for a reliable active component. Biol. Signals Recept. 199;8:143–146.
30. Williamson BL, Tomlinson AJ, Mishra PK, Gleich GJ, Naylor S. Structural characterization of contaminants found in commercial preparations of

melatonin: similarities to case-related compounds from L-tryptophan associated with eosinophilia-myalgia syndrome. *Chem. Res. Toxicol.* 1998;11:234–240.

31. Stephenson SA, Bryant DK, Thomson CM, Walsgrove TC, Webb ML. An analytical study of the interaction of low levels of formaldehyde with active pharmaceuticals. *J. Pharm. Pharmacol.* 1998;50:122.
32. Akimova TI, Soldatkina OA, Ivanenko ZA, Savchenko VG. Methods of synthesis of alicyclic 1,5,9Triketones. reaction of transaminomethylation. *Russ J Org Chem.* 2017;53(5):720–728.
33. Akimova TI, Kravchenko NS, Denisenko VA. An alicyclic 1,5,9-triketone 2,6.bis[(2-*oxocyclohexyl*)*methyl*]cyclohexanone, its cyclic foem and reactions with *N*-nucleophiles. *Tetrahedron*. 2008;64:9548–9554.

3.2 Supplementary Information

Synthesis, Isolation and Identification of a Methylene-Bridged Naloxone "Dimer" Formed by Formaldehyde

Philipp Schmidt[1], Christine Kolb[2], Andreas Reiser[2], Markus Philipp[2], Hans-Christian Müller[2]*, Konstantin Karaghiosoff[1]*

[1]Department Chemie, Ludwig-Maximilians-Universität München, Butenandtstraße 5-13, Haus D, 81377 Munich, Germany, [2]Analytical Development, Hexal AG, Industriestraße 25, 83607 Holzkirchen, Germany,

Table of Contents

The programs used to produce the images in these supporting informations were *Compass Hystar* from Bruker, *Chromeleon* from Thermo Scientific as well as *MestreNova* from Mestrelab Research.

I UV Chromatogram

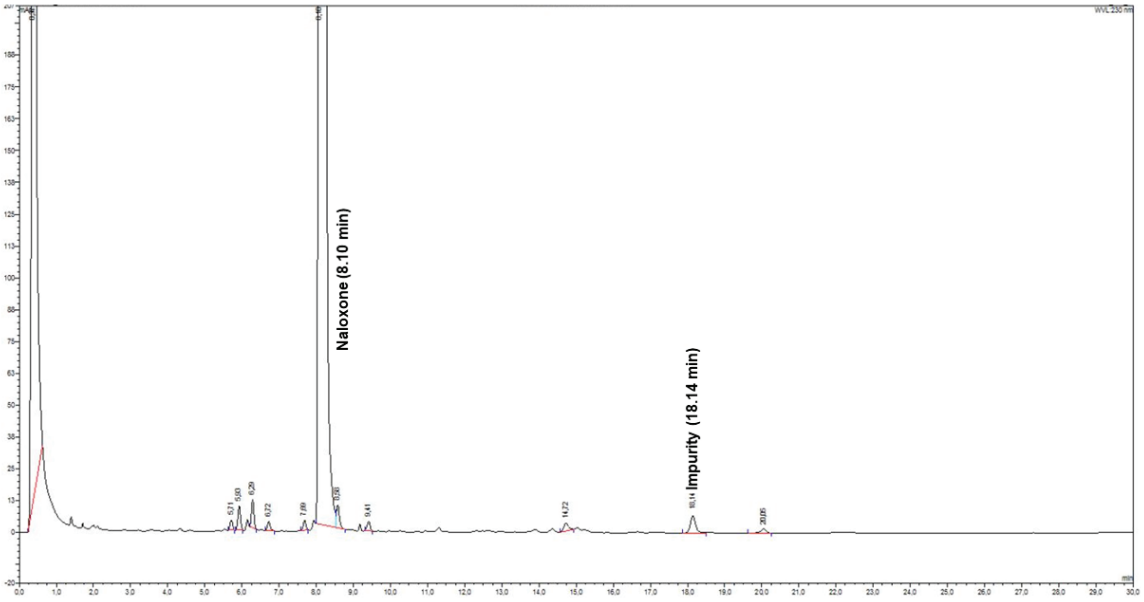

Figure S1. Excerpt of a UV Chromatogram of the discovery of **2** within an experimental Naloxone oral film. Naloxone (8.10 min) and Impurity **2** (18.14 min) are marked. As can be observed, only one of the three stereoisomers of **2** are visible in this sample. This may be due to the small amounts of **2** within the sample, resulting in only the predominately formed of the three stereoisomers being visible. The method used is described below (Table S1).

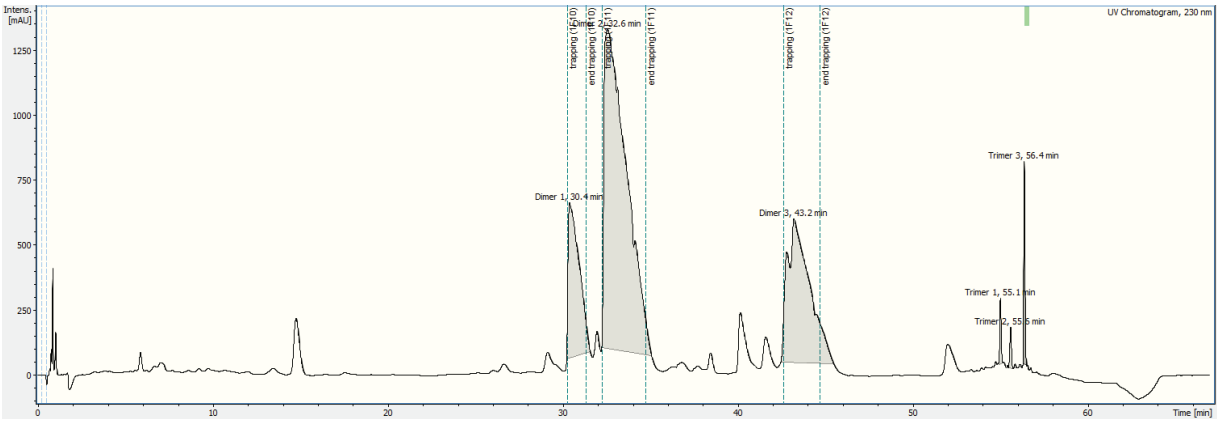

Figure S2. UV chromatogram of the separation and isolation of the individual stereoisomers of **2** from the reaction solution. The beginning and end of the tapping process is marked by dashed lines. The sudden falls and rises visible in the chromatogram in the regions of isolation are caused by changes of the flow and pressure, caused by the addition of the make-up flow and the diversion of the flow to the SPE cartridges.

Figure S3. UV chromatogram of fraction one after isolation, showing that all three stereoisomers had reformed.

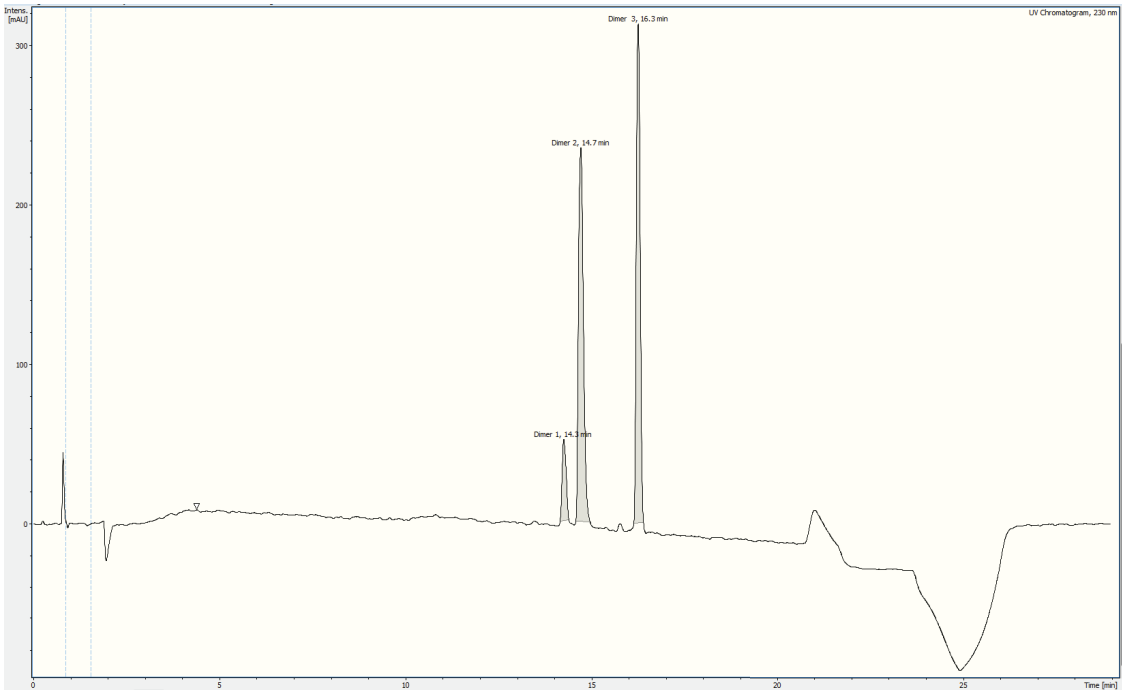

Figure S4. UV chromatogram of fraction two after isolation, showing that all three stereoisomers had reformed.

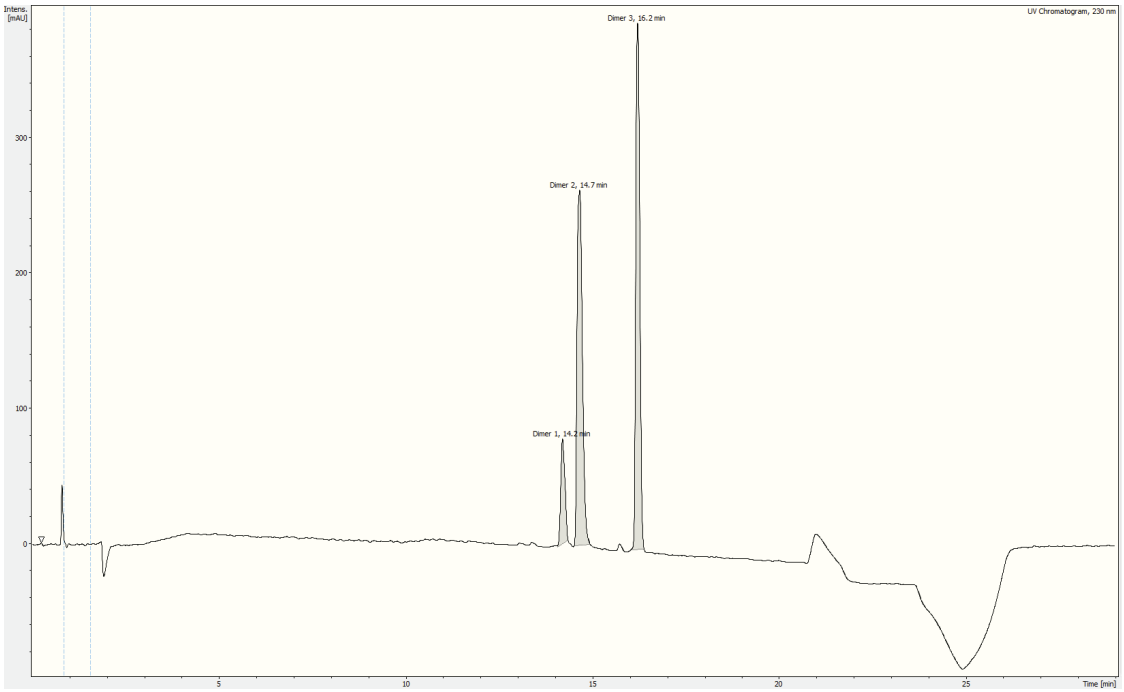

Figure S5. UV chromatogram of fraction three after isolation, showing that all three stereoisomers had reformed.

II MS Spectra

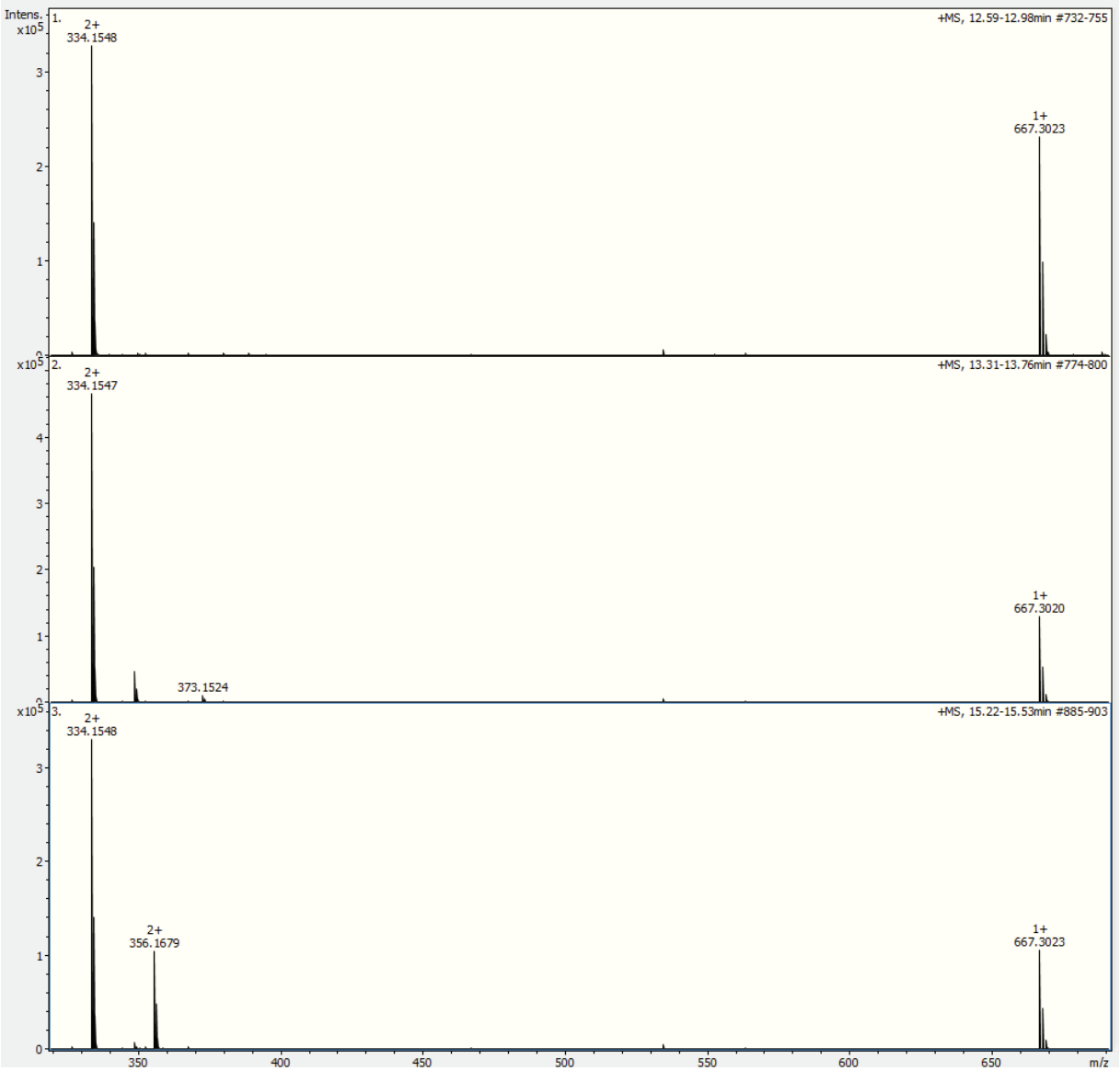

Figure S6. HRMS Data (ESI positive) of the three diastereomers of **2** in order of elution.

III NMR Spectra

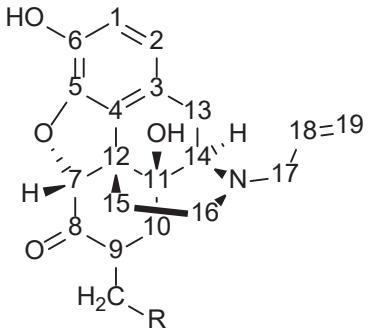

Figure S7. Numbering scheme for the assignment of ^{1}H and ^{13}C NMR signals of **2**. With R representing a second Naloxone unit with an identical numbering scheme to the first. (As depicted in Figure 2 of the main article)

III.I NMR Spectra of Naloxone Recorded in Deuterated Water

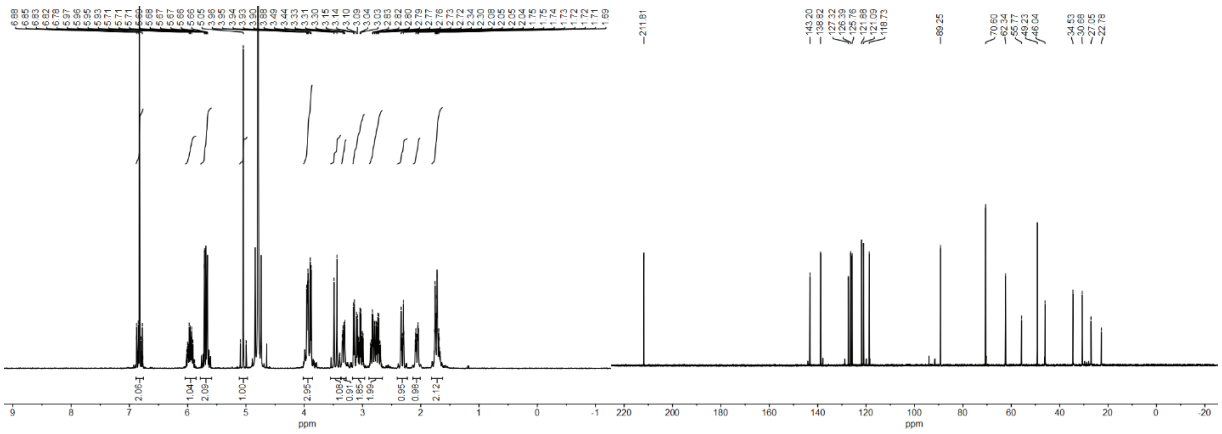

Figure S8. ^{1}H (left) and ^{13}C NMR (right) spectra of Naloxone.

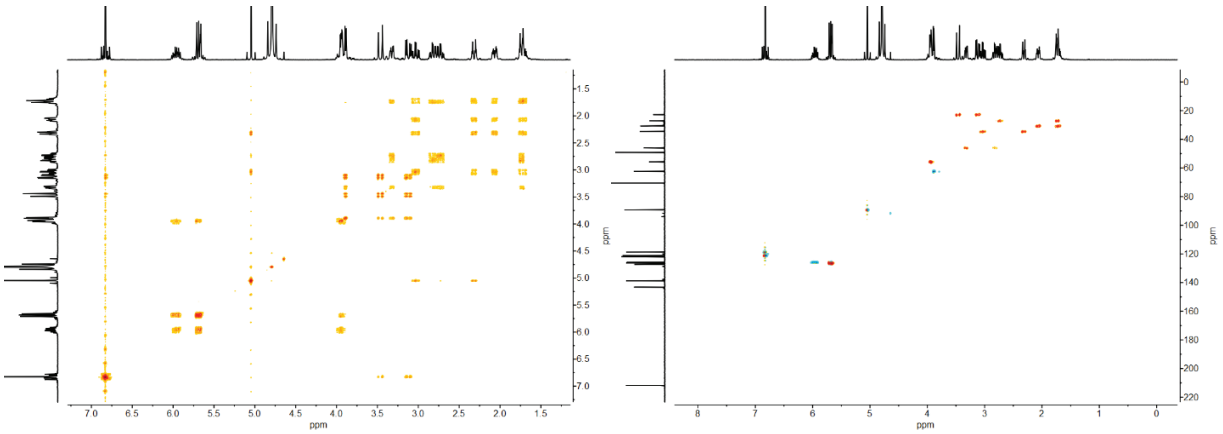

Figure S9. ^{1}H-^{1}H COSY (left) and ^{1}H-^{13}C HSQC (right) NMR spectra of Naloxone.

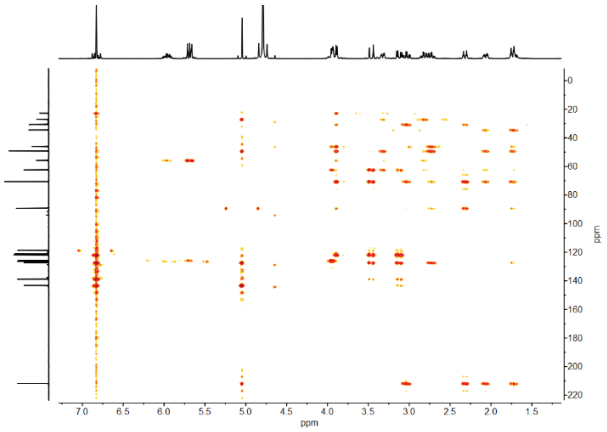

Figure S10. ^{1}H-^{13}C HMBC NMR spectrum of Naloxone.

III.II NMR Spectra of the Naloxone-Impurity Recorded in Deuterated Acetonitrile

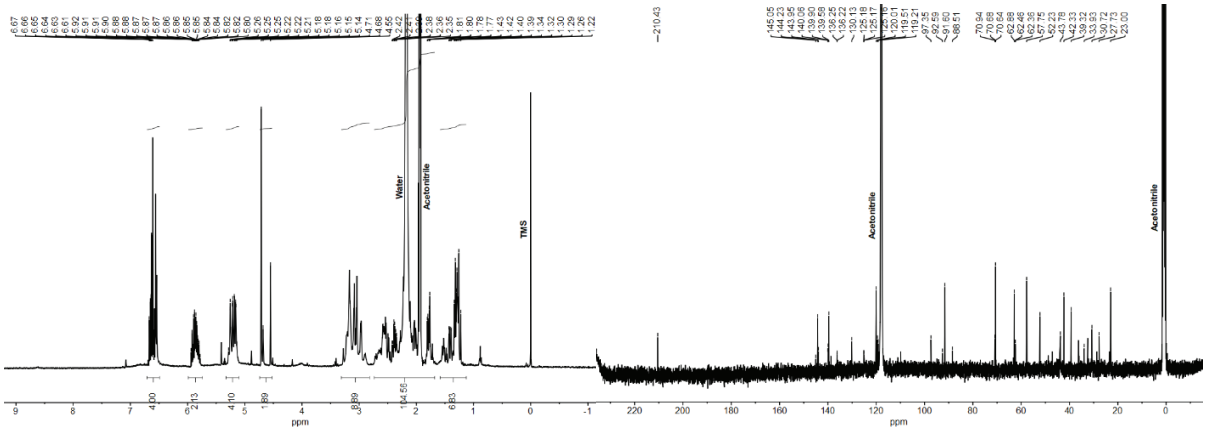

Figure S11. ^{1}H (left) and ^{13}C NMR (right) spectra of **2** (recorded in deuterated acetonitrile).

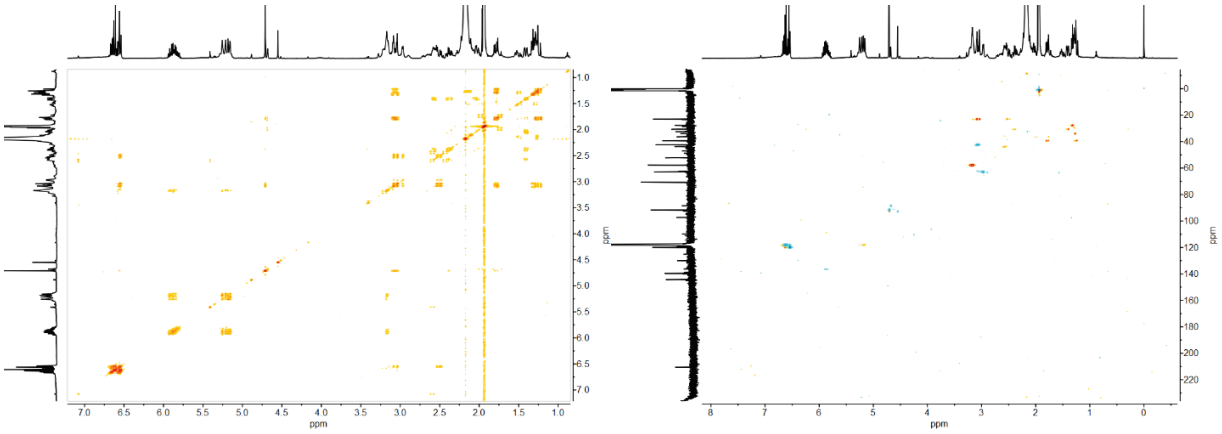

Figure S12. ^{1}H-^{1}H COSY (left) and ^{1}H-^{13}C HSQC (right) NMR spectra of **2** (recorded in deuterated acetonitrile).

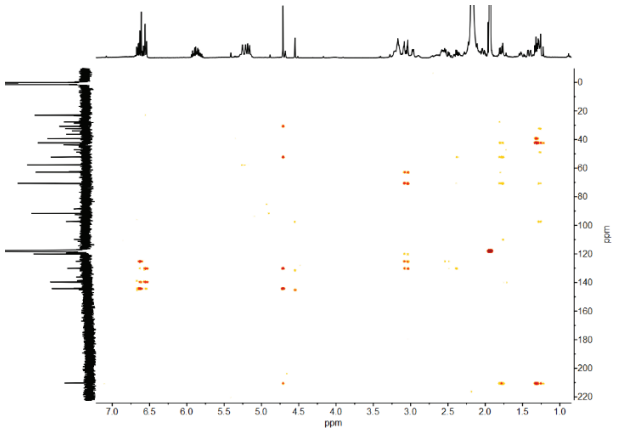

Figure S13. ^{1}H-^{13}C HMBC NMR spectrum of **2** (recorded in deuterated acetonitrile).

III.III NMR Spectra of the Naloxone-Impurity Recorded in Deuterated Methanol

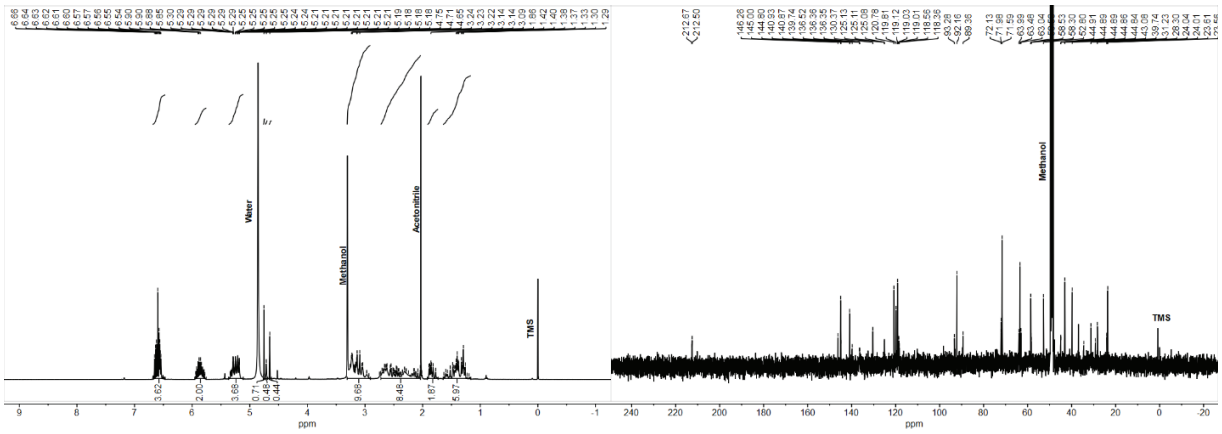

Figure S14. ^{1}H (left) and ^{13}C NMR (right) spectra of **2** (recorded in deuterated methanol).

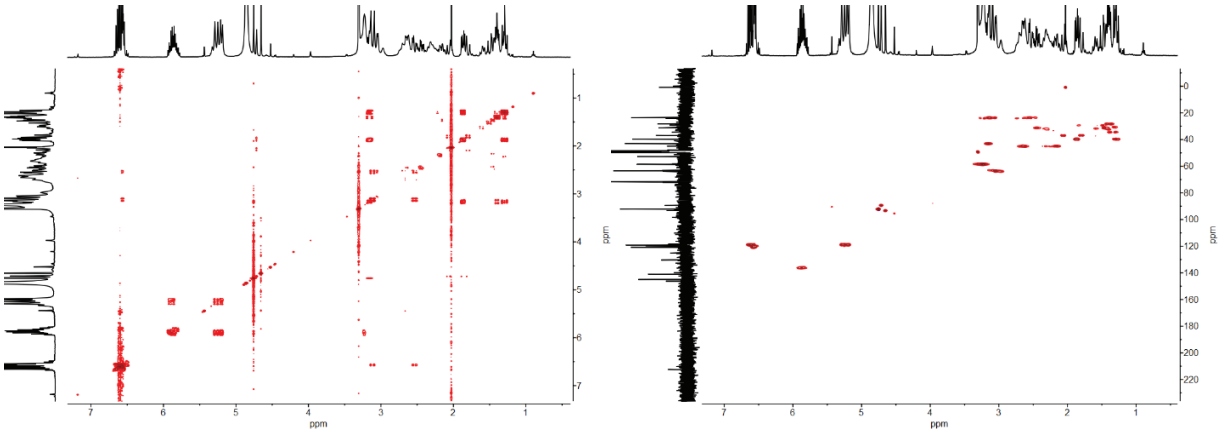

Figure S15. ^{1}H-^{1}H COSY (left) and ^{1}H-^{13}C HSQC (right) NMR spectra of **2** (recorded in deuterated methanol).

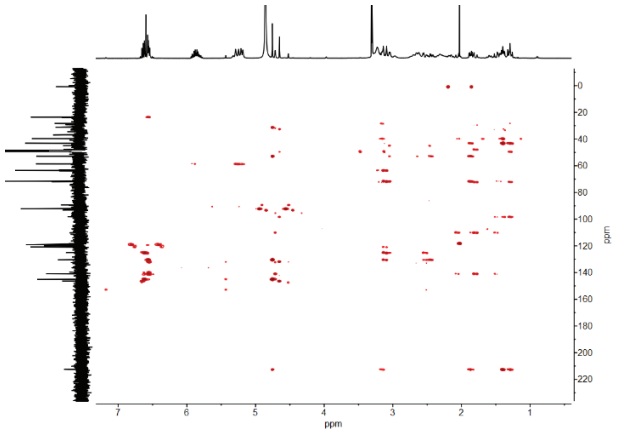

Figure S16. ^{1}H-^{13}C HMBC NMR spectrum of **2** (recorded in deuterated methanol).

III.IV Enlarged 2D NMR Spectra of the Naloxone-Impurity and Naloxone

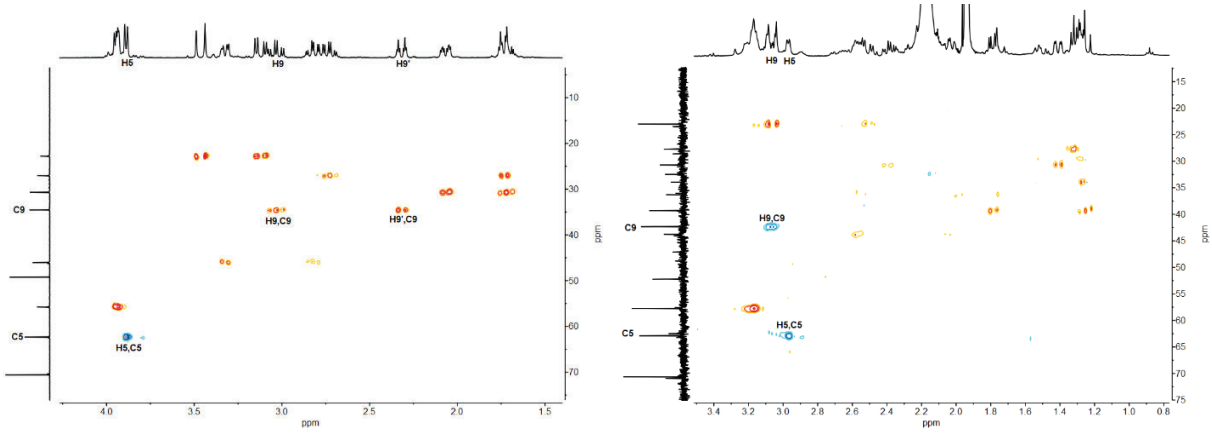

Figure S17. Aliphatic region of the ^{1}H-^{1}H HSQC NMR spectrum of Naloxone (left, recorded in D_2O) and ^{1}H-^{1}H HSQC NMR spectrum of **2** (right, recorded in deuterated acetonitrile). The phase for CH_2 groups is depicted in orange and for CH (and CH_3) groups is depicted in blue. In the case of Naloxone only one blue CH group is visible as group 5, while an additional CH group is visible as group 9, previously visible as orange CH_2 group, indicating the reaction at group 9.

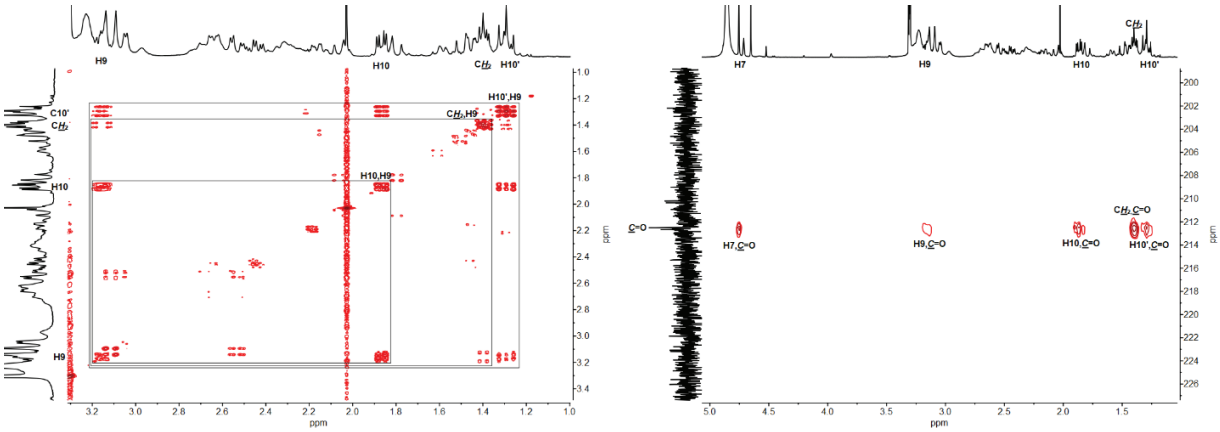

Figure S18. Enlarged sections of the ^{1}H-^{1}H COSY (left) and ^{1}H-^{13}C-HMBC (right) NMR spectra of **2** (recorded in deuterated methanol). The COSY depicts the coupling between H9 and H10, H10' and the protons of the bridging CH_2 group. The HMBC depicts the coupling of the keto group's carbon atom (C15) with H7, H9, H10, H10' and the protons of the bridging CH_2 group.

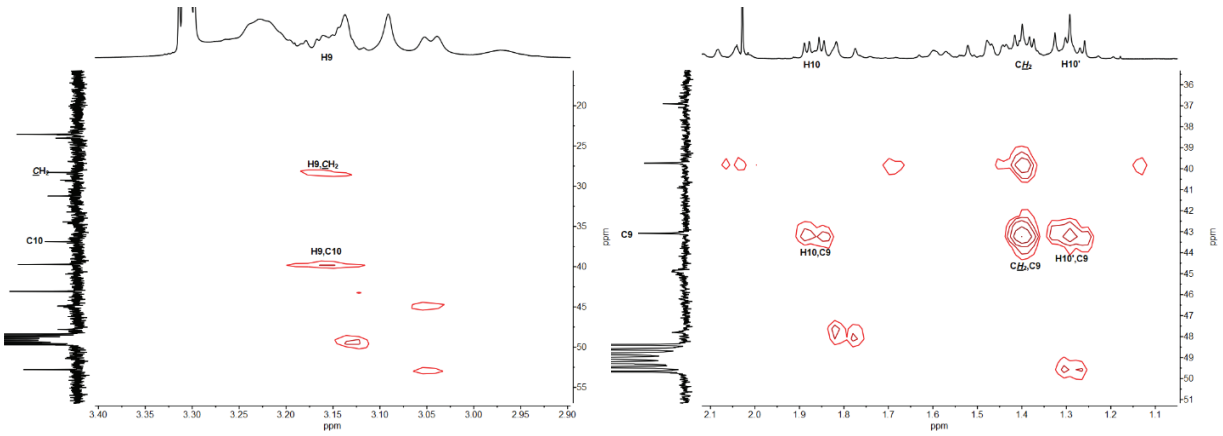

Figure S19. Enlarged sections of the ^{1}H-^{13}C HMBC NMR spectrum of **2** (recorded in deuterated methanol). The coupling of H9 with the carbon of the bridging CH_2 group and C10 is depicted on the left, whilst the coupling of C9 with H10, H10' and the protons of the bridging CH_2 group is depicted on the right.

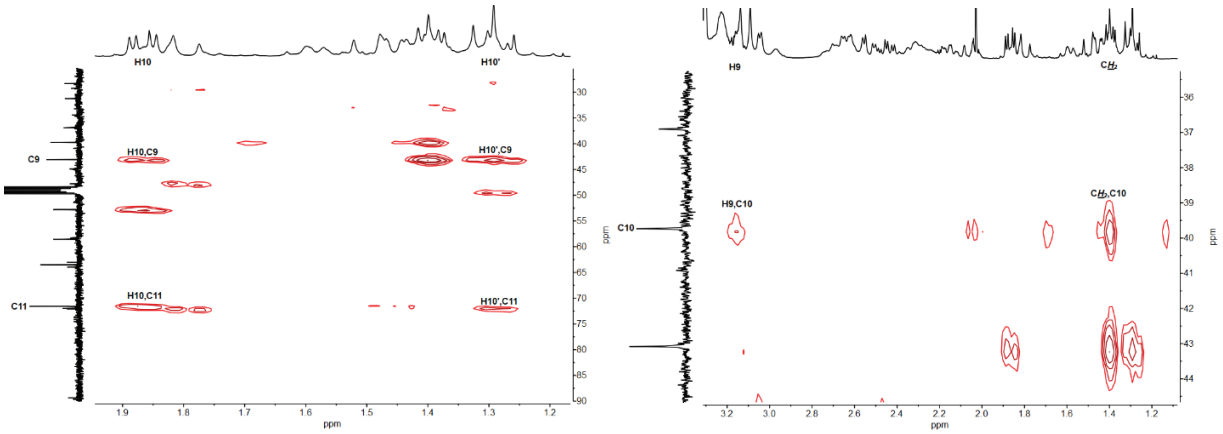

Figure S20. Enlarged sections of the ^{1}H-^{13}C HMBC NMR spectrum of **2** (recorded in deuterated methanol). The coupling of H10 and H10' with C9 and C11 is depicted on the left, whilst the coupling of C10 with H9 and the protons of the bridging CH_2 group is depicted on the right.

IV 3-D Models of the Stereoisomers of the Naloxone-Impurity

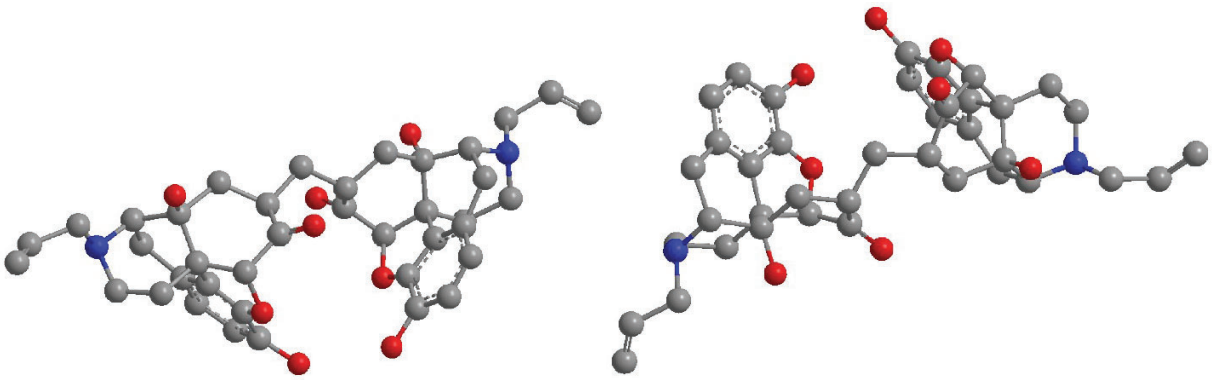

Figure S21. (R,R)-stereoisomer (left) and (S,S)-stereoisomer (right) of **2**.

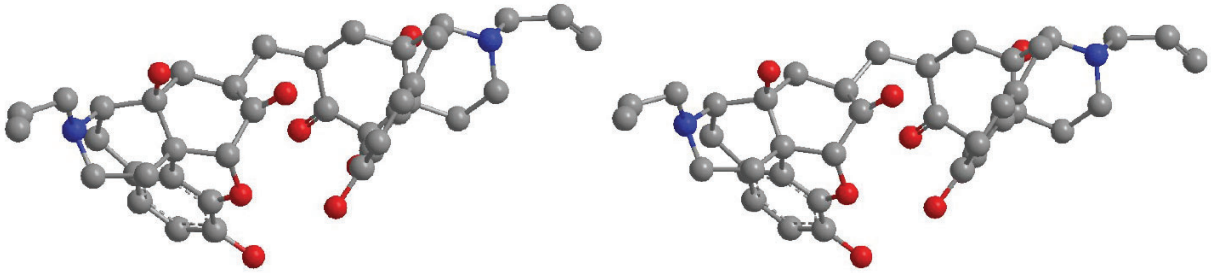

Figure S22. (R,S)-stereoisomer (left) and (S,R)-stereoisomer (right) of **2**. As seen comparing the two models, the (R,S)- and (S,R)-stereoisomers are identical molecules.

V Proposed Reaction Mechanisms for the Formation of the Naloxone-Impurity

The following are the proposed base (Fig. S24) and acid catalyzed (Fig. S25) mechanisms for the formation of **2**. Addition reactions and proton transfers that lead to the creation of one of the two new stereocenters in **2** are marked by dashed arrows and the stereo centers are marked by an asterisk (*). The mechanism is depicted in a simplified version, only depicting the parts of the cyclohexanone ring participating in the reaction. For better visualization Naloxone (**1**), compound **2** and intermediate compounds **3** and **4** are also depicted (Fig. S23).

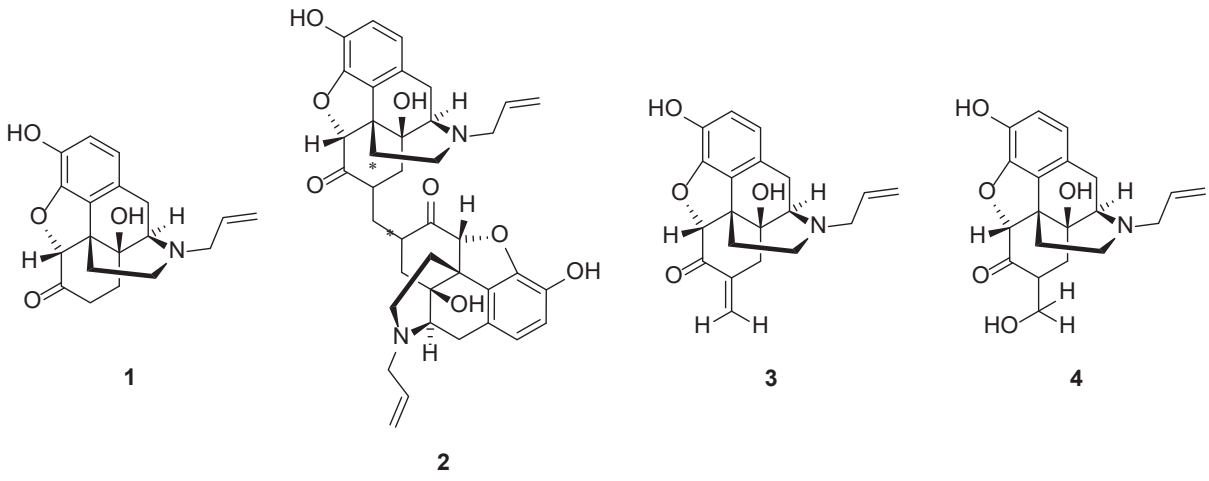

Figure S23. Structures of Naloxone (**1**), compound **2** and intermediate compounds **3** and **4**.

Base catalyzed aldol condensation:

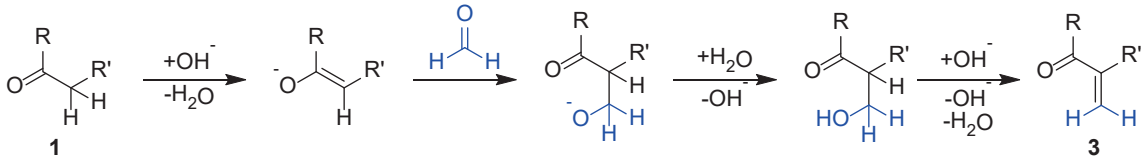

Base catalyzed Michael reaction:

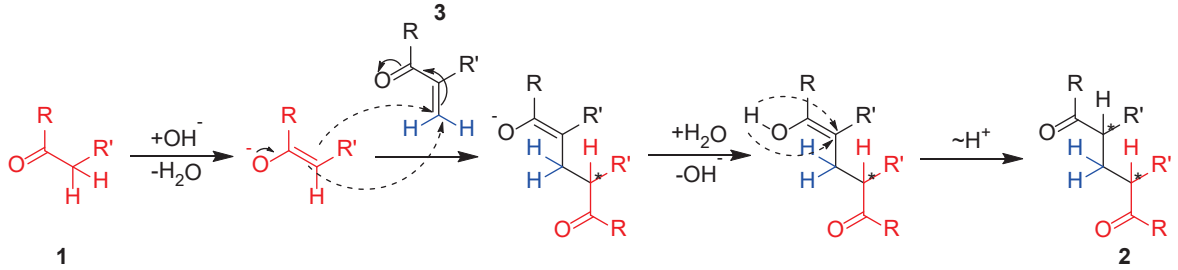

Figure S24. Proposed base catalyzed mechanism for the formation of **2**.

Acid catalyzed aldol addition:

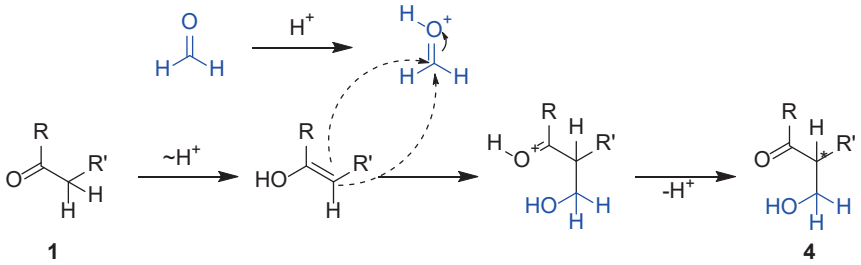

Acid catalyzed condensation reaction:

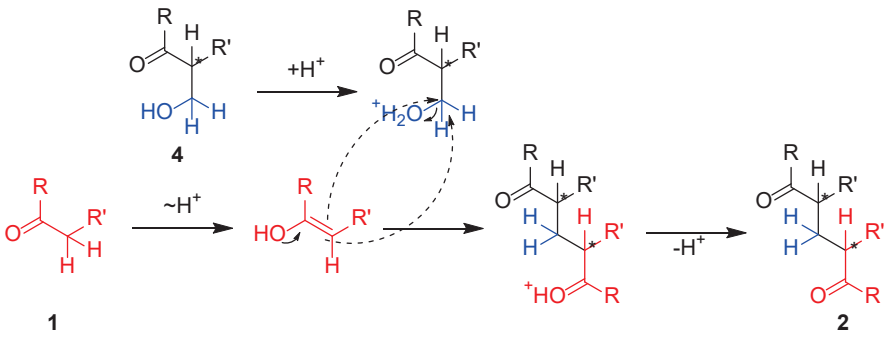

Figure S25. Proposed acid catalyzed meachanism for the formation of **2**.

VI Formulation of the Investigational Naloxone/Buprenorphine and Naloxone Oral Films

The experimental oral films were produced by ARx Drug Delivery Systems in the USA. The excipients used in the formulation as well as the solvents used in production are listed below (Table S1) however, the exact amounts used are not given, to not reveal company practice. The impurity was first detected in the oral films after 4 months and stress conditions: 40 °C and 75 %relative humidity.

It should be mentioned that the ratio of Tri-sodium citrate to citric acid are approximately 1:3, meaning an excess of protons is present within the formulation leading to acidic conditions within the oral films.

Table S1. List of Excipients and APIs used in the investigational oral films.

Name	Comment
Naloxone HCl	
Buprenorphine HCl	Only in the mixed oral films
Tri-sodium citrate water free	
Citric acid monohydrate	
Acesulfame K	
Maltitol	
PEG 100000	
PEG 200000	
PEG 900000	
Hydroxypropyl methylcellulose (HPMC)	
Acetone	Used during the production of the oral films
Water	Used during the production of the oral films

VII Additional HPLC Methods

Table S2. Method for the analysis of the experimental Buprenorphine-Naloxone and Naloxone oral films.

Instrument	Agilent 1100		
Column	Waters XBridge – 2.5 µm – 50 x 3.0 mm		
Temperature	40 °C		
Mobile Phase A	Na Octane-1-sulfonic acid solution (ultra-pure water) pH 2.0 : CAN = 92 : 8		
Mobile Phase B	Na Octane-1-sulfonic acid solution (ultra-pure water) pH 2.0 : CAN = 54 : 46		
Gradient	**Time (min)**	**% A**	**% B**
	0	100	0
	2	100	0
	8	68	32
	27	47	53
	32	0	100
	35	0	100
	37	100	0
	42	100	0
Flow	0.85 mL/min		
Wavelength	230 nm		
Injection Volume	7.5 – 100 µL		
Sample Concentration	2 mg/mL		
Solvent	Ultra-pure water with H3PO4 (85 %) pH = 2.0		
Run Time	42 min		

3.3 Discussion

Synthesis attempts showed that the impurity forms under both acidic and basic conditions. However, as the yield was much higher in the presence of a base, alkaline conditions were selected for the synthesis. In this case, UV/Vis and HRMS data gave the first indications for the dimer-like, methylene-bridged structure of the compound. However, to make exact statements on the structure and the connectivity of the impurity, more robust NMR data were necessary.

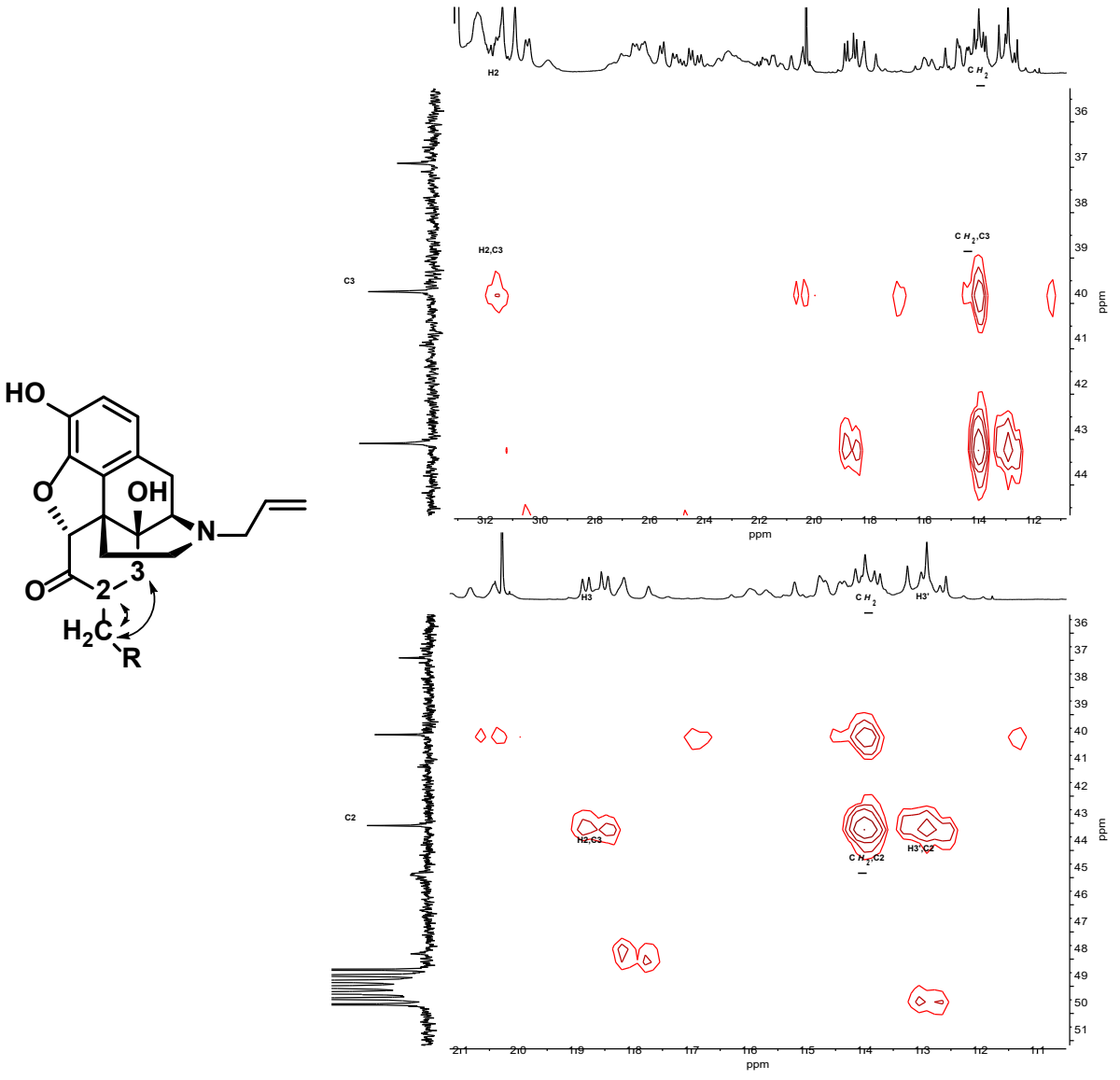

Figure 1. Sections of the ^{1}H-^{13}C HMBC spectrum of the dimeric Naloxone impurity showing the correlations between the carbons marked as 2 and 3 with the protons of the bridging methylene group used to confirm the location of the methylene bridge.

As UV/Vis and HRMS data had already implied that Naloxone itself was the base structure for the impurity, 1D and 2D NMR data were recorded of the API as reference. By comparing these 1D and 2D NMR data with those obtained from the impurity, all protons and carbon atoms of the compound could be assigned, and the precise location of the methylene bridge identified. By observing the structure, a

reaction mechanism was once again postulated, which gave a plausible explanation for both an acidic and a basic reaction pathway.

Additionally, further insight into the operation of the hyphenated system was obtained during these experiments in regard to SPE isolation. As HPLC analysis in the pharmaceutical industry is mainly performed using reversed-phase columns, the analytes in question are usually fairly nonpolar. For this reason, hydrophobic divinylbenzene (DVB) polymers were selected as material for the SPE cartridges, although other resins, such as ion-exchange materials or polar modified polymers, were also available. In the case of the Naloxone-formaldehyde "dimer", it was discovered that the DVB material did not sufficiently retain the analyte. It was ascertained that the reason for this lack of retention was the acidic conditions during the HPLC separation, which led to protonation of the amine groups in the two Naloxone units. The thereby formed positive charges make the analyte too polar to be retained on the DVB resin. Rather than changing the separation conditions, which would take much time and would be less economic in real pharmaceutical quality control, the easier way of adjusting the pH value of the SPE unit's make-up flow was selected. For this a slightly basic buffer was applied, that had a p*K*s- value based on the Naloxone amino groups, which was meant to convert them into their neutral state, thereby decreasing the impurities polarity and improving retention on the DVB resin.

Overall, this project showed that the data obtained by using this hyphenated system was sufficient for the complete structural elucidation of even complex molecules. It was demonstrated that comparing the obtained data to data of the original API, which is easily obtainable as pure substance, was all that was necessary. In cases where the impurity is formed by degradation of an excipient, the same principle can be applicable. Nonetheless, for projects such as this one, a certain amount of knowhow may be needed for the evaluation of the data obtained, as well as the application of the individual methods, especially in regard to the NMR spectroscopy.

4 Flurbiprofen – The Proof-of-Concept

The previous two projects demonstrated the applicability of the hyphenated system for complete structural elucidation of impurities and the identification of the reaction mechanisms that lead to their formation. As these results were obtained from synthetic samples, the final project was performed on real samples obtained from stability studies, which are commonly performed in pharmaceutical environments. This was meant to prove the applicability of the system in real life pharmaceutical quality control while at the same time exploring its analytical capabilities and limitations.

4.1 Flurbiprofen Research Article

Author contributions:

Philipp Schmidt:

- *Artificial synthesis of the Flurbiprofen impurities for analysis using the HPLC-DAD-HRMS/SPE-NMR system*
- *Design of the method of for analysis of the mono- and diesters on the HPLC-DAD-HRMS/SPE-NMR system*
- *Separation, enrichment, isolation and data acquisition using the artificial samples on the HPLC-DAD-HRMS/SPE-NMR system*
- *Evaluation of the data, followed by the complete structural elucidation of six Flurbiprofen-PEG monoesters and six Flurbiprofen-PEG diesters, including the assignment of all ^{1}H and ^{19}F NMR signals*
- *Extraction of the Flurbiprofen-PEG ester impurities from Flurbiprofen lozenges*
- *Method development for the separation, analysis and isolation using the lozenge extracts on an HPLC-DAD-HRMS/SPE-NMR system*
- *Evaluation of the data obtained from the lozenge extracts, followed by the complete structural elucidation of six Flurbiprofen-PEG monoesters and six Flurbiprofen-PEG diesters, including the assignment of all ^{1}H and ^{19}F NMR signals*
- *Writing of the Research Article*

Christine Kolb and Andreas Reiser:

- *Performed the initial investigations regarding the identity and formation of the Naloxone impurity, when it was first discovered, including degradation and enrichment experiments*

Markus Godejohann:

- *Performed the separation, data acquisition and isolation of the mono- and diesters in an external lab, on an HPLC-DAD-HRMS/SPE-NMR system using the provided lozenge extracts and the method designed by Philipp Schmidt*

Markus Philipp:

- *Performed a role as supervisor of the project*

Hans-Christian Müller and Konstantin Karaghiosoff:

- *Performed an advisory role in the preparation of the manuscript and aided in proof-reading*

Journal of Pharmaceutical and Biomedical Analysis 222 (2023) 115068

Contents lists available at ScienceDirect

Journal of Pharmaceutical and Biomedical Analysis

journal homepage: www.journals.elsevier.com/journal-of-pharmaceutical-and-biomedical-analysis

Separation and identification of a complex flurbiprofen-polyethylene glycol mono- and diester mixture via a hyphenated HPLC-DAD-HRMS/SPE NMR system

Philipp Schmidt [a], Christine Kolb [b], Markus Godejohann [c], Andreas Reiser [b], Markus Philipp [b], Hans-Christian Müller [b,*,1], Konstantin Karaghiosoff [a,**,2]

[a] Department Chemie, Ludwig-Maximilians-Universität München, Butenandtstraße 5-13, Haus D, 81377 Munich, Germany
[b] Analytical Development, Hexal AG, Industriestraße 25, 83607 Holzkirchen, Germany
[c] Bruker BioSpin GmbH, Rudolf-Plank-Str. 23, 76275 Ettlingen, Germany

ARTICLE INFO

Keywords:
Flurbiprofen
PEG-ester
Solid-phase extraction (SPE)
HPLC-SPE NMR
LC-HRMS
Hyphenation

ABSTRACT

We report the use of a hyphenated HPLC-DAD(diode array detector)-HRMS/SPE NMR system for the separation and isolation of a complex mixture of esters, containing substances with very similar LC retention times. The literature known mono- and diesters of the drug Flurbiprofen and polyethylene glycol, which form a large number of substances with varying chain lengths, were chosen for this study. We demonstrate the use of this hyphenated system to quickly and effectively isolate sixteen of these highly similar individual esters in an automated fashion, demonstrating its applicability in standard pharmaceutical analysis and quality control of drugs. Both, synthetic solutions of these esters and extracts from Flurbiprofen lozenges were used for this purpose. By the sole use of this system, the individual compounds were isolated and UV, HRMS and 1D and ^{2}D NMR data could be collected, enabling the identification and differentiation of the individual esters.

1. Introduction

Flurbiprofen (**1**, Fig. 1) is a nonsteroidal anti-inflammatory drug (NSAID) of the phenylalkanoic acid group, which also includes the common pain killer Ibuprofen [1,2]. It functions by inhibiting the prostaglandin biosynthesis via cyclooxygenase-1 and − 2, reducing inflammation, pain and fever and is often administered orally in the form of lozenges [3,4].

As the categorization as phenylalkanoic acid implies, one of Flurbiprofen's main functionalities is a carboxylic acid group, which is capable of reactions such as esterifications with hydroxyl groups [4,6]. As esterifications can occur under several conditions, such as basic and acidic catalysis [5], and since many common medicine excipients (sugars or sugar derivatives, like microcrystalline cellulose (MCC)) contain hydroxyl groups [6,7], formulations of Flurbiprofen may lead to a variety of esters forming during production or storage [4]. Many ester variants of Flurbiprofen are known, such as menthyl ester, which can be found as impurity in medication using menthol as flavor [4]. Some Flurbiprofen esters of basic alcohols have also been intentionally synthesized for possible use as prodrugs [5].

A common used excipient in medical products such as lozenges is the polymer polyethylene glycol (PEG) [4]. PEG exists in various chain lengths and depending on the average chain length of a mixture, the aggregate state may vary from viscous liquid to solid [4,8,9]. When these mixtures are introduced to a formulation they are capable of forming a large array of chemically similar degradation products with Flurbiprofen [4]. This results in difficulties when separating them during HPLC.

Despite the knowledge that PEG is capable of side reactions, such as esterifications, its use in drugs and cosmetics is still widespread, due to its many favorable properties [8,9]. These range from PEG's application as solubilizer for hydrophobic substances, permeation enhancer and anti-fouling agent, to its use as plasticizer and binding agent [8,9].

HPLC analysis of medical products containing Flurbiprofen and PEG

* Correspondence to: Analytical Development, Hexal AG, 83607 Holzkirchen, Germany.
** Correspondence to: Department Chemie, Ludwig-Maximilians-Universität München, 81377 Munich, Germany.
E-mail addresses: dhcm@gmx.de (H.-C. Müller), klk@cup.uni-muenchen.de (K. Karaghiosoff).
[1] orcid.org/0000-0001-9367-6066
[2] orcid.org/0000-0002-8855-730X

https://doi.org/10.1016/j.jpba.2022.115068
Received 7 January 2022; Received in revised form 13 September 2022; Accepted 19 September 2022
Available online 29 September 2022

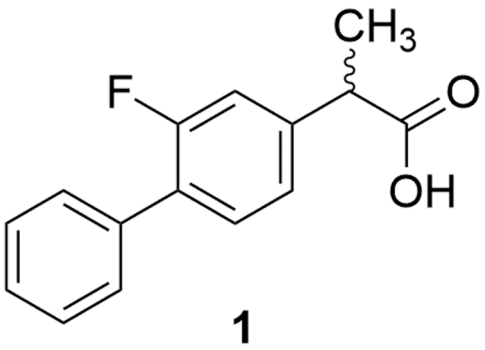

Fig. 1. Chemical structure of anti-inflammatory medication Flurbiprofen (**1**).

often reveal two sets of impurities, which presented themselves as two "hedgehog-like" hills in the UV-chromatogram (Fig. S1). These impurities consist of a mixture of literature known PEG esters with either one or two Flurbiprofen units (Fig. 2) [4].

Complex mixtures of substances, such as this collection of very similar impurities, only varying in their PEG chain length, prove a significant challenge when their quantitative separation and structural elucidation is required. Identification of impurities in medication is usually performed by one of two methods. Either the impurity is compared to a synthesized standard of the suspected impurity via their relative retention time in LC-UV analysis, or the impurity is isolated and fully characterized by MS spectrometry and NMR spectroscopy [10]. The first method requires the collection of prior knowledge on the impurity in question in order to synthesize or purchase the standard sample. This process may be both time consuming and, depending on the molecule in question, expensive. The latter method can prove less time consuming, however separation of substances with nearly identical retention times and the collection of sufficient sample quantities for NMR studies may prove challenging, as is the case with the Flurbiprofen-PEG esters.

This paper presents the application of a hyphenated HPLC-DAD-HRMS/SPE NMR system, capable of precisely isolating even very similar compounds. This system uses time criteria and UV or HRMS intensity inputs to isolate fractions from the mobile phase stream onto solid phase cartridges. This happens in an automated fashion, allowing the collection of sufficient quantities for NMR analysis (both 1 and 2D) during a series of consecutive HPLC runs. This hyphenated system is becoming increasingly popular in the analysis of metabolites [11–15], natural compounds [11,16–22], and environmental samples, such as water samples [23,24], but its application in the identification of impurities occurring in pharmaceutical analysis and quality control of medication is still comparatively uncommon [17,25]. A SciFinder^n search for the terms HPLC, SPE and NMR and subsequent search within secondary citations, revealed only six cases of this, and similar hyphenated systems used in the identification of impurities in medication (Scifinder search performed on 12/17/2021) [26–31].

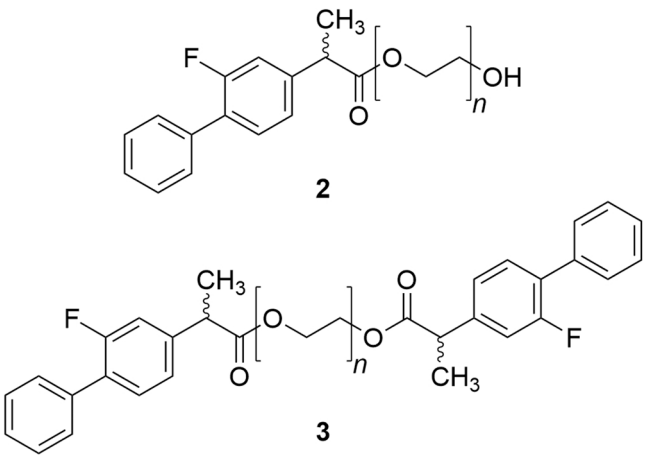

Fig. 2. Structures of the Flurbiprofen-PEG mono- and diesters (**2** and **3**), with *n* representing the chain length of the PEG unit in integral numbers.

To demonstrate the potential of this system in the separation and identification of compounds detected during stability analysis of medication, the aforementioned literature known Flurbiprofen-PEG-ester mixture was chosen as a common example and due to its complexity. First experiments were performed on synthetic mixtures of these esters, before the applicability was demonstrated on Flurbiprofen lozenges. Here we show how standard analytical methods, used during routine quality control, can be easily and swiftly adjusted for use by this hyphenated system, to achieve the isolation and structural elucidation of these individual mono- and diesters. Hereby we hope to demonstrate the potential of this hyphenated system to reduce the time from detection of an impurity to its complete characterization.

2. Materials and methods

2.1. Chemicals and reagents

All chemicals and solvents were used as purchased without further purification. Concentrated sulfuric acid, sodium bicarbonate and polyethylene glycol 300 were purchased from Merck. Ammonium acetate was purchased from Merck and Supelco. Acetonitrile for liquid and mass spectrometry in their respective qualities were purchased from Merck and Riedel-de-Haen. Dichloromethane for liquid chromatography was purchased from Merck. Deuterated acetonitrile was purchased from Sigma-Aldrich. Pure Flurbiprofen was acquired from AESICA, whilst Lozenges containing 8.75 mg Flurbiprofen were acquired from Hexal. Ultra-pure water was produced by an in-house Merck Millipore-Q and a Merck MilliQ Simplicity System.

2.2. NMR spectroscopy

2.2.1. Conditions for the synthetic samples

All ^{1}H and ^{13}C NMR spectra were recorded in deuterated acetonitrile at 298 K and were referenced to residual solvent signals using literature values (1.94 ppm for ^{1}H spectra and 118.26 ppm for ^{13}C spectra for acetonitrile) [32]. The spectra were acquired using a 400 MHz Bruker Avance Neo 400 (400.15 MHz for ^{1}H, 100.63 MHz for ^{13}C and 376.46 MHz for ^{19}F) and a 400 MHz Bruker AV400TR (400.13 MHz for ^{1}H, 100.62 MHz for ^{13}C and 376.44 MHz for ^{19}F). Measurements were performed in 2.5 mm NMR capillaries.

2.2.2. Conditions for the lozenge-extracts

All ^{1}H and ^{13}C NMR spectra were recorded in deuterated acetonitrile at 298 K and were referenced to residual solvent signals using literature values (1.94 ppm for ^{1}H spectra and 118.26 ppm for ^{13}C spectra for acetonitrile) [32]. The spectra were acquired using a 600 MHz Bruker Avance Neo 600 (600.18 MHz for ^{1}H and 150.93 MHz for ^{13}C). Measurements were performed in 3.0 mm NMR capillaries.

2.3. HPLC-DAD system

HPLC-UV analysis was performed using an Agilent 1100 system.

2.4. Hyphenated HPLC-DAD-HRMS/SPE system

2.4.1. Synthetic samples

The system used for the analysis of the synthetic ester solutions consisted of an Agilent 1290 Infinity II system, a Bruker/Spark LC-SPE Interface (3.0 CPL), a UHR-Q-TOF Bruker impact II in ESI positive mode and an Azura Knauer pump. Spark SPE cartridges (10 ×2 mm,

Hysphere-Resin GP, 10–12 μm pore size, polyvinyl benzene) were used for collection of the samples. Elution into 2.5 mm Bruker NMR capillaries was performed by a Bruker SamplePro SPE TT system.

2.4.2. Lozenge-extracts

The system used for the analysis of the lozenge-extracts consisted of an Agilent 1260/1200 Spark Prospect 2, a Bruker/Spark LC-SPE Interface (3.0 CPL), a Bruker Daltonic MicroTOF-QII HRMS in ESI positive mode and an Azura Knauer pump. Spark SPE cartridges (10 ×2 mm, Hysphere-Resin GP, 10–12 μm pore size, polyvinyl benzene) were used for collection of the samples. Elution into 3.0 mm SampleJet NMR tubes was performed manually.

2.5. Synthesis of the Flurbiprofen-PEG mono- and diester mixture

Flurbiprofen (1 equiv, 407.28 mg, 1.67 mmol) was dissolved in PEG-300 (excess, 1.32 mL) and a catalytic amount of sulfuric acid (50 μL) was added. The solution was heated to 80 °C for 3 h and then used for analysis and separation without further workup.

2.6. Extraction of impurities from lozenges containing 8.75 mg Flurbiprofen

A total of 40 Flurbiprofen lozenges were ground in a mortar and dissolved in a mixture of 150 mL dichloromethane and 150 mL of a 0.1% sodium bicarbonate solution under strong stirring. Using a separatory funnel, the organic phase was separated and washed twice with 100 mL of a 0.1% sodium bicarbonate solution. The organic phase was dried over magnesium sulfate and the solvent was removed via rotary evaporation. The residue was dissolved in 1 mL of a 1:1 acetonitrile/water solution, resulting in the solution for hyphenation analysis.

2.7. In-House HPLC-UV method for lozenges containing 8.75 mg Flurbiprofen

The following, regulatory approved, analytical method for 8.75 mg Flurbiprofen lozenges served as the basis for all further methods developed in this study and was itself not applied for analysis during research. The method uses a 0.175 mg/mL sample solution in methanol/water (1:1) solvent mixture. The analysis is performed on a Zorbax SB-C18 Column with 1.8 μm particle size and dimensions of 50 × 3.0 mm, using a 25.5 min HPLC method at a temperature of 40 °C. The solvent system consists of ammonium acetate, dissolved in a solvent mixture of water and acetonitrile (75/25 v/v-%) that is adjusted to a pH value of 3.0 (mobile phase A) and acetonitrile (mobile phase B). The UV detector is set to 254 and 270 nm with a DAD range from 190 to 450 nm. The injection volume is 25 μL and the flow rate is set to 1.0 mL/min. For the first 1.9 min the solvent composition is set to 0% B, before it is increased to 70% B within 17.6 min. This level is held for 1 min, after which B is reduced back to 0% within 2 min and is held at this level for the remaining 3 min

2.8. HPLC-UV-analysis, specifically developed for both mono- and diesters

The sample was prepared by dissolving 10 μL of the reaction solution (see 2.5) in 500 μL of a 1:1 methanol/acetonitrile solution. The analysis was performed on a ProntoSIL EuroBOND C18 Column with 5.0 μm particle size and dimensions of 125 × 4.0 mm, using a 85 min HPLC method at a temperature of 40 °C. The solvent system consisted of ammonium acetate, dissolved in a solvent mixture of water and acetonitrile (75/25 v/v-%) that had been adjusted to a pH value of 6.6 (mobile phase A) and acetonitrile (mobile phase B). The UV detector was set to 254 nm with a DAD range from 190 to 450 nm. The injection volume was 25 μL and the flow rate was set to 1.0 mL/min. For the first 40 min the solvent composition was set to 13% B, before it was increased to 58% B within 9.5 min. This level was held for 30 min, after which B was further increased to 70% within 5 min. B was then reduced to 15% within 2 min and was then returned to the initial 13% within 3 min

2.9. Separation and Isolation via a Hyphenated HPLC-DAD-MS/SPE NMR system

The synthetic samples (see 2.5) were prepared by mixing 0.2 mL of the reaction solution with 0.5 mL of a 1:1 acetonitrile/water solution. The separation was performed by applying an HPLC method that lasted 100.5 min for the mono- and 65 min for the diesters, using a ProntoSIL EuroBOND C18 column with 5.0 μm particle size and dimensions of 125 × 4.0 mm for the monoesters and a Nucleosil 100 C18 column 5.0 μm particle size and dimensions of 250 × 4.0 mm for the diesters. The lozenge-extract (see 2.6) was analyzed without further preparation. The separation was performed by applying an HPLC method running 100.5 min for the mono- and 40.0 min for the diesters, using a Nucleosil C18 column with 5.0 μm particle size and dimensions of 125 × 4.0 mm for the monoesters and a Waters Nova-Pak C18 column with 4 μm particle size and dimensions of 150 × 3.9 mm for the diesters. All four methods used a solvent system consisting of ammonium acetate dissolved in a solvent mixture of water and acetonitrile (75/25 v/v-%) that had been adjusted to a pH value of 6.6 (mobile phase A) and acetonitrile (mobile phase B). 10 μL of sample solution were injected and separated at a temperature of 40 °C.

2.9.1. Monoester HPLC methods

The HPLC methods for the Flurbiprofen-PEG monoesters were mostly equivalent for the synthetic mixtures and the lozenge-extracts, with the only difference being the flow rate of the make-up flow. Both methods held a constant flow of 1.0 mL/min and started with a long isocratic part that held a value of 8% B for 60 min. B was then increased to 10% in 2 min and held at this value for 18 min before it was further increased to 70% within 9.5 min. After 5 min at 70%, the level of B was decreased back to the initial value of 8% within 2 min, where it was held for the remaining 4 min. The water make-up flow of the LCE-SPE unit was set to 0.01 mL/min and increased to 2.5 mL/min between 40 and 80 min for the synthetic samples and was set to 0.01 mL/min and increased to 2.0 mL/min between 40 and 90 min for the lozenge-extracts.

2.9.2. Diester HPLC methods

The HPLC method for the Flurbiprofen-PEG diesters from the synthetic samples started with a flow of 1.5 mL/min and a value of 11% B, which was increased to 52% B within 5 min. The level of B and the flow were held at these values for 25 min, before the flow was decreased to 1.0 mL/min within 5 min. The lower flow was held for 25 min, before both the flow and the level of B were reset to their original values of 1.5 mL/min and 11% within 2 min. These values were held for the remaining 3 min. The water make-up flow of the LCE-SPE unit was set to 0.01 mL/min and increased to 2.5 mL/min between 30 and 60 min

The diester method for the lozenge-extracts started with a flow of 1.5 mL/min and a value of 11% B, which was increased to 52% B within 5 min. The level of B and the flow were held at these values for 5 min, before the flow was decreased to 1.0 mL/min within 5 min. The lower flow was held for 10 min, before it was reset to 1.5 mL/min and B was increased to 70% within 5 min. The level of B was then reset to the original 11% within 5 min and held at this value for the remaining 5 min. The water make-up flow of the LCE-SPE unit was set to 0.01 mL/min and increased to 2.5 mL/min between 10 and 35 min

After separation via HPLC, 5% of the eluting solution was split off, diluted by acetonitrile and analyzed by HRMS in ESI positive mode. At the beginning of every sample injection the HRMS was calibrated using a 0.1% trifluoroacetic acid solution. The remaining solution was directed through a DAD detector with a range of 190 – 640 nm that recorded a separate chromatogram at 254 nm, as this wavelength was used for SPE

separation.

2.9.3. Trapping method for the monoesters

The time window for the isolation of the synthetic samples onto the SPE cartridges was set to 40.0 – 80.0 min using a threshold of 300 mAU (for 254 nm). Whenever the UV intensity rose above this value, the effluent was directed toward the SPE organizer until the intensity fell below 300 mAU once again.

The time window for the isolation of the lozenge-extracts onto the SPE cartridges was set to 42.90 – 80.0 min using a threshold of 75 mAU (DAD range from 190 to 640 nm). Whenever the UV intensity rose above this value, the effluent was directed toward the SPE organizer until the intensity fell below 75 mAU once again.

2.9.4. Trapping method for the diesters

Three time windows were set for the synthetic samples. 38.0 – 48.0 min at 514 mAU, 48.0 – 51.0 min at 340 mAU and 51.5 – 53.4 min at 100 mAU. Whenever the UV intensity rose above these values within the set time windows, the effluent was directed toward the SPE organizer, until the intensity fell below the set values once again.

The time window for the isolation of the lozenge-extracts onto the SPE cartridges was set to 15.0 – 30.0 min using a threshold of 75 mAU (DAD range from 190 to 640 nm). Whenever the UV intensity rose above this value, the effluent was directed toward the SPE organizer until the intensity fell below 75 mAU once again.

Each collected fraction was trapped on a separate SPE polyvinyl benzene cartridge in order of elution. For the synthetic solution, six consecutive HPLC runs used the same cartridges in the same order. Two sets of six separations were performed collecting a total of twelve fractions per collected ester, split onto two cartridges. For the extracts from the lozenges only five fractions were collected per ester. In the case of the synthetic samples, all loaded cartridges were then dried for 30 min under nitrogen flow and eluted using deuterated acetonitrile for NMR analysis. 60 μL of solvent were used per cartridge, pooling both cartridges containing the same fraction in one 2.5 mm NMR capillary. For the lozenge-extracts, all loaded cartridges were dried under nitrogen flow for 2–3 days and were eluted manually into 3.0 mm NMR capillaries using 120 μL deuterated acetonitrile.

2.10. Analytical data for the Flurbiprofen-PEG monoesters

NMR, UV-Vis and HRMS data of the Flurbiprofen-PEG monoesters are listed below. Only the data of the collected esters (n = 3 – 8) are listed. For easier assignment of the ^{1}H NMR signals a numbering scheme of the nuclei for the monoesters is depicted in Fig. 11. The results listed below are the data collected from the synthetic samples. The results of the extracts from the lozenges are identical within measurement precision and are listed in the supplementary material Fig. 11.

2.10.1. Monoester n = 3

^{1}H NMR (400.15 MHz, CD_3CN): δ = 7.60 – 7.52 (m, 2 H, H7) 7.50 – 7.37 (m, 4 H, H5, H6, H8), 7.22 (dd, ^{3}J(H4,H5) = 8.1, ^{4}J(H3,H4) = 1.8 Hz, 1 H, H4), 7.18 (dd, ^{3}J(H3,F) = 12.0, ^{4}J(H3,H4) = 1.7 Hz, 1 H, H3), 4.23 – 4.17 (m, 2 H, H10), 3.84 (q, ^{3}J(H1,H2) = 7.2 Hz, 1 H, H2), 3.65 – 3.58 (m, 2 H, H9), 3.62 – 3.41 (m, 8 H, H_{PEG}), 2.82 (t, ^{3}J(H_{OH}, H_{PEG}) = 5.8 Hz, 1 H, H_{OH}), 1.48 ppm (d, ^{3}J(H1,H2) = 7.2 Hz, 3 H, H1). ^{19}F NMR (376.46 MHz, CD_3CN): δ = −119.6 ppm (ddtd, ^{3}J(H3,F) = 12.0, ^{4}J(H5,F) = 8.4, ^{5}J(H6,F) = 1.6, ^{5}J(H4,F) = 0.4 Hz). HRMS (ESI+): *m/z* calculated for $C_{21}H_{25}FO_5 + H^+$ [M + H^+]: 377.1759. Found: 377.1773.

2.10.2. Monoester n = 4

^{1}H NMR (400.15 MHz, CD_3CN): δ = 7.59 – 7.53 (m, 2 H, H7) 7.50 – 7.37 (m, 4 H, H5, H6, H8), 7.22 (ddd, ^{3}J(H4,H5) = 7.8, ^{4}J(H3,H4) = 1.9, ^{5}J(H4,F) = 0.4 Hz, 1 H, H4), 7.18 (dd, ^{3}J(H3,F) = 11.9, ^{4}J(H3, H4) = 1.8 Hz, 1 H, H3), 4.22 – 4.18 (m, 2 H, H10), 3.84 (q, ^{3}J(H1,H2) = 7.2 Hz, 1 H, H2), 3.62 – 3.59 (m, 2 H, H9), 3.59 – 3.43 (m, 12 H, H_{PEG}), 2.74 (t, ^{3}J(H_{OH},H_{PEG}) = 5.8 Hz, 1 H, H_{OH}), 1.49 ppm (d, ^{3}J(H1, H2) = 7.2 Hz, 3 H, H1). ^{19}F NMR (376.46 MHz, CD_3CN): δ = −119.5 ppm (ddtd, ^{3}J(H3,F) = 12.0, ^{4}J(H5,F) = 8.4, ^{5}J(H6,F) = 1.6, ^{5}J(H4,F) = 0.6 Hz). HRMS (ESI+): *m/z* calculated for $C_{23}H_{29}FO_6 + H^+$ [M + H^+]: 421.2021. Found: 421.2033.

2.10.3. Monoester n = 5

^{1}H NMR (400.15 MHz, CD_3CN): δ = 7.57 – 7.53 (m, 2 H, H7) 7.50 – 7.37 (m, 4 H, H5, H6, H8), 7.22 (ddd, ^{3}J(H4,H5) = 7.8, ^{4}J(H3,H4) = 1.9, ^{5}J(H4,F) = 0.5 Hz, 1 H, H4), 7.18 (dd, ^{3}J(H3,F) = 11.9, ^{4}J(H3,

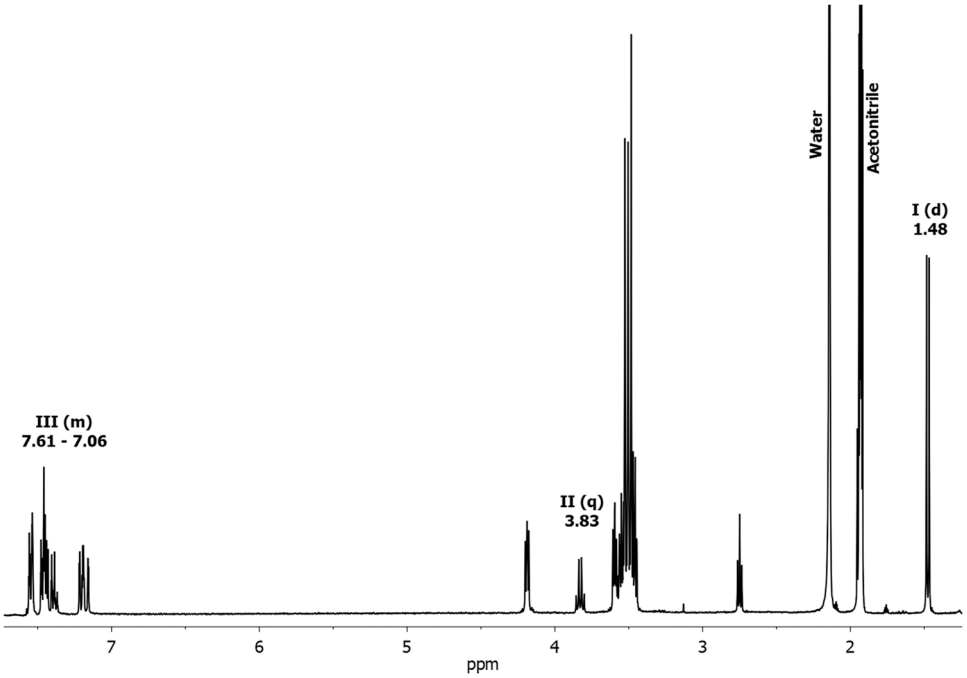

Fig. 3. Exemplary ^{1}H NMR spectrum of the Flurbiprofen-PEG monoester with a chain length of n = 5. The signals arising from the Flurbiprofen unit are marked (I – III).

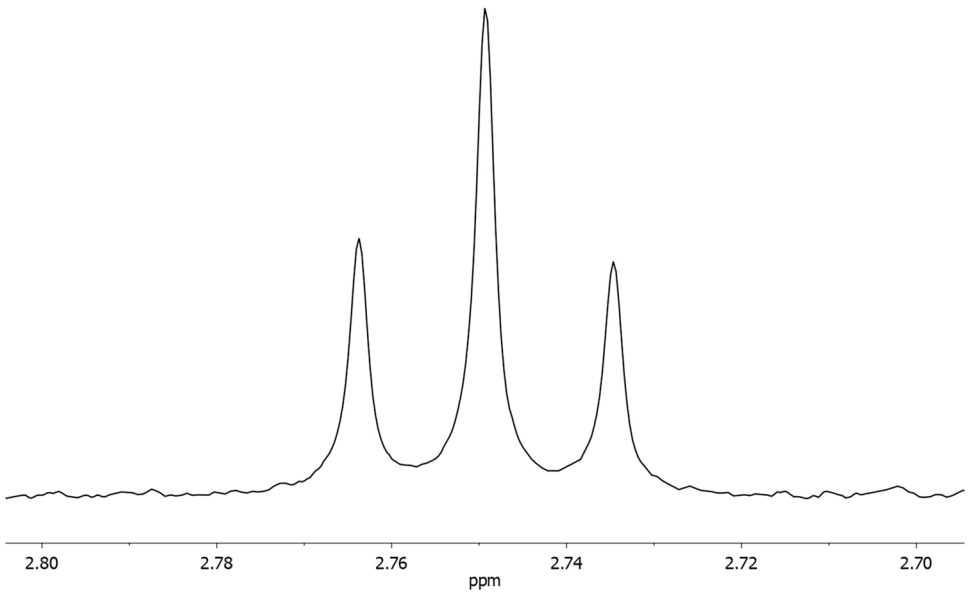

Fig. 4. Exemplary ^{1}H NMR signal arising from the PEG-OH group within the Flurbiprofen-PEG monoesters with a chain length of n = 5.

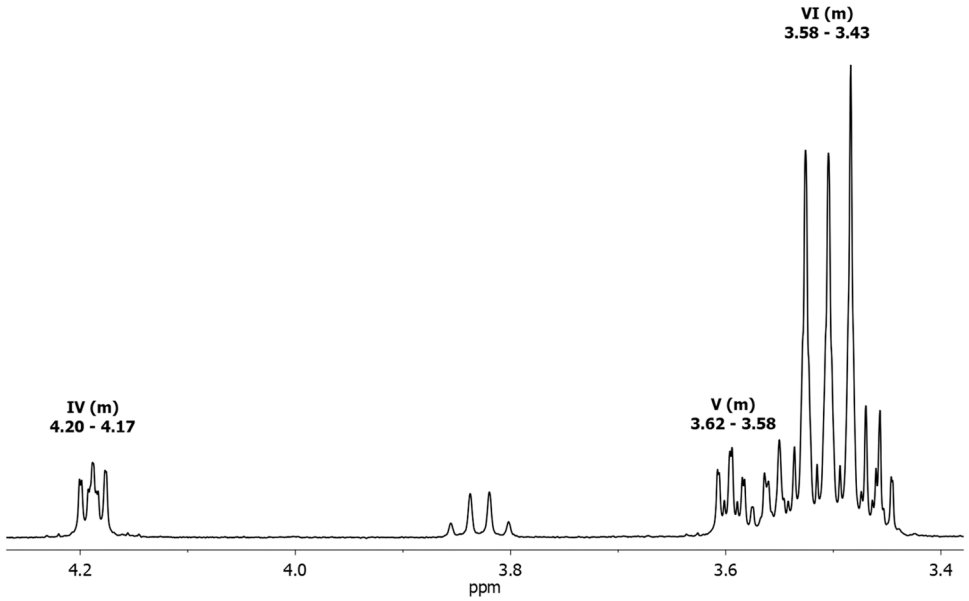

Fig. 5. Exemplary ^{1}H NMR spectrum of the aliphatic region for the Flurbiprofen-PEG monoester with a chain length of n = 5.

H4) = 1.8 Hz, 1 H, H3), 4.23 – 4.16 (m, 2 H, H10), 3.84 (q, ^{3}J(H1,H2) = 7.1 Hz, 1 H, H2), 3.64 – 3.57 (m, 2 H, H9), 3.60 – 3.43 (m, 16 H, H_{PEG}), 2.81 (t, $^{3}J(H_{OH},H_{PEG})$ = 5.8 Hz, 1 H, H_{OH}), 1.49 ppm (d, ^{3}J(H1, H2) = 7.2 Hz, 3 H, H1). ^{19}F NMR (376.46 MHz, CD_3CN): δ = −119.5 ppm (dddt, ^{3}J(H3,F) = 11.9, ^{4}J(H5,F) = 8.4, ^{5}J(H6,F) = 1.9, ^{5}J(H4,F) = 0.5 Hz). HRMS (ESI+): *m/z* calculated for $C_{25}H_{33}FO_7 + H^+$ [M + H^+]: 465.2283. Found: 465.2300.

2.10.4. Monoester n = 6

^{1}H NMR (400.15 MHz, CD_3CN): δ = 7.60 – 7.53 (m, 2 H, H7) 7.51 – 7.37 (m, 4 H, H5, H6, H8), 7.22 (dd, ^{3}J(H4,H5) = 7.9, ^{4}J(H3,H4) = 1.9 Hz, 1 H, H4), 7.18 (dd, ^{3}J(H3,F) = 11.9, ^{4}J(H3,H4) = 1.8 Hz, 1 H, H3), 4.23 – 4.16 (m, 2 H, H10), 3.84 (q, ^{3}J(H1,H2) = 7.1 Hz, 1 H, H2), 3.63 – 3.58 (m, 2 H, H9), 3.58 – 3.45 (m, 20 H, H_{PEG}), 2.76 (t, $^{3}J(H_{OH}$, H_{PEG}) = 5.8 Hz, 1 H, H_{OH}), 1.49 ppm (d, ^{3}J(H1,H2) = 7.2 Hz, 3 H, H1). ^{19}F NMR (376.46 MHz, CD_3CN): δ = −119.5 ppm (dddt, ^{3}J(H3,F) = 11.9, ^{4}J(H5,F) = 8.3, ^{5}J(H6,F) = 1.6, ^{5}J(H4,F) = 0.5). HRMS (ESI+): *m/z* calculated for $C_{27}H_{37}FO_8 + H^+$ [M + H^+]: 509.2545. Found: 509.2562.

2.10.5. Monoester n = 7

^{1}H NMR (400.15 MHz, CD_3CN): δ = 7.59 – 7.53 (m, 2 H, H7) 7.50 – 7.37 (m, 4 H, H5, H6, H8), 7.22 (ddd, ^{3}J(H4,H5) = 7.9, ^{4}J(H3,H4) = 1.9, ^{5}J(H4,F) = 0.5 Hz, 1 H, H4), 7.18 (dd, ^{3}J(H3,F) = 11.7, ^{4}J(H3, H4) = 1.8 Hz, 1 H, H3), 4.23 – 4.16 (m, 2 H, H10), 3.84 (q, ^{3}J(H1,H2) = 7.0 Hz, 1 H, H2), 3.64 – 3.57 (m, 2 H, H9), 3.60 – 3.44 (m, 24 H, H_{PEG}), 2.77 (t, $^{3}J(H_{OH},H_{PEG})$ = 5.8 Hz, 1 H, H_{OH}), 1.49 ppm (d, ^{3}J(H1, H2) = 7.2 Hz, 3 H, H1). ^{19}F NMR (376.46 MHz, CD_3CN): δ = −119.5 ppm (dddt, ^{3}J(H3,F) = 11.8, ^{4}J(H5,F) = 8.4, ^{5}J(H6,F) = 1.6, ^{5}J(H4,F) = 0.5 Hz, 1 F). HRMS (ESI+): *m/z* calculated for $C_{29}H_{41}FO_9 + H^+$ [M + H^+]: 553.2807. Found: 553.2825.

2.10.6. Monoester n = 8

^{1}H NMR (400.15 MHz, CD_3CN): δ = 7.59 – 7.53 (m, 2 H, H7) 7.50 –

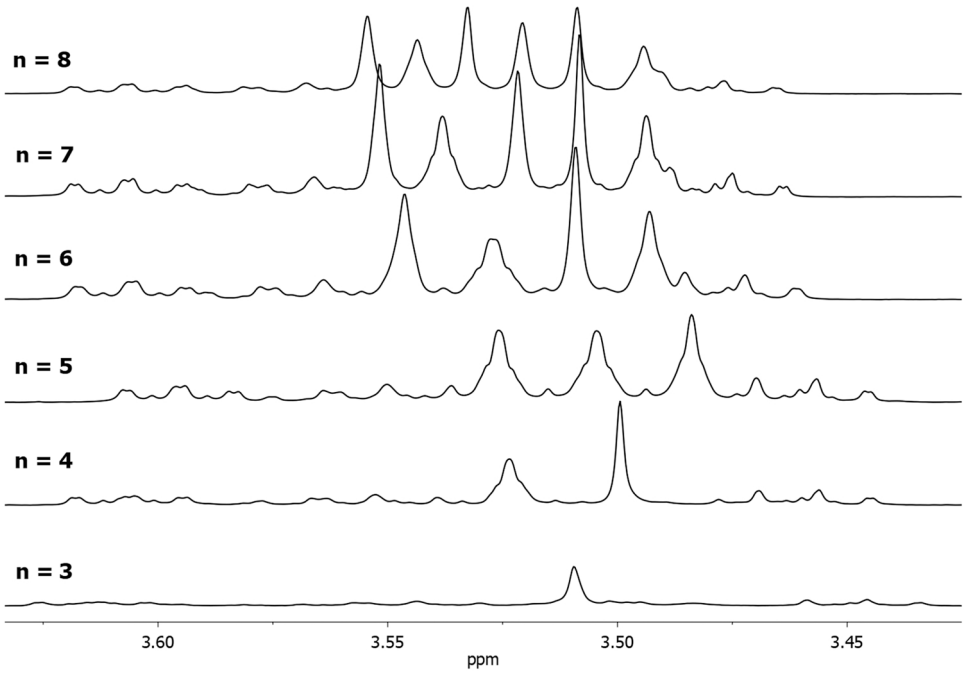

Fig. 6. Comparison of the large signals arising from the central EG units for the Flurbiprofen-PEG monoesters in the ^{1}H NMR spectrum (chain lengths n = 3 – 8).

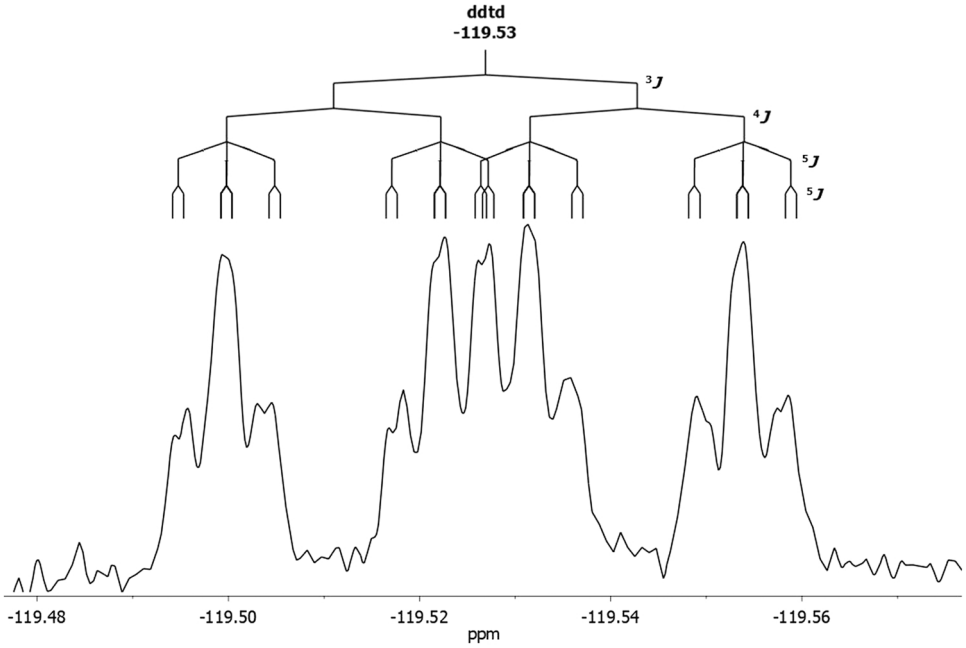

Fig. 7. Exemplary ^{19}F NMR signal for the Flurbiprofen-PEG monoester with a chain length of n = 5.

7.37 (m, 4 H, H5, H6, H8), 7.22 (ddd, ^{3}J(H4,H5) = 7.9, ^{4}J(H3,H4) = 1.9, ^{5}J(H4,F) = 0.5 Hz, 1 H, H4), 7.18 (dd, ^{3}J(H3,F) = 11.9, ^{4}J(H3, H4) = 1.7 Hz, 1 H, H3), 4.23 – 4.17 (m, 2 H, H10), 3.84 (q, ^{3}J(H1,H2) = 7.2 Hz, 1 H, H2), 3.62 – 3.59 (m, 2 H, H9), 3.59 – 3.45 (m, 28 H, H_{PEG}), 2.77 (t, $^{3}J(H_{OH},H_{PEG})$ = 5.8 Hz, 1 H, H_{OH}), 1.48 ppm (d, ^{3}J(H1, H2) = 7.2 Hz, 3 H, H1). ^{19}F NMR (376.46 MHz, CD_3CN): δ = −119.5 ppm (dddt, ^{3}J(H3,F) = 11.9, ^{4}J(H5,F) = 8.4, ^{5}J(H6,F) = 1.6, ^{5}J(H4,F) = 0.5 Hz). HRMS (ESI+): *m/z* calculated for $C_{31}H_{45}FO_{10}$ + H^{+} [M + H^{+}]: 597.3070. Found: 597.3086.

2.11. Analytical data for the Flurbiprofen-PEG diesters

NMR, UV-Vis and HRMS data of the Flurbiprofen-PEG diesters are listed below. Only the data of the collected esters (n = 3 – 8) are listed. For easier assignment of the ^{1}H NMR signals a numbering scheme of the nuclei for the diesters is depicted in Fig. 12. The results listed below are the data collected from the synthetic samples. The results of the extracts from the lozenges are identical within measurement precision and are listed in the supplementary material Fig. 12.

2.11.1. Diester n = 3

^{1}H NMR (400.15 MHz, CD_3CN): δ = 7.58 – 7.50 (m, 4 H, H7), 7.50 –

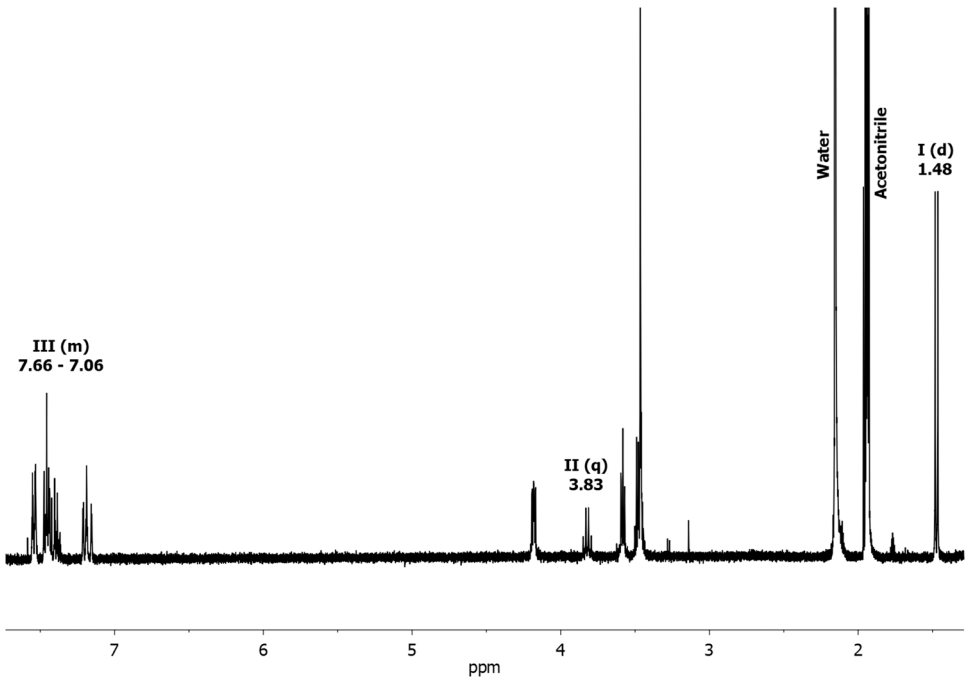

Fig. 8. Exemplary ^{1}H NMR spectrum of the Flurbiprofen-PEG diester with a chain length of n = 5. The signals arising from the Flurbiprofen unit are marked (I – III).

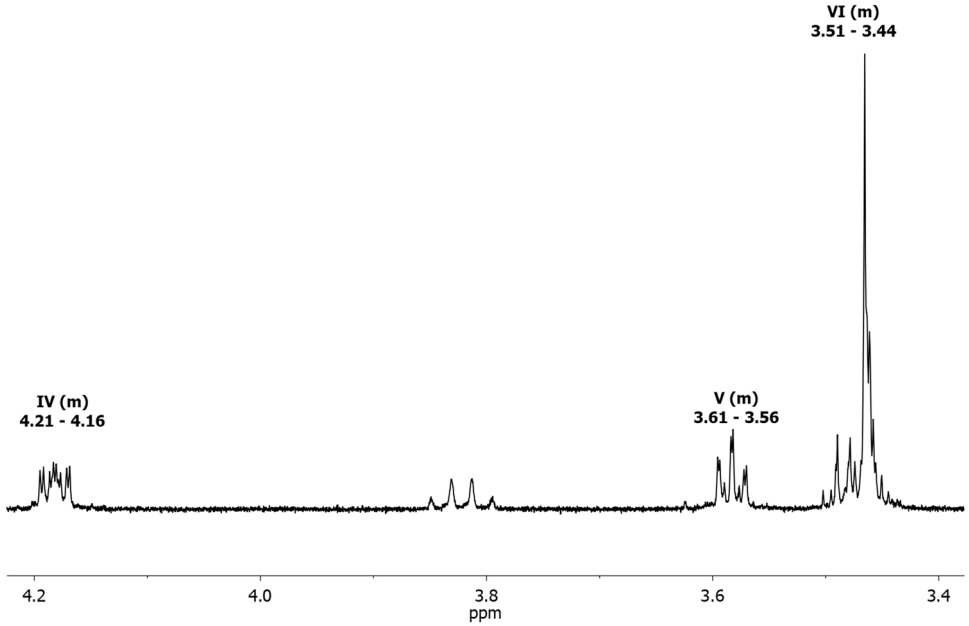

Fig. 9. Exemplary ^{1}H NMR spectrum of the aliphatic region for the Flurbiprofen-PEG diester with a chain length of n = 5.

7.35 (m, 8 H, H5, H6, H8), 7.24 – 7.12 (m, 4 H, H3, H4), 4.20 – 4.14 (m, 4 H, H10), 3.83 – 3.78 (m, 2 H, H2), 3.63 – 3.52 (m, 4 H, H9), 3.53 – 3.41 (m, 4 H, H_{PEG}), 1.46 ppm (d, ^{3}J(H1,H2) = 7.1 Hz, 6 H, H1). ^{19}F NMR (376.46 MHz, CD_3CN): $\delta = -119.5$ ppm (dddt, ^{3}J(H3,F) = 12.0, ^{4}J(H5,F) = 8.1, ^{5}J(H6,F) = 1.8, ^{5}J(H4,F) = 0.6 Hz). HRMS (ESI+): *m/z* calculated for $C_{36}H_{36}F_2O_6 + H^+$ [M + H^+]: 603.2553. Found: 603.2583.

2.11.2. Diester n = 4

^{1}H NMR (400.15 MHz, CD_3CN): $\delta = 7.56 – 7.52$ (m, 4 H, H7), 7.48 – 7.36 (m, 8 H, H5, H6, H8), 7.22 – 7.14 (m, 4 H, H3, H4), 4.20 – 4.13 (m, 4 H, H10), 3.82 (q, ^{3}J(H1,H2) = 7.2 Hz, 2 H, H2), 3.62 – 3.53 (m, 4 H, H9), 3.52 – 3.41 (m, 8 H, H_{PEG}), 1.47 ppm (d, ^{3}J(H1,H2) = 7.2 Hz, 6 H, H1). ^{19}F NMR (376.46 MHz, CD_3CN): $\delta = -119.5$ ppm (dddt, ^{3}J(H3,F) = 11.9, ^{4}J(H5,F) = 8.2, ^{5}J(H6,F) = 1.6, ^{5}J(H4,F) = 0.6 Hz). HRMS (ESI+): *m/z* calculated for $C_{38}H_{40}F_2O_7 + K^+$ [M + K^+]: 685.2374. Found: 685.2383.

2.11.3. Diester n = 5

^{1}H NMR (400.15 MHz, CD_3CN): $\delta = 7.57 – 7.52$ (m, 4 H, H7), 7.49 – 7.36 (m, 8 H, H5, H6, H8), 7.22 – 7.15 (m, 4 H, H3, H4), 4.21 – 4.16 (m, 4 H, H10), 3.83 (q, ^{3}J(H1,H2) = 7.2 Hz, 2 H, H2), 3.61 – 3.56 (m, 4 H, H9), 3.51 – 3.44 (m, 12 H, H_{PEG}), 1.48 ppm (d, ^{3}J(H1,H2) = 7.2 Hz, 6 H, H1). ^{19}F NMR (376.46 MHz, CD_3CN): $\delta = -119.5$ ppm (dddt, ^{3}J(H3,F) = 11.9, ^{4}J(H5,F) = 8.2, ^{5}J(H6,F) = 1.6, ^{5}J(H4,F) = 0.6 Hz). HRMS (ESI+): *m/z* calculated for $C_{40}H_{44}F_2O_8 + K^+$ [M + K^+]: 729.2636. Found: 729.2650.

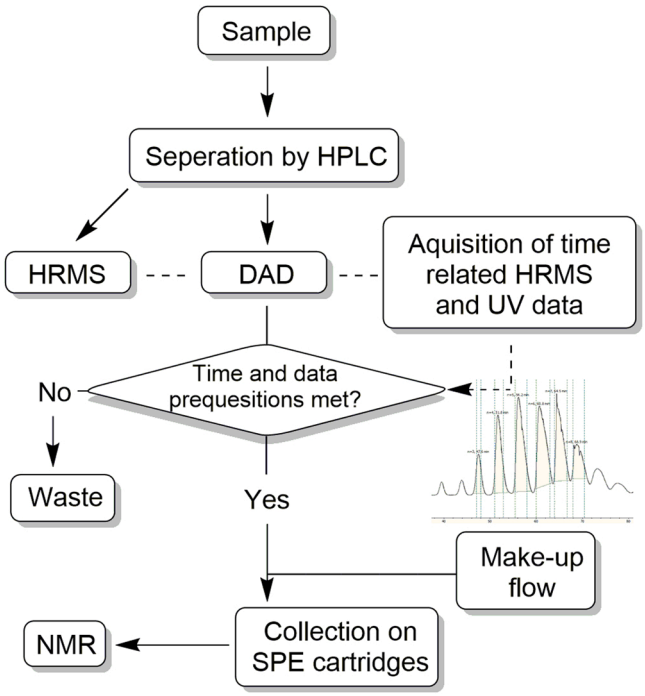

Fig. 10. Flow chart for the setup and function of the hyphenated HPLC-DAD-HRMS/SPE NMR system, with a representative image of an UV chromatogram of the Flurbiprofen-PEG monoesters, with dashed lines marking the beginning and end of the trapping processes.

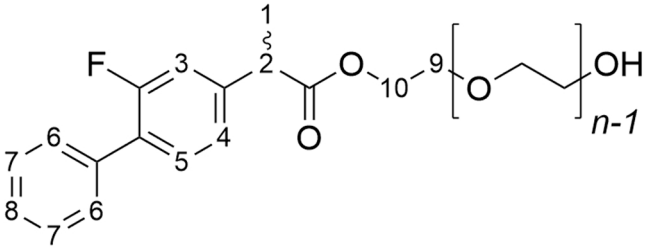

Fig. 11. Numbering scheme for the assignment of ^{1}H NMR signals of **2**, for n = 3 – 8.

2.11.4. Diester n = 6

^{1}H NMR (400.15 MHz, CD_3CN): δ = 7.57 – 7.52 (m, 4 H, H7), 7.49 – 7.36 (m, 8 H, H5, H6, H8), 7.22 – 7.15 (m, 4 H, H3, H4), 4.21 – 4.16 (m, 4 H, H10), 3.82 (q, ^{3}J(H1,H2) = 7.1 Hz, 2 H, H2), 3.61 – 3.57 (m, 4 H, H9), 3.51 – 3.44 (m, 16 H, H_{PEG}), 1.47 ppm (d, ^{3}J(H1,H2) = 7.2 Hz, 6 H, H1). ^{19}F NMR (376.46 MHz, CD_3CN): δ = −119.5 ppm (dddt, ^{3}J(H3,F) = 11.9, ^{4}J(H5,F) = 8.5, ^{5}J(H6,F) = 1.5, ^{5}J(H4,F) = 0.5 Hz). HRMS (ESI+): *m/z* calculated for $C_{42}H_{48}F_2O_9 + K^+$ [M + K^+]: 773.2898. Found: 773.2922.

2.11.5. Diester n = 7

^{1}H NMR (400.15 MHz, CD_3CN): δ = 7.57 – 7.52 (m, 4 H, H7), 7.49 – 7.36 (m, 8 H, H5, H6, H8), 7.23 – 7.15 (m, 4 H, H3, H4), 4.22 – 4.16 (m, 4 H, H10), 3.83 (q, ^{3}J(H1,H2) = 7.1 Hz, 2 H, H2), 3.63 – 3.57 (m, 4 H, H9), 3.54 – 3.43 (m, 20 H, H_{PEG}), 1.48 ppm (d, ^{3}J(H1,H2) = 7.2 Hz, 6 H, H1). ^{19}F NMR (376.46 MHz, CD_3CN): δ = −119.5 ppm (dddt, ^{3}J(H3,F) = 11.9, ^{4}J(H5,F) = 8.5, ^{5}J(H6,F) = 1.5, ^{5}J(H4,F) = 0.4 Hz). HRMS (ESI+): *m/z* calculated for $C_{44}H_{52}F_2O_{10} + K^+$ [M + K^+]: 817.3160. Found: 817.3194.

2.11.6. Diester n = 8

^{1}H NMR (400.15 MHz, CD_3CN): δ = 7.58 – 7.52 (m, 4 H, H7), 7.49 – 7.36 (m, 8 H, H5, H6, H8), 7.26 – 7.13 (m, 4 H, H3, H4), 4.23 – 4.12 (m, 4 H, H10), 3.83 (q, ^{3}J(H1,H2) = 7.2 Hz, 2 H, H2), 3.64 – 3.54 (m, 4 H, H9), 3.53 – 3.44 (m, 24 H, H_{PEG}), 1.48 ppm (d, ^{3}J(H1,H2) = 7.2 Hz, 6 H, H1). ^{19}F NMR (376.46 MHz, CD_3CN): δ = −119.5 ppm (dddt, ^{3}J(H3,F) = 11.8, ^{4}J(H5,F) = 8.5, ^{5}J(H6,F) = 1.7, ^{5}J(H4,F) = 0.5 Hz). HRMS (ESI+): *m/z* calculated for $C_{46}H_{56}F_2O_{11} + K^+$ [M + K^+]: 861.3422. Found: 861.3432.

3. Results and discussion

The impurities described and isolated in this article are known to form in Flurbiprofen medication containing PEG and have already been identified in literature [4]. This work does not focus on the process of identification of these substances but rather on their isolation using the aforementioned HPLC-DAD-HRMS/SPE NMR system, in an attempt to highlight the speed, efficiency and potential of this system for pharmaceutical analysis. If not stated otherwise, the analytical data listed were collected using this system. The first samples were synthesized in a solvent free reaction of Flurbiprofen and an excess of PEG under catalysis by sulfuric acid.

3.1. Analytical data

The two sets of Flurbiprofen-PEG-esters both show absorption maxima at approximately 204 and 247 nm during HPLC-UV analysis (method 2.8) (Figs. S7 and S8 of the Supporting Information), very similar to Flurbiprofen (208 and 248 nm). As there is no particular change in the chromophore system during the reaction these results are as expected for the known Flurbiprofen-PEG-mono- and diesters.

Analysis of the synthetic solution by HPLC-HRMS (ESI positive, method 2.9) resulted in a sequence of data for 21 individual substances for the mono- and 16 for the diesters. In the case of the monoester the first identified compound shows an *m/z* value of 289 for $[M+H]^+$, along with several other positively charged aggregates. This corresponds with the theoretical *m/z* value of the monoester of Flurbiprofen (*m/z* = 244) and PEG (*m/z* = 44 per EG (ethylene glycol) unit with a chain length of n = 1. Further observed compounds increased by an *m/z* value of 44 with each additional EG unit up to 1187 for $[M+NH_4]^+$ for a PEG chain

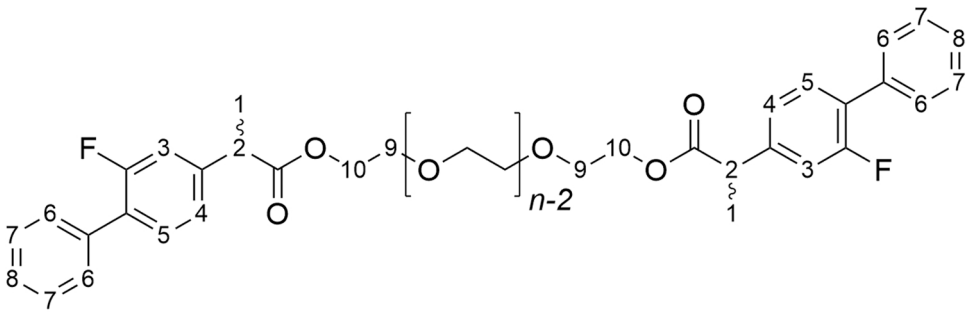

Fig. 12. Numbering scheme for the assignment of ^{1}H NMR signals of **3**, for n = 3 – 8.

length of n = 21. In the case of the diesters, the order of the eluting compounds was reversed, with long chained esters eluting earlier. As such the first compound that could be detected in HPLC-HRMS analysis had an *m/z* value of 1193 for $[M+NH_4]^+$ for a diester with a PEG length of n = 16, followed by compounds with *m/z* values decreasing by 44 down to a PEG chain length of n = 1 (*m/z* = 532 for $[M+NH_4]^+$). A full list of the HRMS data of the mono- and diesters and their corresponding aggregates are depicted in the Supporting Information (Table S1, Figs. S9 and S11).

In addition to UV and HRMS data, the final characterization was performed by NMR spectroscopy, requiring the isolation of the individual compounds. This was achieved using the hyphenated HPLC-DAD-HRMS/SPE NMR system.

For comparison of the NMR spectra of the mono- and diesters, a set of six esters with increasing chain length were collected, beginning from chain length n = 3 to n = 8. Chain lengths of n = 1 and 2 and larger than n = 8 were not collected, as their concentration was below the reporting limit set by relevant ICH guidelines within the Flurbiprofen lozenges.

In preparation for the isolation of the mono- and diesters, two specific HPLC methods were developed (Method 2.9, Figs. S2 and S4), based on the in-house analytical method (2.7) for 8.75 mg Flurbiprofen lozenges, registered with the regulatory authorities. The methods were easily adapted within one day by research staff with little prior experience in method development. In particular, the pH value of the methods was changed from 3.0 to 6.6, as this leads to earlier elution of Flurbiprofen, removing it from the sample, whilst the pH value remains low enough for ESI+ HRMS analysis. Also, the use of a broader column allowed the injection of larger sample concentrations per run, whilst the increased length of the column made up for the reduced efficiency of the separation due to the use of column material with a larger particle size. Due to the use of a longer column, the flow rate was also increased. The methods contained prolonged isocratic sections in the regions of the two ester "hedgehogs" in order to sufficiently separate the individual compounds. Time and UV data were used as parameters for the SPE isolation.

Both methods were repeated twelve times each with the fractions of interest collected in order of elution. Two sets of SPE cartridges were used to collect the individual UV peaks onto a set of two SPE cartridges per ester, with six fractions on each, resulting in a total of twelve fractions per ester. All cartridges were then dried using nitrogen and each ester was eluted into individual NMR capillaries using deuterated acetonitrile.

For the six collected monoesters, a series of ^{1}H- and ^{19}F NMR spectra were collected. In the case of a PEG chain length n = 5, a series of 2D spectra (COSY, HSQC, HMBC) were recorded. To examine the performance limit of the method, an attempt to measure 2D spectra for a chain length of n = 3 was also made, as this was the compound amongst the collected samples with the lowest intensity in the UV-chromatogram. In this case COSY and HSQC spectra could be recorded for the monoester, but the amount of sample was insufficient to generate adequate HMBC data. Sufficient amounts of sample for these experiments may be collected by increasing the number of HPLC runs in the collection process, but for the purpose of comparability, this was not done in this study. For comparison a series of 1D (^{1}H, ^{19}F and ^{13}C) and 2D (COSY, HSQC, HMBC) spectra were collected of Flurbiprofen in deuterated acetonitrile.

Like Flurbiprofen, all monoesters showed a doublet around 1.47–1.49 ppm (I) stemming from the methyl group of the Flurbiprofen unit and its ^3J coupling with the proton of the neighboring methine group (Fig. 3). This single proton in turn was present as a quartet at 3.84 ppm (II), and the eight protons of the fluorobiphenyl rings were visible around 7.18–7.62 ppm (III). The coupling constant of 7.2 Hz between I and II is also identical to Flurbiprofen.

One distinct feature differentiating Flurbiprofen from its PEG-monoesters is the presence of a triplet at around 2.76–2.82 ppm, caused by the hydroxyl group at the end of the respective PEG chain (Fig. 4). Whilst these protons all showed a consistent coupling constant of 5.8 Hz with the neighboring methylene group, their chemical shifts were shown to vary strongly for each sample and measurement. As such, it was observed that the same sample measured on different days could result in a change of the chemical shift of around 0.1 ppm and broadening or even further splitting of the signal was occasionally observed. In some instances, the signal disappeared completely for a time. This fluctuation can likely be explained by an occurring proton exchange with residual water within the solvent, especially seeing as the effect increased over time, during which the acetonitrile gathered additional moisture from the air.

Amongst the remaining protons of the PEG unit, the methylene groups adjacent to the ester group are visible as two multiplets at around 4.22–4.17 (IV) and 3.62–3.58 ppm (V), with the former (IV) representing the methylene group directly neighboring the ester group (Fig. 5). The remaining PEG protons form a large set of multiplets between 3.62 and 3.41 ppm (VI). The integrals of these sets of multiplets coincide with the growing chain length. For a length of n = 3 twelve protons can be counted, with the proton count rising by four for each additional EG unit up to thirty-two for n = 8.

A further observation is the presence of one large signal amongst the set of eight protons for a chain length of n = 3, resulting from the central unit of the PEG chain (neither adjacent to the ester nor the OH group). With increasing chain length a further one of these signals can be observed up until six signals for n = 8 (Fig. 6). It can be assumed that this trend continues for chain lengths larger than n = 8 but will eventually become less distinct, as the signals of the protons begin to overlap increasingly.

The fluorine spectra of the monoesters all show similar coupling patterns, visible as doublets of doublets of triplets with a further small split into doublets (ddtd) as is the case for Flurbiprofen. This pattern results from fluorine coupling with various protons of the biphenyl ring up to a distance of ^5J (Fig. 7). The coupling constants of the monoesters are once again almost identical to Flurbiprofen.

Like the monoesters, a series of ^{1}H- and ^{19}F NMR spectra were collected for the diesters with chain lengths n = 3 – 8. Due to less substance, the overall quality of the measured spectra was lower than for the monoesters. This meant that impurities of the deuterated solvent were visible more distinctly and that the sample signals were less defined. All important coupling constants and integrals could however be determined accurately for the collected samples, providing sufficient data for the characterization of the individual diesters.

As expected, the ^{1}H- and ^{19}F NMR spectra of the mono- and diesters were almost identical. The signals of the Flurbiprofen unit (I – III) showed similar patterns, coupling constants and chemical shifts as Flurbiprofen and the monoesters, with the only major difference being the integrals in the ^{1}H NMR spectra that were twice as high due to the additional Flurbiprofen unit (Fig. 8). Naturally the triplet caused by the OH group of PEG was no longer visible due to the double esterification and the only other visible differences were the shape and integrals of the PEG unit (Fig. 9).

Due to the second Flurbiprofen unit replacing the OH group in the diesters, the four protons adjacent to the hydroxyl group are shifted, reducing the integral of the signals in the area around 3.64 – 3.41 ppm (VI) by four, compared to the monoesters. Instead, the integrals of the signals in the area of 3.54 – 3.41 (V) and 4.23 – 4.12 ppm (IV), stemming from the methylene groups adjacent to the ester group, are doubled.

3.2. Analysis of extracts from Flurbiprofen lozenges

The methods established for the analysis of the synthetic solutions, were adapted for the analysis of extracts from lozenges, to test if the analysis and identification of the impurities can also be performed directly from the medical products.

The samples were prepared from 40 Flurbiprofen lozenges (see 2.6). To increase the concentration of the impurities, compared to other

ingredients, the tablets were dissolved in a 1:1 dichloromethane and 0.1% sodium bicarbonate solution. This was done with the intention of separating sugars, the major components of the tablets, from the non-polar impurities by extracting them into the aqueous phase, whilst the analytes of interest remained in the organic phase. The use of sodium bicarbonate also reduced the amount of Flurbiprofen by deprotonating and thereby ionizing the API, transferring it into the aqueous phase.

Using this method, the proportion of Flurbiprofen-PEG mono- and diesters could be increased sufficiently for NMR analysis after separation. As the analytical equipment for the separation, used during the synthetic-route analysis, was not accessible for further experiments, the separation of the components of the lozenge-analyte solution was performed with different, but comparable equipment and analytical columns. The monoester separation method remained the same, whilst the diester separation was performed on a shorter column using a compressed method (see 2.9, Figs. S3 and S5). This was possible due to lower concentrations of the diesters, resulting in less column overload and improved peak separation.

As the NMR measurements of the impurities from the lozenge-extracts were performed on a more accurate 600 MHz NMR spectrometer using a cryo probe head, the sample collection onto the SPE cartridges was reduced to five cycles from originally twelve for the synthetic samples. Despite an overall lower concentration of esters within the sample, the five cycles and the use of solvent suppression during measurements proved sufficient for the necessary NMR analysis. Both the chemical shifts and coupling constants, as well as the integrals of the individual samples, were identical to the synthetic samples. In the case of the monoesters the 2D measurements (COSY, HSQC, HMBC) were successfully performed. In case of the diesters only COSY and HSQC spectra of acceptable quality could be obtained. Due to low sample concentration, the spectra of the diesters with a chain length of $n = 3$ and 4 were of low quality but proved sufficient for analysis. A further observation showed, that the signals of the hydroxyl groups within the monoester were present with the correct coupling constants, but the integrals did not have the predicted value of one. This may be due to the previously mentioned proton exchange of the hydroxyl group with the solvent, leading to a false value for the integrals. Lastly, UV and HRMS data were also identical to the synthetic samples, though the predominant masses collected during HRMS measurements were those of the ammonium aggregates (S10 and S11).

Despite lower sample concentrations and a lower number of collection cycles, adequate data for complete structural elucidation of the impurities of interest could be collected from the lozenge-extracts. Even impurities far below the reporting limit specified by the ICH could be enriched in sufficient amounts and purity for complete structural elucidation. In the case of the diester with a chain length of $n = 3$, the approximate assay during the analysis of the Flurbiprofen lozenges was as low as 0.016%.

3.3. The hyphenated system: function, advantages and limitations

Hyphenated systems come in varying set-ups with an array of coupled analytical methods [19]. The HPLC-DAD-HRMS/SPE NMR (Fig. 10) system applied in this work simultaneously allows both effective separation and isolation via HPLC and SPE as well as the collection of high-quality data via DAD, HRMS and NMR, that in combination allow the unambiguous identification of a compound.

At first the sample is separated by HPLC chromatography, allowing the separation of complex mixtures with many substances. The separation at this point is merely limited by the LC method and available columns. After passing through the column, the effluent is flow-split into two parts. Approximately 5% is diluted by MS grade solvent, using a binary pump, and is constantly infused into the HRMS. The remaining 95% of the stream pass through the DAD detector, which records the UV absorption in a selected range, 190 – 640 nm in this case. In doing so, time correlated HRMS and UV data are collected for the separated compounds within the continuous effluent flow. Based on this data, elusion times can be determined, which can be used as data parameters for the collection of the individual fractions in the trapping method of the SPE system. This method is then used in subsequent HPLC runs. A single trapping parameter consists of the elusion time window and either the UV absorption level threshold or HRMS intensity threshold. The trapping method can contain several trapping parameters to enable the collection of many samples at a time. If, in the elusion time window, the absorption of the UV data or the intensity of the HRMS data rise above the specified threshold, the effluent is channeled toward the SPE cartridges (via the LC-SPE organizer).

The SPE cartridges consist of polymers and other substances usually used as column materials, in this case polyvinylbenzene. The type of cartridge may be chosen to best retain the substances in question, depending on characteristics of the analyte such as polarity, charge, or presence of certain functional groups, like aromatic rings. Before use, the cartridges are conditioned by an appropriate solvent system, in this case a 1:1 system of water and acetonitrile.

To prevent the trapped materials from simply being washed off the cartridges when the effluent is channeled to the SPE cartridges, the solvent composition is adjusted by a make-up pump that adds a solvent of choice to the system. This usually serves to switch the polarity of the solvent system to enable better trapping on the cartridges. Buffer solutions may also be used to change the polarity of the analyte itself. After the end of the trapping process, the make-up flow continues for a short, preset time to wash any salts or eluent-additives from the cartridges. The make-up flow must be significantly higher than the flow of the HPLC pump to ensure a sufficient switch of polarity. If the flow is too high however, it may result too rapid and strong pressure increase within the system. One way to avoid this increase in pressure and to reduce the make-up flow, is by using an HPLC method that reduces the HPLC flow in the section of interest.

The great advantage of this hyphenated system is that the trapping process may be repeated as often as desired for several consecutive HPLC runs in an automated fashion, using the same cartridges for the corresponding fractions. This allows the collection of sample quantities high enough for less sensitive methods such as NMR spectroscopy. The amount of substance that can be collected per cartridge depends on the substance itself, the cartridge in use and the solvent system. The system requires adjustment from case to case to prevent cartridge overload. If more substance is required than can be stored on an individual cartridge, additional cartridges can be used for the individual fractions.

Once the desired number of HPLC runs has been performed, the loaded cartridges are dried by nitrogen flow and the enriched compound is transferred into NMR capillaries (2.5 and 0.3 mm in this case) using deuterated solvents. The solvent that best elutes the analyte from the SPE cartridges should be chosen for the transfer, acetonitrile in this case. The use of NMR capillaries, instead of NMR tubes, requires less deuterated solvent and has the advantage that the signals of the enriched compounds are less disturbed by undeuterated solvent and impurities contained in the NMR solvent. These may otherwise overshadow or overlap with the signals of the analyte, especially in cases when only small amounts of substance are collected. The use of capillaries instead of standard NMR tubes also increases the number of nuclei in the active volume and allows the use of optimized probe heads with better filling factors.

Once the fractions have been pooled in their individual NMR capillaries, any type of NMR study may be performed depending on the amount of substance and type of atoms it contains. Hereby UV, HRMS and NMR data of a single or several separated sample components may be acquired in a fast, automated fashion.

The variable methods and conditions of the hyphenated HPLC-DAD-HRMS/SPE NMR system may be adjusted to accommodate a large range of samples. The amount and concentration of any given analyte however, remains a limiting factor for the system, as NMR studies require a comparatively large amount of sample. Although the trapping process

can potentially be repeated as often as desired, too low sample concentration will still make NMR measurements difficult.

4. Conclusion

In this report we demonstrated the use of a hyphenated HPLC-DAD-HRMS/SPE NMR system for the separation and isolation of a complex mixture of very similar compounds, for the specific case of Flurbiprofen-PEG mono- and diesters. This method enables the effective separation and isolation of compounds with very similar retention times in a quick and automated fashion that allows the collection of UV, HRMS and even NMR data within only a few days. The method was successfully applied to the identification of impurities from the pharmaceutical product Flurbiprofen Lozenges, with the impurity concentration successfully analyzed ranging from as low as 0.016–0.354% within the medical product. The extended analytical information delivered by this type of hyphenated system, its ease and speed of use, as well as the quick adaptability of existing HPLC methods qualify this system for a more widespread use in the analysis of pharmaceutical samples and quality control. The ability to directly isolate impurities from pharmaceuticals and effectively identify them with modern analytical methods such as NMR spectroscopy, without the need for the classical extensive investigation into the formation of the unknown analyte, for example via degradation experiments, may significantly reduce the time from detection of an impurity to its identification. The possibility of repeating the collection process as often as required and the ability to freely vary the SPE cartridges used for fraction collection, means that this method is only truly limited by the same parameters as any other HPLC separation. In case of difficulties separating individual components of a sample however, the system may even be modified employing a 2D-HPLC system, thus allowing more powerful separation on the LC part [25].

Statement on funding

Hexal AG, Industriestraße 25, 83607 Holzkirchen, Germany.

Author agreement

The manuscript was written through contributions of all authors. All authors have given approval to the final version of the manuscript.

Supplementary information

The supplementary information contains additional data, chromatograms, figures and spectra including detailed images of both 1D and ^{2}D NMR spectra.

CRediT authorship contribution statement

Philipp Schmidt: Conceptualization, Methodology, Software, Validation, Formal analysis, Investigation, Data curation, Writing – original draft, Writing – review & editing, Visualization. **Christine Kolb:** Methodology, Software, Validation, Formal analysis, Investigation, Data curation. **Markus Godejohann**: Software, Formal analysis, Investigation, Resources, Data curation, Visualization. **Andreas Reiser**: Methodology, Software, Validation, Formal analysis, Investigation, Data curation. **Markus Philipp**: Conceptualization, Supervision, Project administration. **Hans-Christian Müller**: Conceptualization, Supervision, Project administration, Funding acquisition. **Konstantin Karaghiosoff**: Conceptualization, Resources, Supervision, Project administration, Funding acquisition.

Declaration of Competing Interest

The authors declare the following financial interests/personal relationships which may be considered as potential competing interests: Philipp Schmidt reports financial support and equipment, drugs, and supplies were provided by Hexal AG.

Data Availability

Data will be made available on request.

Acknowledgements

We thank the Hexal AG for providing funds, materials as well as the facilities, equipment and analytical machines necessary for the research of this paper. Also, we greatly thank Bruker BioSpin GmbH fort the measurement of the lozenge-extracts.\.

Appendix A. Supporting information

Supplementary data associated with this article can be found in the online version at doi:10.1016/j.jpba.2022.115068.

References

[1] L. Gasparini, E. Ongini, D. Wilcock, D. Morgan, Activity of flurbiprofen and chemically related anti-inflammatory drugs in models of Alzheimer's diseas, Brain Res. Rev. 48 (2005) 400–408.
[2] T. Timocin, H.B. Ila, Investigation of flurbiprofen genotoxicity and cytotoxicity in rat bone marrow cells, Drug Chem. Toxicol. 38 (2015) 355–360.
[3] T.G. Kantor, Physiology and treatment of pain and inflammation: analgesic effects of flurbiprofen, Am. J. Med. 80 (1986) 3–9.
[4] K. Sawicka, J. Takhar, P. Marrshall, M. Fanfarillo, Production Process for NSAID-Containing Lozenges, Their Compositions, Their Medical Use. WO 2006/092569 A1, September 8, 2006.
[5] R. Mohan, C.S. Ramaa, Ester prodrugs of flurbiprofen: Synthesis, plasma hydrolysis and gastrointestinall toxicity, Indian J. Chem. 46 (2007) 1164–1168.
[6] S.P. Chaudhari, P.S. Patil, Pharmaceutical excipients: a review, IJAPBC 1 (2012) 21–34.
[7] I. Sopyan, N.M.W.S. Santi, A.V. Berlian, N.E. Meilina, Q. Fauza, R.A. Apriyandi, A review: pharmaceutical excipients of solid dosage forms and characterizations, Int. J. Res. Pharm. Sci. 11 (2020) 1472–1480.
[8] A.A. D'souza, R. Shegokar, Polyethylene glycol (PEG): a versatile polymer for pharmaceutical applications, Expert Opin. Drug Deliv. 13 (2016) 1257–1275.
[9] K. Knop, R. Hoogenboom, D. Fischer, U.S. Schubert, Poly(ethylene glycol) in drug delivery: pros and cons as well as potential alternatives, Angew. Chem. Int. Ed. 49 (2010) 6288–6308.
[10] F. Qiu, D.L. Norwood, Identification of pharmaceutical impurities, J. Liq. Chrom. Relat. Tech. 30 (2007) 877–935.
[11] O. Corcoran, M. Spraul, LC NMR-MS in drug discovery, DDT 8 (14) (2003) 624–631.
[12] J.M. Garcia-Manteiga, S. Mari, M. Godejohann, M. Spraul, C. Napoli, S. Cenci, G. Musco, R. Sitia, Metabolomics of B to plasma cell differentiation, J. Proteome Res 10 (2011) 4165–4176.
[13] M. Godejohann, L.-H. Tseng, U. Braumann, J. Fuchser, M. Spraul, Characterization of paracetamol metabolite using on-line LC-SPE NMR-MS and a cryogenic NMR probe, J. Chromatogr. A. 1058 (2004) 191–196.
[14] A.W. Nicholls, I.D. Wilson, M. Godejohann, J.K. Nicholson, J.P. Shockcor, Identification of phenacetin metabolites in human urine after administration of phenacetin-C^{2}H$_3$: measurement of futile metabolic deacetylation via HPLC/MS-SPE NMR and HPLC-ToF MS, Xenobiotica 36 (7) (2006) 615–629.
[15] H. Tang, C. Xiao, Y. Wang, Important roles of the hyphenated HPLC-DAD-MS-SPE NMR technique in metabonomics, Magn. Reason. Chem. 47 (2009) 157–162.
[16] J. Fu, Y.-N. Wang, S.-G. Ma, L. Li, X.-J. Wang, Y. Li, Y.-B. Liu, J. Qu, S.-S. Yu, Xanthanoltrimer A–C: three xanthanolide sesquiterpene trimers from the fruits of Xanthium italicum Moretti isolated by HPLC-MS-SPE NMR, Org. Chem. Front. 8 (2021) 1288–1293.
[17] S. Gummadi, D.S. Siyyadri, Nuclear magnetic resonance and hyphenations – a review, IJPSR 11 (12) (2020) 5932–5950.
[18] K. Iqbal, J. Iqbal, D. Staerk, K.T. Kongstad, Characterization of antileishmanial compounds from lawsonia intermis L. leaves using semi-high resolution antileishmanial profiling combined with HPLC-HRMS-SPE NMR, Front. Pharmacol. 8 (337) (2017) 1–7.
[19] K.T. Johansen, S.J. Ebild, S.B. Christensen, M. Godejohann, J.W. Jaroszewski, Alkaloid analysis by high-performance liquid chromatography-solid phase extraction-nuclear magnetic resonance: new strategies going beyond the standard, J. Chromatogr. A 1270 (2012) 171–177.
[20] K.T. Johansen, S.G. Wubshet, N.T. Nyber, HPLC NMR revisited: using time-slice high-performance liquid chromatography–solid-phase extraction–nuclear magnetic resonance with database-assisted dereplication, Anal. Chem. 85 (2013) 3183–3189.
[21] F. Liu, Y.-N. Wang, Y. Li, S.-G. Ma, J. Qu, Y.-B. Liu, C.-S. Niu, Z.-H. Tang, Y.-H. Li, L. Li, S.-S. Yu, Triterpenoids from the twigs and leaves of Rhododendron latoucheae by HPLC-MS-SPE NMR, Tetrahedron 75 (2019) 296–307.

[22] C. Seger, M. Godejohann, L.-H. Tseng, M. Spraul, A. Girtler, S. Sturm, H. Stuppner, LC-DAD-MS/SPE NMR Hyphenation. A tool for the analysis of pharmaceutically used plant extracts: identification of isobaric iridoid glycoside regioisomers from harpagophytum procumbens, Anal. Chem. 77 (2005) 878–885.
[23] M. Godejohann, L. Heintz, C. Daolio, J.-D. Berset, D. Muff, Comprehensive non-target analysis of contaminated groundwater of a former ammunition destruction site using ^{1}H NMR and HPLC-SPE-MR/TOF-MS, Environ. Sci. Technol. 43 (2009) 7055–7061.
[24] M. Godejohann, J.-D. Berset, D. Muff, Non-targeted analysis of wastewater treatment plant effluents by high performance liquid chromatography-time slice-solid phase extraction- nuclear magnetic resonance/time-of-flight-mass spectrometry, J. Chromatogr. A 1218 (2011) 9202–9209.
[25] A.J. Alexander, F. Xu, C. Bernard, The design of a multi-dimensional LC-SPE NMR system (LC^{2}-SPE NMR) for complex mixture analysis, Magn. Reason. Chem. 44 (2006) 1–6.
[26] J.R. Kesting, J. Huang, D. Sørensen, Identification of adulterants in Chinese herbal medicine by LC-HRMS and LC-MS-SPE/NMR and comparative in vivo with standards in a hypertensive rat model, J. Pharm. Biomed. 51 (2010) 705–711.
[27] J. Larsen, D. Staerk, C. Cornett, S.H. Hansen, J.W. Jaroszewski, Identification of reaction products between drug substances and excipients by HPLC-SPE NMR: ester and amide formation between citric acid and 5-aminosalicylic acid, J. Pharm. Biomed. 49 (2009) 839–842.
[28] C. Pan, F.L. Liu, Q. Ji, W. Wang, D. Drinkwarer, R. Vivilecchia, The use of LC/MS, GC/MS, and LC/NMR hyphenated techniques to identify a drug degradation product in pharmaceutical development, J. Pharm. Biomed. 40 (2006) 581–590.
[29] M. Sandvoss, B. Bardsley, T.L. Beck, E. Lee-Smith, S.E. North, P.J. Moore, A. J. Edwards, R.J. Smith, HPLC-SPE NMR in pharmaceutical development: capabilities and applications, Magn. Reason. Chem. 43 (2005) 762–770.
[30] B. Schmidt, J.W. Jaroszewski, R. Bro, M. Witt, D. Stærk, Combination PARAFAC analysis of HPLC-PDA profiles and structural characterization using HPLC-PDA-SPE NMR-MS experiments: commercial preparations of St. John's Wort, Anal. Chem. 80 (2008) 1978–1987.
[31] P. Schmidt, C. Kolb, A. Reiser, M. Philipp, H.-C. Müller, K. Karaghiosoff, Isolation, identification and structural verification of a methylene-bridged naloxone "dimer" formed by formaldehyde, J. Pharm. Sci. 00 (2021) 1–8.
[32] N.R. Babij, E.O. McCusker, G.T. Whiteker, B. Canturk, N. Choy, L.C. Creemer, C. V. De Amicis, N.M. Hewlett, P.L. Johnson, J.A. Knobelsdorf, F. Li, B.A. Lorsbach, B. M. Nugent, S.J. Ryan, M.R. Smith, Q. Yang, NMR chemical shifts of trace impurities: industrially preferred solvents used in process and green chemistry, Org. Process Res. Dev. 20 (2016) 661–667.

4.2 Supporting Information

Separation and Identification of a Complex Flurbiprofen-Polyethylene Glycol Mono- and Diester mixture via a Hyphenated HPLC-DAD-HRMS/SPE-NMR System

Philipp Schmidt [a], Christine Kolb [b], Markus Godejohann [c] Andreas Reiser [b], Markus Philipp [b], Hans-Christian Müller [b]*, Konstantin Karaghiosoff [a]*

[a] Department Chemie, Ludwig-Maximilians-Universität München, Butenandtstraße 5-13, Haus D, 81377 Munich, Germany, [b] Analytical Development, Hexal AG, Industriestraße 25, 83607 Holzkirchen, Germany, [c] Bruker BioSpin GmbH, Rudolf-Plank-Str. 23, 76275 Ettlingen, Germany

Table of Contents

The programs used to produce the images in these supporting informations were *Compass Hystar* from Bruker, *Chromeleon* from Thermo Scientific as well as *MestreNova* from Mestrelab Research.

Data was acquired both from the synthetic samples and the lozenge-extracts. The source of the Data, spectra and images is mentioned at the relevant points.

I UV Chromatograms

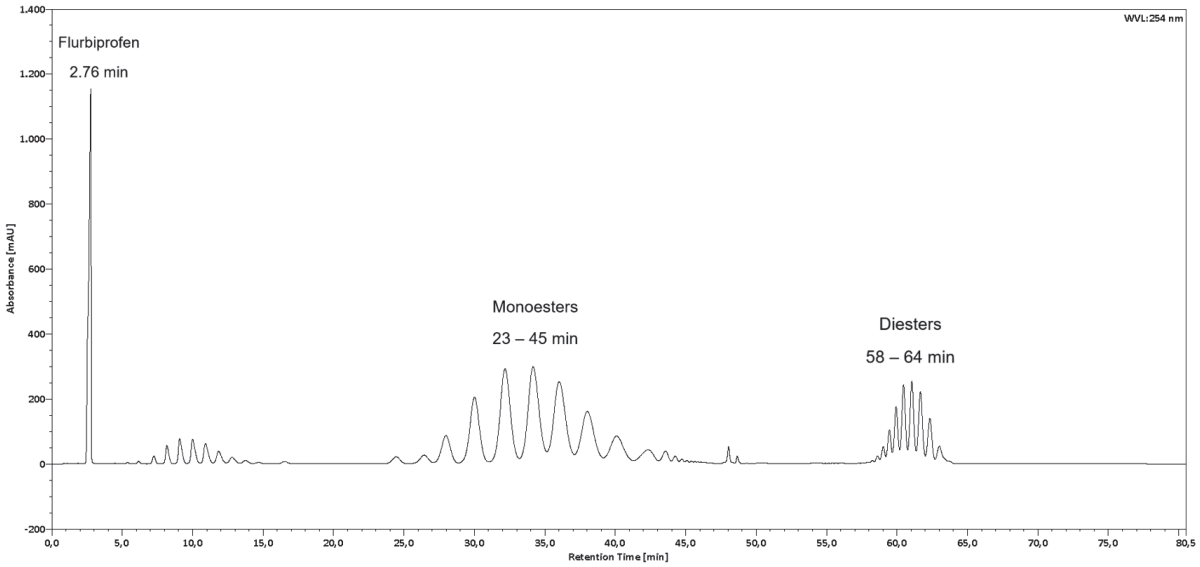

Figure S1. UV Chromatogramm of the reaction solution of the Flurbiprofen-PEG ester mixture with Flurbiprofen (2.76 min), the monoesters (23 – 45 min) and the diesters (58 – 64 min) marked. The substances around 10 min are a mixture of Sulfuric acid-PEG esters (acquired from synthetic samples).

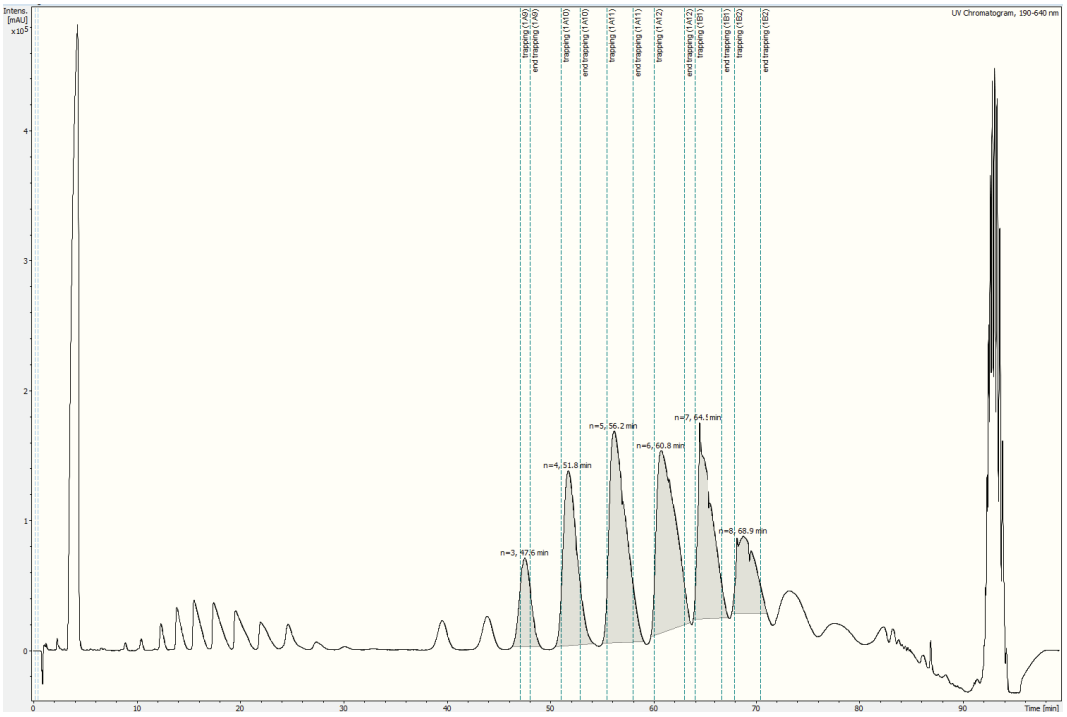

Figure S2. UV chromatogram of the separation and isolation of the Flurbiprofen-PEG monoesters. The beginning and end of the trapping process is marked by dashed lines (acquired from synthetic samples).

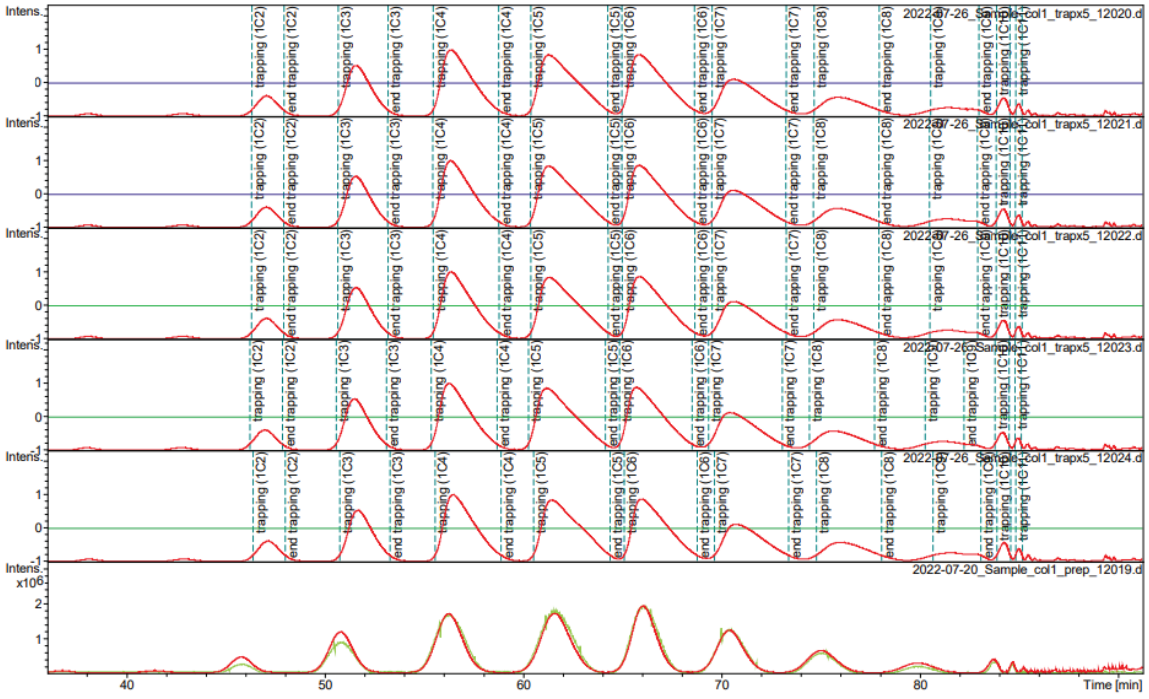

Figure S3. UV chromatogram of the separation and isolation of the Flurbiprofen-PEG monoesters. The beginning and end of the trapping process is marked by dashed lines (acquired from lozenge-extracts).

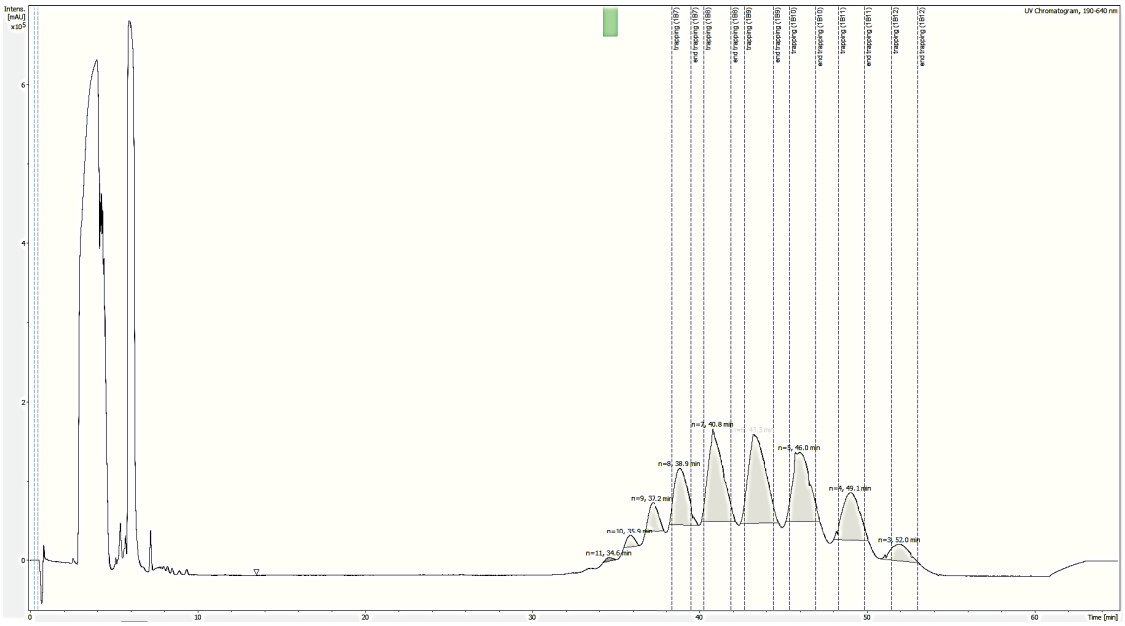

Figure S4. UV chromatogram of the separation and isolation of the Flurbiprofen-PEG diesters. The beginning and end of the trapping process is marked by dashed lines (acquired from synthetic samples).

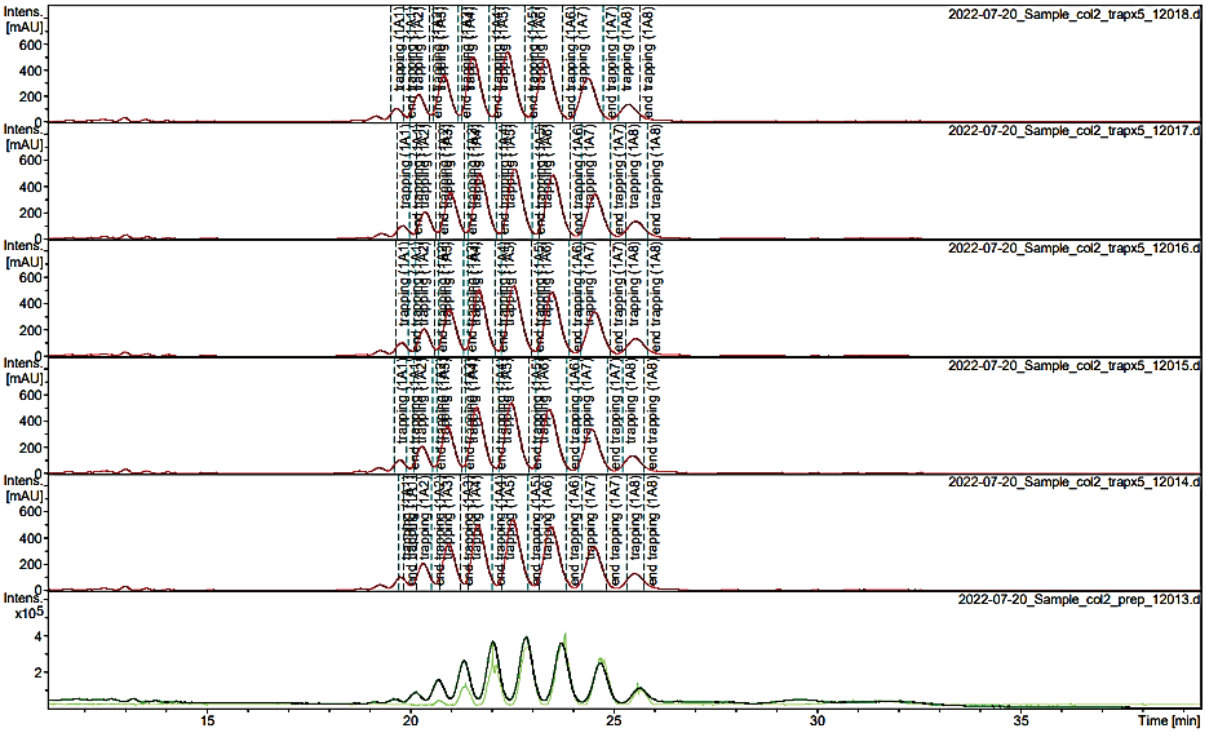

Figure S5. UV chromatogram of the separation and isolation of the Flurbiprofen-PEG diesters. The beginning and end of the trapping process is marked by dashed lines (acquired from lozenge-extracts).

II UV-Vis Spectra

II.I UV-Vis Spectrum of Flurbiprofen

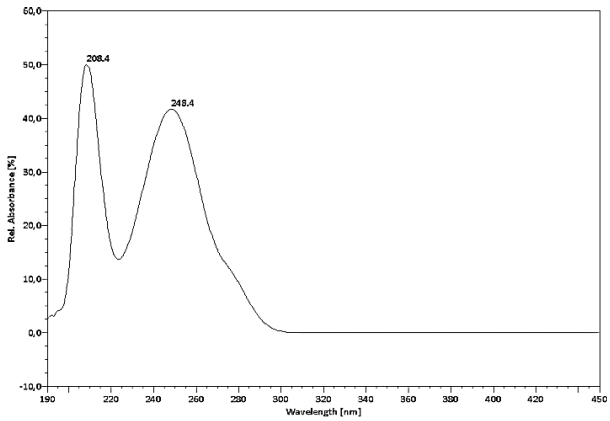

Figure S6. UV-Vis spectrum of Flurbiprofen.

II.II UV-Vis Spectra of the Flurbiprofen-PEG Monoesters

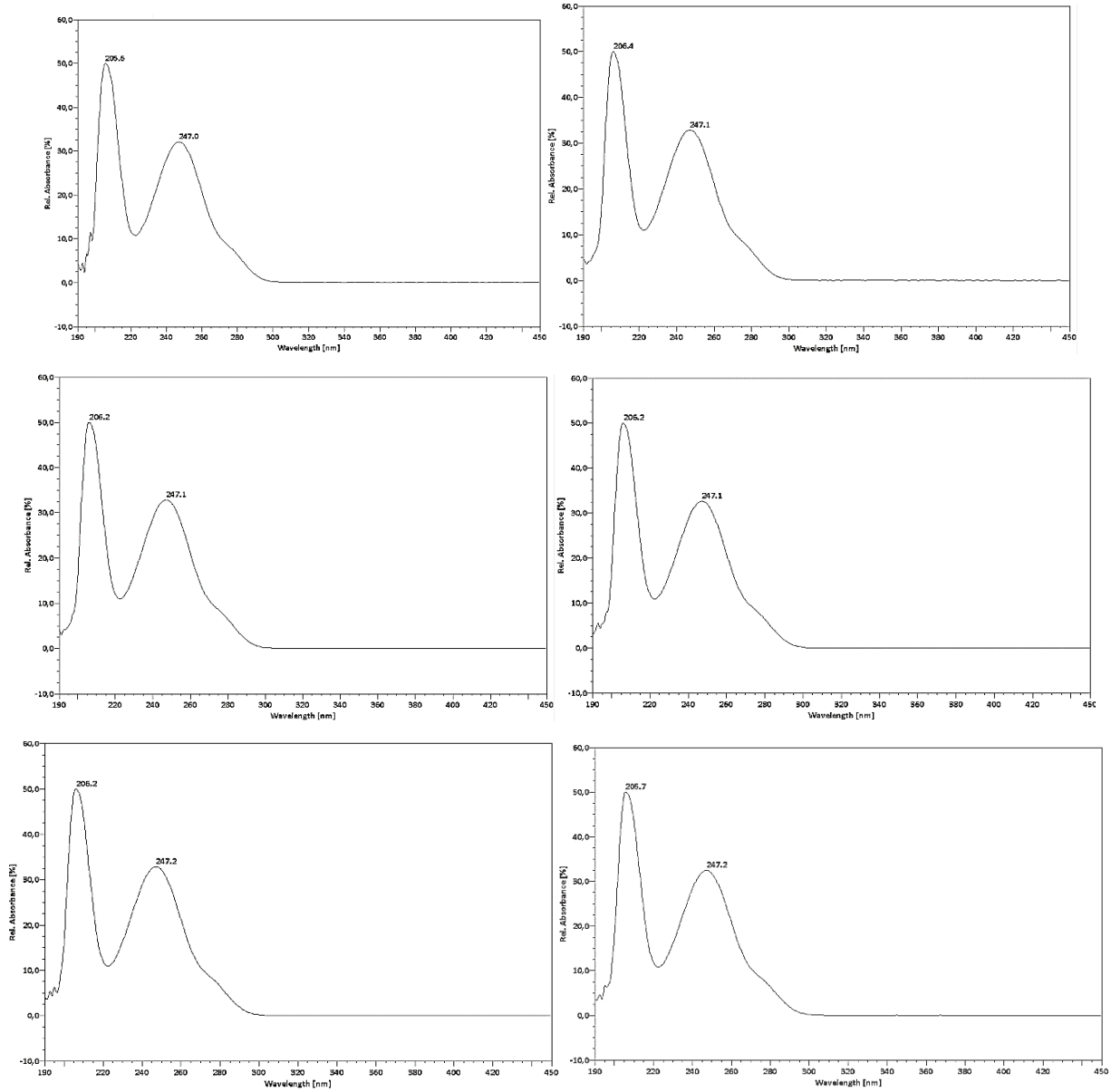

Figure S7. UV-Vis spectra of the Flurbiprofen-PEG monoesters with chain lengths n = 1 to 8 (starting top left to bottom right, acquired from synthetic samples).

II.III UV-Vis Spectra of the Flurbiprofen-PEG Diesters

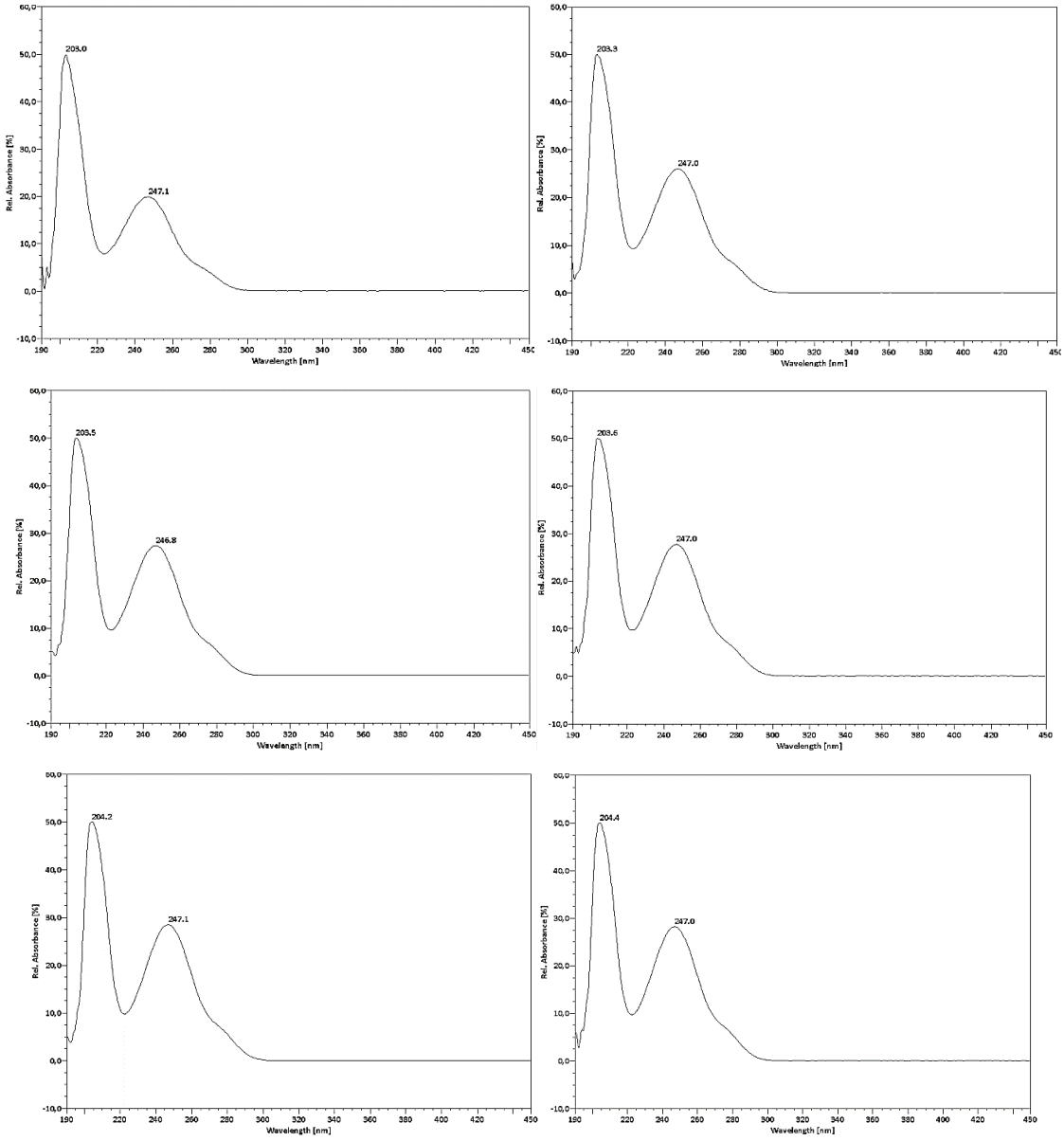

Figure S8. UV-Vis spectra of the Flurbiprofen-PEG diesters with chain lengths n = 1 to 8 (starting top left to bottom right, acquired from synthetic samples).

III. MS Spectra

III.I Mass Spectra of the Flurbiprofen-PEG Monoesters

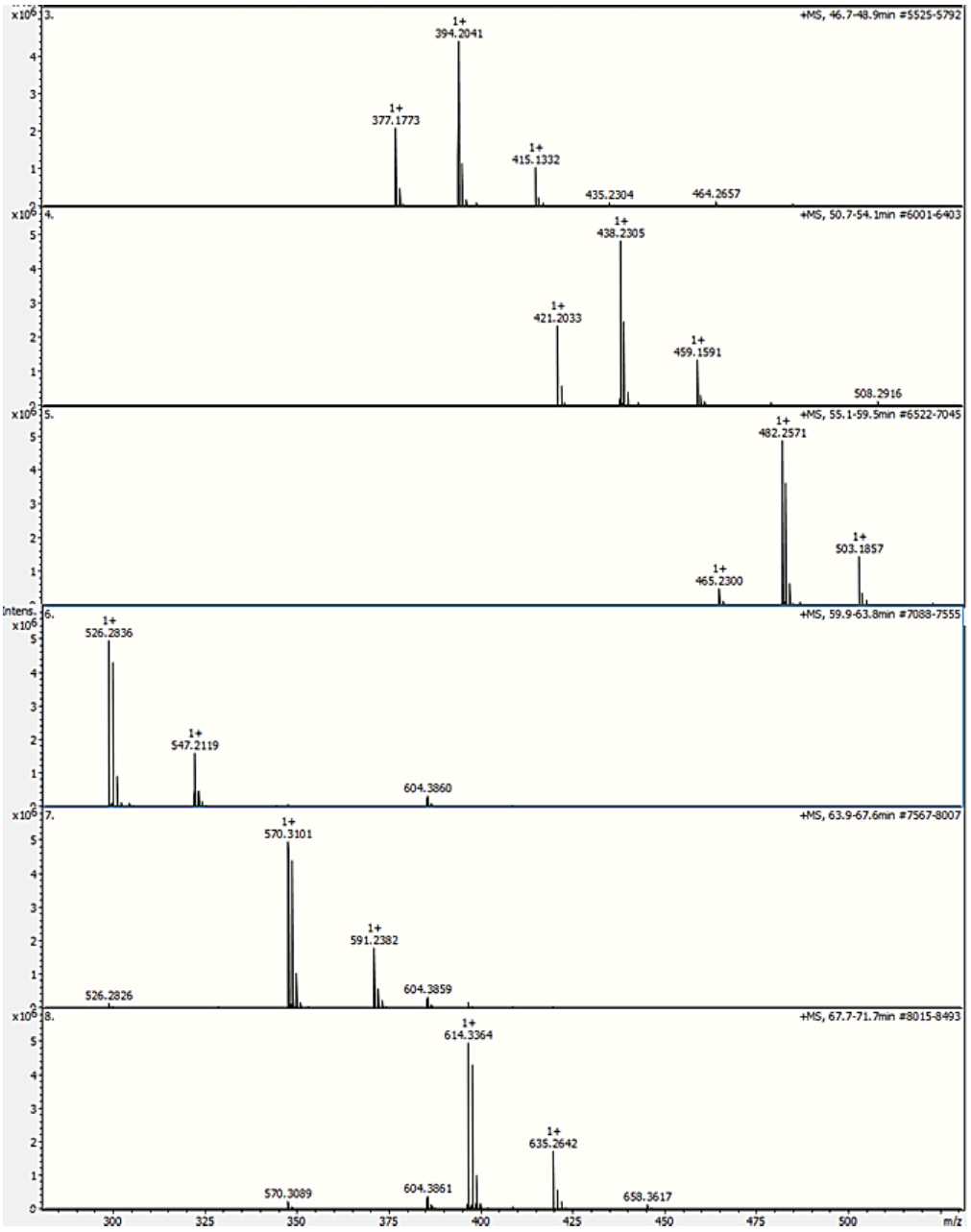

Figure S9. HRMS Data of the Flurbiprofen-PEG monoesters n = 3 – 8 (from top to bottom, acquired from synthetic samples).

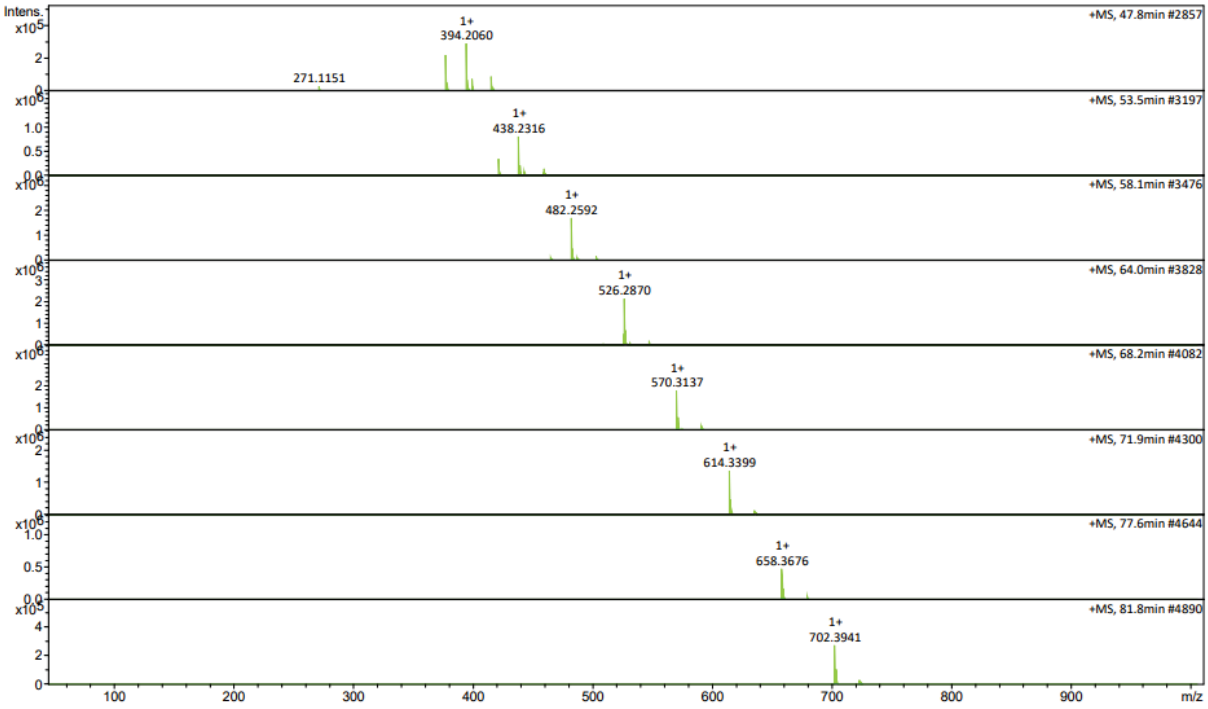

Figure S10. HRMS Data of the Flurbiprofen-PEG monoesters n = 3 – 10 (acquired from lozenge-extracts).

III.II Mass Spectra of Flurbiprofen-PEG Diesters

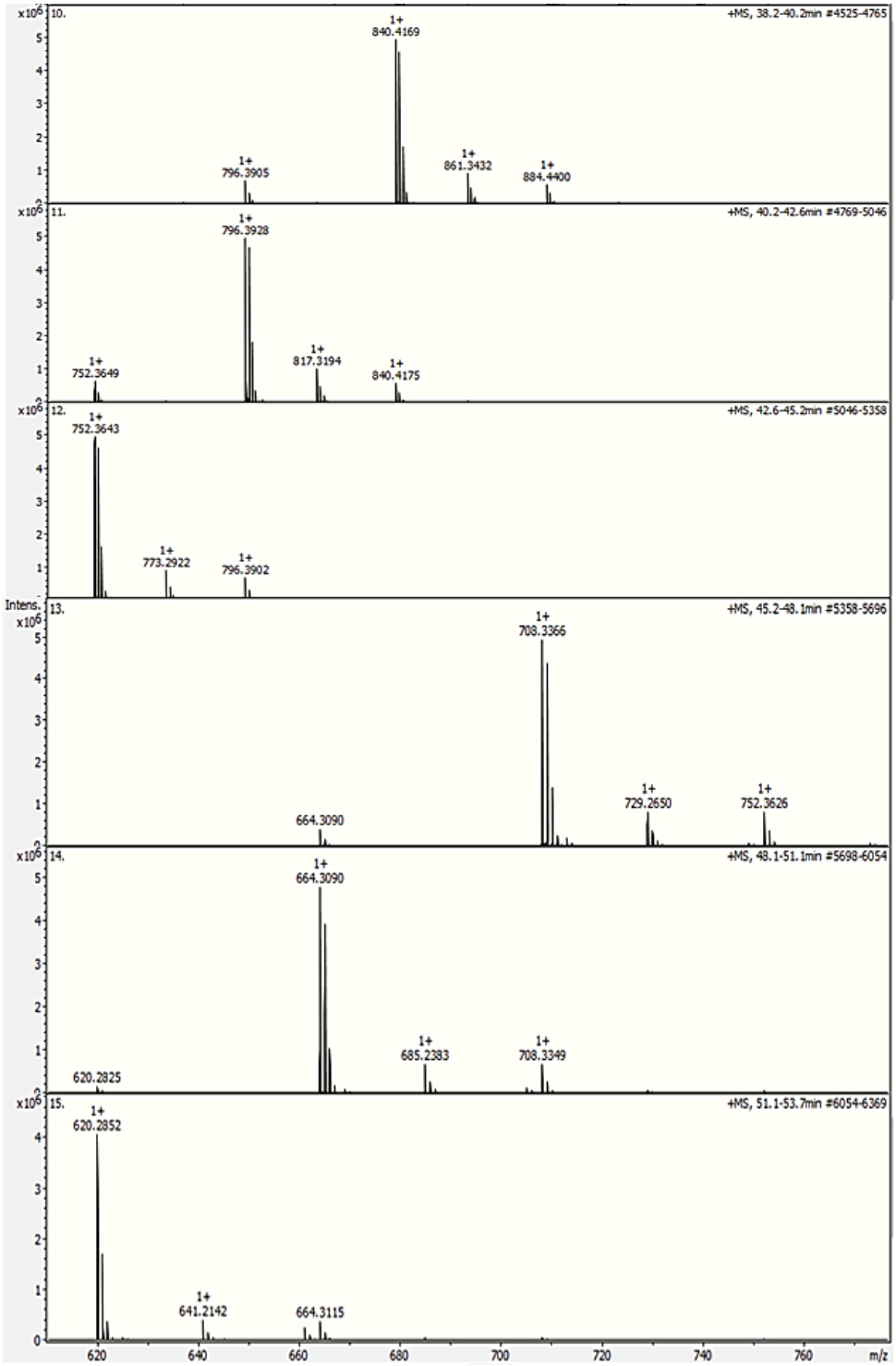

Figure S11. HRMS Data of the Flurbiprofen-PEG diesters n = 3 – 8 (from bottom to top, acquired from synthetic samples).

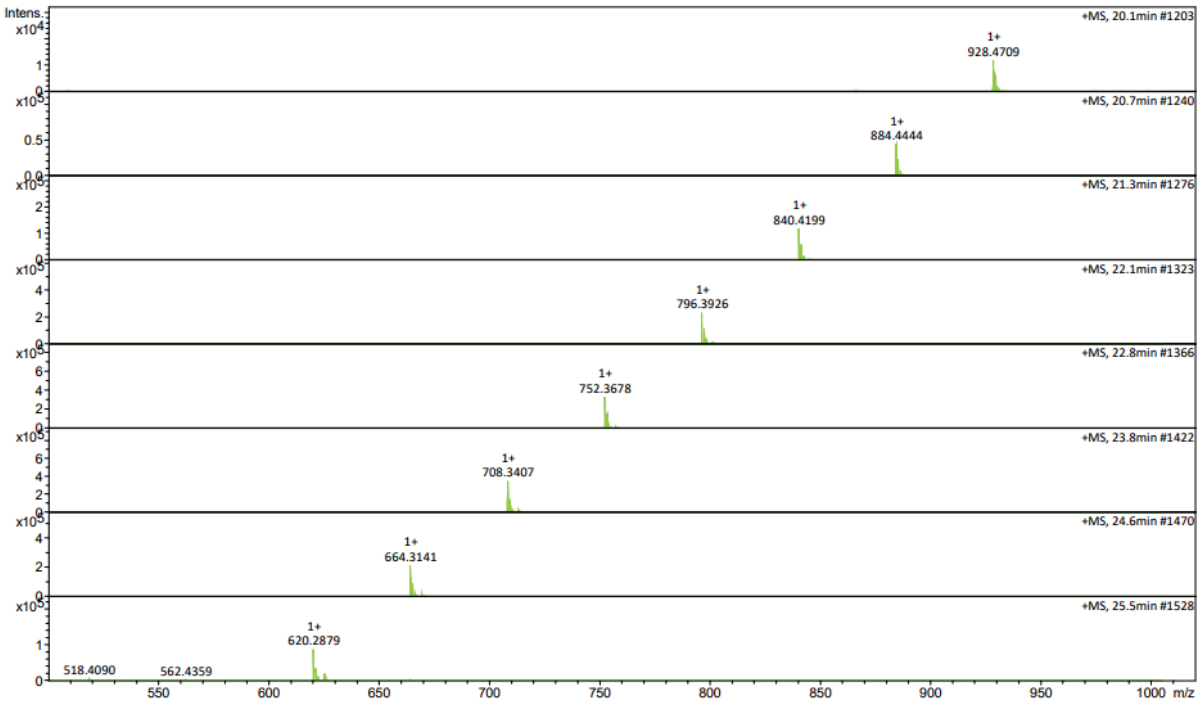

Figure S12. HRMS Data of the Flurbiprofen-PEG diesters n = 3 – 10 (from bottom to top, acquired from lozenge-extracts).

IV. NMR-Spectra

IV.I NMR Spectra of the Flurbiprofen-PEG Monoesters

IV.I.I NMR Spectra of Monoester n = 3

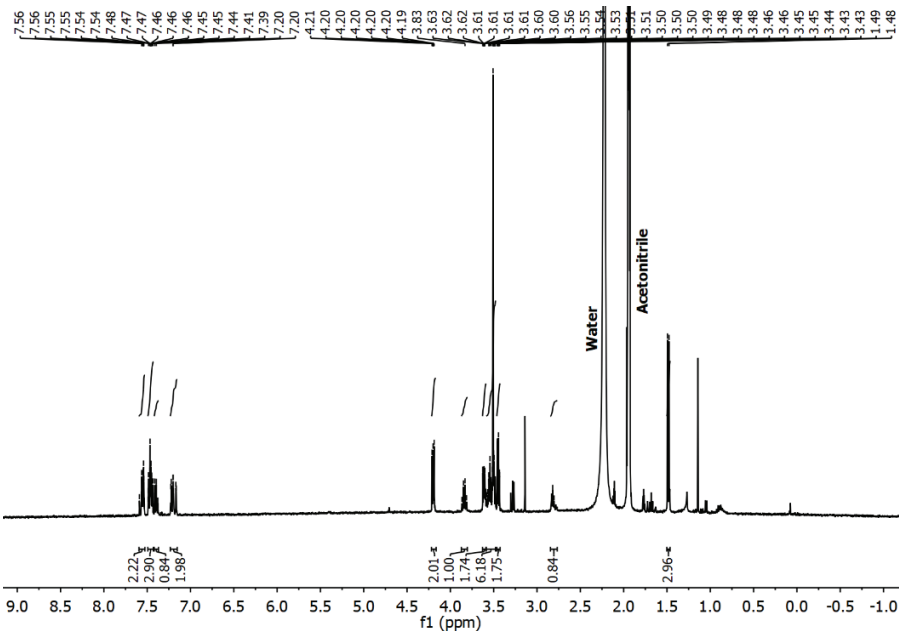

Figure S13. ^{1}H NMR spectrum of the Flurbiprofen-PEG monoester with a chain length of n = 3 (acquired from synthetic samples).

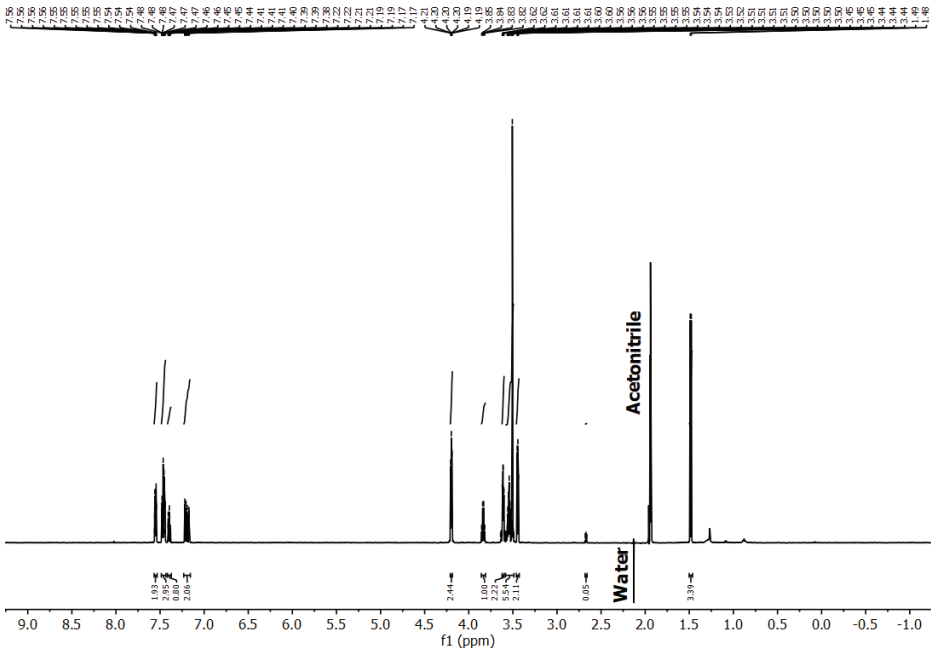

Figure S14. ^{1}H NMR spectrum of the Flurbiprofen-PEG monoester with a chain length of n = 3 (acquired from lozenge-extracts).

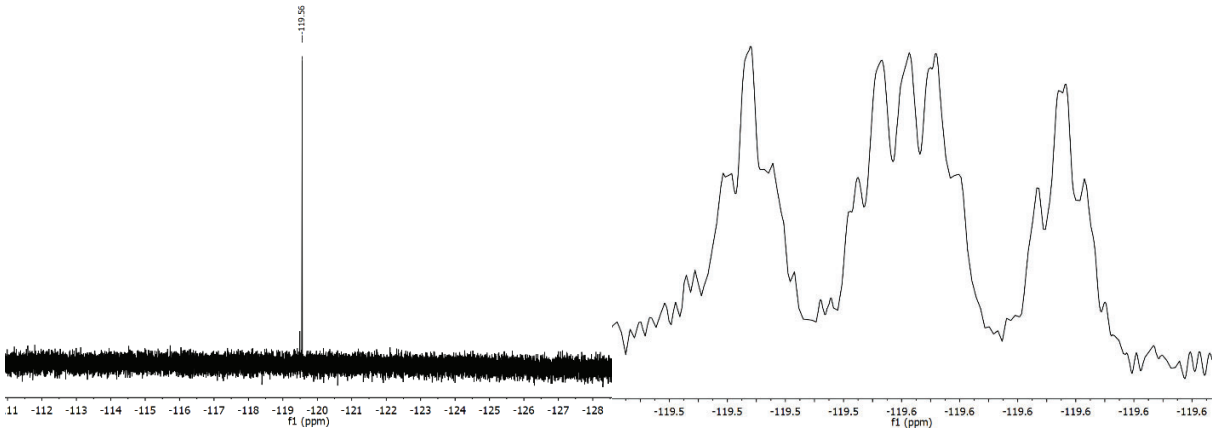

Figure S15. Decoupled (left) and coupled (right) ^{19}F NMR spectra of the Flurbiprofen-PEG monoester with a chain length of n = 3 (acquired from synthetic samples).

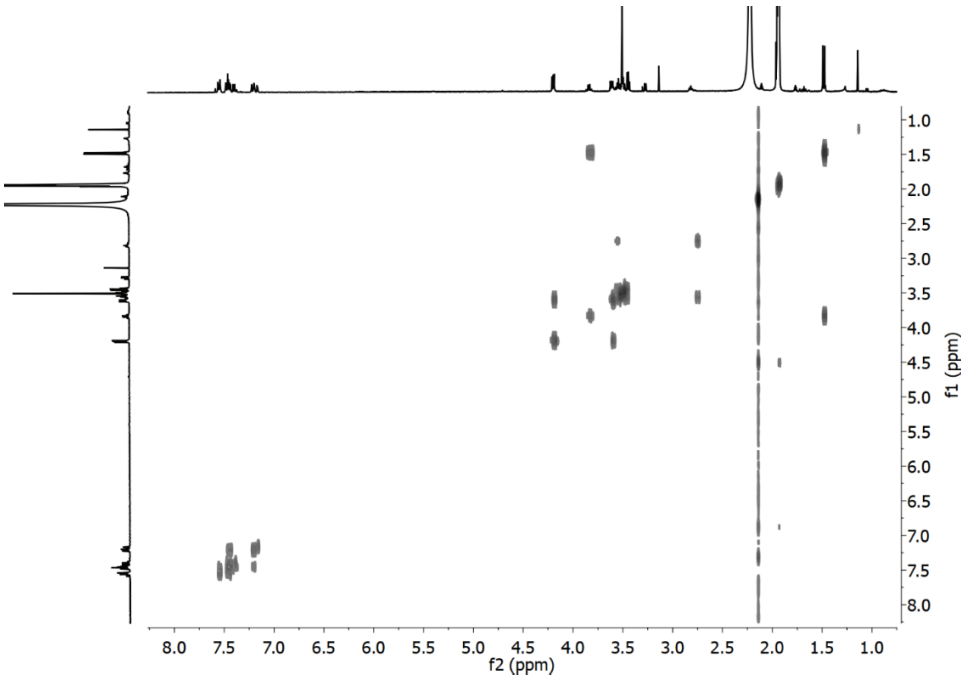

Figure S16. ^{1}H-^{1}H COSY NMR spectrum of the Flurbiprofen-PEG monoester with a chain length of n = 3 (acquired from synthetic samples).

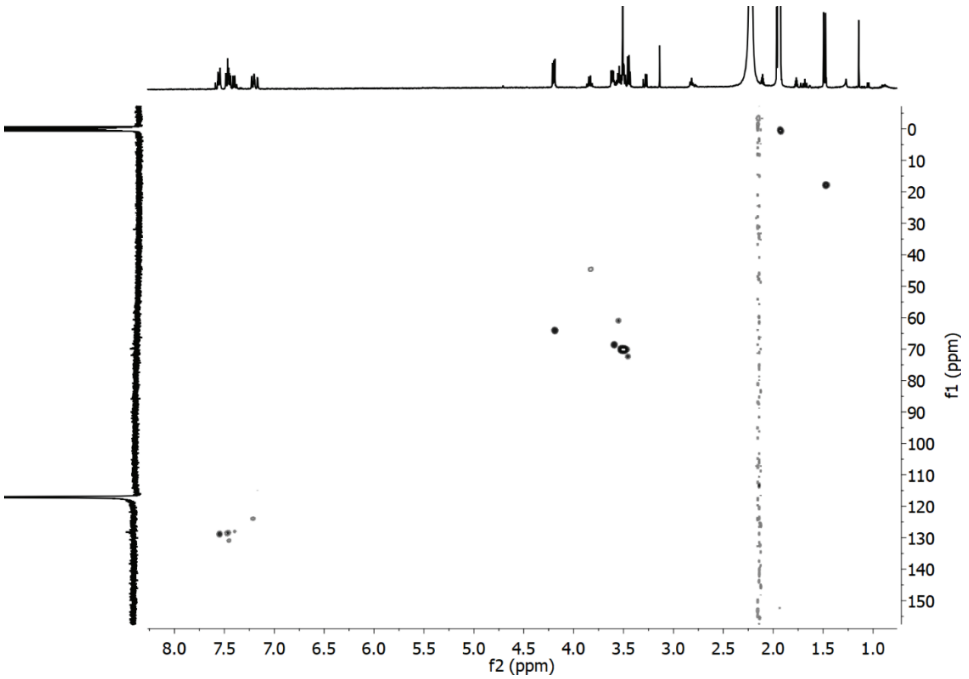

Figure S17. ^{1}H-^{13}C HSQC NMR spectrum of the Flurbiprofen-PEG monoester with a chain length of n = 3 (acquired from synthetic samples).

IV.I.II NMR Spectra of Monoester n = 4

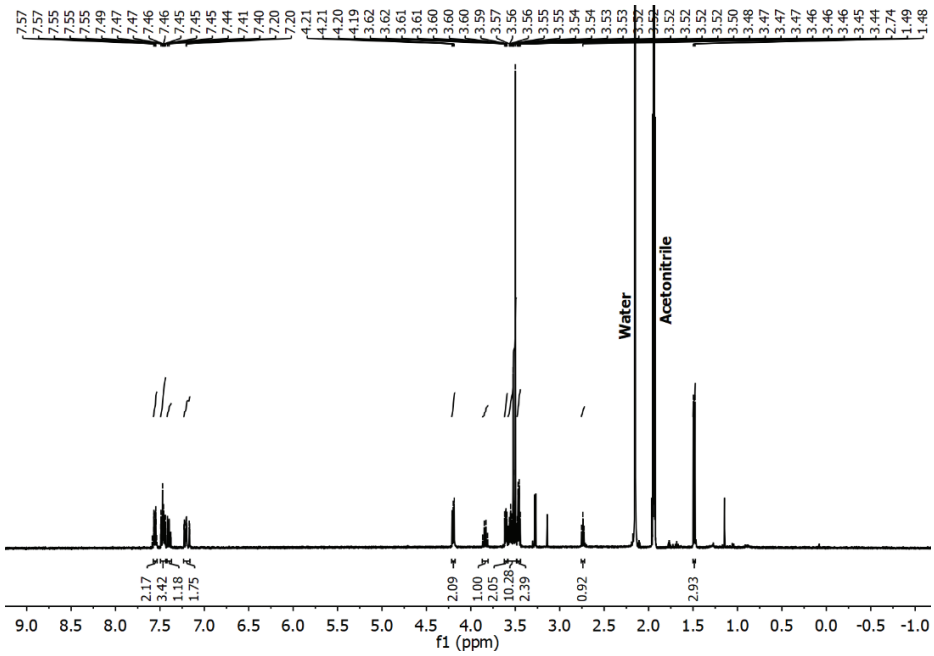

Figure S18. ^{1}H NMR spectrum of the Flurbiprofen-PEG monoester with a chain length of n = 4 (acquired from synthetic samples).

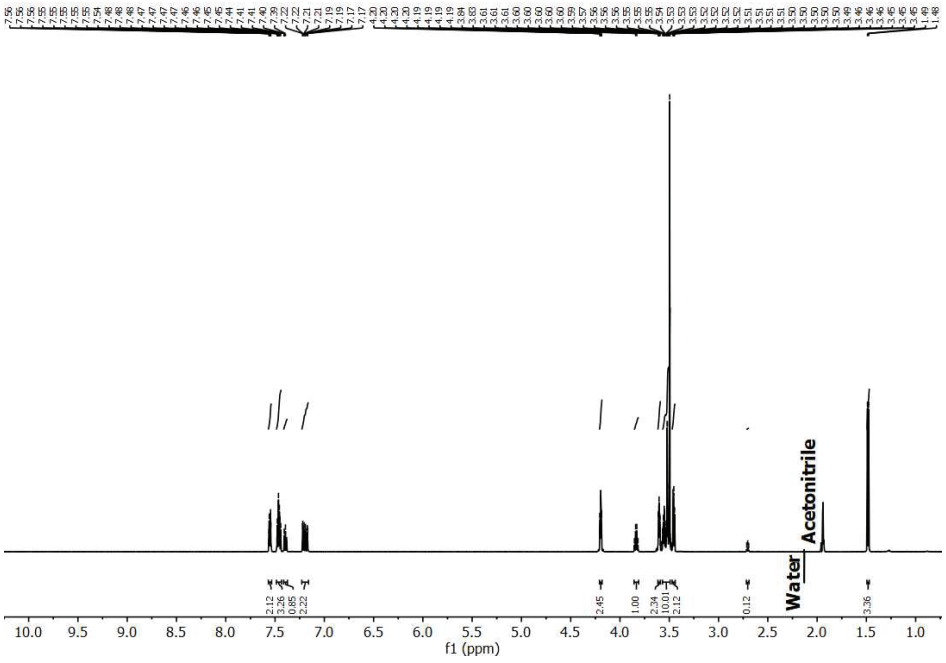

Figure S19. ^{1}H NMR spectrum of the Flurbiprofen-PEG monoester with a chain length of n = 4 (acquired from lozenge-extracts).

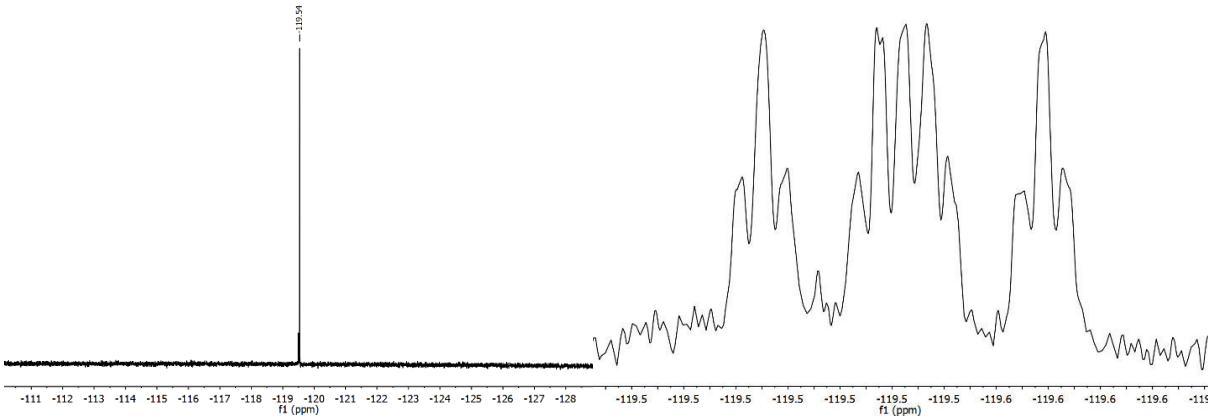

Figure S20. Decoupled (left) and coupled (right) ^{19}F NMR spectra of the Flurbiprofen-PEG monoester with a chain length of n = 4 (acquired from synthetic samples).

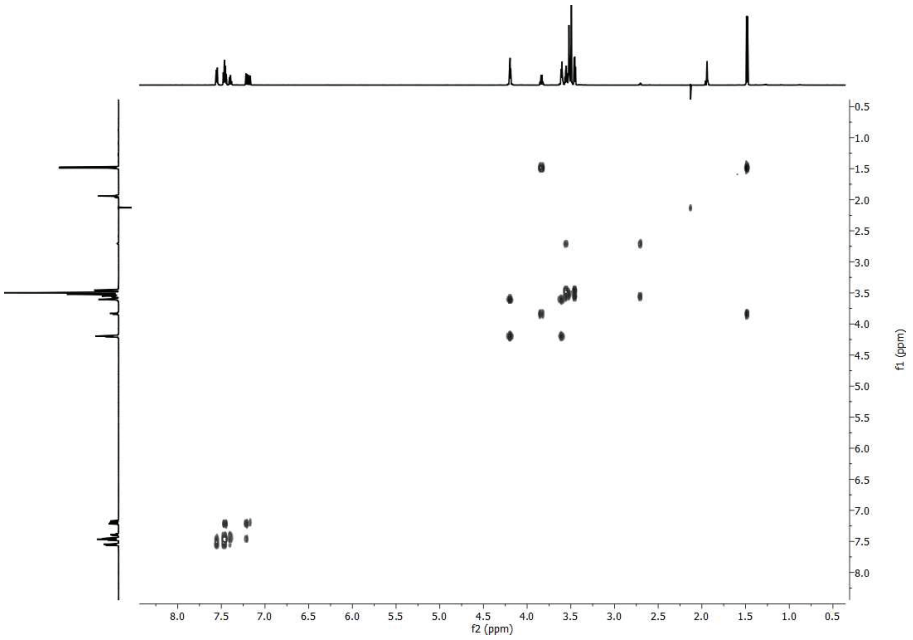

Figure S21. ^{1}H-^{1}H COSY NMR spectrum of the Flurbiprofen-PEG monoester with a chain length of n = 4 (acquired from lozenge-extracts).

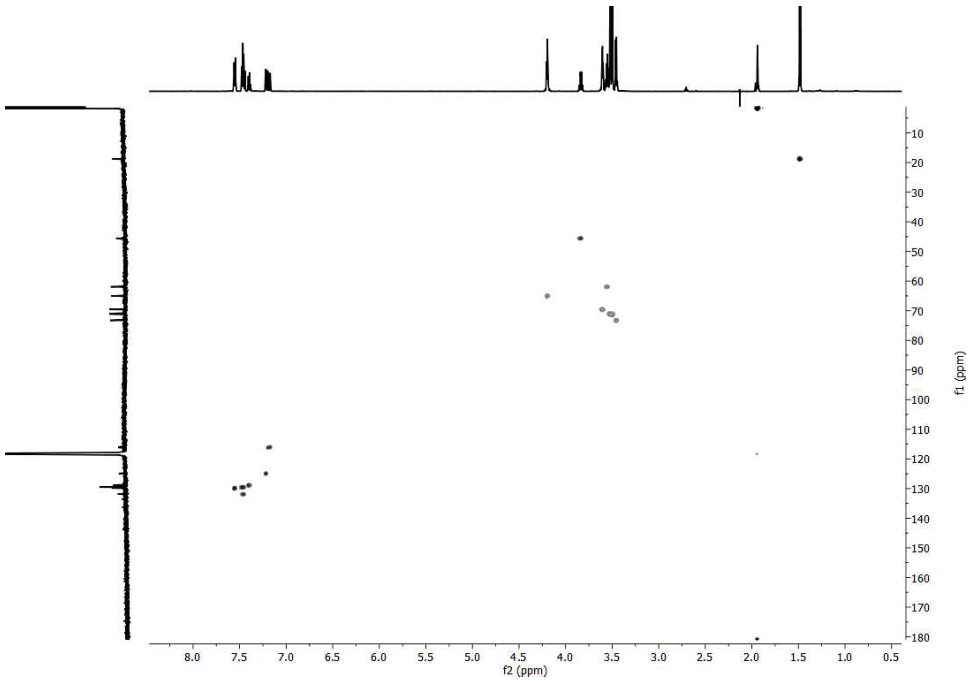

Figure S22. ^{1}H-^{13}C HSQC NMR spectrum of the Flurbiprofen-PEG monoester with a chain length of n = 4 (acquired from lozenge-extracts).

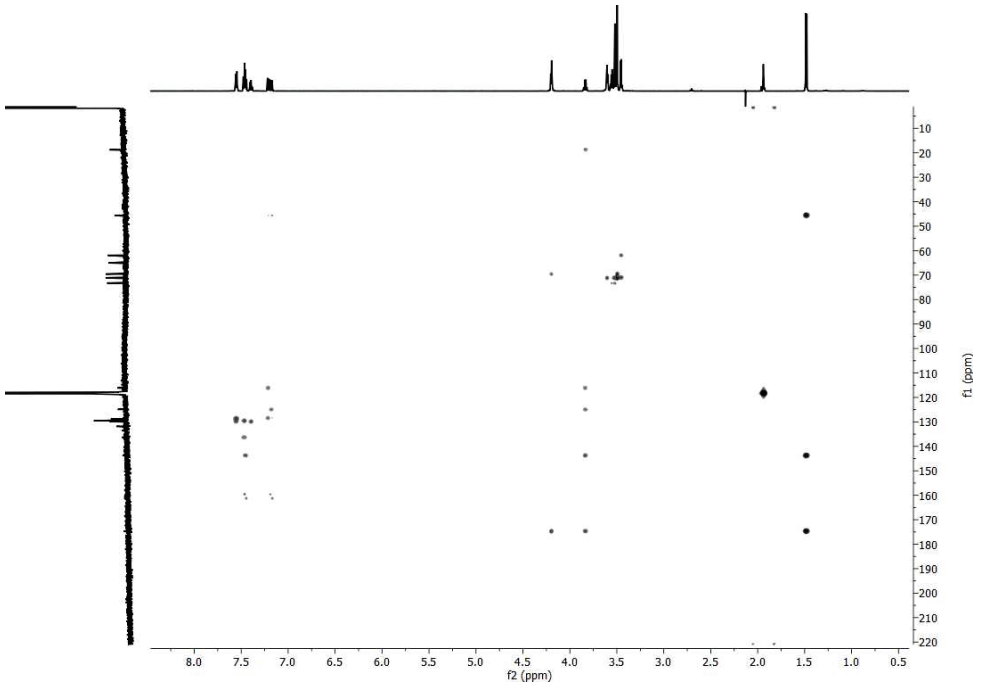

Figure S23. ^{1}H-^{13}C HMBC NMR spectrum of the Flurbiprofen-PEG monoester with a chain length of n = 4 (acquired from lozenge-extracts).

IV.I.III NMR Spectra of Monoester n = 5

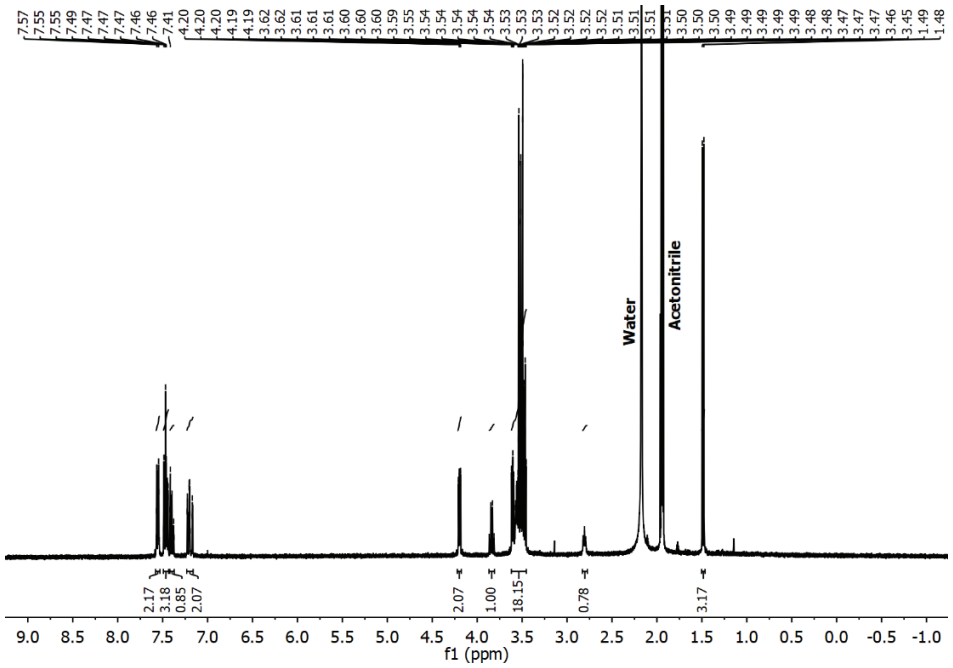

Figure S24. ^{1}H NMR spectrum of the Flurbiprofen-PEG monoester with a chain length of n = 5 (acquired from synthetic samples).

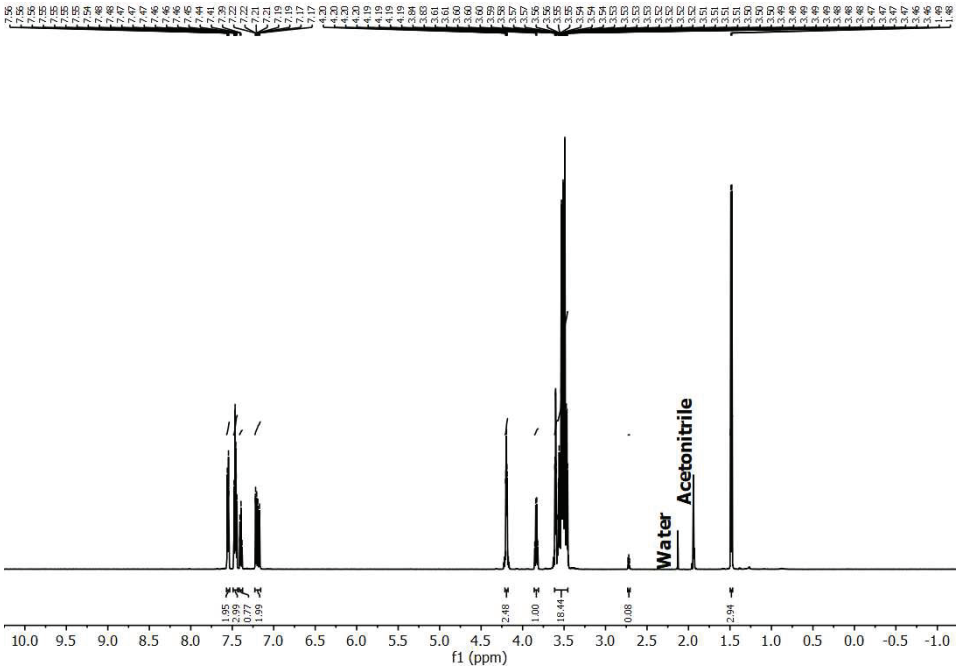

Figure S25. ^{1}H NMR spectrum of the Flurbiprofen-PEG monoester with a chain length of n = 5 (acquired from lozenge-extracts).

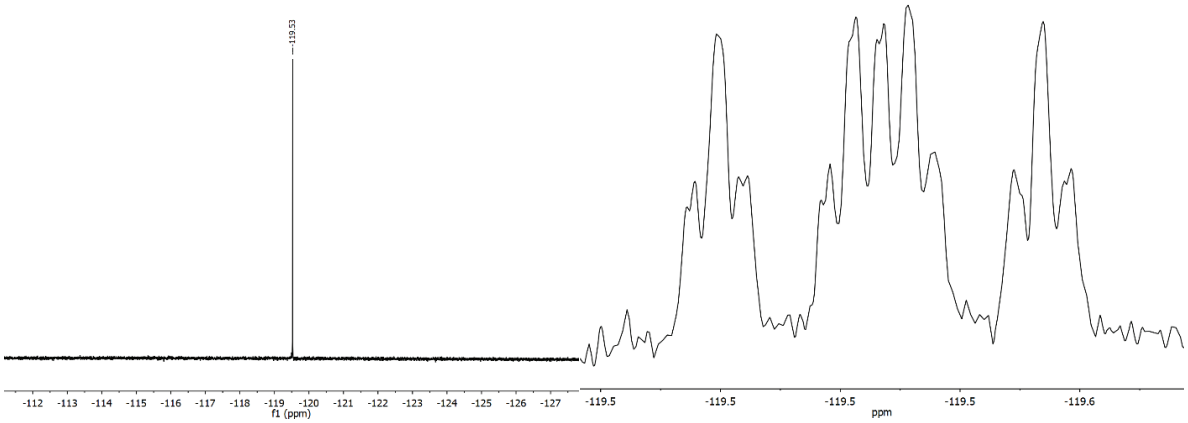

Figure S26. Decoupled (left) and coupled (right) ^{19}F NMR spectra of the Flurbiprofen-PEG monoester with a chain length of n = 5 (acquired from synthetic samples).

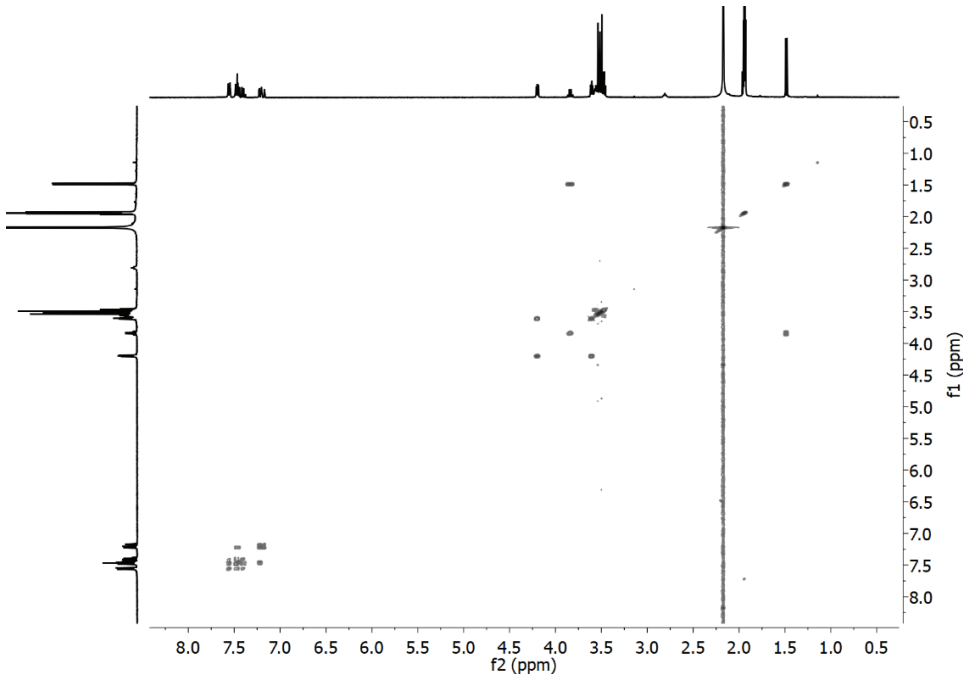

Figure S27. ^{1}H-^{1}H COSY NMR spectrum of the Flurbiprofen-PEG monoester with a chain length of n = 5 (acquired from synthetic samples).

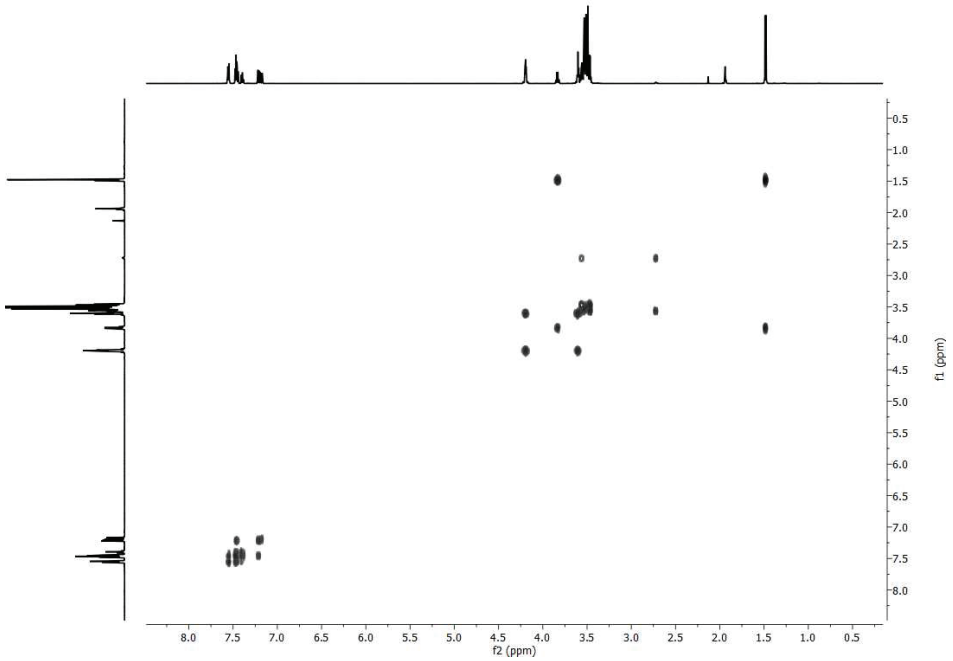

Figure S28. ^{1}H-^{1}H COSY NMR spectrum of the Flurbiprofen-PEG monoester with a chain length of n = 5 (acquired from lozenge-extracts).

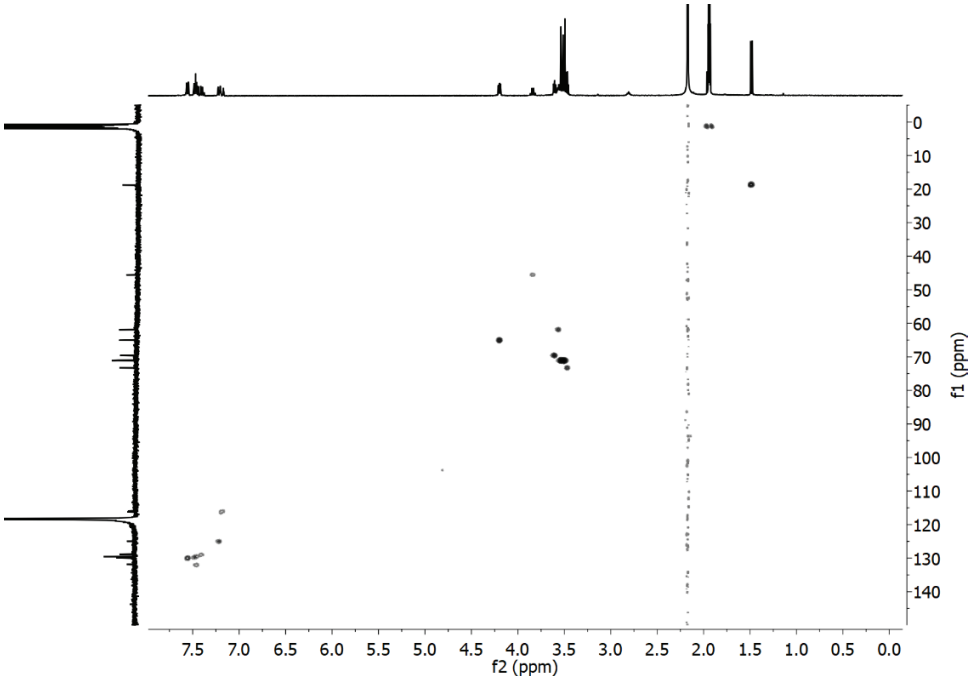

Figure S29. ^{1}H-^{13}C HSQC NMR spectrum of the Flurbiprofen-PEG monoester with a chain length of n = 5 (acquired from synthetic samples).

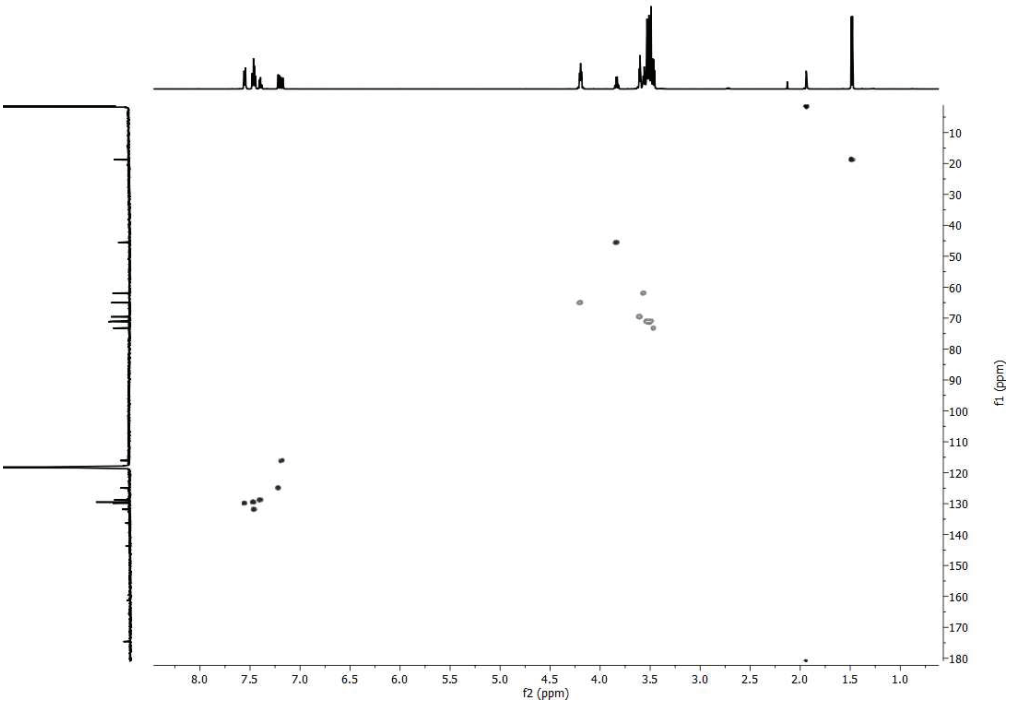

Figure S30. ^{1}H-^{13}C HSQC NMR spectrum of the Flurbiprofen-PEG monoester with a chain length of n = 5 (acquired from lozenge-extracts).

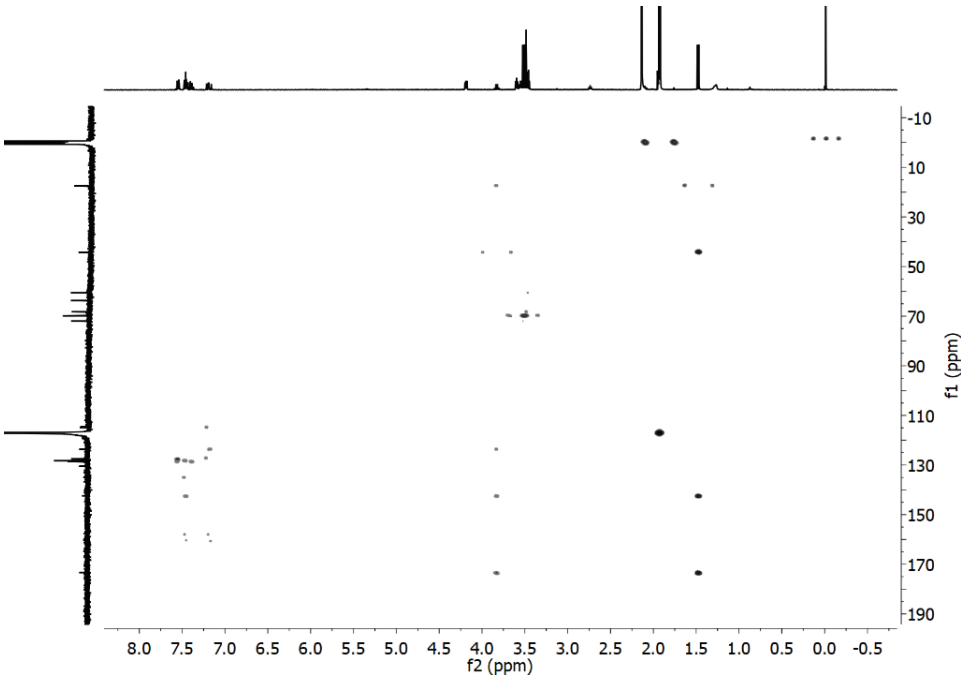

Figure S31. ^{1}H-^{13}C HMBC NMR spectrum of the Flurbiprofen-PEG monoester with a chain length of n = 5 (acquired from synthetic samples).

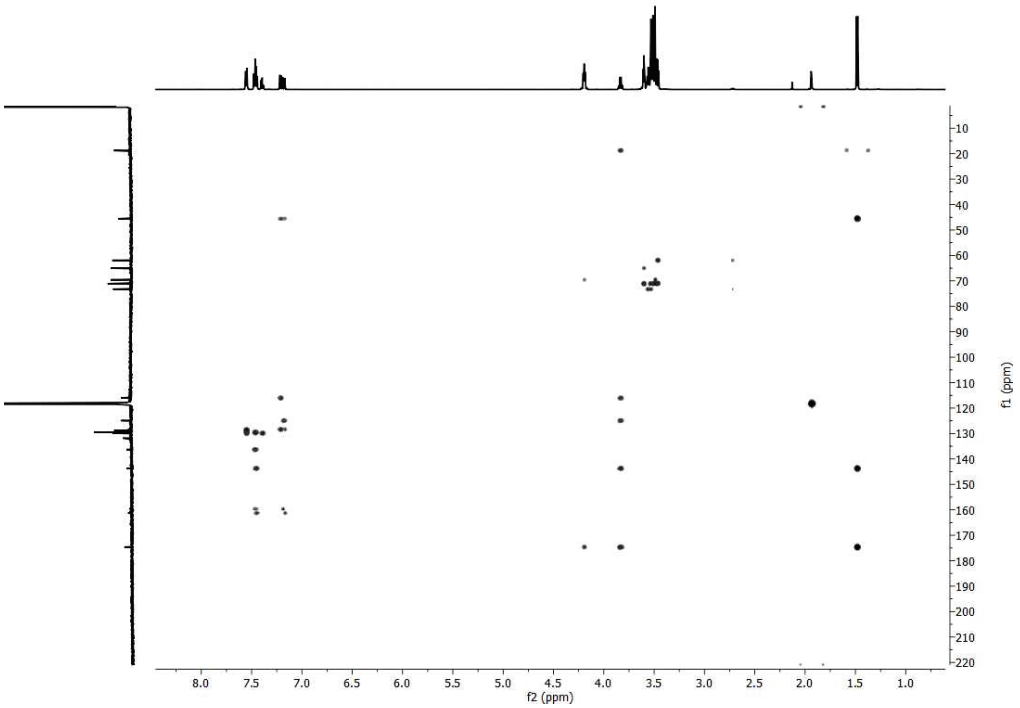

Figure S32. ^{1}H-^{13}C HMBC NMR spectrum of the Flurbiprofen-PEG monoester with a chain length of n = 5 (acquired from lozenge-extracts).

IV.I.IV NMR Spectra of Monoester n = 6

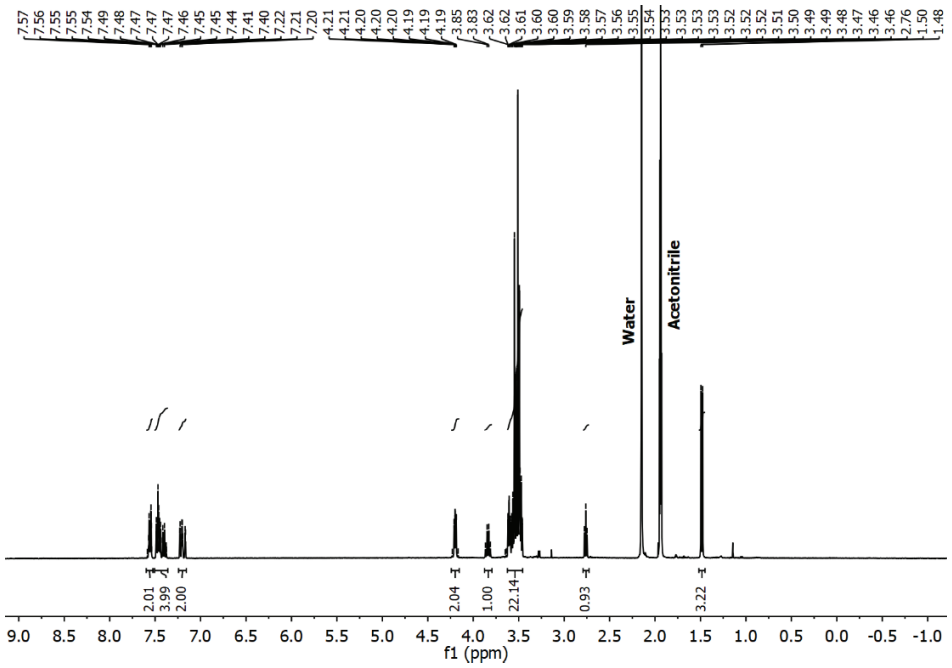

Figure S33. [1]H NMR spectrum of the Flurbiprofen-PEG monoester with a chain length of n = 6 (acquired from synthetic samples).

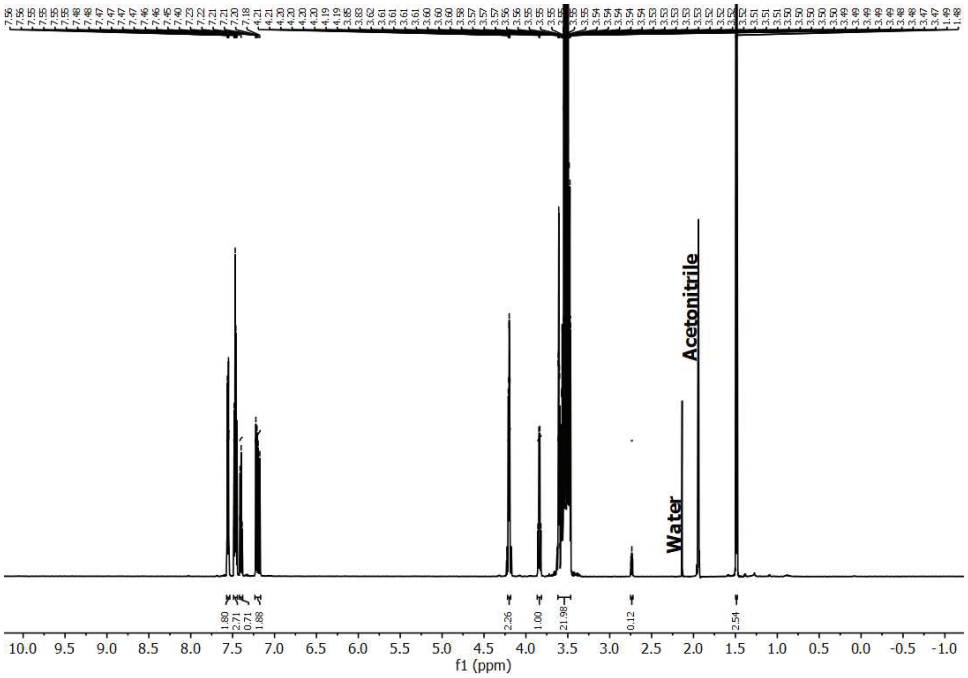

Figure S34. [1]H NMR spectrum of the Flurbiprofen-PEG monoester with a chain length of n = 6 (acquired from lozenge-extracts).

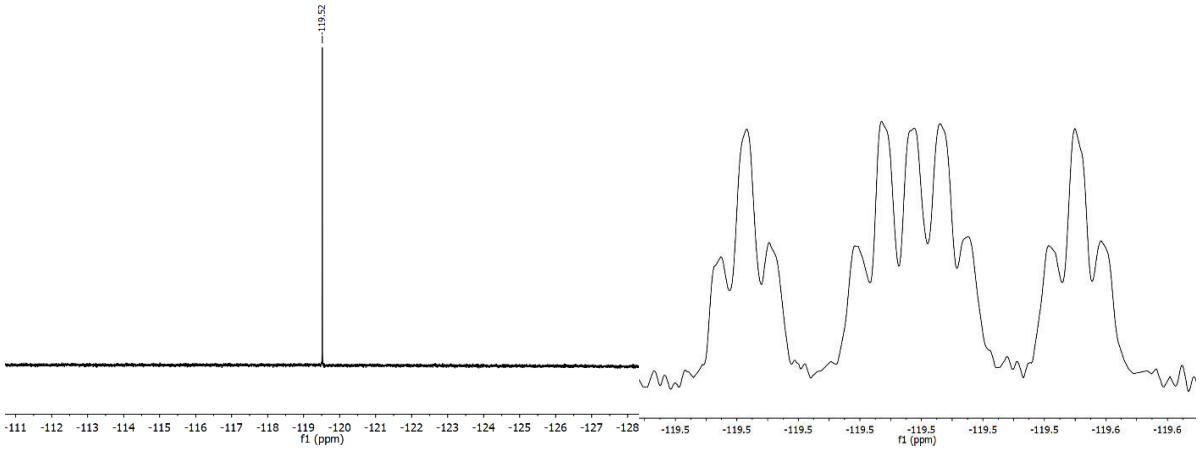

Figure S35. Decoupled (left) and coupled (right) ^{19}F NMR spectra of the Flurbiprofen-PEG monoester with a chain length of n = 6 (acquired from synthetic samples).

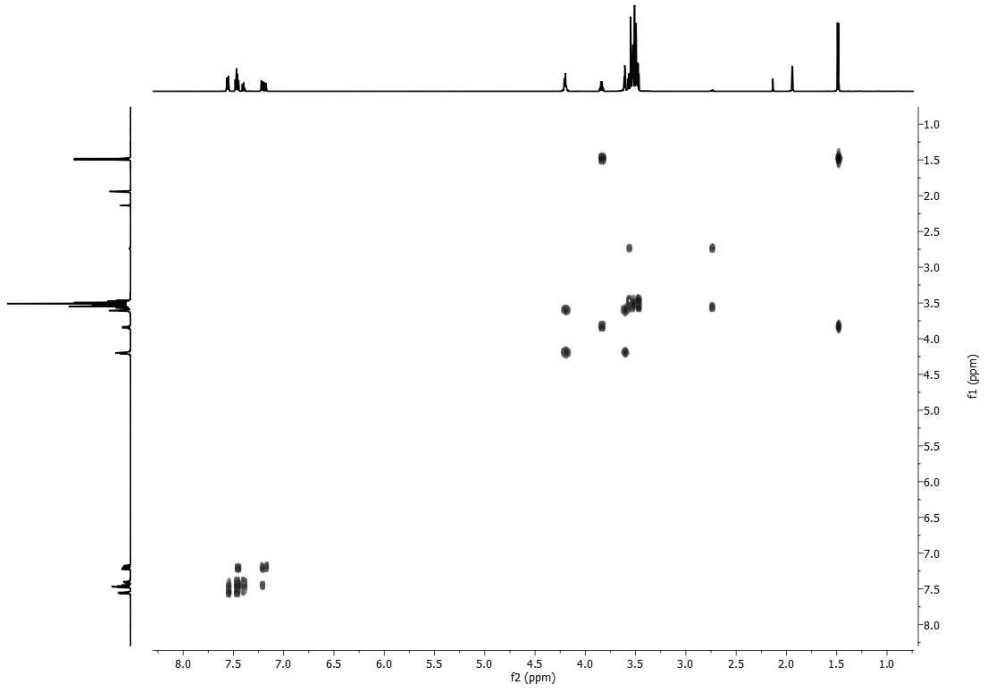

Figure S36. ^{1}H-^{1}H COSY NMR spectrum of the Flurbiprofen-PEG monoester with a chain length of n = 6 (acquired from lozenge-extracts).

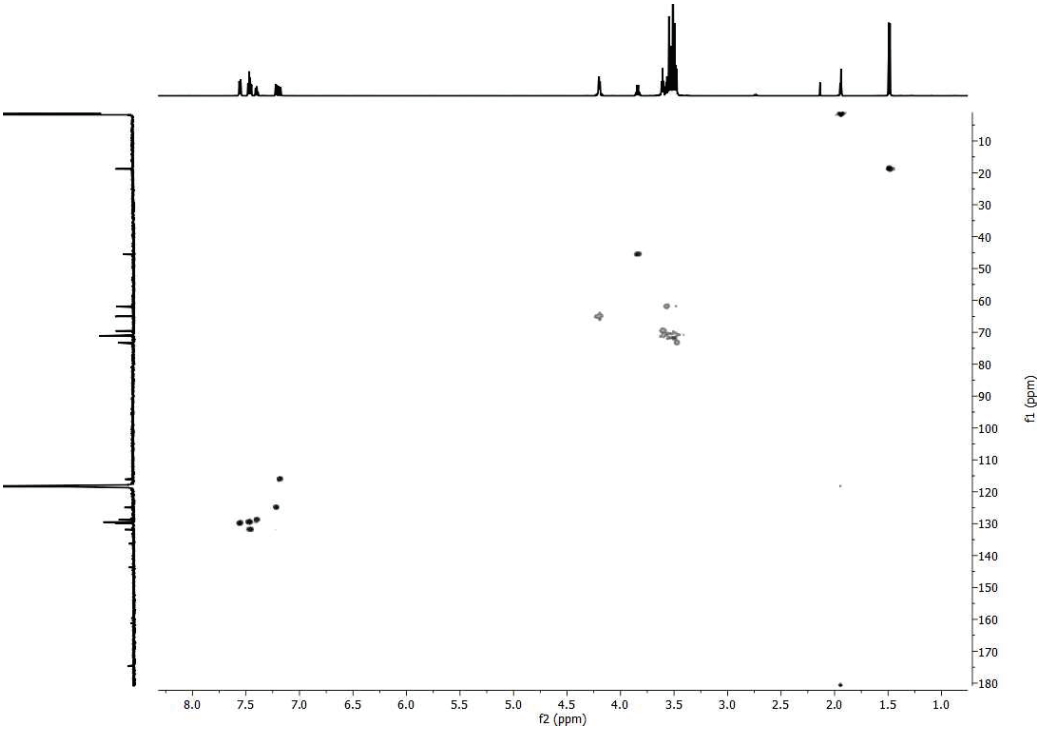

Figure S37. ^{1}H-^{13}C HSQC NMR spectrum of the Flurbiprofen-PEG monoester with a chain length of n = 6 (acquired from lozenge-extracts).

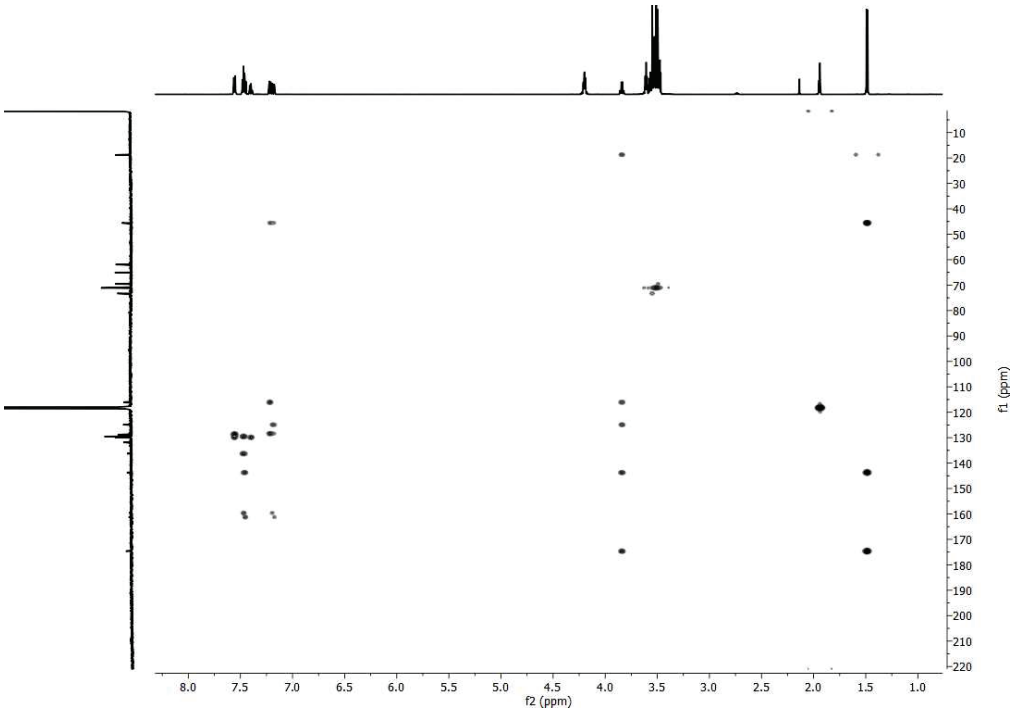

Figure S38. ^{1}H-^{13}C HMBC NMR spectrum of the Flurbiprofen-PEG monoester with a chain length of n = 6 (acquired from lozenge-extracts).

IV.I.V NMR Spectra of Monoester n = 7

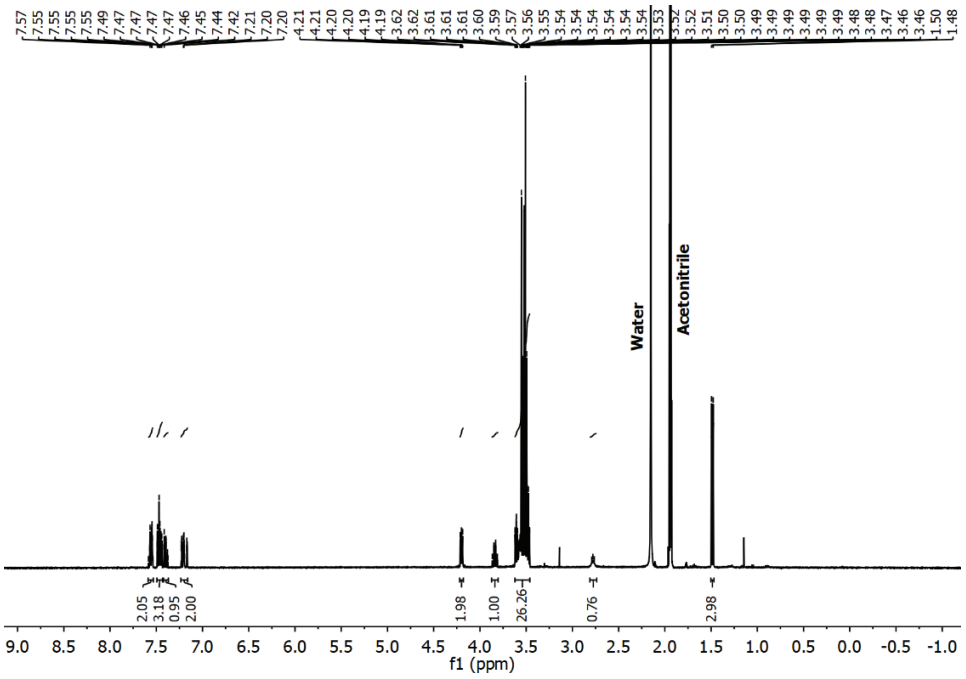

Figure S39. [1]H NMR spectrum of the Flurbiprofen-PEG monoester with a chain length of n = 7 (acquired from synthetic samples).

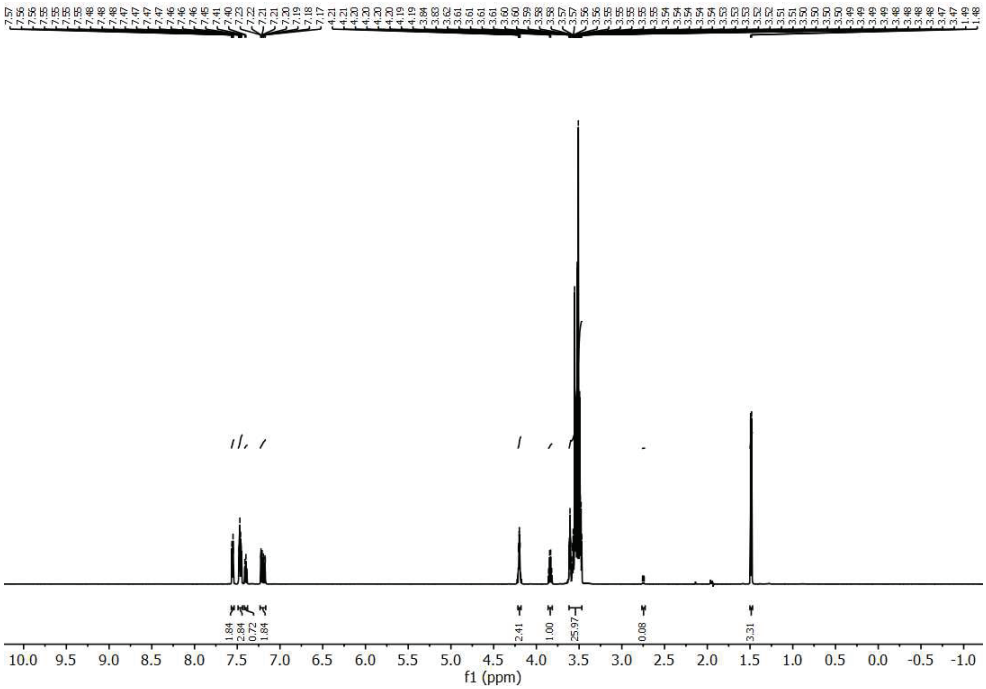

Figure S40. [1]H NMR spectrum of the Flurbiprofen-PEG monoester with a chain length of n = 7 (acquired from lozenge-extracts).

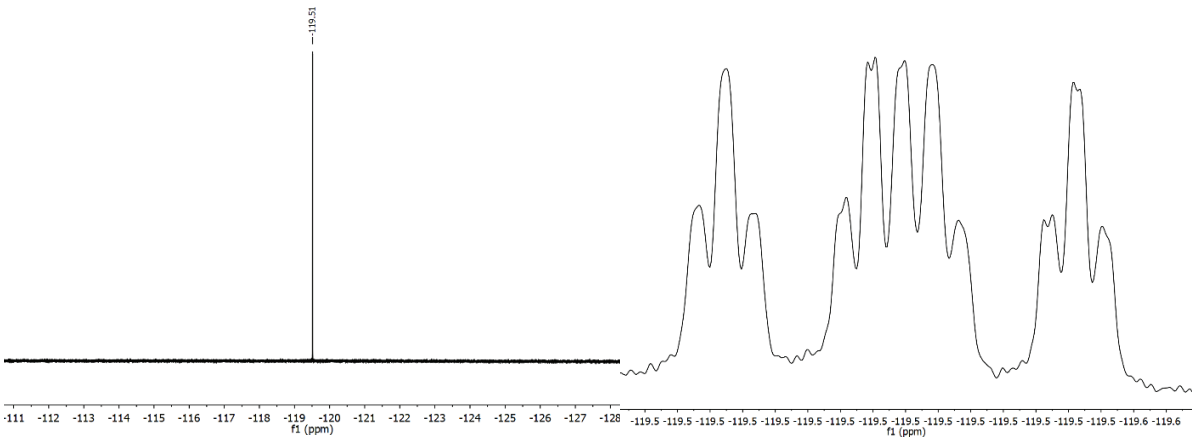

Figure S41. Decoupled (left) and coupled (right) ^{19}F NMR spectra of the Flurbiprofen-PEG monoester with a chain length of n = 7 (acquired from synthetic samples).

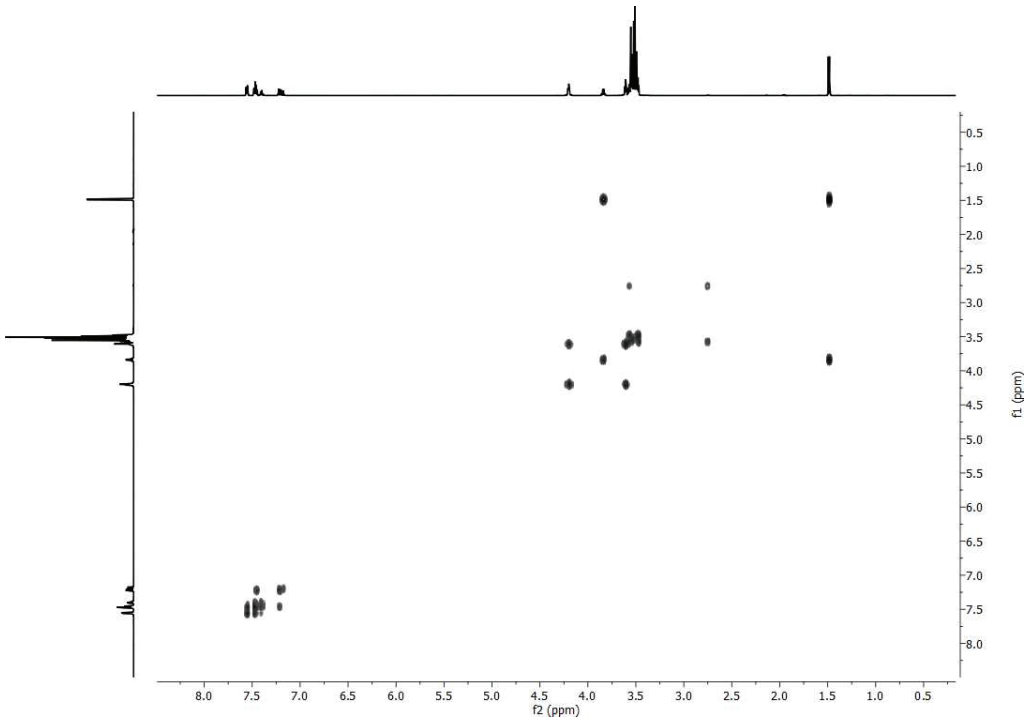

Figure S42. ^{1}H-^{1}H COSY NMR spectrum of the Flurbiprofen-PEG monoester with a chain length of n = 7 (acquired from lozenge-extracts).

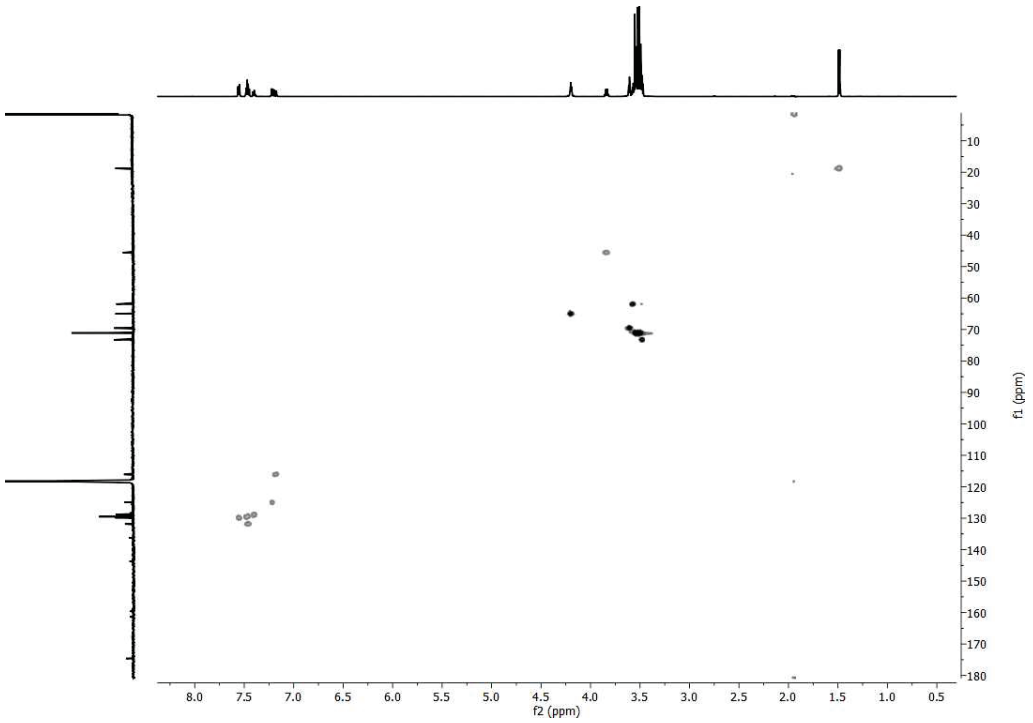

Figure S43. ^{1}H-^{13}C HSQC NMR spectrum of the Flurbiprofen-PEG monoester with a chain length of n = 7 (acquired from lozenge-extracts).

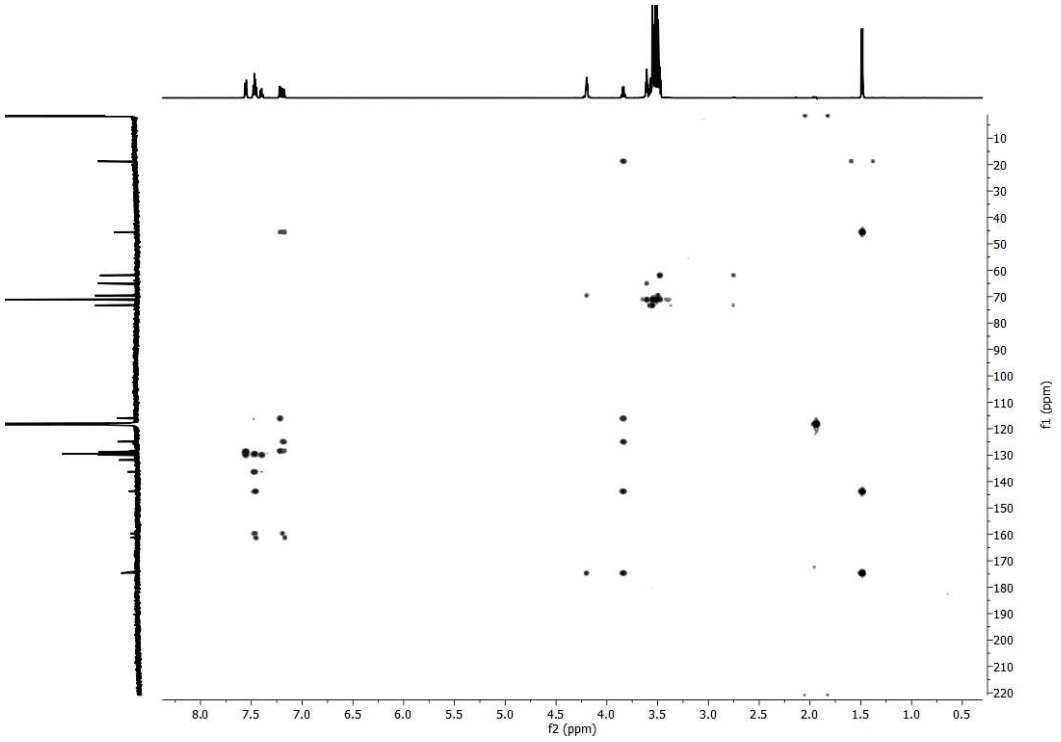

Figure S44. ^{1}H-^{13}C HMBC NMR spectrum of the Flurbiprofen-PEG monoester with a chain length of n = 7 (acquired from lozenge-extracts).

IV.I.VI NMR Spectra of Monoester n = 8

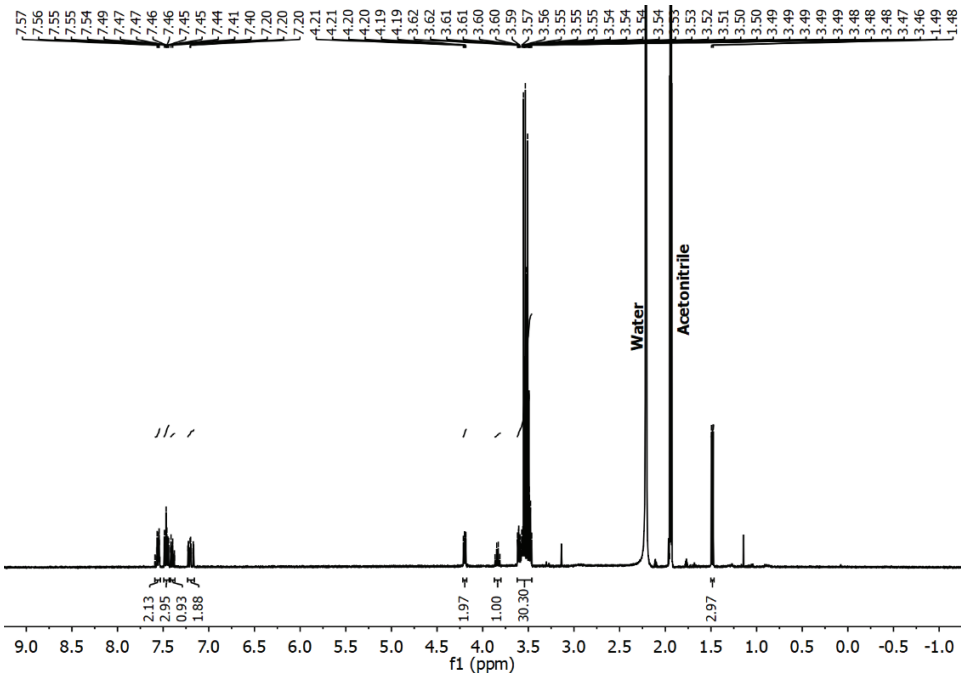

Figure S45. ^{1}H NMR spectrum of the Flurbiprofen-PEG monoester with a chain length of n = 8 (acquired from synthetic samples).

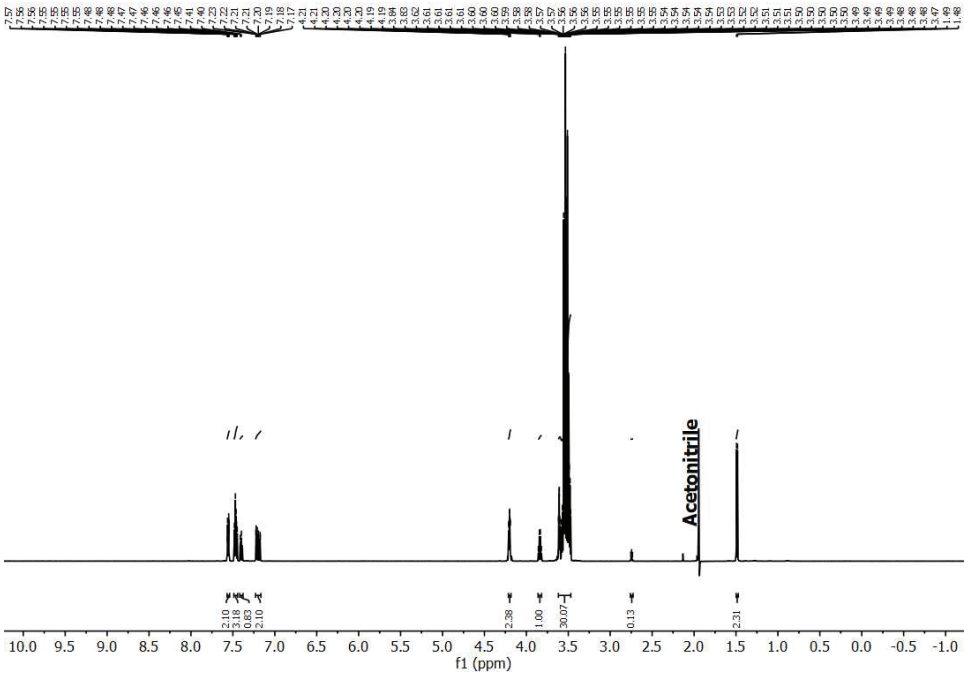

Figure S46. ^{1}H NMR spectrum of the Flurbiprofen-PEG monoester with a chain length of n = 8 (acquired from lozenge-extracts).

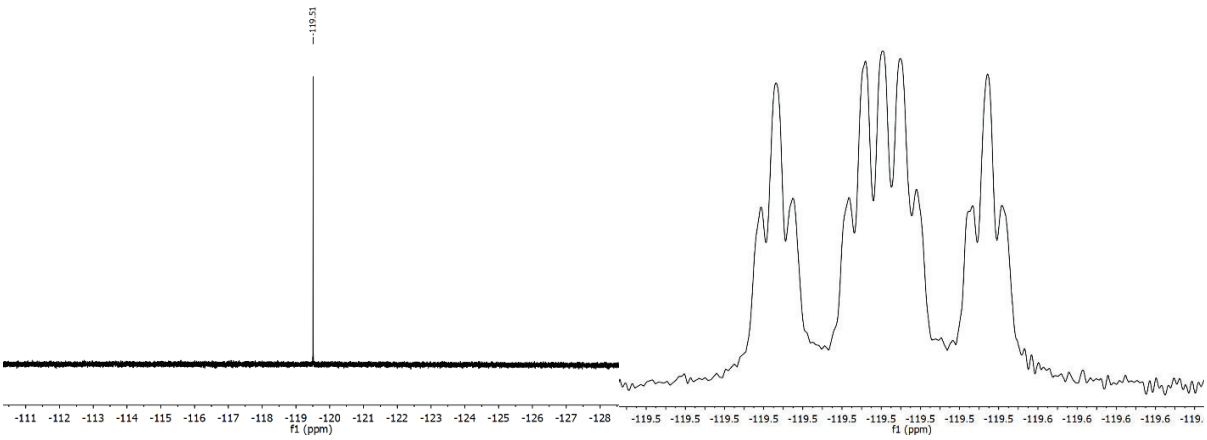

Figure S47. Decoupled (left) and coupled (right) ^{19}F NMR spectra of the Flurbiprofen-PEG monoester with a chain length of n = 8 (acquired from synthetic samples).

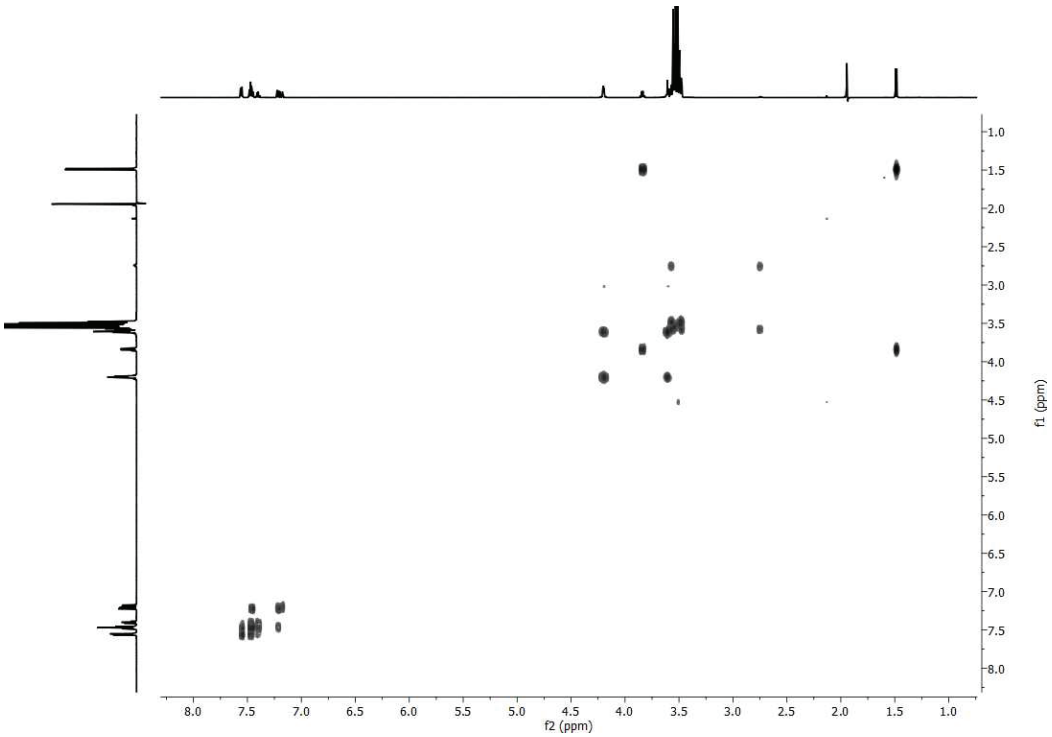

Figure S48. ^{1}H-^{1}H COSY NMR spectrum of the Flurbiprofen-PEG monoester with a chain length of n = 8 (acquired from lozenge-extracts).

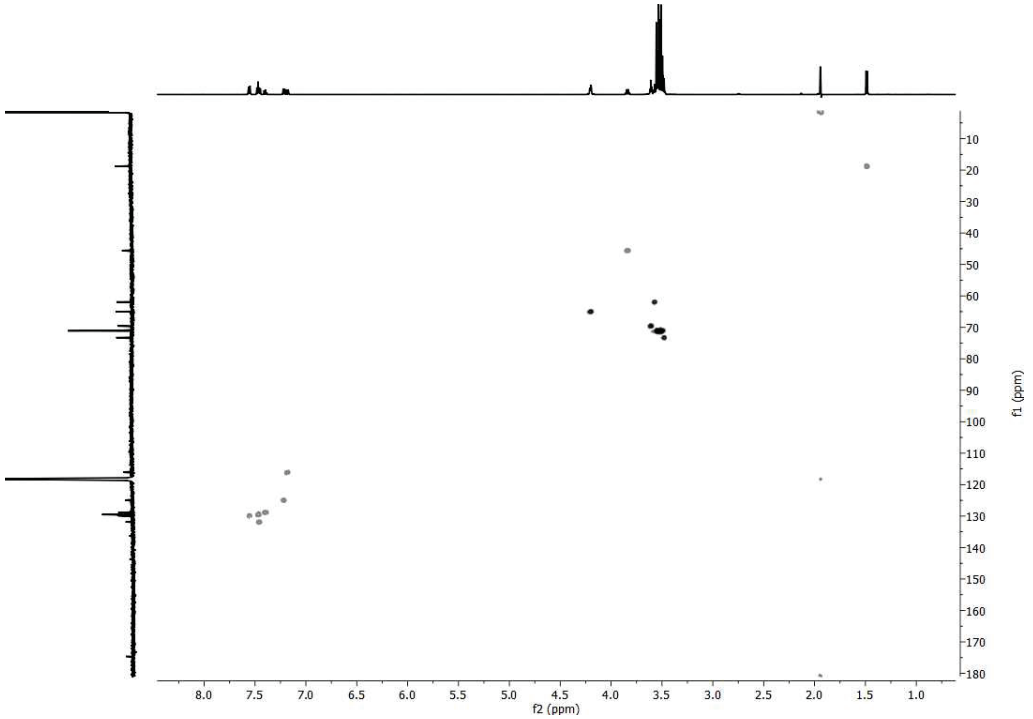

Figure S49. ^{1}H-^{13}C HSQC NMR spectrum of the Flurbiprofen-PEG monoester with a chain length of n = 8 (acquired from lozenge-extracts).

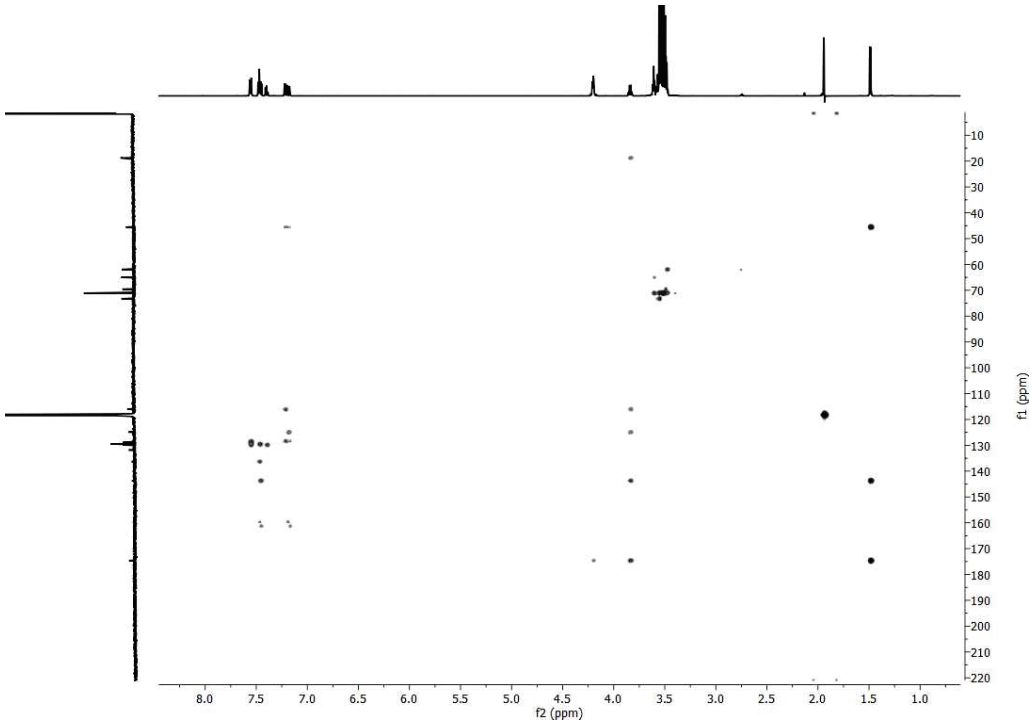

Figure S50. ^{1}H-^{13}C HMBC NMR spectrum of the Flurbiprofen-PEG monoester with a chain length of n = 8 (acquired from lozenge-extracts).

IV.II NMR Spectra of the Flurbiprofen-PEG Diesters

IV.II.I NMR Spectra of Diester n = 3

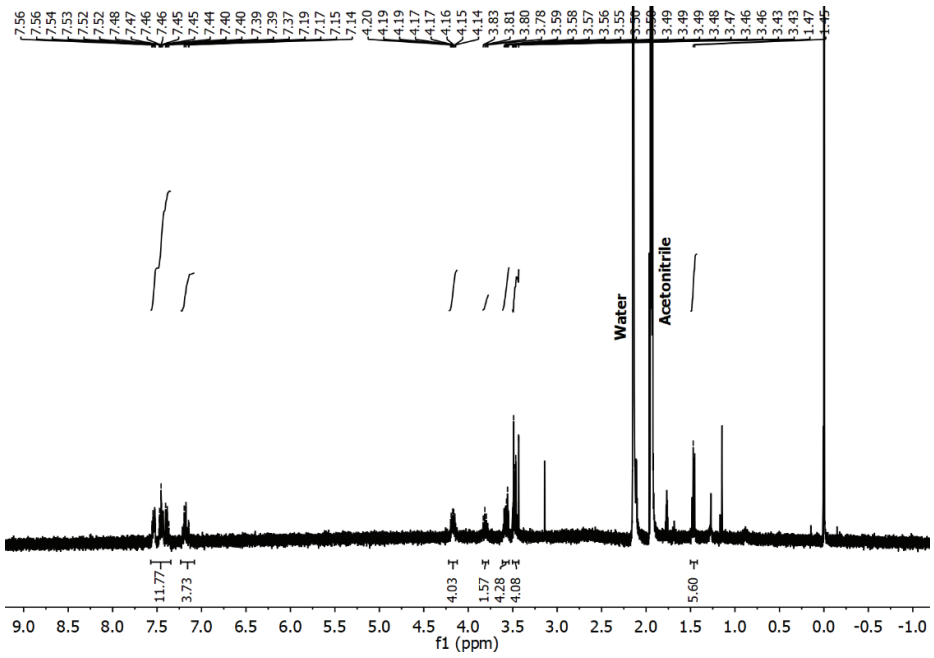

Figure S51. ^{1}H NMR spectrum of the Flurbiprofen-PEG diester with a chain length of n = 3 (acquired from synthetic samples).

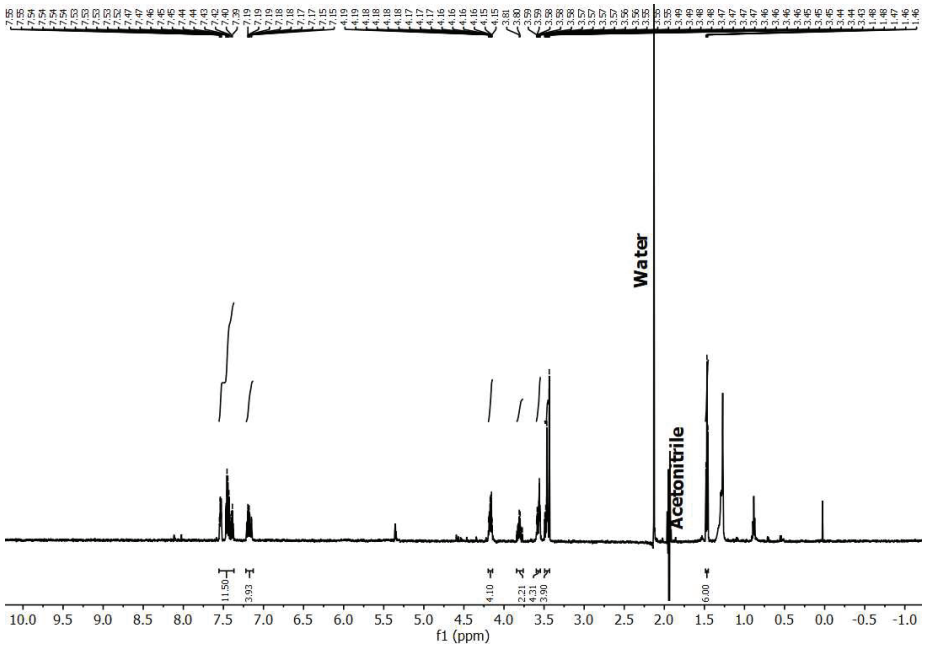

Figure S52. ^{1}H NMR spectrum of the Flurbiprofen-PEG diester with a chain length of n = 3 (acquired from lozenge-extracts).

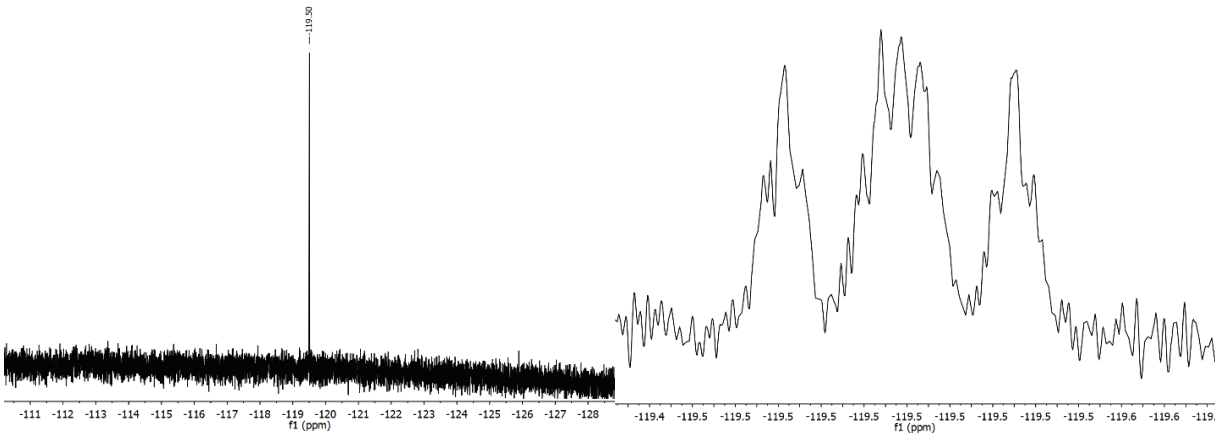

Figure S53. Decoupled (left) and coupled (right) ^{19}F NMR spectra of the Flurbiprofen-PEG diester with a chain length of n = 3 (acquired from synthetic samples).

IV.II.II NMR Spectra of Diester n = 4

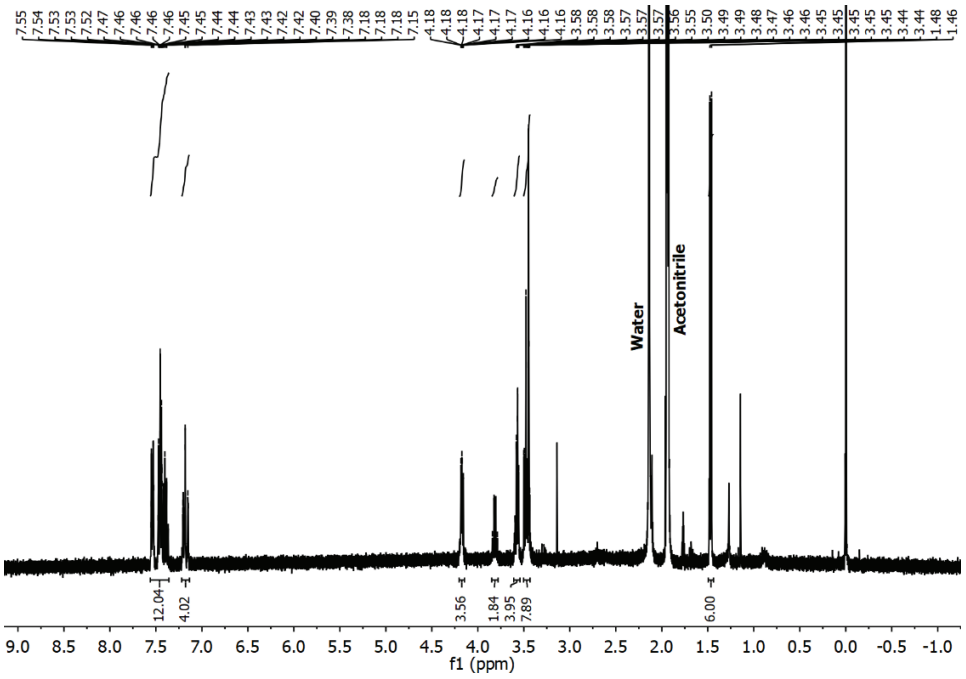

Figure S54. ^{1}H NMR spectrum of the Flurbiprofen-PEG diester with a chain length of n = 4 (acquired from synthetic samples).

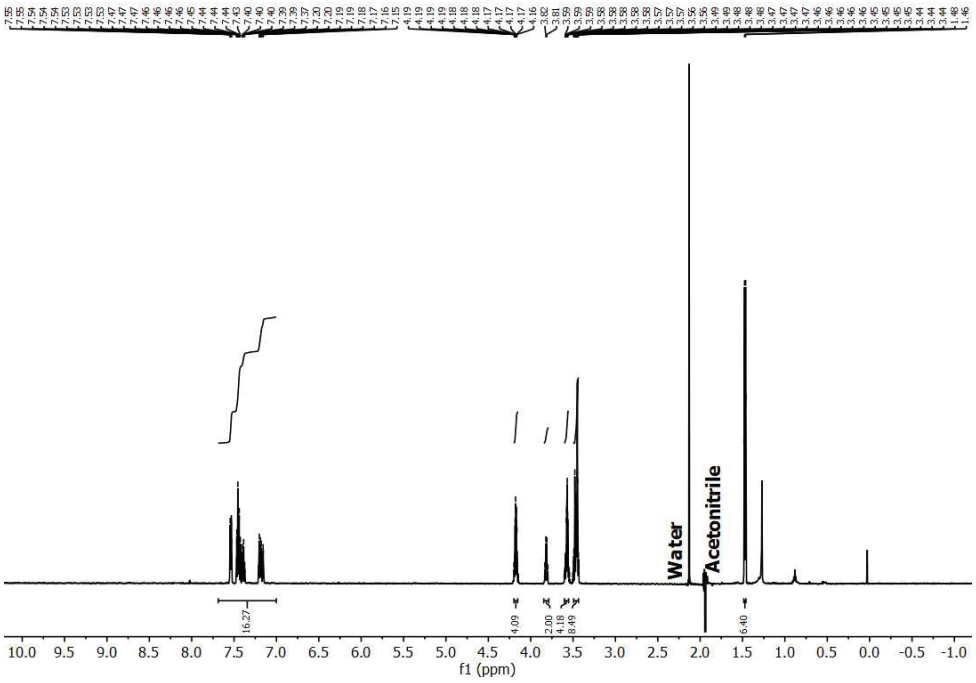

Figure S55. ^{1}H NMR spectrum of the Flurbiprofen-PEG diester with a chain length of n = 4 (acquired from lozenge-extracts).

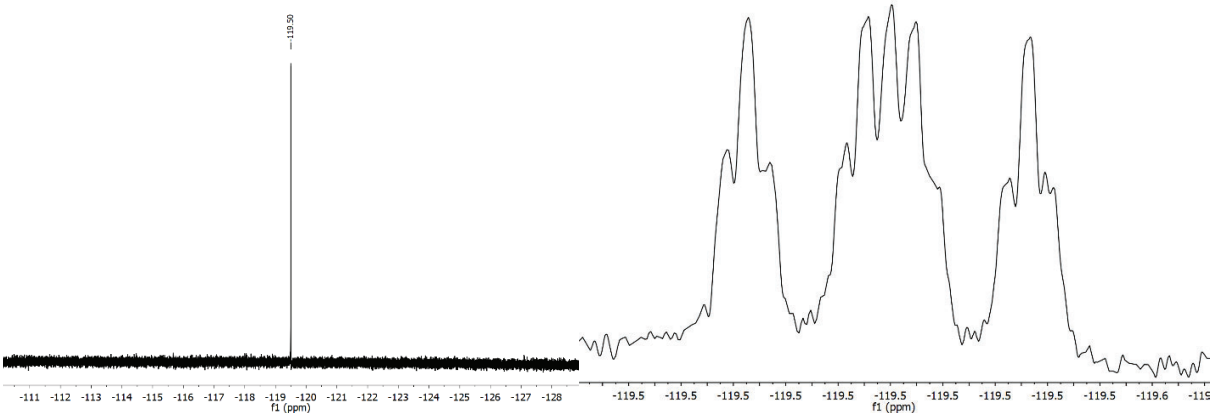

Figure S56. Decoupled (left) and coupled (right) ^{19}F NMR spectra of the Flurbiprofen-PEG diester with a chain length of n = 4 (acquired from synthetic samples).

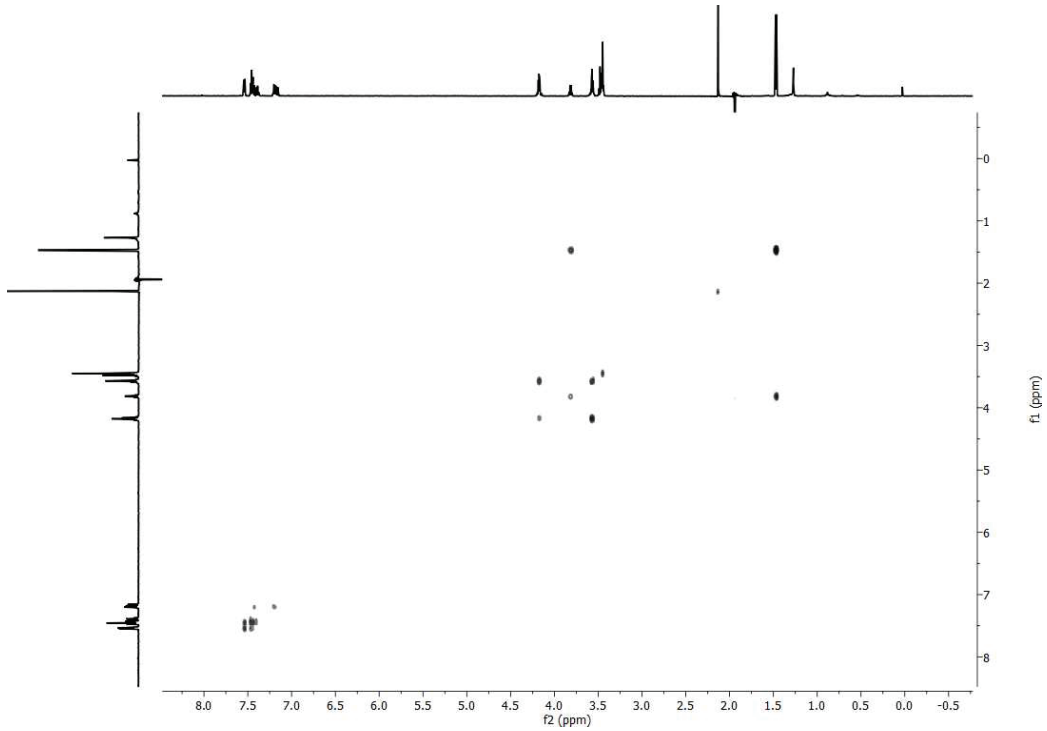

Figure S57. ^{1}H-^{1}H COSY NMR spectrum of the Flurbiprofen-PEG diester with a chain length of n = 4 (acquired from lozenge-extracts).

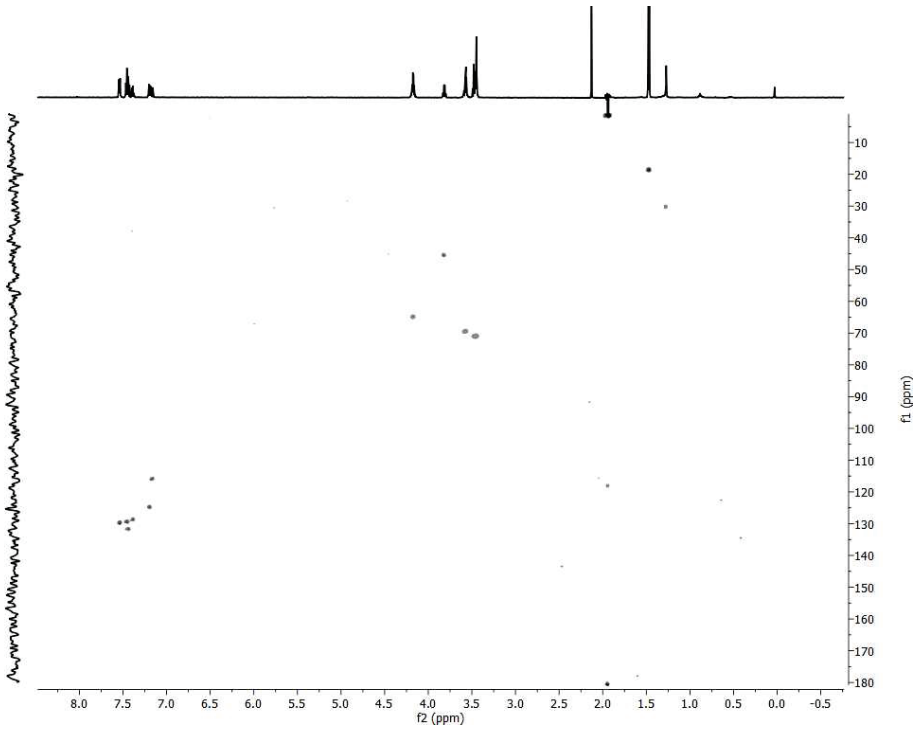

Figure S58. ^{1}H-^{13}C HSQC NMR spectrum of the Flurbiprofen-PEG diester with a chain length of n = 4 (acquired from lozenge-extracts).

IV.II.III NMR Spectra of Diester n = 5

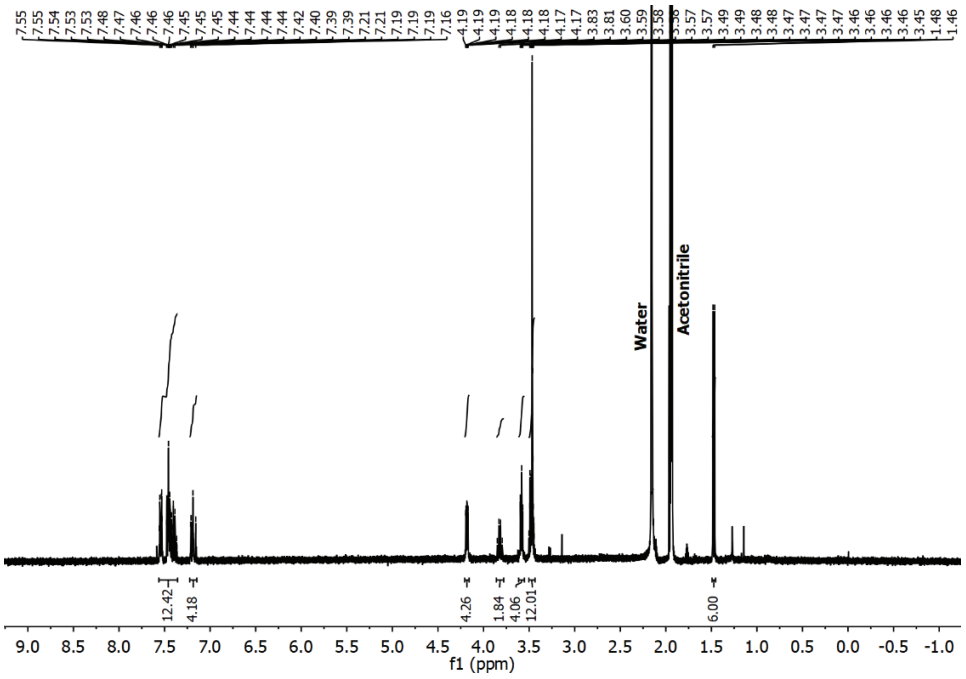

Figure S59. ^{1}H NMR spectrum of the Flurbiprofen-PEG diester with a chain length of n = 5 (acquired from synthetic samples).

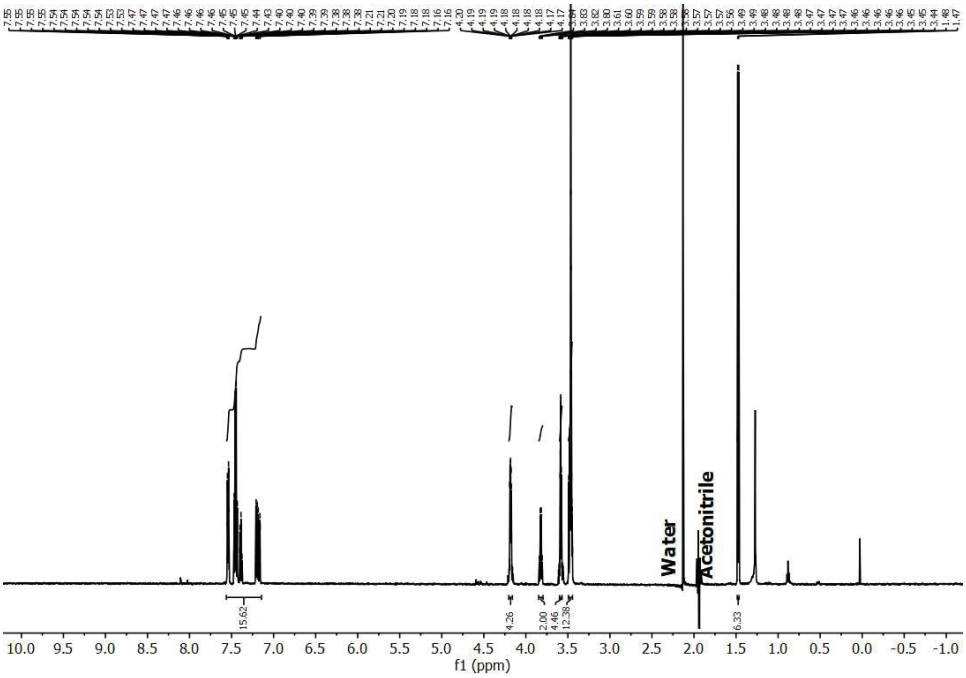

Figure S60. ^{1}H NMR spectrum of the Flurbiprofen-PEG diester with a chain length of n = 5 (acquired from lozenge-extracts).

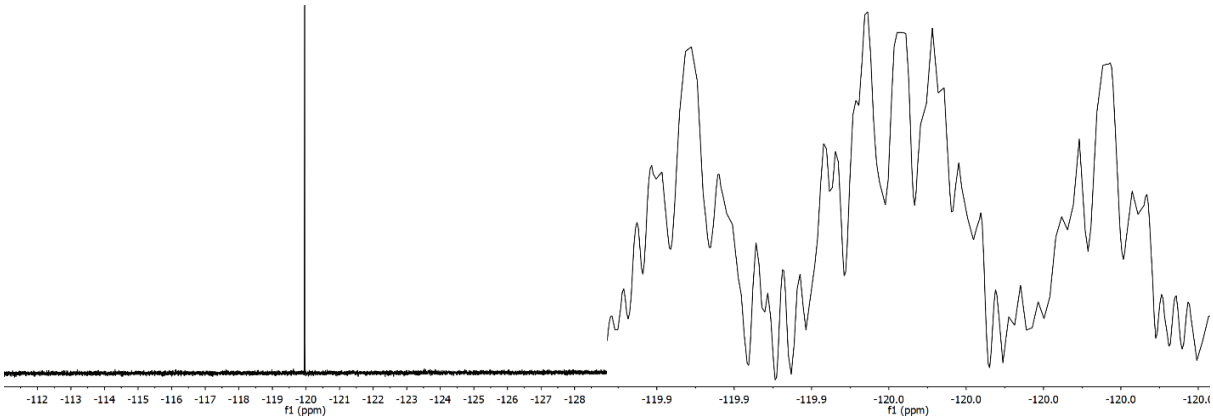

Figure S61. Decoupled (left) and coupled (right) ^{19}F NMR spectra of the Flurbiprofen-PEG diester with a chain length of n = 5 (acquired from synthetic samples).

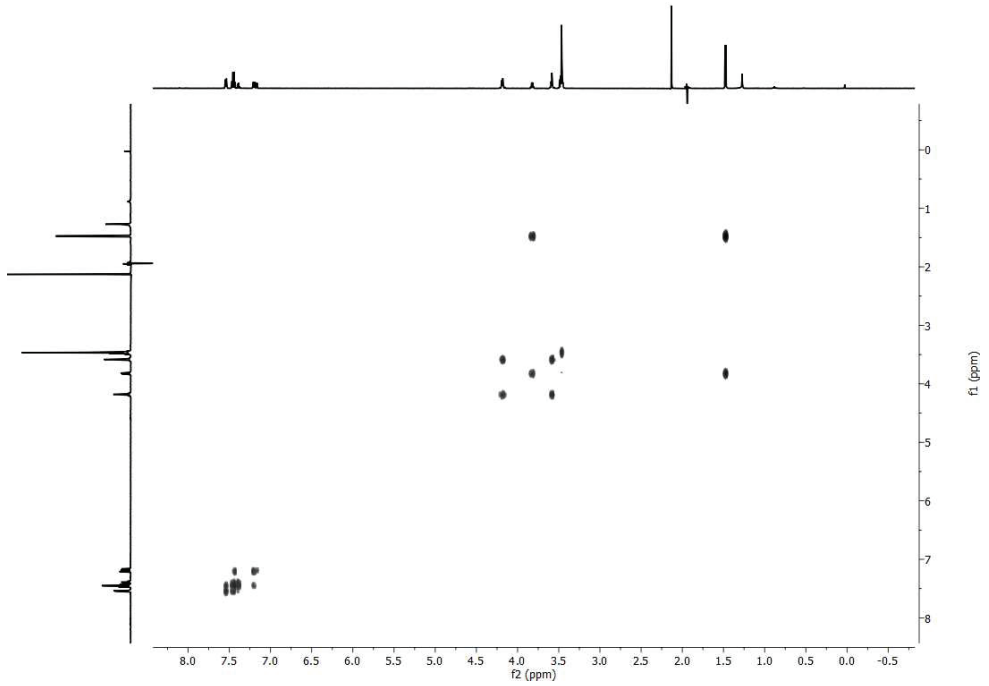

Figure S62. ^{1}H-^{1}H COSY NMR spectrum of the Flurbiprofen-PEG diester with a chain length of n = 5 (acquired from lozenge-extracts).

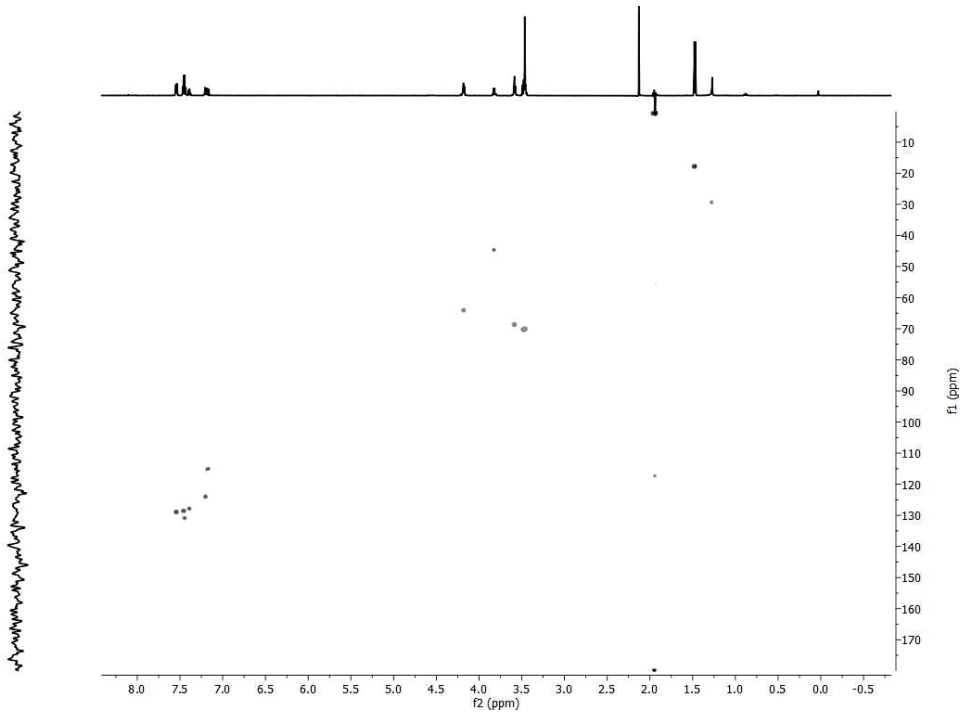

Figure S63. ^{1}H-^{13}C HSQC NMR spectrum of the Flurbiprofen-PEG diester with a chain length of n = 5 (acquired from lozenge-extracts).

IV.II.IV NMR Spectra of Diester n = 6

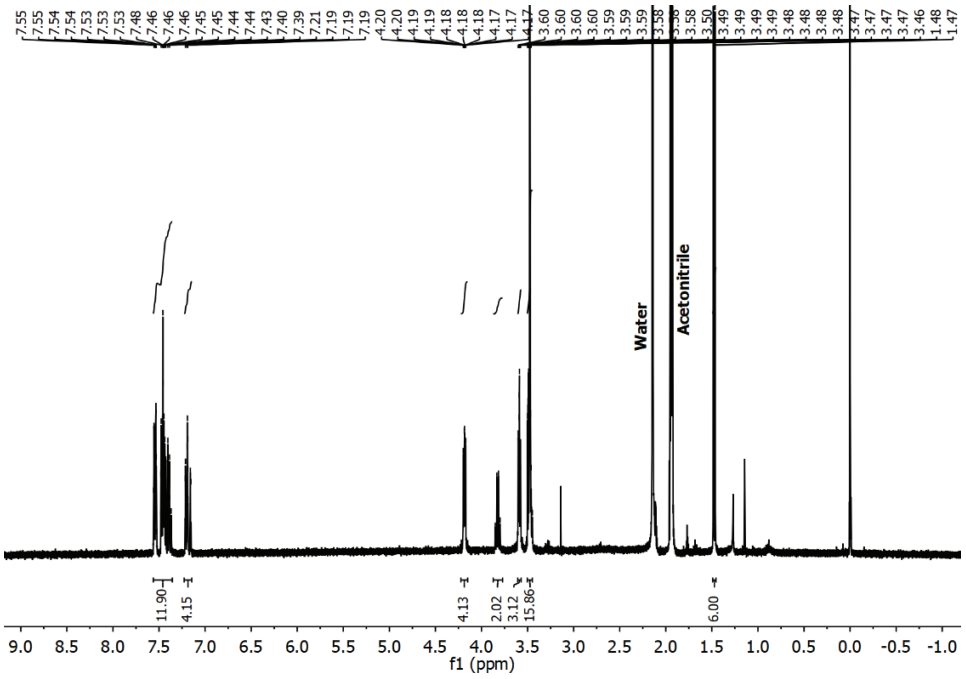

Figure S64. ^{1}H NMR spectrum of the Flurbiprofen-PEG diester with a chain length of n = 6 (acquired from synthetic samples).

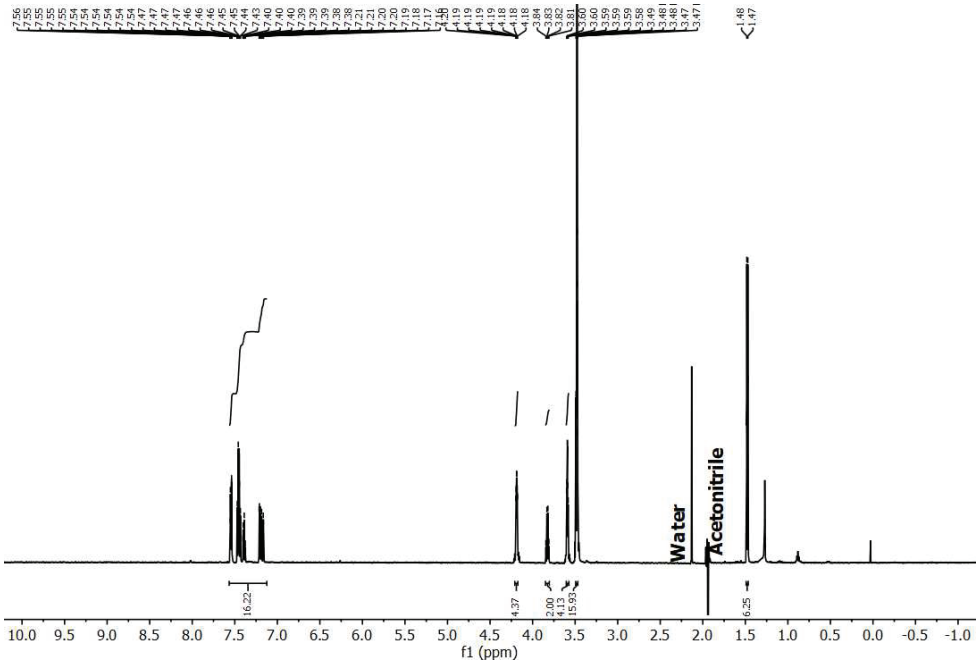

Figure S65. ^{1}H NMR spectrum of the Flurbiprofen-PEG diester with a chain length of n = 6 (acquired from lozenge-extracts).

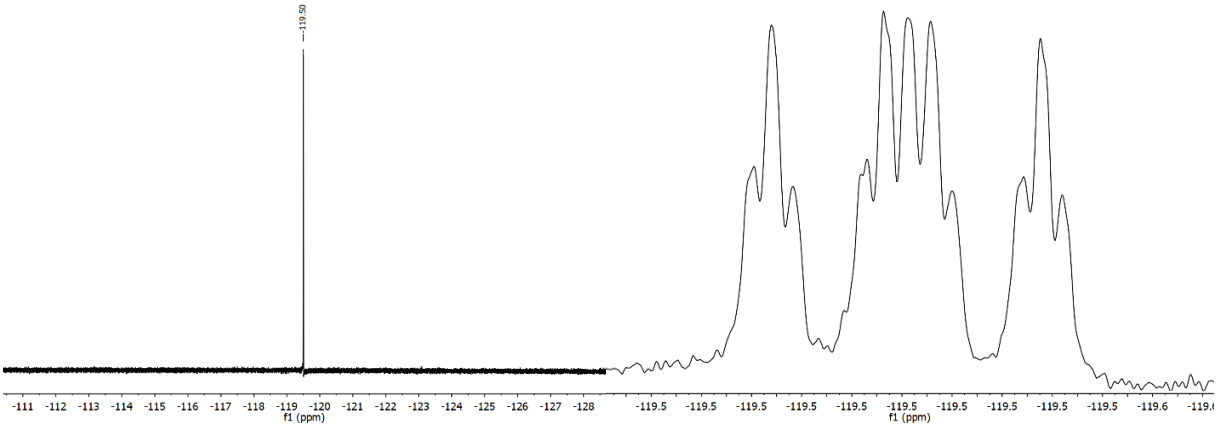

Figure S66. Decoupled (left) and coupled (right) ^{19}F NMR spectra of the Flurbiprofen-PEG diester with a chain length of n = 6 (acquired from synthetic samples).

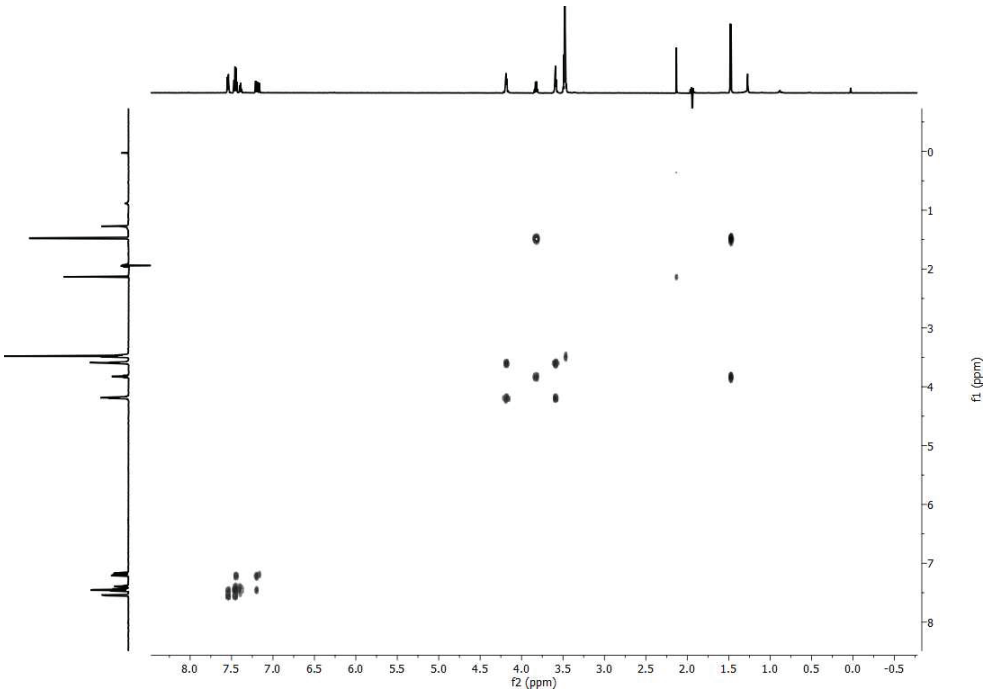

Figure S67. ^{1}H-^{1}H COSY NMR spectrum of the Flurbiprofen-PEG diester with a chain length of n = 6 (acquired from lozenge-extracts).

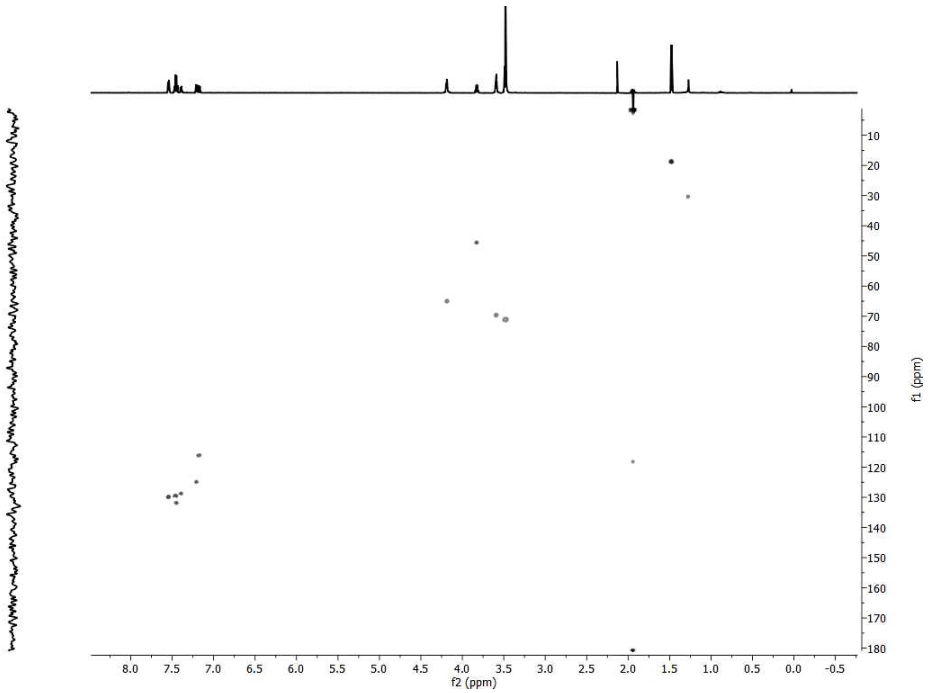

Figure S68. ^{1}H-^{13}C HSQC NMR spectrum of the Flurbiprofen-PEG diester with a chain length of n = 6 (acquired from lozenge-extracts).

IV.II.V NMR Spectra of Diester n = 7

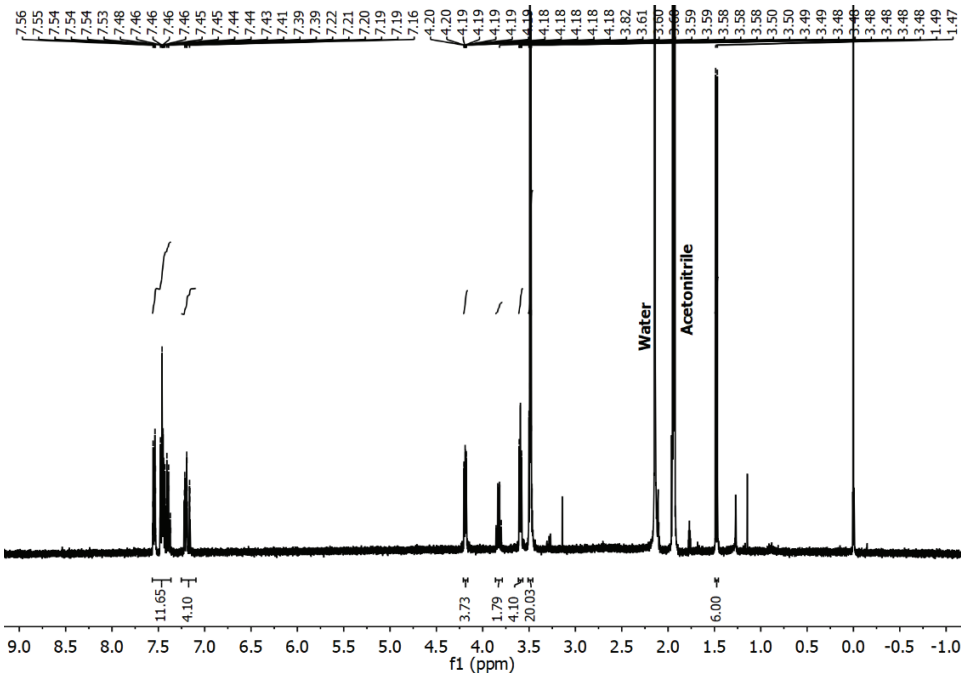

Figure S69. ^{1}H NMR spectrum of the Flurbiprofen-PEG diester with a chain length of n = 7 (acquired from synthetic samples).

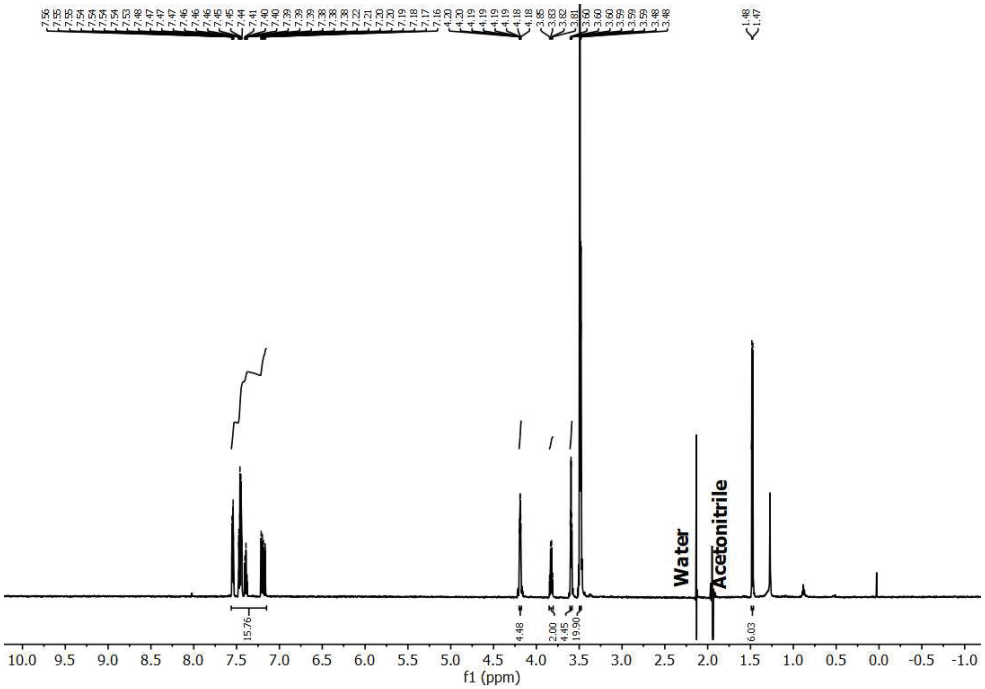

Figure S70. ^{1}H NMR spectrum of the Flurbiprofen-PEG diester with a chain length of n = 7 (acquired from lozenge extracts).

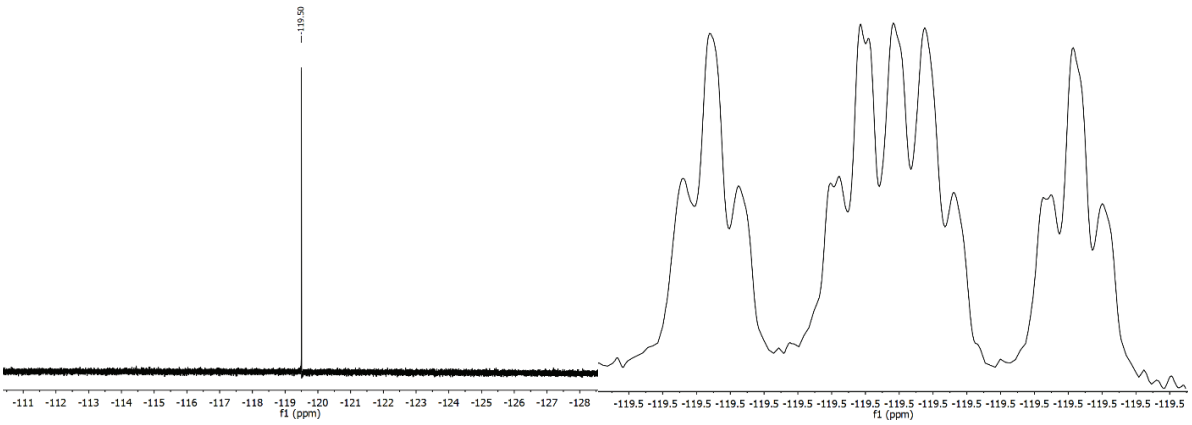

Figure S71. Decoupled (left) and coupled (right) ^{19}F NMR spectra of the Flurbiprofen-PEG diester with a chain length of n = 7 (acquired from synthetic samples).

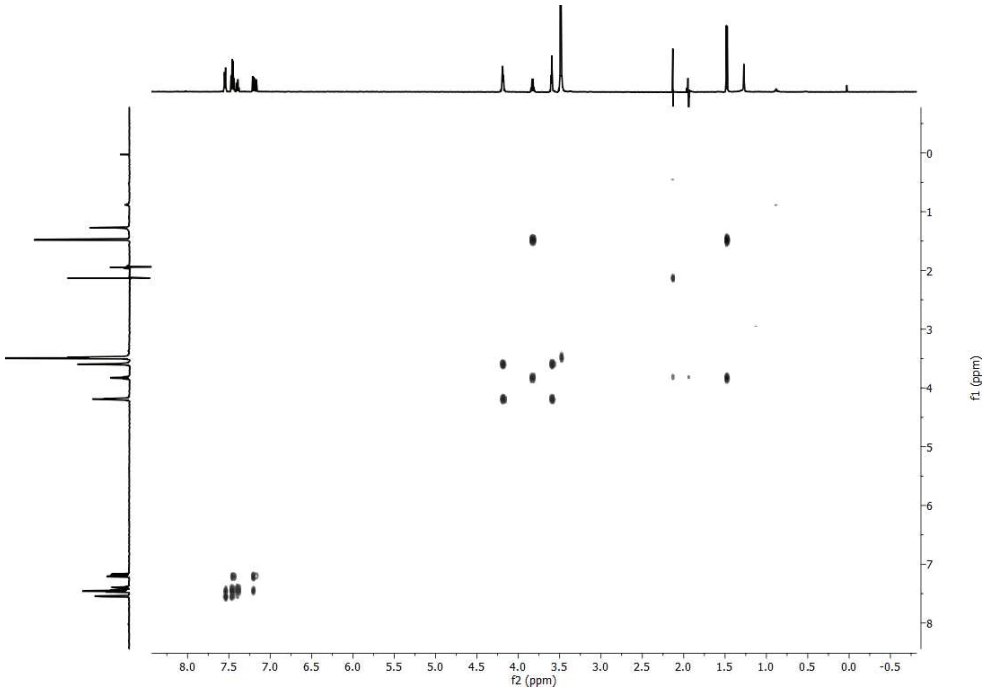

Figure S72. ^{1}H-^{1}H COSY NMR spectrum of the Flurbiprofen-PEG diester with a chain length of n = 7 (acquired from lozenge-extracts).

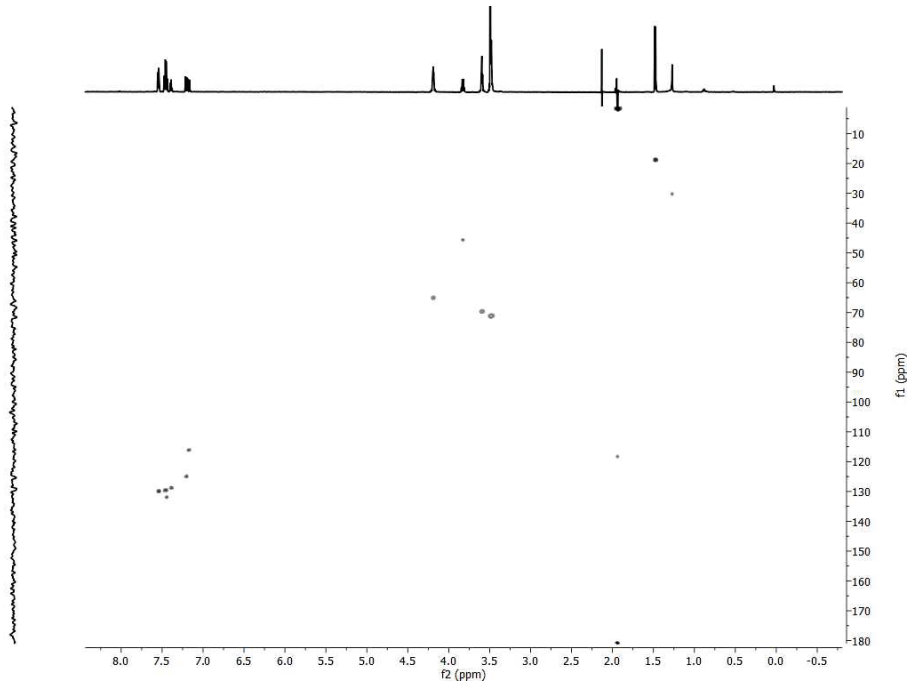

Figure S73. ^{1}H-^{13}C HSQC NMR spectrum of the Flurbiprofen-PEG diester with a chain length of n = 7 (acquired from lozenge-extracts).

IV.II.VI NMR Spectra of Diester n = 8

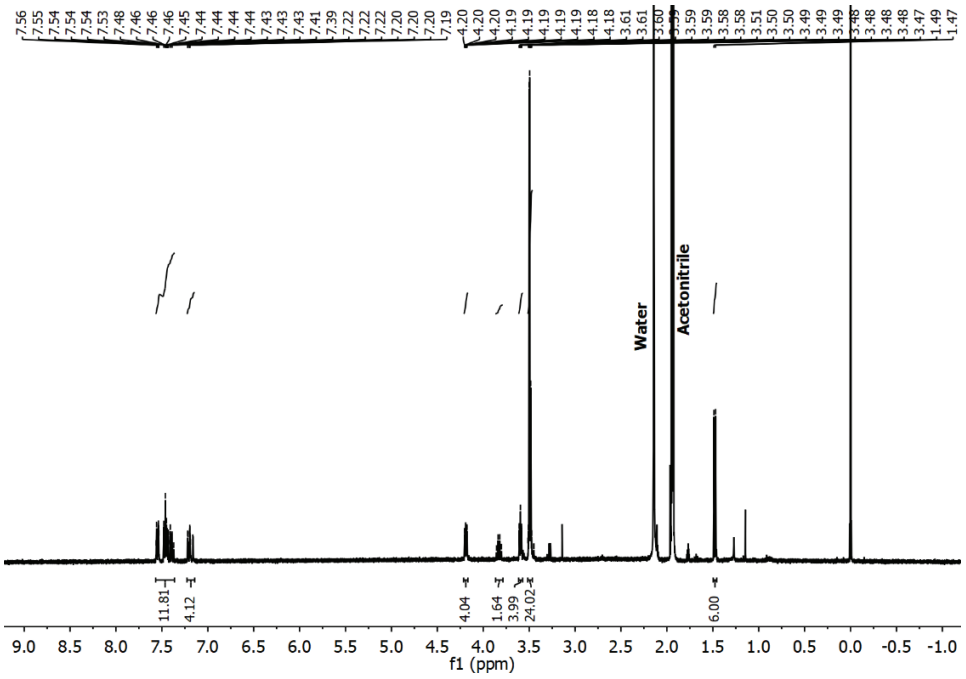

Figure S74. ^{1}H NMR spectrum of the Flurbiprofen-PEG diester with a chain length of n = 8 (acquired from synthetic samples).

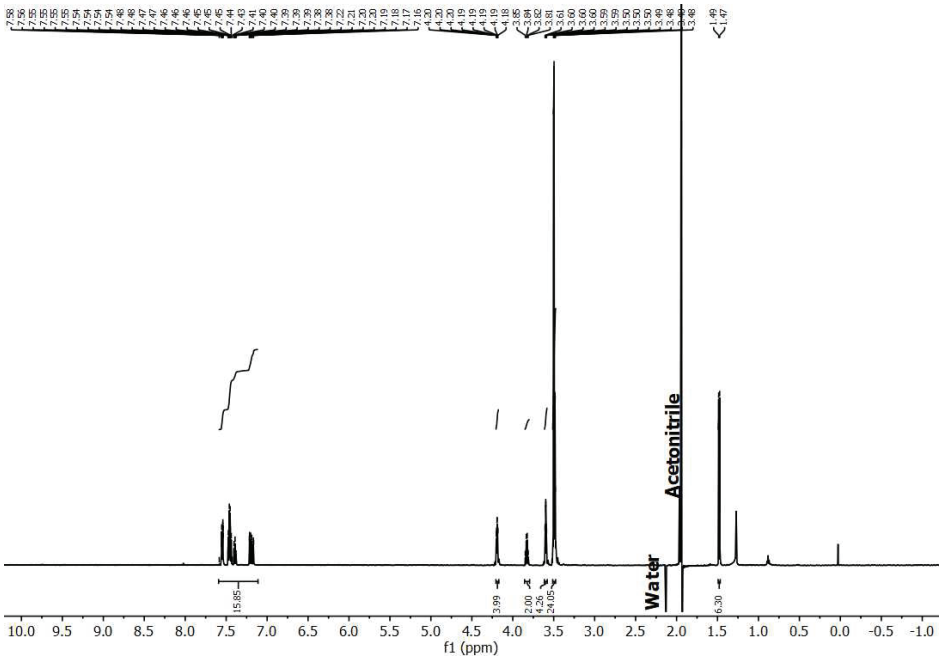

Figure S75. ^{1}H NMR spectrum of the Flurbiprofen-PEG diester with a chain length of n = 8 (acquired from lozenge-extracts).

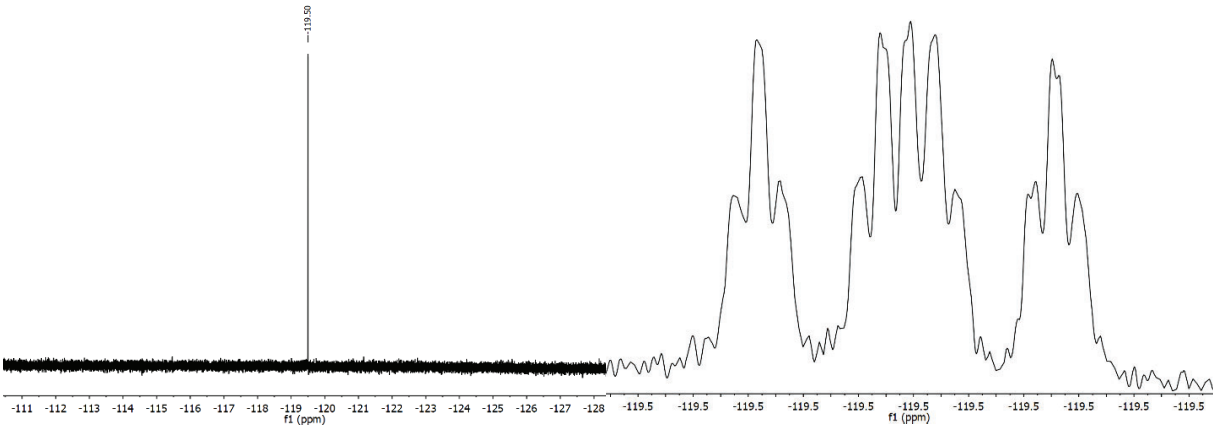

Figure S76. Decoupled (left) and coupled (right) ^{19}F NMR spectra of the Flurbiprofen-PEG diester with a chain length of n = 8 (acquired from synthetic samples).

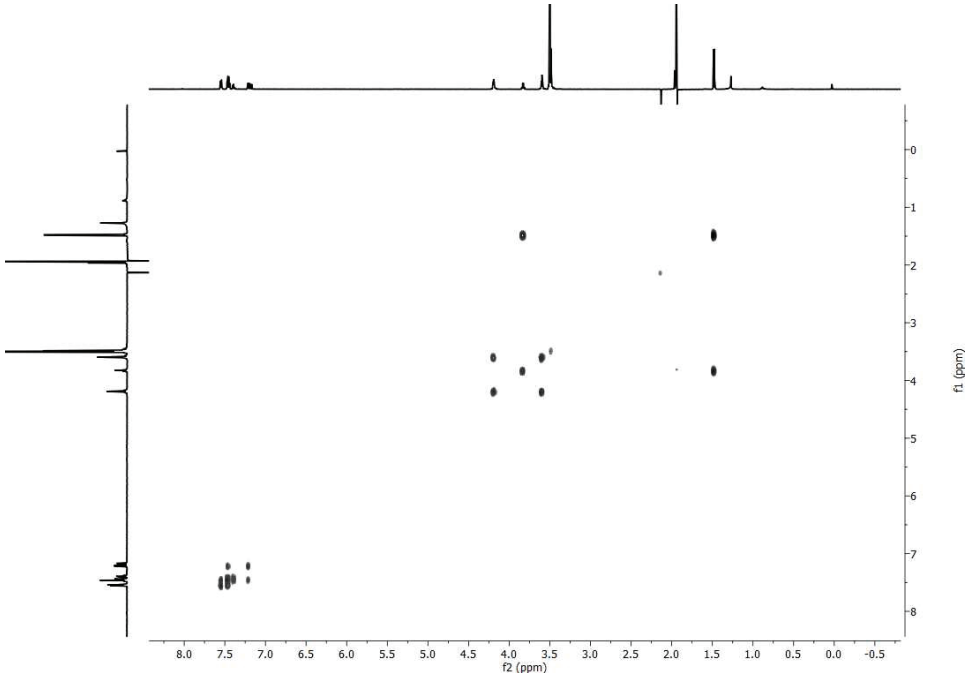

Figure S77. ^{1}H-^{1}H COSY NMR spectrum of the Flurbiprofen-PEG diester with a chain length of n = 8 (acquired from lozenge-extracts).

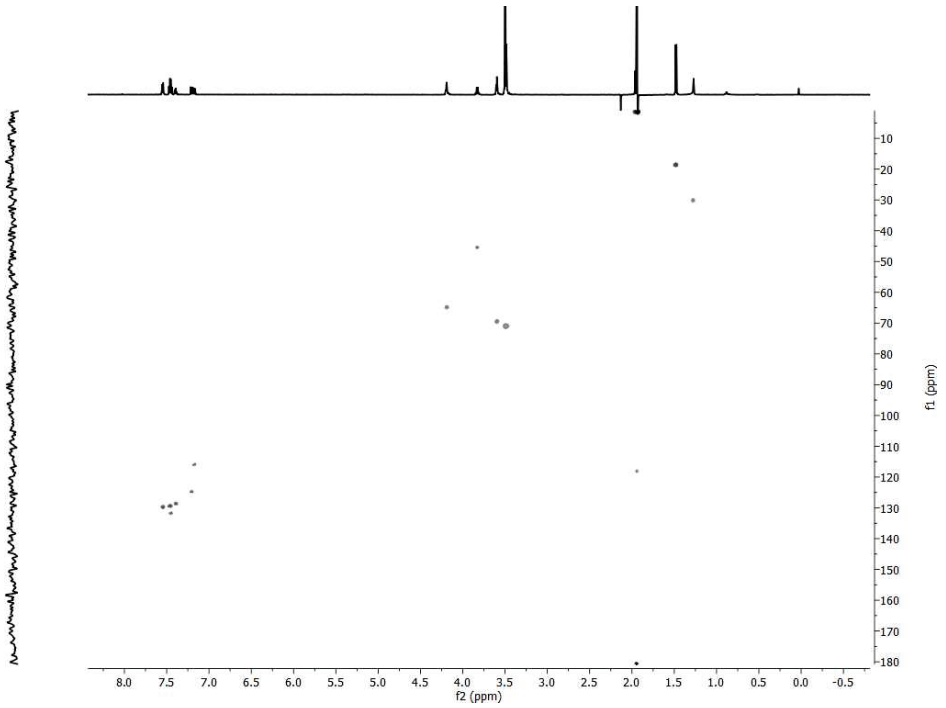

Figure S78. ^{1}H-^{13}C HSQC NMR spectrum of the Flurbiprofen-PEG diester with a chain length of n = 8 (acquired from lozenge-extracts).

V HRMS-Data of Individual Flurbiprofen-PEG Esters

Table S1. List of the m/z values for the Flurbiprofen-PEG-mono- and diesters and their aggregates, detected during LC-HRMS analysis. Aggregates that were not detected or deviated by more than 5 ppm are marked as *not detected* (n.d., acquired from synthetic samples).

Flurbiprofen-PEG-Monoesters				Flurbiprofen-PEG-Diesters			
n	$[M+H]^+$	$[M+NH_4]^+$	$[M+K]^+$	n	$[M+H]^+$	$[M+NH_4]^+$	$[M+K]^+$
1	289.1245	306.1512	327.0805	**1**	n.d.	532.2307	553.1601
2	333.1510	350.1776	371.1070	**2**	559.2302	576.2569	597.1863
3	377.1773	394.2041	415.1332	**3**	603.2583	620.2852	641.2142
4	421.2033	438.2305	459.1591	**4**	n.d.	664.3090	685.2383
5	465.2300	482.2571	503.1857	**5**	n.d.	708.3366	729.2650
6	509.2562	526.2836	547.2119	**6**	n.d.	752.3643	773.2922
7	553.2825	570.3101	591.2382	**7**	n.d.	796.3928	817.3194
8	597.3086	614.3364	635.2642	**8**	n.d.	840.4169	861.3432
9	n.d.	658.3626	679.2912	**9**	n.d.	884.4411	905.3692
10	n.d.	702.3885	723.3172	**10**	n.d.	928.4648	949.3930
11	n.d.	746.4153	767.3400	**11**	n.d.	972.4897	993.4184
12	n.d.	790.4420	811.3707	**12**	n.d.	1016.5157	1037.4448
13	n.d.	834.4678	855.3967	**13**	n.d.	1060.5403	1081.4695
14	n.d.	878.4936	899.4228	**14**	n.d.	1104.5679	1125.4970
15	n.d.	922.5192	n.d.	**15**	n.d.	1148.5957	1169.5286
16	n.d.	966.5458	n.d.	**16**	n.d.	1192.6254	1213.5547
17	n.d.	1010.5718	n.d.	**17**	n.d.	n.d.	n.d.
18	n.d.	1054.5983	n.d.	**18**	n.d.	n.d.	n.d.
19	n.d.	1098.6246	n.d.	**19**	n.d.	n.d.	n.d.
20	n.d.	1142.6502	n.d.	**20**	n.d.	n.d.	n.d.
21	n.d.	1184.6774	n.d.	**21**	n.d.	n.d.	n.d.

4.3 Discussion

During this study, real stability samples of Flurbiprofen lozenges were used. These developed an array of closely eluting impurities, that formed by esterification of the API with the excipient polyethylene glycol (PEG) during storage. The concentration distribution of these impurities is dependent on the average mass of the PEG used in the formulation of the lozenges. This provided an array of analytes with similar retention times and varying concentrations suitable to both test the chromatographic limitations, as well as the detection limits of the system.

The samples for analysis were obtained by dissolving and extracting the lozenges, without the need for further treatment of the samples. Using only the hyphenated system, the separation, isolation, enrichment, and structural elucidation of a wide range of Flurbiprofen-PEG mono and diesters was performed successfully. The obtained UV/Vis, HRMS, 1D, and, in many cases, 2D NMR data were sufficient for the complete characterization of the compounds.

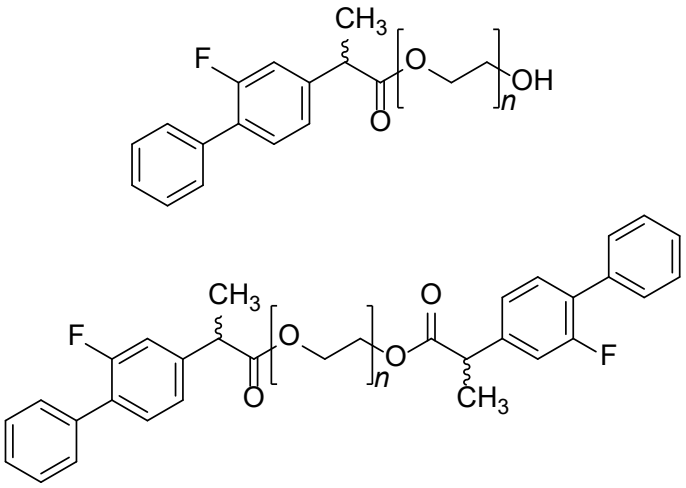

Figure 1. Structures of the Flurbiprofen-formaldehyde mono- and diesters, as elucidated by HRMS and NMR spectroscopy.

Depending on the daily dose of an API, ICH guidelines define a threshold of down to 0.05% for qualification, 0.05% for identification and 0.03% for reporting of a newly discovered impurity. These values are determined by comparing the peak area of an impurity peak in a chromatogram (usually UV/Vis) to the peak area of the API within the drug at the time of production, without considering the response factors of the impurity.[1,2,3] If the area percent-value of the impurity rises above one of the given thresholds the required action needs to be performed. During this project, complete structural elucidation and characterization was successfully performed for impurities that were contained in the lozenges at a value of 0.016% - far lower than the threshold demanded by the ICH.

Hereby, it was shown that a complete and comprehensive characterization of impurities can be performed from real stability samples without the need for further, extensive and time-consuming stress tests.

1. International Conference on Harmonization (ICH) guidelines. Impurities in new Drug Substances Q3A (R2), October 2006.
2. International Conference on Harmonization (ICH) guidelines. Impurities in new Drug Products Q3B (R2), June 2006.
3. International Conference on Harmonization (ICH) Guidance for Industry. Impurities in new Drug Products Q3B (R2), August 2006.

5 Conclusion

During this dissertation, the suitability of a hyphenated analytical system, consisting of HPLC, DAD, HRMS, SPE and NMR spectroscopy, for the use in pharmaceutical analysis was evaluated. Herein, the focus was placed on the identification of impurities in drugs. The system was designed to perform detection, separation, purification, enrichment, isolation and structural elucidation all in one, while being faster and more efficient than standard procedures that usually rely on time-consuming degradation and enrichment experiments.

5.1 Montelukast – the Early beginnings

The first project addressed the method transfer from standard analytical procedures, such as those described in the European Pharmacopoeia, to the hyphenated system. Using the degradation product of the asthma medication Montelukast as case study, it was shown that the method transfer could be performed with little effort and time, producing data of sufficient quality and quantity for a complete structural elucidation. This information was then used to deduce the formation mechanism of the impurity.

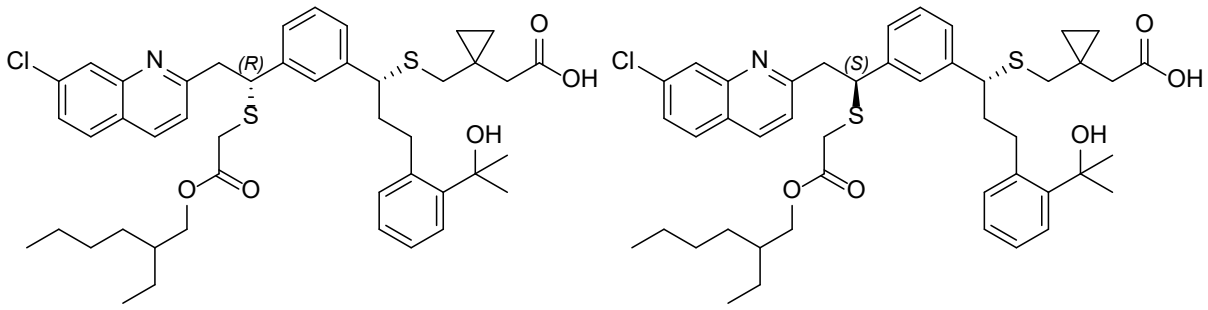

Figure 1. Structures of the two stereoisomers of the thiol-ene addition product of Montelukast and 2-ethylhexyl thioglycolate as elucidated using the data acquired using the hyphenated system.

5.2 Naloxone – A Complex Case

The second project was designed to prove the applicability of the hyphenated system for the structural elucidation of complex structures. By using SPE, sufficient amounts of sample for comprehensive 1D and 2D NMR measurements were obtained, allowing the full elucidation of the large Naloxone “dimer”.

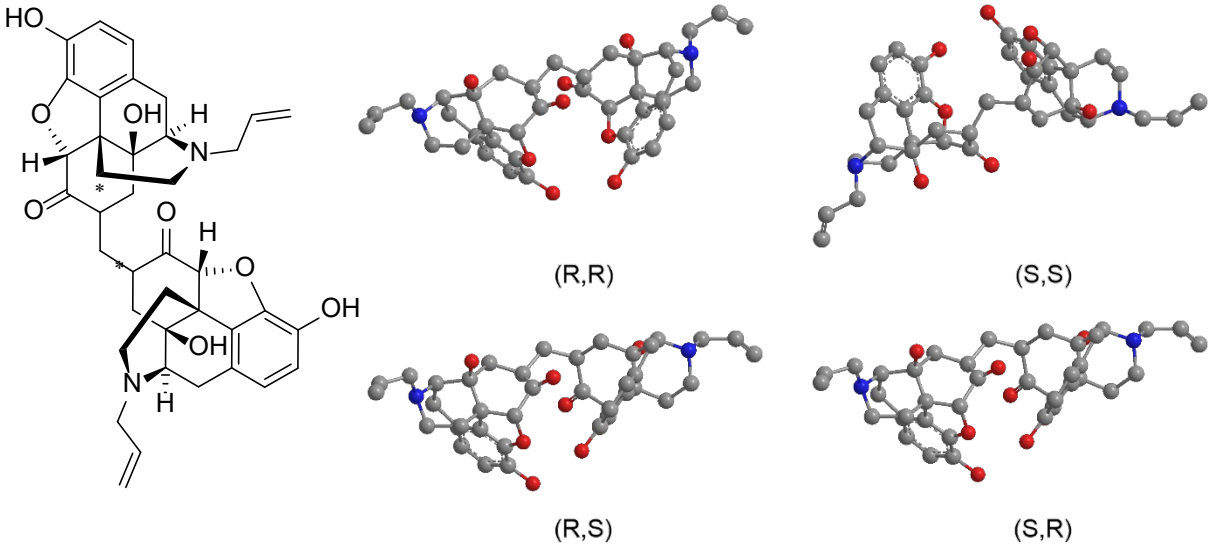

Figure 2. Structure and 3D models of the four stereoisomers of the methylene bridged Naloxone “dimer”, as elucidated using the hyphenated system.

5.3 Flurbiprofen – The Final Test

Lastly, it was shown that the hyphenated system could be used to isolate and identify impurities directly from stability samples as they are used in regular pharmaceutical quality control. Usually, the low concentrations of impurities in these samples are the major limiting factor, preventing NMR spectroscopy. However, by using SPE cartridges to enrich the target molecules, impurities that were only present in trace amounts within the medication could be identified. PEG mono- and diesters of Flurbiprofen, with levels as low as 0.016% within the samples could be isolated and fully characterized. A value, far below the ICH thresholds defined for the report of a medication impurity.

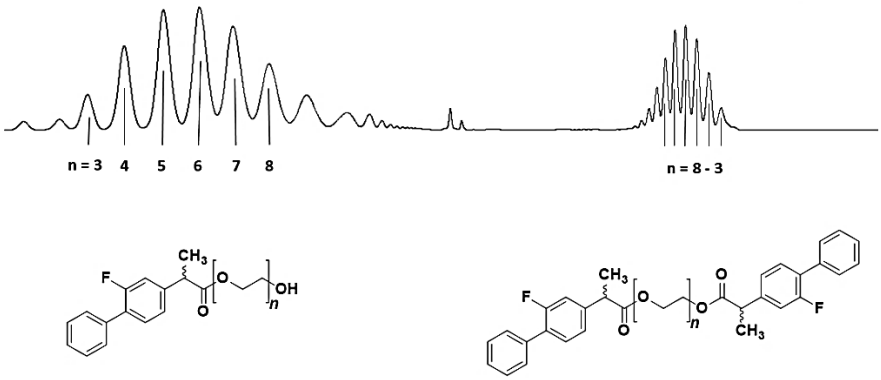

Figure 3. UV chromatogram of two Flurbiprofen-PEG mono- (left) and diester (right) impurities with varying chain lengths. The numbers beneath the chromatogram depict which chain lengths were detected during HRMS analysis.

5.4 Hyphenated Systems – A Worthwhile Investment

Overall, this hyphenated system shows high potential for the identification and characterization of trace impurities in pharmaceutical quality control. It enables the complete analysis of a newly detected impurity during synthesis, production, or stability tests, without the need for further enrichment experiments, by producing comprehensive UV/Vis, HRMS as well as 1D and 2D NMR data. The “classic” way of identification, first requires experiments to determine how the impurity is formed, followed by experiments to enrich the substance, before the actual structural elucidation can be performed. Depending on the case, this process, from detection to elucidation, may take weeks and in the worst case, may even lead to false results, should the analyte enriched during experiments turn out not to be the actual impurity in question, but a coeluting and/or artificially created substance with a similar UV/Vis-spectrum. The use of the described hyphenated system significantly expedites the process from the detection of an impurity to its identification, allowing a swift risk assessment and, if necessary, a quick implementation of measures to prevent its formation in the future. Additionally, as the entire process from detection, over separation and identification can be performed using the original sample, the risk of analyzing the wrong substance is minimized. Hereby the safety of patients and the availability of medication can be assured more reliably. It should however be noted, that though this process may significantly reduce the time of analysis, the evaluation of the data remains time consuming and requires trained personnel. Also, the cost for the acquisition, operation and maintenance of the analytical equipment remains high, with additional costs arising from the interfaces and modules required to combine these various analytical methods. In this case the additional costs amounted to approximately 250 000€ for the SPE module, connectors and pumps and 200 000€ for an update to the NMR console. Overall, the long-term savings in time, material and personnel as well as the heightened efficiency should outweigh the initial costs of acquisition.

6 Appendix – Trade Magazine Article

For additional reading on the topic of complex hyphenated systems in pharmaceutical analytics, this additional article from the German *GIT Laborzeitschrift* titled *HPLC in der pharmazeutischen Analytik* by Hans-Christian Müller and Philipp Schmidt, has been added to the appendix of this dissertation.

This article is meant to provide additional insights into the topic from the perspective of the pharmaceutical industry. Unlike most of this dissertation, the article is written in German and parts of the article are grayed out, as they are intended for the placement of adverts in the printed version of the article.

Author contributions:

Hans-Christian Müller:

Performed the literary research and writing of the following article "HPLC in der pharmazeutischen Analytik".

Philipp Schmidt:

Performed an advisory role in the preparation of the manuscript, aided in proof-reading and provided data and images.

HPLC in der pharmazeutischen Analytik

Neue Techniken für alte Herausforderungen und neue Fragestellungen

Hans-Christian Müller[1], Philipp Schmidt[2]

In vielen Unternehmen und Behörden steigt die Komplexität der zu bearbeitenden Fragestellungen und zu kontrollierenden Anforderungen an Produkte und Prozesse. Damit steigen quasi automatisch auch die Anforderungen an die analytischen Untersuchungen. Infolgedessen wird eine zunehmend größere Bandbreite an analytischen Techniken zur Beantwortung der Fragestellungen und zur Überwachung der Produkte und Prozesse notwendig. Immer mehr kommen dabei Kombinationssysteme aus Separations- und verschiedenen Detektionstechniken (Hyphenation) zum Einsatz. Am Beispiel der Strukturaufklärung von unbekannten Verunreinigungen in pharmazeutischen Produkten konnte gezeigt werden, was mit einem solchen Kombinationssystem heute möglich ist und wo die Herausforderungen liegen. Mit den steigenden Fähigkeiten dieser Systeme wachsen Komplexität und Kosten. Insbesondere stellen sie hohe Anforderungen an die Benutzer und deren Training. Der Umfang des erforderlichen Wissens wächst und muss später auch bei geringer Geräteauslastung aufrechterhalten werden. Das stellt insbesondere für kleine Unternehmen eine Herausforderung dar.

Die HPLC im pharmazeutischen Labor

Im pharmazeutischen Umfeld – in der Produktentwicklung wie der Qualitätskontrolle – ist die HPLC-Technik die wichtigste analytische Schlüsseltechnologie zur Trennung von Stoffgemischen und der nachfolgenden qualitativen und quantitativen Bewertung der Komponenten. Diese Technik hat von ihren Anfängen mit dem Auswiegen von ausgeschnittenen Papierschreiberausdrucken einen sehr weiten Weg zurückgelegt bis zur heute möglichen, vollautomatischen Auswertung und direkten Ergebnisübertragung in Laborinformationssysteme.

Viele dieser Fortschritte sind der unglaublichen Entwicklung der Mathematik und der Computertechnologie zu verdanken. Ebenso zu nennen sind die geradezu gewaltigen technischen Fortschritte zur Verbesserung der Detektoren, der erhöhten Bauteilpräzision zur Erreichung genauerer Arbeitsspezifikationen und nicht zuletzt weitreichende Optimierungen der Säulenmaterialien. Alles zusammengenommen hat zum großen Erfolg der HPLC, insbesondere der HPLC-UV, im pharmazeutischen Umfeld geführt.

Die erreichte Automatisierung, die technischen Verbesserungen sowie neue Detektionsverfahren (Brechungsindex, Fluoreszenz, Charged Aerosol Detektion, Leitfähigkeit, etc.) konnten bisher allerdings nicht über die grundlegende Einschränkung der Technologie hinweghelfen.

Die HPLC-Technik ist in ihrem Wesen eine relative Bestimmungsmethode. Das Quantifizieren von Substanzen ist nur unter Zuhilfenahme einer bekannten und spezifizierten Referenzsubstanz möglich. Und auch

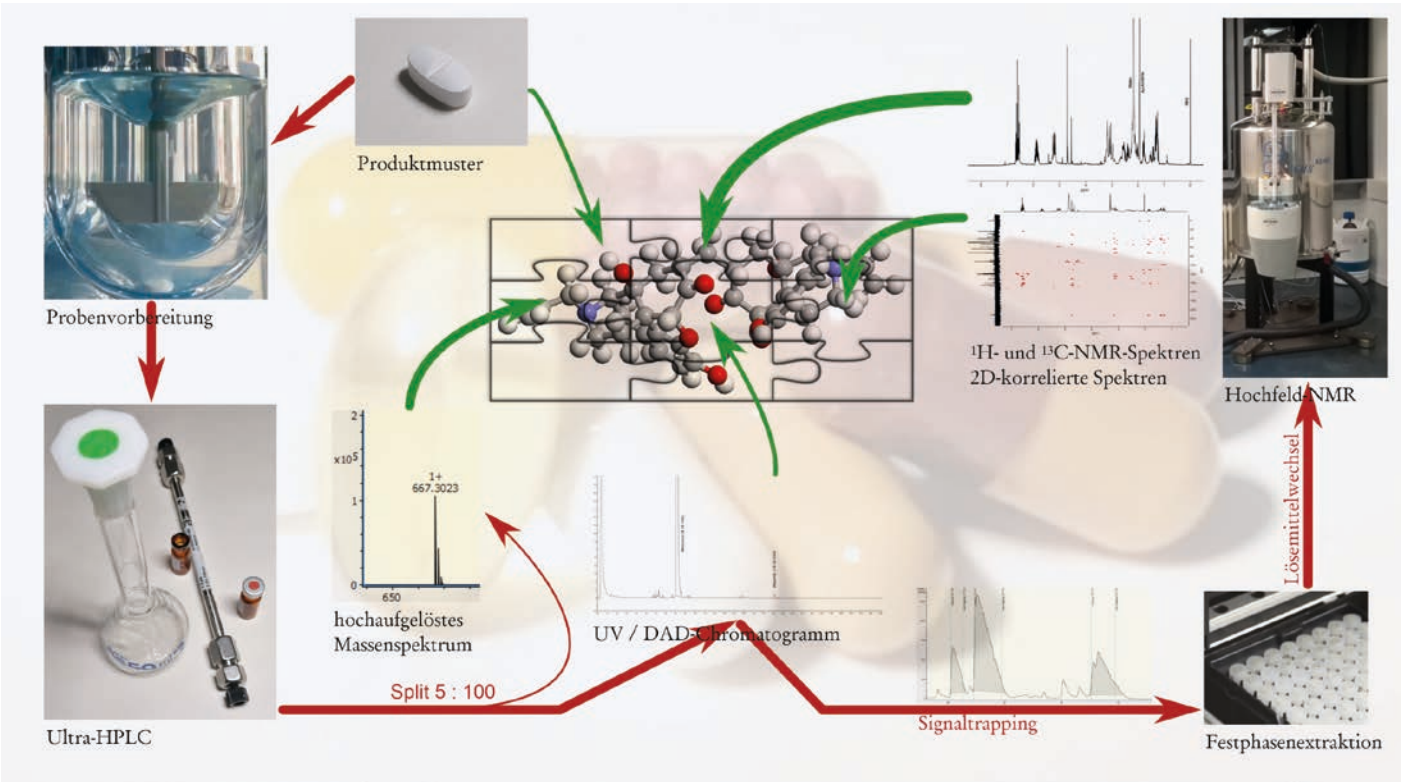

Abb 1: Prinzip des verwendeten HPLC-DAD-HRMS/SPE-NMR Systems.

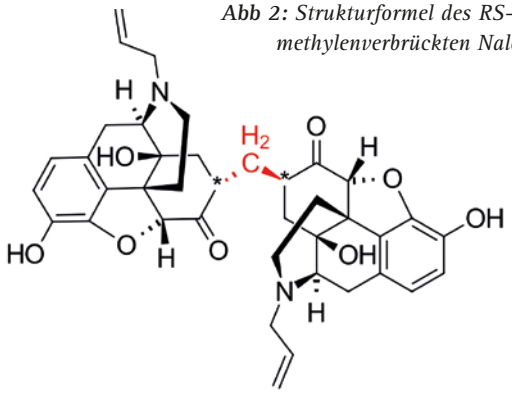

Abb 2: Strukturformel des RS-Isomers des methylenverbrückten Naloxondimers.

das Identifizieren ist nur eingeschränkt unter standardisierten Rahmenbedingungen, die denen der Methodenentwicklung entsprechen, möglich. Eingebettet in ein komplexes Qualitätsmanagementsystem muss das dann kaum eine Einschränkung mehr darstellen. Und dennoch treten im Betriebsalltag immer wieder Situationen auf, die diese Limitierung schmerzlich bewusst machen.

Der klassische Weg zur Identifizierung von Verunreinigungen

Eine solche Situation begann mit der Entdeckung einer bisher unbekannten Verunreinigung bei der Reinheitsanalyse während der Stabilitätsstudie zu einem pharmazeutischen Entwicklungsprodukt mit dem Wirkstoff Naloxon [1]. Aufgrund der beschriebenen Limitierung waren trotz Einsatz eines DAD-Detektors nur wenige Informationen zur Identität der Verunreinigung verfügbar. Die Substanz zeigte fast identische UV-Vis-Signale wie der Wirkstoff. Darüber hinaus konnte eine Ähnlichkeit der Substanz mit den Hilfsstoffen mit hoher Wahrscheinlichkeit ausgeschlossen werden. Das fast unveränderte UV-Spektrum gegenüber dem Wirkstoff deutete darauf hin, dass sich das chromophore System des Wirkstoffmoleküls wohl kaum verändert hatte und die entsprechende Abbaureaktion in einem anderen Teil des Moleküls stattgefunden haben musste. Das waren leider schon alle Informationen aus der HPLC-UV.

Nun wurde auf klassischem Wege mittels selektierter Versuche zum Abbau des Wirkstoffes gearbeitet und die HPLC-Chromatogramme der entstandenen Verbindungsgemische verglichen. Im Zuge dieser Untersuchungen wurde die Beteiligung von Formaldehyd bei der Bildung der Verunreinigung entdeckt. Formaldehyd ist eine bekanntermaßen in Spuren auftretende Verunreinigung in mehreren weitverbreiteten pharmazeutischen Hilfsstoffen [2 – 8].

Auf Basis von Überlegungen zu möglichen Reaktionsverläufen in der vorhandenen Produktmatrix wurden nun vor allem Versuche zur direkten Synthese und Isolierung mittels

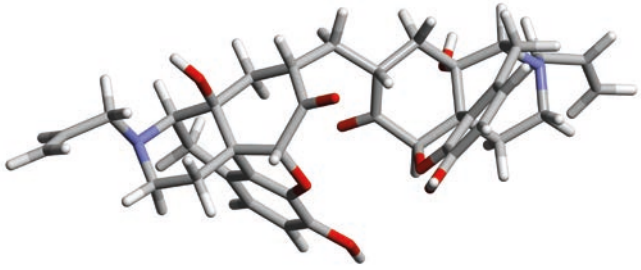

Abb 3: Molekülmodell des RS-Isomers des methylenverbrückten Naloxondimers.

präparativer HPLC durchgeführt. Für die Arbeiten zur Identifizierung war dann der Einsatz der HPLC-UV-HRMS Technik erforderlich. Die notwendige Umschreibung der Trennmethode auf Eluenten mit massenspektrometerverträglichen Komponenten erforderte einigen Aufwand, da hierdurch die Chromatogrammvergleichbarkeit nicht mehr gegeben war. Dafür lieferte diese Technik aber wertvolle Informationen zur Natur der Verunreinigung.

Bei den zugehörigen ESI-Experimenten im positiven Modus wurden ein einfach geladenes Ion mit einem m/z Verhältnis von 667 für $[M + H]^+$ und ein doppelt geladenes Ion mit einem m/z Wert von ungefähr 666 nachgewiesen, verglichen mit 327 bei Naloxon. Diese Ergebnisse legten den Schluss nahe, dass es sich bei der Verunreinigung um zwei miteinander verbundene Naloxon-Einheiten handelt. Die Differenz von 14 atomaren Einheiten entspricht dabei einer CH_2-Einheit.

Bei den Syntheseexperimenten konnten schließlich größere Konzentrationen der Verunreinigung hergestellt werden. Dabei wurden drei Isomere entdeckt, was auf die Anwesenheit von mindestens zwei Stereozentren im Molekül hinwies. Aber erst mit Hilfe von sehr aufwendig auszuwertenden 1D- und 2D-NMR-Experimenten in deuteriertem Methanol an Isolaten aus der direkten Synthese konnte die finale Strukturbestimmung abgeschlossen werden.

Hiernach reagieren zwei Naloxon-Moleküle in Anwesenheit von Formaldehyd zunächst in einer Aldolkondensation, gefolgt von einer Michael Addition. Hierbei entstehen zwei neue optische Zentren, die die drei experimentell gefundenen Stereoisomere (RR, SS sowie RS, welches identisch mit SR ist) bilden.

> *Die HPLC-Technik ist in ihrem Wesen eine relative Bestimmungsmethode.*

Die anschließende Direktsynthese und Aufreinigung der Verbindung zeigte, dass jede der drei gezielt isolierten Reinsubstanzen immer wieder alle drei Stereoisomere in ähnlichem Mengenverhältnis enthielt. Dies erklärt sich durch eine Keto-Enol-Tautomerie zwischen den Ketofunktionen und den neu gebildeten Stereozentren.

Ein neuer Weg zur Identifizierung von Verunreinigungen?

Während die Identifizierung der Verunreinigung im klassischen Stil mit Degradations- und Syntheseexperimenten stattfand, wurde anschließend eine komplexe Kombinationstechnik angewandt, um deren Fähigkeiten zu evaluieren. Die erste Anwendung dieses HPLC-DAD-HRMS/SPE-NMR Systems wurde noch mit Syntheselösungen durchgeführt. Diese enthielten im Vergleich zu Extrakten aus einem Produktmuster eine vergleichsweise hohe Konzentration der Verunreinigung.

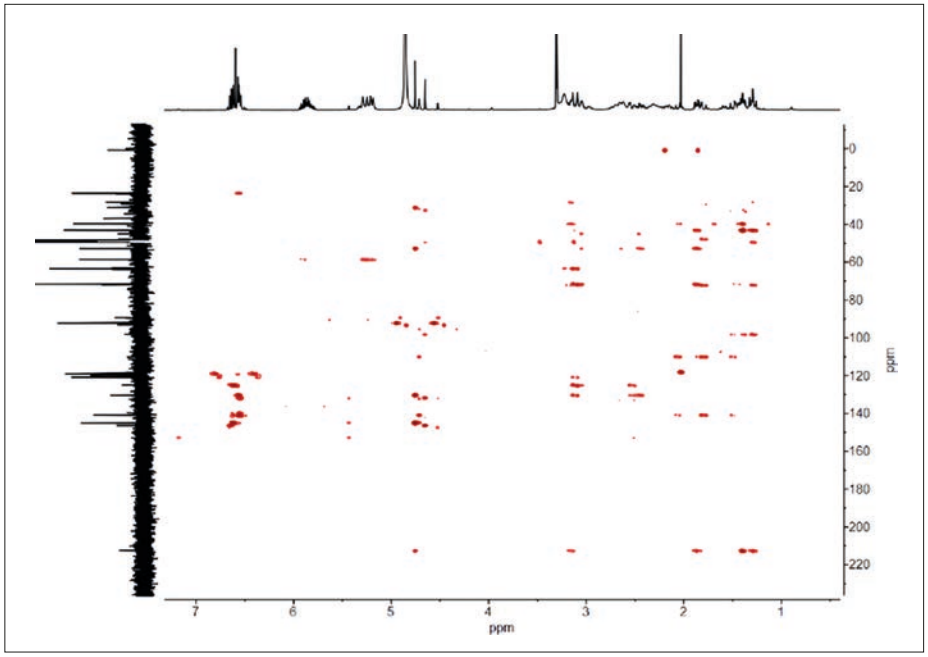

Abb 4: ^1H-^{13}C-HMBC-NMR-Spektrum der Verunreinigung (gemessen in deuteriertem Methanol). Reprinted from [1, Figure S16] with permission from Elsevier.

Nach einigen Anlaufschwierigkeiten konnte eine vollständige Isolierung und Charakterisierung mit allen beteiligten Analysetechniken aus nur einer Probe der Syntheselösung erfolgreich durchgeführt werden. Das stimmte zuversichtlich, dass mit einigen Adaptionen, weiterer Einarbeitung und einigem Lernen durch Ausprobieren, eine Isolierung direkt aus einem Produktmuster gelingen könnte.

Die Gelegenheit dazu kam schnell [9]. Bei der Untersuchung einer Lutschtablette mit dem Wirkstoff Flurbiprofen wurde schon immer ein Muster von pharmakologisch unbedenklichen Verunreinigungen beobachtet, deren Identität im Prinzip bekannt war, aber ohne exakte Zuordnung zu den einzelnen Peaks im Chromatogramm. Der Hilfsstoff Polyethylenglykol mit seinen verschiedenen Kettenlängen reagiert mit dem Wirkstoff und bildet eine Gruppe von Estern mit unterschiedlichen Kettenlängen. Die vollständige Strukturaufklärung dieser Gruppe von Estern direkt aus der Lutschtablette wurde mit dem komplexen HPLC-DAD-HRMS/SPE-NMR Kombinationssystem parallel zur klassischen Aufklärung versucht.

Das stellt derzeit für das System noch eine erhebliche Herausforderung dar, denn die NMR benötigt für jede Analyse, die mehr als ein Protonenspektrum liefert, ausreichend Substanz im Bereich von Millimol. Eine Menge, die bei der Separation einer Verunreinigung aus einem Fertigarzneimittel mittels HPLC-Säule selten erreicht wird. Hier liegen die Mengen eher im Bereich von Pikomol, also einige Zehnerpotenzen niedriger. Und dennoch gelang unter Ausreizung vieler Möglichkeiten an jeder der beteiligten Techniken eine ausreichende Optimierung und die Isolation von genügend Substanz auf den speziellen SPE-Kartuschen, um für die Mehrzahl der Verunreinigungen nicht nur ^1H und ^{13}C, sondern auch korrelierte 2D-NMR-Spektren erhalten zu können.

So war die vollständige Strukturaufklärung mehrerer Komponenten aus Lutschtabletten in vergleichsweise kurzer Zeit möglich. Gleichzeitig wurde aber auch klar, dass trotz der ausgeklügelten Technik das gleiche chemische, produktspezifische und methodische Wissen zur Aufklärung erforderlich war, wie bei der klassischen Herangehensweise.

Fazit

Bei einem Produkt in der Entwicklung mag es akzeptabel sein, wenn die Aufklärung einer Verunreinigung einige Wochen dauert. Ganz anders, wenn eine neue Verunreinigung bei einer Freigabe- oder Stabilitäts-

untersuchung auftritt und damit auf eine Änderung oder Abweichung bei den Ausgangsstoffen, im Herstellungs- oder auch im Analyseprozess hinweist. Die Identität der Verunreinigung und damit die Ursache muss schnellstmöglich gefunden werden, um die Produktion des betroffenen Produkts wieder aufnehmen zu können und auch die Chargenfreigabe für den Markt nicht zu lange zu blockieren.

Durch die Kombination der HPLC mit verschiedenen Techniken werden die analytischen Möglichkeiten erheblich erweitert, aber deren Anwendung auch immer komplizierter. Denn die Voraussetzungen und Einschränkungen der einzelnen Techniken müssen in ihrer Kombination optimal abgestimmt werden. Dieses erfordert sehr viel Fachwissen und beachtliche Erfahrung in Bedienung, Methodenentwicklung und auch der Auswertung. Schließlich müssen die Ergebnisse der unterschiedlichen Messmethoden richtig interpretiert werden, damit nicht das aus den Daten herausgelesen wird, was man gerne hätte.

Die komplexen Kombinationssysteme können die Identifizierung und Charakterisierung von neuen Verunreinigungen deutlich beschleunigen. Aber der nicht monetäre Preis dafür ist die deutlich zeitaufwendigere Einarbeitung und Aufrechterhaltung des Wissens- und Erfahrungsniveaus. Ein Fakt den Labor- und Abteilungsleitungen besser akzeptieren sollten.

Ferner sind durchaus Kooperationen vorstellbar, bei denen die in die verschiedenen Kombinationstechniken investierenden Firmen oder Einrichtungen zwecks Geräteauslastung und zum weiteren Training der eigenen Spezialisten mit externen Partnern zusammenarbeiten. Für das Management stellt ein solcher Vorschlag natürlich eine Herausforderung dar, denn es erfordert beachtlichen Mut, die eingetretenen Pfade vom Unternehmen als Einzelkämpfer zu verlassen und solche Zusammenarbeiten zu wagen. Schließlich steigt der Kostendruck beständig und gefährdet sinnvolle Zukunftsinvestitionen, weil viel zu viele Manager irgendwelchen artifiziellen Zahlen hinterher hecheln, statt sinnvolle Ziele zu verfolgen.

Zugehörigkeiten
[1]Selbständiger Berater für Qualitätsmanagement, Brannenburg, Deutschland
[2]Department Chemie, Ludwig-Maximilians-Universität München, Deutschland

KONTAKT

Dr. Hans-Christian Müller
Selbständiger Berater für Qualitätsmanagement
Brannenburg, Deutschland
ORCID: 0000-0001-9367-6066
beratung@dm-hc.org

Weitere Beiträge zum Thema:
https:// bit.ly/WAS-D-HPLC

[1] Literatur:
https://bit.ly/GIT-Mueller-1

References

1. Schmidt P, Kolb C, Reiser A, Philipp M, Müller HC, Karaghiosoff K. Isolation, Identification and Structural Verification of a Methylene-Bridged Naloxon “Dimer” Formed by Formaldehyde. J Pharm Sci 2021;11(6):1682–1689.
2. Qiu F, Norwood DL. Identification of Pharmaceutical Impurities. J Liq Chrom Relat Tech 2007;30:877–935.
3. del Barrio MA, Hu J, Zhou P, Cauchon N. Simultaneous determination of formic acid and formaldehyde in pharmaceutical excipients using headspace GC/MS. J Pharm Biomed Anal 2006;41:738–743.
4. Bergh M, Magnusson K, Nilsson JL, Karlberg AT. Formation of formaldehyde and peroxides by air oxidation of high polyoxyethylene surfactants. Contact Derm 1998;39(1):14–20.
5. Bindra DS, Williams TD, Stella VJ. Degradation of O^6-benzylguanine in aqueous polyethhylene glycol 400 (PEG 400) solutions: concerns with formaldehyde in PEG 400. Pharm Res 1994;11:1060–1064.
6. Fujita M, Ueda T, Handa T. Generation of Formaldehyde by pharmaceutical excipients and its absorption by meglumine. Chem Pharm Bull 2009;57:1096–1099.
7. Nassar MN, Nesarikar VN, Lozano R, Parker WL, Huang Y, Palaniswamy V, Xu W, Khaselev N. Influence of formaldehyde impurity in polysorbate 80 and PEG-300 on stability of parenteral formulation of BMS-204352: identification and control of degradation product. Pharm Dev Technol 2004;9(2):189–195.
8. Qin XZ, Ip DP, Chang KH, Dradransky PM, Brooks MA, Sakuma T. Pharmaceutical application of LC-MS. 1 − Characterization of a famotidine degradate in a package screening study by LC-APCI MS. J Pharm Biomed Anal 1994;12(2):221–233.
9. Schmidt P, Kolb C, Godejohann M, Reiser A, Philipp M, Müller HC, Karaghiosoff K. Separation and identification of a complex flurbiprofen-polyethylene glycol mono- and diester mixture via a hyphenated HPLC-DAD-HRMS/SPE-NMR system. J Pharm Biomed Anal 2023;222:1–12.
10. Dettlaff H, Dufter-Münster AMW, Karaghiosoff K, Klapötke TM, Müller HC, Sabatini JJ. Microscopic Studies and Application of a Stabilized Ceric Ammonium Nitrate Oxidizer in Environmentally Friendly Pyrotechnic Strobes. Inorg Chem 2022;61(26):9930–9934.